Optimising calcium phosphate cement formulations to widen clinical application.

By

Sarika Patel

A thesis submitted to the
School of Chemical Engineering of the
University of Birmingham
for the degree of
Doctor of Philosophy

School of Chemical Engineering,
College of Engineering and
Physical Science,
University of Birmingham,
Egdbaston,
Birmingham,
B15 2TT
UK

Abstract

As a result of our ageing population, the demand for novel approaches to the repair of bone defects caused by trauma, infection and surgical intervention is ever increasing. This increase in clinical demand has highlighted the deficiencies of autogenous grafts, such as poor availability and donor site morbidity and consequently there has been a drive to develop new synthetic bone replacement materials. Since the 1980's calcium phosphate cements (CPC's) have attracted a great deal of interest due to their chemical similarities to natural bone; chemical, physical and mechanical characteristics have been investigated and manipulated to maximise osteoconductivity and osteointegration. Despite these advanatageous properties, the CPC has not surplanted the autogenous tissue graft as the gold-standard bone replacement material owing to perceived difficulties in clinical application and long-term stability following implantation.

In this thesis, a range of approaches to address issues that have prevented the widespread clinical uptake of CPC's by: (1) limiting water availability during the setting reaction of a brushite cement to produce monetite (the anhdydrous form of brushite) based cement, which is known to be extensively resorbed during implantation, but previously could not be formed by a cementing reaction; (2) encapsulating the aqueous component of the cement to produce a material that can be supplied in a 'ready-mixed' form and will set following a change in temperature from 4 °C to 37 °C; (3) incorporating therapeutic molecules as a prophylactic measure to prevent implant-associated infections; and (4) Manipulating the degradation properties of the material by incorporating porosity with a non-toxic pore former.

Acknowledgments

I owe many thanks to my supervisor Dr. Liam Grover who has provided motivation, direction and encouragement throughout my PhD. I would also like to thank Dr Adrian Wright whose knowledge of X-ray diffraction aided much of my work. I would like to extend my appreciation to David Farrar at the Smith and Nephew Research Centre.

Thanks to those from other academic institutions who have also helped with a number of aspects of my PhD. I am particularly grateful to Dr. Uwe Gbureck and his research group at the University of Wurzburg, Germany.

Thanks to my fellow PhD students who have been a great support to me during my PhD; many thanks to Jiana-Pei Jing, Amina Bolariwa and Nicola Hunt and in particular to my best friend Yi-Pei Hung.

My sincerest thanks go to my parents and grandparents for their ongoing financial and emotional support. Most importantly I would like to thank my sisters Poonam and Chandni who have both been a great inspiration to me throughout my academic study.

Finally I would like to thank Bhagwan Swaminarayan and Guru Hari Pramukh Swami Maharaj; for keeping me focussed and composed in times of stress and difficulties. Without their grace and blessings, I would not have been able to reach this level of academia.

“Swami Shreeji”

Abbreviations

(α/β-) TCP – (Alpha/Beta-) Tricalcium Phosphate

ACP – Amorphous Calcium Phosohate

ALP – Alkaline Phosphatase

BCP – Bisphasic Calcium Phosphate

BMA – Bone Marrow Aspirate

BMP – Bone Morphogenic Proteins

C:B - Cement to Bead Ratio

CaO – Calcium Carbonate

CDHA – Calcium-deficient Hydroxyapatite

CO_2 – Carbon Dioxide

CPC – Calcium Phosphate

CPC – Calcium Phosphate Cements

CS – Compression Strength

CSD – Calcium Sulphate Dihydrate

CSH – Calcium Sulphate Hemihydrates

DBM – Demineralised Bone Matrix

DCM – Dichloromethane

DCP – Dicalcium Phosphate

DCPA – Dicalcium Phosphate Anhydrate

DCPD – Dicalcium Phosphate Dehydrate (Brushite)

DCPP – Dicalcium Pyrophosphate

EDS – Energy Dispersive System

EPG – Eudragit Polyethyleneglycol

E-SEM – Environmental Scanning Electron Microscope

FTIR – Fourier Transform Infrared Spectroscopy

GS – Gentamicin Sulphate

HA – Hydroxyapipatie

HCA – Hydroxycarbonate Apatite

HCl – Hydrochloric Acid

Hep B/C – Hepertitis B/C

HIV – Human Immunosupressant Virus

IAP – Internal Aqueous Phase

KCl – Potassium Chloride

LCVR – Liquid to Cement Volume Ratio

MCPA – Monocalcium Phosphate Anhydrous

MCPM – Monocalcium Phosphate Monohydrate

M-CSF – Macrophage Colony Stimulating Factors

Micro CT – X-ray Computed Microtomagraphy

MRSA – Methacilin Resistant Straphylococcus *aureus*

O/W/O – Oil-in-Water-in-Oil

OA – Orthophosphoric Acid

P:L – Powder to Liquid Ratio

PBS – Phosphate Buffer Solution

PCL – Poly-Caprolactone

PEG – Polyethyleneglycol

PGA – Polyglycolide

PLA – Polylactide

PLGA – Poly(DL-Lactide-co-glycolide)

PMMA – Polymethylmethacrylate

PPA – Pyrophosphoric Acid

PSD – Particle Size Distribution

PTFE – Polytetraflouroethylene

PTH – Parathyroid Hormone

PVA – Polyvinyl Alcohol

S. *aureus* – Staphylococcus *aureus*

S. *epi* – Staphylococcus *epidermidis*

SD – Standard Deviation

SEM – Scanning Electron Microscopy

SHA – Stoichiometric Hydroxyapatite

TTCP – Tetracalcium Phosphate

UCS – Ultimate Compression Strength

VH – Vancomyicin Hydrochloride

W/O – Water-in-Oil

W/O/W – Water-in-Oil-in-Water

XRD – X-ray Diffraction

Table of Contents

Chapter 1 Introduction 1

Chapter 2 Bone 4

2.1 Bone cells 4
2.1.1 Osteoprogenitor 5
2.1.2 Osteoblast 5
2.1.3 Osteocyte 5
2.1.4 Osteoclast 6
2.2 Structure 7
2.2.1 Types of bone 9
2.2.2 Cortical 9
2.2.3 Cancellous 10
2.2.4 Comparison of cortical and cancellous bone 11
2.3 Function 11
2.3.1 Support and Protection 12
2.3.2 Minal storage 12
2.3.3 Production of blood cells 13
2.3.4 Movement 13
2.4 Factors influencing the mechanical properties of bone 13
2.4.1 Age 14
2.4.2 Gender 14
2.4.3 Diet 15
2.4.4 Loading 15
2.5 The need for bone replacement materials 16
2.5.1 Diseases and infections 16
2.5.2 Congenital disorders 18
2.5.3 Trauma 18
2.6 Bone grafting 19
2.6.1 Biological materials 20
2.6.2 Synthetic materials 23
2.6.3 Ideal graft material properties 28

Chapter 3 Calcium phosphate ceramics 29

3.1 Charaterisation of calcium phosphate ceramics 29
3.1.1 Struture 32
3.1.2 Porosity 32
3.1.3 Solubility 33
3.2 Hydroxyapatite 33
3.3 Tricalcium phosphate (TCP) 36

3.3.1 β-TCP 37
3.3.2 α-TCP 38
3.4 Biphasic calcium phosphate (BCP) 38
3.5 Commercially avaliable ceramics 39
3.6 Drawbacks of calcium phosphate ceramics 40

Chapter 4 Calcium phosphate cements 42

4.1 Advantages of CPC's 42
4.2 Hydroxyapatite 43
4.2.1 Chemistry of setting reactions 43
4.2.2 Setting properties 47
4.2.3 Rheological properties 50
4.2.4 Mechanical properties 52
4.2.5 *In-vitro* ageing 55
4.2.6 Clinical applications 57
4.3 Brushite 59
4.3.1 Chemistry of setting reactions 59
4.3.2 Setting properties 61
4.3.3 Rheological properties 63
4.3.4 Mechanical properties 64
4.3.5 *In-vitro* ageing 65
4.3.6 Clinical applications 66
4.4 Conclusions 67

Chapter 5 Formulation of a monetite based cement 69

5.1 Introduction 69
5.1.1 Problems with CPC's 69
5.1.2 Possible solutions 70
5.1.3 Aims 71
5.2 Materials and methods 73
5.2.1 Materials 73
5.2.2 Cement formulation 73
5.2.3 Cement paste stability and setting 74
5.2.4 Cement mechanical properties 74
5.2.5 Perfusion through the cement pastes 75
5.2.6 Cement composition 75
5.3 Results 77
5.3.1 Slow setting monetite cement 77
5.3.2 Comparing gelling agents 87
5.4 Discussion 92
5.5 Conclusions 98

Chapter 6 Controlled-setting cement pastes using polymer encapsulation 99

6.1 Introduction 99
6.1.1 Microencapsulation 99
6.1.2 Emulsions 102
6.1.3 Materials 103
6.1.4 Aims 105
6.2 Materials and methods 106
6.2.1 Production of microspheres 106
6.2.2 Release study 110
6.3 Results 112
6.3.1 Release from Eudragit® microspheres 112
6.3.2 Cement compostion 122
6.3.3 Storage of microsphere-cement pastes 127
6.3.4 Poly-caprolactone (PCL) microspheres 128
6.3.5 Mechanical properties of microsphere cements 131
6.4 Discussion 134
6.5 Conclusions 142

Chapter 7 Antimicrobial CPC matrices 143
7.1 Introduction 143
7.1.1 Aims 144
7.2 Materials and methods 145
7.2.1 Matrix Preparation 145
7.2.2 Sample elution 145
7.2.3 Microbiological activity assay 146
7.2.4 Mechaincal testing 147
7.2.5 Physicochemical charaterisation 147
7.3 Results 148
7.3.1 Comparisons of CPC's 148
7.3.2 Brushite cements 153
7.4 Discussion 164
7.5 Conclusions 170

Chapter 8 Degradation of calcium phosphate cements 171
8.1 Introduction 171
8.1.1 Problems with CPC's 171
8.1.2 Macroporosity of CPC's 172
8.1.3 Aims 173
8.2 Materials and methods 174
8.2.1 Materials 174
8.2.2 Calcium phosphate cement synthesis 174

8.2.3 Preperation of calcium-alginate beads 174
8.2.4 Macroporous cements 175
8.2.5 Mechanical studies 176
8.2.6 Charaterisation of macroporous cement schaffolds 176
8.2.7 Degradation 177
8.3 Results 178
8.3.1 Comparing CPC degradation 178
8.3.2 Addition of macroporosity 181
8.3.3 Long term degradation of brushite cements 185
8.4 Discussion 188
8.5 Conclusions 191

Chapter 9 Thesis conclusions 192

Chapter 10 Future work 195

Chapter 11 Appendices 197

Chapter 12 References 253

List of Figures

Figure 2.1: The processes of bone remodelling (Russell T.Turner & Jean D.Sibonga 2009). (A) Quiescent phase is when bone surface is inactive. Neither bone resorption nor bone formation is occurring on this region of bone surface; (B) Resorption phase where osteoclasts remove a discrete packet of bone, creating a cavity, a temporary weak spot or link; (C) Formation phase when osteoblasts form a bone matrix, which fills in the cavity (the cement line defines the boundary between the newly formed bone and the surface excavated by osteoclasts at the end of the resorption phase (B)); (D) Quiescent phase again the inactive bone surface, this time after a completed remodelling cycle (the new surface may be under filled (1), exactly filled (2), or overfilled (3), reflecting a local decrease, no change, or increase in bone mass, respectively). **7**

Figure 2.2: The hierarchical structure of bone (M.A.K.Liebschner & M.A.Wettergreen 2003). **8**

Figure 5.1: Image of spheres of the cement paste during immersion in PBS; (A) MCPM control cements (β-TCP + MCPM + water) and (B) MCPM cement paste (β-TCP + MCPM + glycerol). Images demonstrate the washout resistance of the paste formulations compared to the control samples; no visible degradation of the cement was evident. **78**

Figure 5.2: Scanning electron micrographs of cement fracture surfaces without (A) and with (B) the addition of sodium alginate and glycerol. The addition of the sodium alginate and glycerol resulted in a marked change in the morphology of the crystals within the cement matrix from predominantly blade-like to irregularly shape. **79**

Figure 5.3: Effect of storage, of the paste formulation (at 4 ºC) prior to setting, on the compressive strengths exhibited by the hardened material. **80**

Figure 5.4: SEM micrographs show microstructure of the fractured surface of the aged cement samples. Samples were aged for 90 days in total; here we can see the minimal effect on the microstructure of the monetite cements over the period of time. Sample A illustrates the sample at day 0; sample B at day 3; sample C at day 7; sample D at day 14; sample E at day 28 and sample F at day 90. **81**

Figure 5.5: A schematic diagram illustrating the sections of cement dissected from the hardened cement cylinder (A) following immersion in PBS for a period of 20 h and the crystalline phase composition of each corresponding layer (B). **83**

Figure 5.6: There was an upper limit on the distance that the methylene blue solution could perfuse the hardening cement paste, with samples of 10 and 15 mm in length being the only samples completely perfused (A), the rate of perfusion reduced significantly with time, showing that the cement hardening reaction provided a barrier to perfusion. B) Shows cement paste cylinders of 10, 20 and 30 mm of length following 9 days immersion in methylene blue solution. **84**

Figure 5.7: XRD results of the different layers of the cement paste sample. Layer 1 = outer most layer and layer 5 = inner most layer. The graph proves that the water-glycerol exchange is more efficient near the surface compared to the inner layer. The various peaks are indicative of the composition of the samples; ■ Monetite; ○ Brushite; ● β-tri-calcium phosphate (β-TCP); □ Monocalcium phosphate monohydrate (MCPM). **85**

Figure 5.8: Compares the diffraction patterns of the MCPM control cement (β-TCP + MCPM + water) (bottom) with the paste formulation before (middle) and after (top) the cement paste has hardened. The various peaks are indicative of the composition of the samples; ■ Monetite; ○ Brushite; ● β-tri-calcium phosphate (β-TCP); □ Monocalcium phosphate monohydrate (MCPM). **86**

Figure 5.9: Compares the diffraction patterns of the MCPM paste formulation (made using glycerol and alginate) with varying amounts of alginate. The various peaks are indicative of the composition of the samples; ■ Monetite; ○ Brushite; ● β-tri-calcium phosphate (β-TCP); □ Monocalcium phosphate monohydrate (MCPM). **87**

Figure 5.10: Effect of the variation in gelling agent of the paste formulation on the compressive strengths exhibited by the hardened material; all samples were prepared in the same manner. **89**

Figure 5.11: Compares the diffraction patterns of the MCPM control cement (β-TCP + MCPM + water) (bottom) with the paste formulation after the cement paste has hardened, using various different gelling agents. The various peaks are indicative of the composition of the samples; ■ Monetite; ○ Brushite; ● β-tri-calcium phosphate (β-TCP); □ Monocalcium phosphate monohydrate (MCPM). **90**

Figure 5.12: SEM micrographs show microstructure of the fractured surface of the different cement samples; each sample is composed using different gelling agent. Sample A illustrates the gelling agent Alginate; sample B uses Agarose; sample C uses Carrageenan; sample D uses Chitosan; sample E uses Gellan gum and sample F uses Gelatine. Here we can see the minimal effect on the microstructure of the monetite cements with varying the gelling agent. **91**

Figure 6.1: Typical forms of spherical microcapsules, which are made by various different methods, depending on the application. Matrix and single-wall are typically relatively easy to manufacture, compared to multi-wall and multi-core, which require more complex processing methods. **101**

Figure 6.2: The chemical structures of Eudragit RS 100 (A) and Eudragit S100 (B) (Reproduced from (Rohm Pharma 2003)). **105**

Figure 6.3: Illustration of the production of Microspheres by the solvent evaporation method using acetone/liquid paraffin system (Azarmi et al. 2002;Oth & Moδs 1989). **109**

Figure 6.4: The graph illustrates the cumulative release, in percentage, of OA released against time in hours, over an 8 h period at the different temperatures; at 37 ºC the thermo-sensitive polymer releases the encapsulated content; at 4 ºC the content should remain encapsulated. The graph illustrates the mean values of the data points from all the batches produced (error bars are also indicated). **113**

Figure 6.5: SEM micrographs of Eudragit S100 microspheres at 200 x magnifications (A) and (B). The morphology illustrated in the SEM micrographs clearly shows all of spheres to be broken. At 5,000 x magnifications (C) it can be seen that the microspheres do produce a hollow sphere, with a relatively smooth surface. Cracks or wrinkled-like surface of the microspheres may be attributed to the heat created by the high voltage of the electron beam. **114**

Figure 6.6: The graph illustrates the cumulative release, in percentage, of OA released against time in hours, over an 8 hour period at the different pH; at pH7.4 the pH-sensitive polymer released the encapsulated content; at pH 4 the content should remain encapsulated. The graph illustrates the mean values of the data points from all the batches produced (error bars are also indicated). **115**

Figure 6.7: Eudragit S100 prepared by solvent evaporation method using acetone/liquid paraffin system **(Figure 6.3)**. The micrograph shows the fragments of the microspheres, the fluffy flake-like structure created by this method does not allow the encapsulation of OA (A) and PPA (B). **116**

Figure 6.8: The graph illustrates the cumulative release in percentage of OA (A) and PPA (B) released against time in hours, at the different pHs; pH7 the pH-sensitive polymer releases the encapsulated content; at pH 4 the content should remain encapsulated, however results show total release of microsphere content. The graph illustrates the mean values of the data points from all the batches produced (error bars are also indicated). Eudragit S100 prepared by solvent evaporation method using acetone/liquid paraffin system **(Figure 6.3)**. **116**

Figure 6.9: (A) Eudragit® RL microspheres without any encapsulated acids. Microspheres were prepared by solvent evaporation method using acetone/liquid paraffin system (**Figure 6.3**). (B) and (C) Higher magnification of the microspheres to emphasize the binding of the microspheres. **117**

Figure 6.10: Eudragit® RL microspheres with OA (A and B) and PPA (C and D) encapsulated. Microspheres were prepared by solvent evaporation method (**Figure 6.3**). Micrographs show the difference in morphology of the two microspheres; with OA encapsulated the surface is smooth, with a porous interior structure; with the PPA the microspheres exhibited a porous surface, on closer inspection the interior was hollow (similar to the non encapsulated microspheres produced) or porous within the same batch. **118**

Figure 6.11: The graph illustrates the particle size distribution of the two microspheres produced; Eudragit S100 (A) and Eudragit RL (B), using the two different methods. **119**

Figure 6.12: Illustrates the cumulative release (%) of OA and PPA over, (A) 24 h period at 37 ºC; (B) OA and (C) PPA release over an 8 h period at the different temperatures; 37 ºC the thermo-sensitive polymer releases the encapsulated content; at 4 ºC the content remain encapsulated. Illustrating the mean values of the data points from all the batches produced (error bars are also indicated). **120**

Figure 6.13: Compares the diffraction patterns of the control cement (β-TCP + OA+ water) with the varying concentrations of OA paste formulations using microspheres staggered on top. The various peaks are indicative of the composition of the samples; ○ Brushite; ● β-tri-calcium phosphate (β-TCP). **122**

Figure 6.14: Compares the diffraction patterns of the control cement (β-TCP + OA (A) or PPA (B) + water) with the paste formulations using Eudragit RL microspheres with the encapsulated OA (A) or PPA (B). The various peaks are indicative of the composition of the samples; ○ Brushite; ● β-tri-calcium phosphate (β-TCP). **124**

Figure 6.15: **(**A) SEM micrographs of the fracture surface of the set cement produced using Eudragit RL microspheres to encapsulate the OA component (500 X magnified); (B) A higher magnification (1,000 X) of the cements needle-like microstructure; and (C) the surface of the cement at 1,500 X magnifications that shows both brushite crystals and Eudragit RL microspheres. Eudragit® RL microspheres were prepared by solvent evaporation method using acetone/liquid paraffin system **(Figure 6.3)**. **125**

Figure 6.16: **(**A) SEM micrographs of the fracture surface of the set cement produced using Eudragit RL microspheres to encapsulate the PPA component (500 X magnified); (B) A higher magnification (1,000 X) of the cements needle-like microstructure; and (C) the surface of the cement at 1,500 X magnifications that shows both brushite crystals and Eudragit RL microspheres fused together; small amounts of degraded polymer is visible, which appears to be fusing the brushite crystal together in some areas. Eudragit® RL microspheres were prepared by solvent evaporation method using acetone/liquid paraffin system **(Figure 6.3)**. **126**

Figures 6.17: The images show the effect of storage at 4 ºC with the use of microspheres S100 (A) and RL100 (B). **127**

Figures 6.18: Illustrates that similarity in the composition of the control pyrophosphate modified brushite cement (bottom) and the Eudragit encapsulated PPA cement after being in storage at 4 ºC for 90 days then; heated to 37 ºC to allow hardening (middle) and without being exposed to a change in the environment to allow hardening (top). The various peaks are indicative of the composition of the samples; ○ Brushite; ● β-tri-calcium phosphate (β-TCP). **128**

Figure 6.19: Shows the particle size distribution of the microspheres produced using PCL; the speed at which there were produced had a large effect on the PSD: 6,000 rpm (A); 3,000 rpm (B); 1,500 rpm (C); and 750 rpm (D). **129**

Figure 6.20: Shows the ESEM micrographs of the microspheres produced using PCL; (A) shows spectrum 1 – outer layer of the microsphere, (B) shows spectrum 2 – the inside of the microsphere, both relate to the EDS analysis in **Table 6.2**. **130**

Figure 6.21: The graph illustrates the cumulative release, in percentage, of PPA released against time in hours, for a total of 2 h at room temperature of 22 ºC the content should remain encapsulated, however, here the contrary is demonstrated. The graph illustrates the mean values of the data points from all the batches produced (error bars are also indicated). **131**

Figure 6.22: The graph illustrates the compressive strengths (A) of the cements compared to the relative porosities (B) at each homogeniser speed (750, 1500, 3000, 6000 rpm). **133**

Figure 7.1: The concentration of the drug in the eluent per day, of VH from the three cement matrices; two brushite based cements are compared to the traditional HA cement, with the MIC line. **148**

Figure 7.2: Illustration of the inhibition zone around the cements in both loaded and unloaded cement matrices (A); the digital images of the inhibition zones (B). **149**

Figure 7.3: SEM images of the microstructure of (A) typical brushite structure, illustrates needle-like thin ling crystals and (B) HA cement, characterised by flat densely packed crystals. **151**

Figure 7.4: Compares the diffraction patterns of the samples as shown in the SEM micrographs of the various cement formulations. The various peaks are indicative of the composition of the samples; ○ Brushite; ● β-tri-calcium phosphate (β-TCP); * Tetracalcium phosphate (TTCP), which remained in small amount in the HA cement (at 28˚ and 29˚ 2θ). **151**

Figure 7.5: FTIR spectra of the apatite cement and brushite cements (both OA and PPA brushite cements). The spectra of all CaP based materials indicated the presence of phosphate groups at the range of 1070-1140 cm $^{-1}$. In addition, the peak at 872 cm $^{-1}$ of the brushite cements was indicative of the presence of HPO_4^{2-} groups. **152**

Figure 7.6: Illustrates the concentration of the antibiotic – gentamicin sulphate and vancomycin hydrochloride released from the β-TCP + OA cement, stored in PBS with at an agitation of 100 spm at 37 °C over a period of 24 days. **154**

Figure 7.7: Illustrates the concentration of the antibiotic – gentamicin sulphate and vancomycin hydrochloride released from the β-TCP + PPA cement, stored in PBS with at an agitation of 100 spm at 37 °C over a period of 24 days. **155**

Figure 7.8: SEM images of the control OA cement sample; (A) illustrates small short brushite-like structure before and (B) demonstrates fused needle-like structures to create irregular globular structures, after being immersed in PBS for 24 days. **156**

Figure 7.9: SEM images of the control PPA cement sample; (A) exhibits obvious needle-like structures indicating presence of brushite, before and (B) illustrates irregular globular structures, after being immersed in PBS for 24 h. **156**

Figure 7.10: SEM images of the GS loaded OA cement sample; (A) before and (B) after being immersed in PBS for 24 days. Sharp defined fine need-like structures, 3–5 μm in length indicative of presence of brushite; no change in morphology indicated here. **157**

Figure 7.11: SEM images of the GS loaded PPA cement sample; (A) illustrates some brushite-like structure before and (B) demonstrates fused needle-like structures to create flat planes (10 μm in length), after being immersed in PBS for 24 days. **157**

Figure 7.12: SEM images of the VH loaded OA cement sample, (A) before and (B) after being immersed in PBS for 24 days. Smooth flat plates over 10 μm in length; slightly needle-like indicating presence of brushite with larger crystals; no change in morphology indicated. **158**

Figure 7.13: SEM images of the VH loaded PPA cement sample; (A) before and (B) after being immersed in PBS for 24 days. Sharp defined need-like structures, 3–7 μm in length indicative of presence of brushite; no change in morphology indicated here. **158**

Figure 7.14: Average inhibition zones produced by OA cements grown on; *S. aureus* samples, after 48 h at 37 °C **(A)** and *S. epidermidis* samples, after 48 h at 37 °C **(B)**. The control cement illustrates some low antimicrobial activity. **159**

Figure 7.15: Average inhibition zones produced by PPA cements grown on; *S. aureus* samples, after 48 h at 37 °C (A), and (B) average inhibition zones of *S. epidermidis* samples, after 48 h at 37 °C. The control cement illustrates some low antimicrobial activity. **159**

Figure 7.16: Images of the Inhibition Zones exhibited by GS **(A)** and VH **(B)** loaded OA cements compared with the inhibition zone produced by control OA cement **(C)**, which indicates that the control cement illustrates some low antimicrobial activity. **160**

Figure 7.17: Images of the Inhibition Zones exhibited by GS **(A)** and VH **(B)** loaded PPA cements compared with the inhibition zone produced by control PPA cement **(C)**, which indicates that the control cement illustrates some low antimicrobial activity. **161**

Figure 7.18: Inhibition Zones exhibited by the cements compared to the mass of cement samples placed in the centre of the lawn of culture; OA cement **(A)** and PPA cement **(B)**. **162**

Figure 8.1: Illustrates the set-up of the set up of the calcium alginate bead production by means of a digital image. The smaller image on the bottom left indicates the final alginate product. The alginate beads are dried and separated by size, due the variance in the production (obvious non-homogenous bead production). **175**

Figure 8.2: Graphs illustrate the degradation of cements over a period of 90 days. Two brushite cements were compared to the HA cement. **178**

Figure 8.3: SEM micrographs illustrate the microstructure of the cements investigated; HA cement (A), orthophosphate brushite cement (B) and pyrophosphate brushite cement (C). **180**

Figure 8.4: The influence of cement:bead mass ratio on the porosity contained within brushite cement and the compression strength exhibited by the hardened material. **182**

Figure 8.5: Illustrates the degradation profiles of macroporous and non-macroporous brushite cements. **183**

Figure 8.6: Compares the diffraction patterns of the control brushite cement (bottom) with and macroporous brushite cement (top). The various peaks are indicative of the composition of the samples; ○ Brushite; ● β-tri-calcium phosphate (β-TCP). **184**

Figure 8.7: A 3D reconstruction of the control brushite cement (A) with and macroporous brushite cement (B). **185**

Figure 8.8: Graphs illustrate the degradation of cements over a period of 730 days. No results were recorded for day 545 and 730, as the samples had degraded too far to be measured using the same conditions; most samples beyond days 365 remained in particulate form. **186**

Figure 8.9: Graphs illustrate the degradation of the non porous orthophosphate brushite cements over a period of 730 days (2 years). The graph is plotted using common logs to allow a clear view of the compressive strengths over this long period of time (n = 6). No results were recorded for day 545 and 730, as the samples had degraded too far to be measured using the same conditions; most samples beyond days 365 remained in particulate form. **187**

Figure 8.10: Graphs illustrate the degradation of cements over a period of 730 days. No results were recorded beyond day 340 (545 and 730), as the samples had degraded too far to be measured using the same conditions; most samples beyond days 365 remained in particulate form. Black plots demonstrate the PPA cement in PBS and the grey plot illustrates the degradation of PPA in serum solution. **187**

Figure A1.1: Illustration of the different types of strain for three forms of stress; compression, tension, and shear (van Eijden 2000). **200**

Figure A1.2: Compression Testing: the compressive forces (C) generate tensile forces (T) in the centre of the specimen acting perpendicular to the vertical axis. **201**

Figure A1.3: The Helium Pycnometer; automatic density analyzer that performs volume and density measurements. **204**

Figure A1.4: Schematic of Dynamic Vapour Sorption (Frank Thielmann & Daniel Burnett 2000). **205**

Figure A1.5: Schematic of the set up of the Micro CT. The sample is placed on a rotating platform; rotation angles can be set to sample specification. As the sample rotates an image is stored for 3D reconstruction using analysis software. **206**

Figure A1.6: X-ray diffraction. A beam of monochromatic X-rays penetrates the crystals of the sample and diffracts to produce a pattern unique to the crystal phases. **207**

Figure A1.7: A schematic illustration of the FTIR equipment set-up. **209**

Figure A1.8: Laser diffraction for measurements of particle size distribution. A laser beam hits the particle flow and diffracts in angles inversely proportional to the particle sizes. **210**

Figure A1.9: A schematic diagram of the SEM apparatus in a typical Joel 7000 SEM. **211**

Figure A2.1: Chemical arrangement of glycerol molecule (McGraw-Hill 2009). **213**

Figure A2.2: Structural illustration for alginates: (A) the monomers in alginate; (B) the alginate chain (Sriamornsak & Sungthongjeen 2007) **215**

Figure A2.3: Structure of Agarose (Normand *et al*. 2000). **216**

Figure A2.4: Schematic representation of the iota-carrageenan (top), kappa-carrageenan (middle), and lambda-carrageenan (bottom) (Serge *et al.* 2009) **217**

Figure A2.5: A schematic diagram of the chemical structure of Chitosan (http://170.107.206.70/drug_info/nmdrugprofiles/nutsupdrugs/chi_0067.shtml). **218**

Figure A2.6: A schematic diagram of the chemical structure Gellan gum (http://commons.wikimedia.org/wiki/File:Gellan_gum_structure.png) **219**

Figure A2.7: Hyaluronic Acid; D-glucuronic acid (left) and D-N-acetylglucosamine (right); (http://www.corgenixonline.com/ed_programs/Intro_to_HA.pdf). **219**

Figure A2.8: Gelatine (http://www.medsafe.govt.nz/Profs/datasheet/p/Prografcapinf.htm) **221**

Figure A2.9: Structure of HPMC; (http://images.chemnet.com/suppliers/chembase/190059_1.gif). **221**

Figure A3.1:A calibration curve for Vancomycin Hydrochloride. **222**

Figure A3.2:A calibration curve for Gentamicin Sulphate. **222**

List of Tables

Table 2.1: Summary of the currently available osteoconductive scaffolds (Giannoudis *et al.* 2005). **20**

Table 2.2: Summary of advantages and disadvantages of both autograft and allograft reconstruction (Amendola & Stolley 2009). **23**

Table 2.3: Mechanical properties of the synthetic graft materials compared to bone (Moore *et al.* 2001). **24**

Table 3.1: Physical properties of various phases of calcium phosphate bioceramics (K.De Groot & J.G.C.Wolke 1990;W.G.Billottee 2002). **30**

Table 3.2: Solubility and pH stability of different calcium phosphates phases (Guo & Li 2004). **31**

Table 3.3: Illustrates the commercialised CP ceramic materials on the market. **40**

Table 4.1: Summarizes the commercialised apatite based cement products with their composition details (Bohner *et al.* 2005) **58**

Table 4.2: Summarizes the commercialised brushite based cement products (Bohner *et al.* 2005). **67**

Table 5.1: The formulations, mechanical and setting properties of the CPCs investigated in this study. **78**

Table 5.2: The effect of the use of different gelling agents on the mechanical and setting properties of the CPCs investigated in this study **88**

Table 6.1: Compares and details the properties of the PCL used in this investigation. **106**

Table 6.2: Shows EDS results of the microspheres produced using PCL, with the table which shows the elements present. **129**

Table 7.1: A summary of the results obtained from the antimicrobial assays performed using the VH eluted from each cement sample. **150**

Table 7.2: Compares the average setting times and the UCS (MPa) for the cements formulated using β-TCP + OA with the addition of antibiotics (GS and VH). **153**

Table 7.3: Compares the average setting times and the UCS (MPa) for the cements formulated using β-TCP + PPA with the addition of antibiotics (GS and VH). **153**

Table 7.4: Average ultimate compression strengths of the cements before and after being placed in PBS for 24 days at an agitation of 100 spm at 37 °C. **163**

Table 8.1: Summarises the key properties of the cements; HA cement, orthophosphate brushite cement and pyrophosphate brushite cement. Comparing the porosity with the strength of the cements and how this affects the degradation rate. **181**

Table 8.2: Compares the composition of the macroporous brushite and non-macroporous brushite cement following immersion in daily refreshed PBS. **184**

Table A2.1: Properties of Degradable Natural Homopolymers that have been Utilization in the Fabrication of Tissue Engineering Scaffolds (Yoon & Fisher 2006). **214**

Chapter One

Introduction

Tissue engineering may be defined as the application of biological, chemical, and engineering principles toward the repair, restoration, or regeneration of living tissue by using biomaterials, cells, and growth factors alone or in combination. Today's world of orthopaedic biomaterials is expanding rapidly driven by ageing demographics, product advances, an increasing number of sport injuries and changing patient care strategies. Strategies to replace damaged bone have employed, such as stem cells, bone growth factors, gene therapy, synthetic bone fillers, implant coatings and various resorbable implantable materials.

At present, the autograft is the gold standard in bone grafting, as it provides an appropriate three-dimensional structure, physiology, associated biological components and an 80–90% success rate (Cook *et al.* 1994). Autografts, however, are not always an option as they are limited by the supply of available donor tissue and the threat of donor-site morbidity (Giannoudis *et al.* 2005). Allografts and synthetic bone graft substitutes are alternative bone grafting methods that are also currently employed (Amendola & Stolley 2009). While a certain amount of success has been achieved using these procedures, both are associated with drawbacks (Arrington *et al.* 1996). The threat of disease transmission and the difficulty of preserving graft bioactivity limit the success of allograft procedures (Friedlaender *et al.* 1999). Furthermore, neither synthetic bone graft substitutes nor allografts incorporate every aspect of natural tissue, such as osteoblastic precursor cells and growth factors, and are therefore unable to match the autograft.

Ceramic materials that are specially developed for use as medical and dental implants are termed bioceramics. They include alumina and zirconia, bioactive glasses, glass-ceramics, coatings and composites, hydroxyapatite and resorbable calcium phosphates, and radiotherapy glasses (Hench 1991). Bioceramics can have structural functions as joint or tissue replacements, can be used as coatings to improve the integration of metal implants, and can function as resorbable lattices which provide temporary structures and a framework that can be replaced by the body's natural healing processes.

The perfect material for medical applications would not only be compatible within the implanted site, but also have physical properties similar to those of the tissue being replaced or repaired. Although ceramics exhibit appropriate chemical and corrosion-resistant properties, they are notoriously brittle. Researchers therefore have required ways of combining desirable ceramics with other materials to tailor properties such as strength and elasticity to meet system requirements (Williams 1979). Composites, functionally gradient materials, and coatings have been studied to optimise material choices to produce solutions for the rapidly growing requirements in clinical applications including orthopaedics, otolaryngology, maxilla-facial and plastic surgery, oral surgery, periodontology, and tumour therapy. Since ceramic materials exhibit such brittle properties and are difficult to fabricate complex shapes, a subdivision of ceramics, cements are explored to be developed and used in place of traditional bioceramics materials.

Since one of the earliest reports of a calcium phosphate cement (CPC) formulation by Brown and Bhow (Brown & Chow 1985) there has been much progress in the development of CPCs. Hydroxyapatite (HA) cements have been used to facilitate adhesion of metal implants (Prado

Da Silva *et al.* 2001) and have also been used as bone graft replacements themselves (Barralet *et al.* 2002c;Charriere *et al.* 2003;Chung & Park 2007). HA has been the core focus in the development of CPCs over the past decade with ceramic materials for bone and dental replacements. However, in recent years other forms of CPC such as the brushite cement has been widely developed to meet the reported issues associated with HA cements. Brushite based cements have an important advantage over HA based cements in that they are sparingly soluble in physiological conditions and hence can be more extensively resorbed following implantation. Although work on brushite based cements means that the material can now be applied either as a putty or through a hypodermic needles, sets in an appropriate timeframe and can be inherently antibacterial, there are still several important drawbacks that mean that the material has not been widely taken up in the clinic. These include:

1. The metastability of brushite, which means that hydrolysis, may occur, resulting in long-term implant stability, as brushite is converted to HA.
2. The need for precise mixing in the operating theatre. Since material mixing and handling are critical to mechanical performance, deviations in the operating theatre may lead to an increased risk of implant failure.
3. An unpredictable degradation rate, meaning that it is difficult to ensure appropriate degradation in all patients.
4. A long-term risk of infection following implantation of the cement.

This thesis presents a collection of studies that aimed to address these shortcomings by modifying cement chemistry (Chapter 5), separating the reactive components of the cement mix using microencapsulation (Chapter 6), loading antibiotics into the cement matrices (Chapter 7), and by incorporating macroporosity using alginate beads (Chapter 8).

Chapter Two

Bone

Bone is a specialised type of connective tissue, characterised by the presence of cells in a hard and dense matrix. The matrix contains collagen, ground substance, and bone mineral. The bone mineral consists of complexes of calcium phosphates in amorphous and crystalline fractions (Horner 2004). The mineral components are approximately 30% amorphous calcium phosphate [$Ca_3(PO_4)_2$] and a little less than 70% nanocrystalline hydroxyapatite [$Ca_{10}(PO_4)_6(OH)_2$] (McTighe *et al.* 1995), which strengthens the whole structure. This chapter presents a concise review of the main functions of the bone, giving details of the structure and types of bone and their mechanical properties. Additionally, a summary of the existing synthetic grafts and the current clinical needs are also outlined.

2.1 Bone cells

The bone cells primarily responsible for the bone deposition and resorption are osteoblasts (bone forming) and osteoclasts (bone resorbing) (Katagiri & Takahashi 2002). Osteoclasts are multinucleated, giant cells derived by differentiation and fusion of haematopoietic cells of the monocyte macrophage lineage. Their bone degradation function depends on the organization of the actin cytoskeleton forming a cavity where protons and proteases degrade mineral and organic matrix, respectively. The relative activity of osteoclasts and osteoblasts determines how bone is remodelled (Kobayashi 2003), the biological process for the renewal of the bone tissue and maintenance of mechanical integrity, metabolic function and calcium homeostasis in healthy adults.

2.1.1 Osteoprogenitor

Osteoprogenitor cells are mesenchymal stem cells that differentiate into osteoblasts and osteocytes (Liu *et al.* 2003). They are immature progenitor cells, located in the periosteum and the bone marrow. Osteoprogenitors differentiate under the influence of growth factors; in particular the bone morphogenetic proteins (BMPs), which stimulate the division of osteoprogenitors and potentially increase osteogenesis, to form osteoblasts.

2.1.2 Osteoblast

Osteoblasts are responsible for bone matrix synthesis. They secrete a collagen rich substance essential for later mineralization of hydroxyapatite. The collagen fibres are organised to form osteoid; spiral fibres of bone matrix. Osteoblasts cause calcium salts to precipitate from the body fluids and bond with the newly formed osteoid to mineralize the bone tissue. Alkaline phosphatase (ALP) is present in high concentrations in osteoblasts and is secreted during osteoblastic activity. Osteoblasts have oestrogen receptors, which can promote the number of osteoblasts, therefore increasing collagen production (Sommerfeldt *et al.* 2001).

2.1.3 Osteocytes

About 90% of all cells of the human skeleton are osteocytes, which are the key in controlling the extracellular concentration of calcium and phosphate, and are directly stimulated by calcitonin and inhibited by the Parathyroid hormone (Vaananen 1996). Osteocytes are derived from osteoblasts and are basically osteoblasts surrounded by the products they secreted. Cytoplasmic processes of the osteocyte extend away from the cell toward other osteocytes in small channels called canaliculi; these enable exchange of nutrients and waste products to maintain the viability of the osteocyte.

2.1.4 Osteoclast

Osteoclasts are formed by the fusion of cells of the monocyte-macrophage cell line. The main feature of osteoclasts is their ability to resorb fully mineralized bone. The osteoclasts secrete growth factors, such as RANK ligand and M-CSF (Macrophage colony-stimulating factor), that stimulate osteoclast differentiation from mononuclear cells. The differentiation, recruitment and inhibition of osteoclasts are controlled by numerous hormonal and growth factors (Vaananen *et al.* 2000). Osteoclasts also express acid phosphatise, carbonic anhydrases, and secrete protons (H+), to degrade bone minerals and extracellular matrix.

Bone Remodelling

In bone remodelling , osteoclastic resorption occurs simultaneous with osteoblastic bone formation (Sommerfeldt *et al.* 2001). Active osteoclasts often have a fine brush-like border where they are in contact with the bone. In the process of bone resorption, the ground substance of bone appears to become modified prior to resorption by osteoclasts. During osteoclastic resorption, the bone marrow cavity is enlarged which leads to an overall reduction in bone tissue. Osteoclasts attach to the tissue surface and proliferate (Vaananen 1996). The renewal of bone is responsible for bone strength throughout our life (**Figure 2.1**). During childhood and the beginning of adulthood, bone becomes larger, heavier and denser; bone formation is favoured over bone resorption. There are several factors that can compromise balanced bone remodelling, such as disease, aging and injuries (O'Flaherty & Ellen 2000).

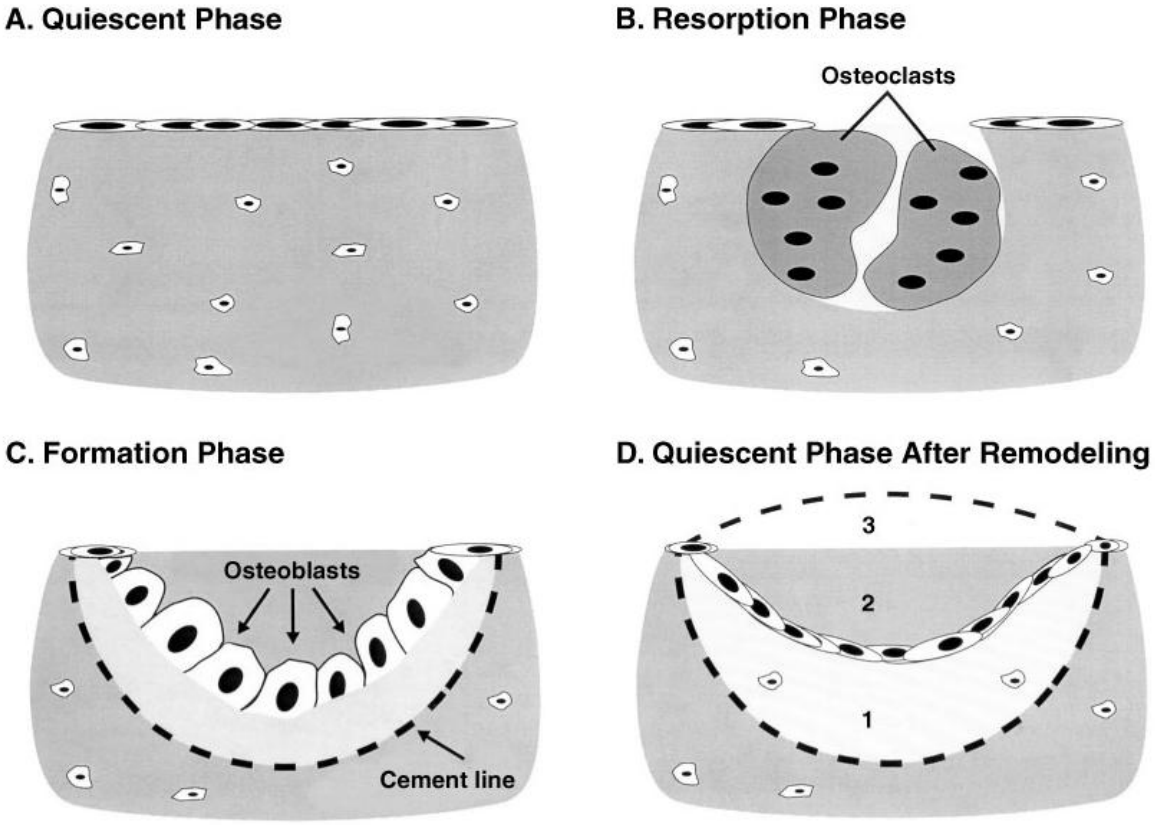

Figure 2.1: The processes of bone remodelling (Russell T.Turner & Jean D.Sibonga 2009). (A) Quiescent phase is when bone surface is inactive. Neither bone resorption nor bone formation is occurring on this region of bone surface; (B) Resorption phase where osteoclasts remove a discrete packet of bone, creating a cavity, a temporary weak spot or link; (C) Formation phase when osteoblasts form a bone matrix, which fills in the cavity (the cement line defines the boundary between the newly formed bone and the surface excavated by osteoclasts at the end of the resorption phase (B)); (D) Quiescent phase again the inactive bone surface, this time after a completed remodelling cycle (the new surface may be under filled (1), exactly filled (2), or overfilled (3), reflecting a local decrease, no change, or increase in bone mass, respectively).

2.2 Structure

Bone is a composite material that exists on at least 5 hierarchical levels (**Figure 2.2**): whole bone, architecture, tissue, lamellar, and ultrastructure (Liebschner & Wettergreen 2003). The macrostructure is the overall shape of the bone, i.e. the Femur; the macrostructure level can dimensionally measure approximately 3–750 mm and is composed of the architectural level, which contains the microstructure that defines the spatial distribution of the bone. The

architectural level can measure from 75–200 µm in cancellous bone and 100–300 µm in cortical bone. Beneath the architectural level is the tissue level, which is inherent to the actual material properties of bone; this level can, in the case of cancellous and cortical bone measure from 20–75 µm and 20–100 µm, respectively. The lamellar level is below the tissue level and is composed of the sheets of collagen and minerals deposited by osteoblasts (Majeska 2001). At the lamellar level for both cancellous and cortical bone the typical measurements of the structure are between 1–20 µm. The final level is the ultrastructural level which incorporates chemical and quantum interactions (van der Linden *et al.* 2001), which can be measure 0.06–0.4 µm for cancellous bone and 0.06–0.6 µm for cortical bone.

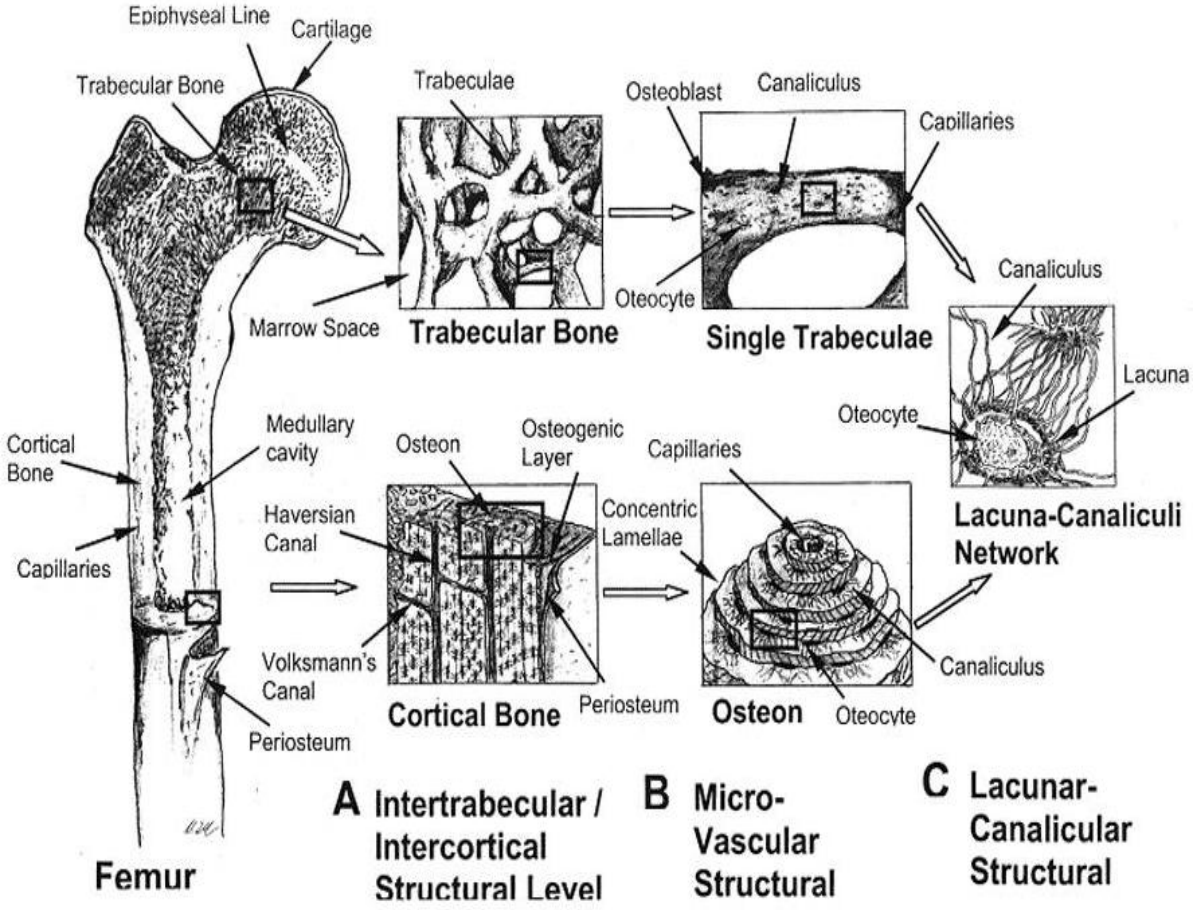

Figure 2.2: The hierarchical structure of bone (Liebschner & Wettergreen 2003).

2.2.1 Types of bone

Bone is categorized into 2 types: cortical (compact) bone and cancellous (trabecular) bone. Although both bone types are composed of the same materials, each one contains different proportions of the organic and inorganic materials, degree of porosity and organization. Furthermore, the combination of cortical and cancellous bone varies according to the location in the body, which is dependent on the applied mechanical loading. Various bone tissue types have different mechanical characteristics that regulate calcium phosphate levels to bear various combinations of the loading modes: tensile, compressive, bending and torsion (Ho 2005). Both cortical and cancellous bones display time dependent mechanical behaviour, as well as damage susceptibility during cyclic loading (Rho *et al.* 1998).

The architecture of bone can be described in two ways: woven and lamellar. Woven bone structure exists in newborns, callus, and metaphyseal regions. It is characterised by a fast growth rate, is very coarse tissue with no uniform collagen orientation and may slowly grow into a lamellar structure. Lamellar bone is slowly formed and highly oriented tissue. Each layer of lamellar bone is embedded with differently oriented collagen. Close to 100% of normal adult bone is lamellar bone (Sikavitsas *et al.* 2001).

2.2.2 Cortical bone

The main structures in cortical bone are the osteon, Haversian canal and interstitial lamella. The Haversian canal contains nerves and blood vessels that transport blood and nutrients to cells, and is surrounded by the cancellous bone. Each osteon is about 20 μm in diameter and located less than 100 μm away from the central blood supply. Therefore, osteons always lie along the Haversian canal; they may branch out and interlock with each other. The interstitial

lamella consists of collagen fibres surrounded by a mineralised matrix. The lamella is continuous with the osteons but is not adjacent to any haversian canal (Mohsin *et al.* 2006). Cortical bone is a dense structure with a porosity ranging between 5–10%. It is primarily found in the shaft of long bones and forms the outer shell around trabecular bone at the end of joints and the vertebrae. Cortical bone is roughly four times the mass of trabecular bone (Augat & Schorlemmer 2006) and contributes significantly to the mechanical strength of bone (Wachter *et al.* 2002). Typically, exhibiting compressive strength of up to 200 MPa and a tensile strength of approximately 130 MPa (Patka *et al.* 1995), when tested longitudinally to the osteons; these values are reduced by approximately half when tested transversely to the long axis of the osteons (Natali & Meroi 1989).

2.2.3 Cancellous bone

Cancellous bone has a spongy or porous nature, found at the ends of all long bones and found within flat and irregular bones, such as the sternum, pelvis, and spine (Keaveny *et al.* 2001). Mainly composed of the interstitial lamellae with small cavities of bone cells called lacunae at the boundaries, and is always surrounded by cortical bone. The microstructural trabeculae that make up the cancellous bone are composed of trabecular tissue material, which is a three dimensional interconnected open porous space, resulting in a cellular solid type of material. The microstructure is typically oriented so that there is a "grain" direction along which mechanical stiffness and strength are greatest. This microstructural directionality gives cancellous bone anisotropy of mechanical properties (Choi & Goldstein 1992). The porosity of cancellous bone ranges from 30–90% with pores containing bone marrow. Cancellous bone is rather weaker then cortical bone, with compressive strength of approximately 1.5–50

MPa and tensile strength of approximately 3–20 MPa; cancellous bone has a high specific impact resistance and due to a higher porosity is considerably lighter (Carter & Hayes 1977).

2.2.4 Comparison of cortical and cancellous bone

The mechanical properties of human cortical bone from the tibia, femur, and humerus have been found to vary between individuals, although the density may remain the same (Augat & Schorlemmer 2006). The cortical bone has less regional heterogeneity compared to the cancellous bone, therefore, the bulk mechanical properties of cortical bones are quite reliable even when comparing various regions of the body (van Eijden 2000). Comparatively, the bulk mechanical properties of cancellous bone have a rather broad range and have shown to vary by a factor of 2–5 MPa from bone to bone (Rho *et al.* 1998). Since the proportion of cortical and cancellous tissue of each bone varies with their shape and mechanical function, the properties of bone in each region cannot be adequately expressed in single values (Goldstein 1987). The elastic moduli in the longitudinal direction were not very different between the various types of cortical bone (Choi *et al.* 1990). The elastic moduli in the radial direction tend to be much lower than the longitudinal direction. In human cancellous bone, mechanical properties vary significantly around the periphery and along the length (Rho *et al.* 1995). However, there is no difference in the mechanical properties of the humerus, the proximal tibia, and the lumbar vertebrae (van Eijden 2000).

2.3 Function

Bone is an incredibly specialised tissue, having several specialised functions. Many of the key functions are discussed in detail in this section. The function of the bone is to provide a framework for the body. Apart from the primary function of providing mechanical support

for movement, the bone also has the marrow where the blood cells are synthesized. Another key function is maintaining calcium homeostasis in the body and also enabling storage of minerals like calcium, phosphorus, and many more. Additionally, bone remodelling is an essential function, this renews and maintains bone health and is involved in growth and development.

2.3.1 Support and Protection

The skeleton acts as a framework for the body; this scaffold-like structure allows the muscles to attach to them for support. This frame defines the basic shape of the body. The human body has many vital organs, which require a certain level of protection from damage by daily trauma. Bone provides protection; the skull protects the brain; the ribs shield the heart and lungs; the vertebrae protect the spinal cord and the pelvis provides protection to portions of the digestive tract (Martini 2001).

2.3.2 Mineral storage

Bone serves as a vast reservoir of calcium; this aids in the homeostasis of bodily fluids. Stimulating net resorption of bone mineral releases calcium and phosphate into blood and suppressing this effect allows calcium to be deposited in bone. Calcitonin is a hormone that functions to reduce blood calcium levels (Talmage *et al.* 1980). It is secreted in response to hypercalcaemia and effects include; (1) suppressed renal tubular and re-absorption of calcium, which increases excretion of calcium into urine; and (2) inhibits osteoclastic activity (bone resorption), which would minimise fluxes of calcium from bone into blood. To counteract this effect when the calcium concentration of bodily fluid is reduced, the release of

parathyroid hormone (PTH) causes an increase in osteoclastic activity resulting in bone resorption and an increase in the calcium levels in bodily fluids (Kurbel *et al.* 2003).

2.3.3 Production of blood cells

Bone marrow is the flexible tissue found in the hollow interior of bones; there are two types of bone marrow. Red marrow consists of connective tissue (stroma) in which exist haemopoetic stem cells and produces the components of blood such as, red blood cells, platelets and most white blood cells (Moghimi 1995). This type of marrow is found mainly in the flat bones, such as the hip bone, sturnum, skull, ribs, vertebrae and shoulder blades, and in the cancellous material at the epiphyseal ends of the long bones such as the femur and humerus. At birth, all bone marrow is red, with age it isconverted to yellow marrow, yet half of adult bone marrow remains as red marrow (Gurevitch *et al.* 2007). Yellow marrow consists of connective tissue containing fat cells and is used as an energy store, which is found in the hollow interior of the middle portion of long bones (Petrakis 1966).

2.3.4 Movement

Bones are connected by joints, attached to muscles via tendons which allow complex movements. As the muscles contract and relax, the complex movements are developed and the body is able to control each movement precisely.

2.4 Factors influencing the mechanical properties of bone

Bone's mechanical properties depend on the structure and microstructure of the bone. Bone has a variety of features that contribute to its resistance to fracture, such as the structural properties of bone which include; thickness and cross-sectional area, but microstructural

properties such as porosity, crystallinity or microcracks also contribute to bone's mechanical integrity (Augat & Schorlemmer 2006). Bone is a damageable, viscoelastic composite and most of all a living material capable of self-repair and therefore exhibits a complex range of mechanical properties. Variables such as race, age, gender, location of the bone and the level of activity of the patient, all lead to a variation in the mechanical properties of bone (Strube *et al.* 2008).

2.4.1 Age

Mineralisation of bone also has a marked effect on the mechanical properties of bone with age. In young bone the hydroxyapatite to collagen ratio of the bone increases so strengthening the bone; the hydroxyapatite to collagen ratio continues increasing until bone is hypermineralised (Zioupos *et al.* 2000). However, once hypermineralisation is reached the bone weakens due to increase in mature crystals which are more brittle. The bone turnover rate is significantly affected with ageing which is about 5% per decade for individuals 30 years of age and is about 25% per decade for individuals 60 years of age (O'Flaherty & Ellen 2000). A high bone turnover rate can lead to a reduction of bone strength and increased fracture risk.

2.4.2 Gender

In post-menopausal women, as their age increases their bone density decreases at a faster rate than other individuals, resulting in osteoporosis and an increase of fracture risk. A study was carried out on cortical thickness which demonstrated that thickness is similar in males and females because endocortical apposition in females contributes to final cortical thickness, even though earlier completion of longitudinal growth and earlier inhibition of periosteal

apposition produces a smaller bone in females (Seeman 2008). A study on children and adolescents showed that in individuals younger than 17 years, the rate of bone mineral density accumulation in the post anterior spine is more rapid in females than in males, whereas in individuals older than 19 years, the reverse was found. Additionally, in children younger than 14 years, bone mineral density measurements taken from the lateral spine, the neck of the femur, and the total hip, correlated with age similarly in both genders (Wu *et al.* 2005).

2.4.3 Diet

The food we consume has a great affect on the bone density and therefore the strength of the bones. The lack of calcium and vitamins (particularly D_3) result in a low bone mineral density due to the inability of the osteoblast to cause mineralisation. This leads to the reduction in the hydroxyapatite to collagen ratio, consequently reducing the strength of bone.

2.4.4 Loading

Loading is required for bone integrity; the absence of continual loading results in resorption by cortical thinning. Hypertrophy is a result of overloading, resulting in a deposition of the mineral phase on the periosteal surface. Several authors conducted animal studies to demonstrate the effect of loading (Kodama *et al.* 1999;Yingling *et al.* 2001); generally concluding that cyclic loading has a significant effect on the bone mineral density. Another study on the effects of loading demonstrated that the cross sectional area of professional tennis players arms had increased by over 39% when comparing the playing arm with the non-playing arm (Jones *et al.* 1977). A more recent animal study demonstrated exercised sheep with elevated estradiol levels (hormone derived from cholesterol; represents oestrogen in humans). The *in vivo* variation in estradiol level alters osteoblast sensitivity to exercise

induced sheep, affecting cortical bone responses to mechanical loading (Devlin & Lieberman 2007). Exercised sheep exhibited higher level of estradiol (levels increased by; 27% in femur, 6% in tibia and 14% in metatarsal).

2.5 The need for bone replacement

An imbalance in formation and resorption of bone may be involved in bone rescue after injury or disease. However, bone has a limited capacity to recover and the missing bone must often be supplied as a biomaterial (Beaman *et al.* 2006). Interactions between the bone replacement material and bone cells determines the success or failure of the repair process (Logeart-Avramoglou *et al.* 2005).

2.5.1 Diseases and Infections

Many diseases can occur leading to the removal or replacement of the natural bone; this section will outline some of these common diseases, infections and congenital disorders.

Osteoporosis

Osteoporosis is a common skeletal disease that may cause severe bone loss and may result in fractures of the vertebra, hip and mandible; most common among the elderly. In osteoporosis the bone mineral density is reduced, bone microarchitecture is disrupted, and the amount and variety of non-collagenous proteins in bone is altered (Rico 1997). The underlying mechanism in all cases of osteoporosis is an imbalance between bone resorption and formation. The three main mechanisms by which osteoporosis develop are; an inadequate peak bone mass (the skeleton develops insufficient mass and strength during growth), excessive bone resorption and inadequate formation of new bone during remodelling (Raisz

2005). The consequence of these three mechanisms underlies the development of fragile bone tissue. Hormonal factors strongly determine the rate of bone resorption; lack of oestrogen increases bone resorption as well as decreasing the deposition of new bone that normally takes place in load-bearing bones (Lee *et al.* 2003). In addition to oestrogen, calcium metabolism plays a significant role in bone turnover, and deficiency of calcium and vitamin D leads to impaired bone deposition. In addition, the parathyroid glands react to low calcium levels by secreting Parathyroid Hormone, which increases bone resorption to ensure sufficient calcium in the blood (Raisz 2005;Kurbel *et al.* 2003). Osteoporosis is most common in women after menopause (Riggs *et al.* 1982;Raisz 2005), but may also develop in men, and in anyone with particular hormonal disorders and other chronic diseases or as a result of medications. Osteoporosis occurs in 20% of people over the age of 70 years and in 16% of postmenopausal women (Dickenson *et al.* 1981).

Osteomyelitis

Osteomyelitis is a bacterial infection of bone and bone marrow in which the resulting inflammation can lead to a reduction of blood supply to the bone. The infection may be localized or it may spread through the periosteum, cortex, marrow, and cancellous tissue and tends to occur near the joints of the limbs (Lew & Waldvogel 2004b). The cause of infection may be due to an open injury to the bone, e.g. open fracture with bone ends piercing the skin. A minor trauma can lead to a blood clot around the bone, cutting off the blood supply to that area. Infection, such as urinary tract infections may lead to bacteria in the bloodstream, which can be deposited in a localized area causing bacterial site growth due to the destruction of bone. The infection can be acute, sudden, and rapidly worsening; or can be chronic, over a long period of time, and not easily resolved (Ratner 1996). Bacteria or fungus is often

responsible for Osteomyelitis causing pus to be produced within the infected bone, which may result in an abscess, depriving the bone of its blood supply (Ellis & O'Brien 1974). The organisms involved are dependent on how the infection was caused, for example, with haematogenous osteomyelitis the infectious agents include; *S. aureus*, Enterobacteriacae organisms, group A and B *Streptococcus* species, and *H. influenza* (Lew & Waldvogel 2004b). In chronic infections, the site of infection may be surgically treated by the removal of dead bone tissue. Spaces left by the removed bone tissue are filled with bone graft or by packing material to promote the growth of new bone tissue.

2.5.2 Congenital disorders

Cleft lip (cheiloschisis) and cleft palate (palatoschisis) are the two main types of clefting congenital deformity caused by abnormal facial development during gestation. A cleft is a split or opening in the uvula; it is the failure of fusion of the body's natural structures that form before birth. A cleft lip or palate can be successfully treated with surgery soon after birth. The hole in the roof of the mouth caused by a cleft connects the mouth directly to the nasal cavity. Cleft lips or palates occur in somewhere between 1 in 600–800 births worldwide (Yavuzer & Jackson 2001). Possible treatment options include speech therapy, prosthetics, augmentation of the posterior pharyngeal wall, lengthening of the palate, and surgical procedures (Sloan 2000).

2.5.3 Trauma

Traumas are severe injuries which cause excessive damage to bodily tissues. In the case of severe trauma bone grafts are used to prevent deformity and restore function, as bone can be broken or damaged which often needs repairing or removal. Motor accidents are the single

most common source of bone trauma, small numbers of falls and personal accidents also account for bone trauma; however these are more common in older or osteoporotic patients. Orthopaedic trauma surgery requires the regular use of bone grafts to help promote appropriate healing of musculoskeletal injuries (De Long *et al.* 2007).

2.6 Bone grafting

Bone is the second most common replaced tissue in the body, after blood. On average annually, there are over 2.2 million bone graft procedures worldwide (Lewandrowski *et al.* 2000). Bone grafts are used to provide structural stability and to stimulate osteogenesis and bone healing in fractures (ADA Division of Science 2002). Bone grafting materials are osteoconductive or osteoinductive (Giannoudis *et al.* 2005). In osteoconduction, the graft acts as a scaffold for the deposition of new bone, facilitating the formation of blood vessels and Haversian systems into the bone scaffold. In osteoinduction, the graft actively stimulates the stem cells from the surrounding tissues to differentiate into osteoblasts to form new bone (Rose & Rosenberg 2001). Osteointegration is also another essential element of bone regeneration; this is the extent to which the host bone bonds to the grafting material.

There are a large number of commercially available bone graft alternatives for orthopaedic applications. These vary in composition, mechanism of action and characteristics. **Table 2.1** demonstrates some of the types of grafts currently in use. However, only 10% of the procedures use synthetic materials because the approved synthetic grafts are considered to be inferior to the use of autograft or allograft (Lewandrowski *et al.* 2000). Conversely, as more research seeks for grafting materials that can provide better osteogenesis, osteoinduction and osteoconduction characteristics, combined with the shortage in biological grafts synthetic

materials for bone replacements expand in all fields of orthopaedics, neurosurgery and dentistry (Cook *et al.* 1995).

Table 2.1: Summary of the currently available osteoconductive scaffolds (Giannoudis *et al.* 2005).

Types	Graft	Advantages
Bone	***Autograft***	Gold standard
	Allograft	Available in many forms
Biomaterials	***DBM (demineralised bone matrix)***	Supplies osteoinductive BMP's, bone graft extender
	Collagen	Good delivery vehicle system
Ceramics	***TCP (tricalcium phosphate), Hydroxyapatite***	Biologically compatible with surrounding tissue
	CPC (calcium phosphate cements)	Some initial structural support
Composite grafts	***β-TCP/BMA (bone marrow aspirate) composite***	Ample supply
	BMP (bone morphogenetic protein)/synthetic composite	Potentially limitless supply

2.6.1 Biological materials

Natural bone tissue may be crushed into powder and placed around a fracture or a fusion site. One of the advantages of using natural materials is that they do not present the problem of toxicity and may carry specific protein binding sites to assist bone healing and integration. An ideal bone graft material should possess four elements: (1) osteogenic cells that allow the

growth of the various stages of bone regeneration, (2) an osteoconductive matrix that provides a scaffold for bone ingrowth, (3) osteoinductive factors that can stimulate osteoprogenitor cells to differentiate into osteoblasts, and (4) structural integrity that can sustain the mechanical loading *in situ*. There are three commonly used biological bone graft materials: autograft, allograft and xenograft (Beaman *et al.* 2006).

Autograft

The use of autologous bone is the "gold standard" for augmentation of bone healing and repair. It is the process of taking bone from the patients's own body; it can be classified as either vascularised or nonvascularised (Schimandle & Boden 1997a). Currently autografts are the most successful graft material available; advantages include the capability of immediate bone formation, ease of incorporation and lack of risk of disease transmission. One of the greatest advantages with these grafts means that the vascularised grafts retain their existing network of nutrient blood vessels which allow immediate adaptation of the bone graft with the implant by providing an instant and intact blood supply. However, autograft harvesting is associated with a complication rate of 8.5–20% including haematoma formation, blood loss, nerve injury, hernia formation, infection, arterial injury, urethral injury, fracture, pelvic instability, cosmetic defects, tumour transplantation, and sometimes chronic pain at the donor site (Giannoudis *et al.* 2005). Autografts are not viable for patients with severe bone damage that require a large amount of bone graft material. Another major drawback to this form of transplant is that the surgical harvesting of vascularised autograft is very time consuming, extremely invasive and can create significant morbidity at the donor site (Vail & Urbaniak 1996).

Allograft

Allograft bone is transplanted from one person to another and is most commonly used as an alternative for autograft bone in spinal fusion surgery (Schimandle & Boden 1997a). The use of allograft bone has been expanding in the last decade as a result of improved methods, preparation and storage, technical advances in surgical methods, and the need to avoid donor site complications associated with using autograft (Giannoudis *et al.* 2005). While allografts are versatile and widely used, especially in spinal surgeries, concerns exist regarding their ability to consistently achieve a successful fusion and the possibility of infectious disease transmission, for example, HIV, Hep B and Hep C (Arrington *et al.* 1996). Allograft has a high infection rate up to 10–12% and more than 80% of infected allografts are associated with clinical failure (Vaccaro *et al.* 2005). Allograft is prepared in fresh, frozen or freeze-dried forms, cortical or cancellous. Fresh allografts are not often used as they might create an immune response or transmit diseases (Friedlaender *et al.* 1999). On the other hand frozen and freeze-dried allograft are more osteoconductive but are considered to have weak osteoinductive capabilities compared with fresh allograft.

Comparison of autografts and allografts

There are several advantages and disadvantages of both autografts and allografts; **Table 2.2** illustrates these. Although 90% of all graft materials used for the replacement of bone tissue is autografts or allografts, these replacement materials posses many disadvantages. This is one of the many stimuli for the research in the development of synthetic bone replacement materials to address and overcome the downfalls of auto/allograft bone exhibit.

Table 2.2: Summary of advantages and disadvantages of both autograft and allograft reconstruction (Amendola & Stolley 2009).

Autograft		**Allograft**	
Advantages	***Disadvantages***	***Advantages***	***Disadvantages***
Minimal risk of infection and disease transmission	Donor-site morbidity	No donor-site morbidity	Possible risk of infection and disease transmission
Improved biologic healing and incorporation	Increased surgical morbidity and complications of graft harvest	Decreased surgical morbidity (time, incisions)	Immunologic response to the allograft
Decreased cost	Increased postoperative pain	Variable grafts (variety of areas can be harvested)	Increased cost
Improved ability to return to pre-implant health of tissue/ functional ablity	Increased recovery time	Decreased postoperative pain and recovery time	Delayed healing and graft incorporation

2.6.2 Synthetic materials

Considerable advances have been made with synthetic alternative materials for bone grafts over the last 30 years. Until recently, synthetics were not in favour compared to autografts and allografts. Synthetic bone grafts at most possess only two of the four characteristics of an ideal bone graft material (osteointegration, osteoconduction). Ideally synthetic bone graft substitutes should be compatible within the host by showing minimal fibrotic reaction, undergo remodelling and support new bone formation. From a mechanical point of view synthetic bone substitutes should have similar strength to that of the bone being replaced. This needs to be matched with a similar modulus of elasticity to that of bone in an attempt to

prevent stress shielding as well as maintaining adequate toughness to prevent fatigue fracture under cyclic loading. Research continues to seek suitable synthetic biodegradable polymers, ceramics, cements and metals to replace the "gold standard" autograft material. The common materials of interest are discussed here; mainly polymers and ceramics.

Table 2.3: Mechanical properties of the synthetic graft materials compared to bone (Moore *et al.*2001).

Material	Fracture Toughness (K1c)	Elastic Modulus (GPa)	Tensile Strength (MPa)
Cancellous Bone	0.1	1	3
Cortical Bone	6.0	15	151
HA	1.0	85	80
Bioglass	0.6	35	42
Glass ceramic – apatite-wollstonite	2.0	118	215
Bioglass – modified with polysulphone	1.2	5	103

Polymethylmethacrylate (PMMA)

PMMA is a commonly used non-degradable polymer in medical devices. It is a self curing material through the polymerisation of methylmethacrylate within a short time, which consists of repeating homologous chains of methylmethacrylate monomer. Through the chemical manipulation of these properties and modification of the polymer, controlled behaviour variations of this material can be achieved. PMMA is typically used as a filler material (bone cement) for joint replacement surgical procedures. It was originally developed for making

dentures; then in 1950s it was also found to be suitable for stabilizing prostheses, and is still used in over 80% of hip and over 90% of knee replacements (Ramakrishna *et al.* 2001).

Medical grade PMMA preparation necessitates manufacturing conditions limited to the clinical situation, which includes lower curing temperatures and pressurization more suitable to *in vivo* applications. When PMMA bone cement cures *in situ*, volumetric shrinkage of PMMA due to density changes has been calculated and experimentally verified to be between 5–7% depending on the type of cement and mixing method (Roques *et al.* 2004). It was also noted that shrinkage of the polymerising cement *in vivo*, might result in the development of porosity, both at the bone-cement and cement-implant in cemented hip replacements (Gilbert *et al.* 2000). The stresses from the shrinkage of PMMA cement may lead to reduced fatigue life of the implant.

Biodegradable polymers

Biodegradable polymers are materials that will eventually be resorbed and metabolised after being introduced into a living organism. No additional surgery is required to remove the implanted material. Biodegradable polymers are used as temporary scaffolds for biomechanical and biochemical support. As new tissue begins to grow within the implantation site, these materials are intended to degrade and leave behind the regenerated tissue.

Poly(DL-lactide-co-glycolide) (PLGA) is a biodegradable polymer. This polymer consists of two monomers: polyglycolide (PGA) and poly-lactide (PLA) from the poly(s-hydroxyl acids). These polymers have been investigated as porous scaffolds for replacement and regeneration

of a variety of tissues and fixation devices for orthopaedic applications (Seal *et al.* 2001;Soriano & Evora 2000;Yao *et al.* 2005). PLA is more hydrophobic and less crystalline than PGA and degrades with a lower degradation rate. The degradation rate of PLGA can thus be easily adjusted by altering the ratio of the two monomers in the formulation. In orthopaedic applications the co-polymer can be exploited to create materials that degrade in concert with bone in-growth. Additionally, porous PLGA is known to support osteoblast migration and proliferation, a necessity for bone tissue regeneration (Soriano & Evora 2000;Wang 2003). However, such polymers on their own are too weak to be used in load bearing situations.

Ceramics

Research in the field of ceramic materials has been widely increasing in the past 50 years for various medical applications, such as hip or knee prosthesis, cardiac valves and dental implants. The bioactive property of ceramic materials has driven most interest in the field of hard tissue replacement. Ceramics provide fixation by osteointegration of the local tissue into the implant pores, or onto the implant surface (Hench 1998b;Hench 1998a).

Commercially common ceramics include; alumina and zirconia, which demonstrate inert nature, which was the driving force for the popularity of their use in biomaterial applications. Alumina increased in popularity due to its loading bearing properties; clinically used as hip prostheses and dental implants because of its combination of excellent corrosion resistance, good *in vivo* compatibility, high wear resistance and high strength (Hench 1991).

Bioactive glasses and glass-ceramics demonstrate bioactive properties, which mean that they are able to bond with bone tissue; ceramics vary in bioactivity, for example some materials are able to bone to both soft and hard tissue. The first bioactive glasses were composed of SiO_2, Na_2O, CaO and P_2O_5 (reported by Hench in 1970's). Upon implantation the surface is modified to form a biologically active hydroxycarbonate apatite (HCA) layer, providing a bonding interface with the tissue (Hench 1991); this bonding present adhesion to the extent that resists considerable mechanical forces.

A number of biodegradable osteoconductive calcium phosphate ceramic bone graft substitutes have received attention as alternatives to autogenous bone but have been used solely as osteoconductive bone graft matrices. Ceramics have the advantage of being compatible with the new bone remodelling process required to attain optimal mechanical strength. A non-resorbable graft material may hinder remodelling and prolong the strength deficiency of new bone, as well as leave permanent stress risers in the fusion mass (Ohura *et al.* 1996). Most calcium phosphate ceramics used in spinal surgeries are synthetic and are composed of hydroxyapatite ($Ca_{10}(PO_4)_6(OH)_2$; HA), tri-calcium phosphate ($Ca_3(PO_4)_2$; TCP), or a combination of the two. These biomaterials are produced commercially as porous or non-porous implants and granular particles with pores and are created with the use of a high-temperature process called sintering along with high-pressure compaction techniques. Calcium phosphate ceramics and their clinical applications are discussed in more detail in chapter 3.

For synthetic implants to function *in vivo*, they must have certain properties: (1) compatibility with surrounding tissues, (2) chemical stability in body fluids, (3) compatibility of mechanical

and physical properties, (4) ability to be fabricated into functional shapes, (5) ability to withstand the sterilisation process, (6) reasonable cost of manufacturing, and (7) reliable quality control. Calcium phosphate ceramics exhibit these properties (Buser *et al.* 1991;Z.Schwartz *et al.* 1996) and have been used successfully as bone graft substitutes in dentistry and maxillofacial surgery, in both animals and humans (Klawitter *et al.* 1977;Lee *et al.* 1976;Nishimura *et al.* 1993;Schimandle & Boden 1997b;Vaughan 1996).

2.6.3 Ideal graft material properties

Ideally, a newly designed bone graft substitute should act as bone filling material that initially provides space filling with dimensional stability and appropriate porosity in a bone defect. The material should then provide an osteoconductive network that degrades at a rate appropriate to bone recovery. Two major concerns in the development of biomaterials are: (1) the material must not impinge on its host (the surrounding biological systems) and (2) in return, the material must not be affected adversely by its host. It is therefore essential to have a good understanding of biological systems prior to developing new biomaterials.

Chapter Three

Calcium Phosphate Ceramics

Calcium phosphate is the name given to a family of minerals containing calcium ions (Ca^{2+}) together with orthophosphates (PO_4^{3-}), metaphosphates or pyrophosphates ($P_2O_7^{4-}$) and occasionally hydrogen or hydroxide ions. The bioactive property of ceramic materials has received much attention in the field of hard tissue replacement. Ceramics provide fixation by biological in-growth of the local tissue into the implant pores, or onto the implant surface a process known as biological fixation (Hench 1998b;Hench 1998a) through the formation of a biologically active hydroxycarbonate apatite layer on their surfaces *in vivo*.

This chapter presents a review of the calcium phosphate ceramics used for medical applications and also reviews current and future clinical applications, as well as focusing on the drawbacks of such calcium phosphate based ceramic materials for the use of bone replacement applications.

3.1 Characteristics of calcium phosphate ceramics

The calcium phosphate (CP) ceramics are formed by a process called sintering. This is a process in which high temperatures (1100-1300 °C), and pressures are used to consolidate calcium phosphate salts into a monolith. Many calcium phosphates can be formed by sintering precipitated poorly crystalline apatites in highly controlled conditions. The stoichiometry of the precipitate and the sintering conditions enable some control over the final calcium phosphate formed. For example, pure HA is formed by using apatite with a Ca/P ratio of 1.7; whereas TCP is formed by using apatite with a Ca/P ratio of 1.5. When apatites

with varying Ca/P ratios are sintered, different amounts of HA and TCP are formed in the final ceramic, resulting in biphasic calcium phosphates (BCPs). Another factor that is determined by the sintering parameters is the residual microporosity (Horner 2004).

Table 3.1: Physical properties of various phases of calcium phosphate bioceramics (Groot & Wolke 1990;Billottee 2002).

Phases	**Chemical formulae**	**Ca/P ratio**	**structure**	**Density (g/cm^3)**
Hydroxyapatite (HA)	$Ca_{10}(PO_4)_6(OH)_2$	10/6	Hexagonal, $P6_3/m$ space group, cell dimensions: $a = b = 9.42$ Å, and $c = 6.88$ Å	3.16
α-Tricalcium phosphate (α-TCP)	$Ca_3(PO_4)_2$	3/2	Monoclinic, $P2_1/a$ space group, lattice constants: $a = 12.887$ Å, $b = 27.280$ Å, $c = 15.219$ Å; $\beta = 126.20°$	2.86
β-Tricalcium phosphate (β-TCP)	$Ca_3(PO_4)_2$	3/2	Pure hexagonal, rhombohedral, space group R3cH, unit cell dimensions: $a = b = 10.439$ Å, $c = 37.375$ Å, and $\alpha = \beta = 90°$, $\gamma = 120°$	3.07
Tetracalcium phosphate (TTCP)	$Ca_4P_2O_9$	2/1	Monoclinic, space group $P2_1$, $a = 7.023$, $b = 11.986$, $c = 9.473$; $\beta = 90.90°$	3.05

CP ceramics are also resistant to microbial attack, pH changes and solvent conditions. They exist in different phases depending on temperature, partial pressure of water and the presence of impurities (Groot & Wolke 1990) and (Hench 1998a). HA, β-TCP, α-TCP, BCP (Wong *et al.* 2002), monocalcium phosphate monohydrate (MCPM) and unsintered apatite are different forms of commercially available calcium phosphates currently used in the biomedical industry. **Table 3.1** summarises the physical properties of various forms of calcium phosphates currently used in the biomedical industry. Different phases are used in different

applications depending upon whether a resorbable or bioactive material is desired (Billottee 2002). HA is the ideal phase for application inside human body because of its excellent stability above pH 4.3, human blood pH being 7.3. **Table 3.2** presents solubility and pH stability of different forms of calcium phosphates in aqueous solution (Guo & Li 2004).

Table 3.2: Solubility & pH stability of different calcium phosphates phases (Guo & Li 2004).

Phases	**Solubility at 25 °C, $-\log(K_{sp})$**	**pH stability range in aqueous solution at 25 °C**
Hydroxyapatite (HA)	116.8	9.5–12
β-Tricalcium phosphate (β-TCP)	28.9	Cannot be precipitated from aqueous solutions
α-Tricalcium phosphate (α-TCP)	25.5	Cannot be precipitated from aqueous solutions
Tetracalcium phosphate (TTCP)	38–44	Cannot be precipitated from aqueous solutions
Dicalcium phosphate dihydrate - Brushite (DCPD)	6.59	2.0–6.0
Dicalcium phosphate anhydrate (DCPA)	6.90	Stable at temperatures above 100 °C
Amorphous calcium phosphate (ACP)	Cannot be measured precisely. However, the following values were reported: 25.7 ± 0.1 (pH 7.40), 29.9 ± 0.1 (pH 6.00), 32.7 ± 0.1 (pH 5.28).	Always metastable. The composition of a precipitate depends on the solution pH value and composition.
Calcium-deficient hydroxyapatite (CDHA)	85.1	6.5–9.5

Crystallization of various salts of calcium phosphates, like HA and β-TCP depends on; Ca/P ratio, presence of water and impurities, and temperature. For example, in a wet environment and at a lower temperature (< 900 °C), the formation of HA is most likely to happen, but in a dry atmosphere and at a higher temperature, β-TCP is more likely to form.

3.1.1 Structure

The crystalline structure of sintered calcium phosphate ceramics can be classified as microcrystalline or macrocrystalline. Microcrystalline structures have a reduced space arrangement, whereas macrocrystalline materials have a well-ordered crystal structure. The diffraction pattern of the ceramics, as determined by x-ray diffraction, can be compared to natural bone, which has a nanocrystalline structure. The comparison of the diffraction patterns provides insight into the resemblance of the crystalline structure of a calcium phosphate to natural bone.

3.1.2 Porosity

Dense and porous ceramics are produced by different sintering techniques. Dense ceramics are produced by compaction under high pressure, resulting in a structure called a green body, and is sintered after the compaction process. Porous ceramics are produced by using appropriate-sized naphthalene particles, incorporated in apatite. After compaction under high pressure, removal of naphthalene is accomplished by sublimation which leaves a macroporous green body. The integrity of this macroporous green body is maintained through the sintering step. Another method of producing porous ceramics relies on the decomposition of hydrogen peroxide to generate a pore-filled structure (Jarcho 1981). The porosity of ceramic materials enables mesenchymal cell migration, adhesion, proliferation and differentiation into osteoblasts within their pores. This unique structure constitutes their osteoconductive characteristics (Spivak & Hasharoni 2001).

3.1.3 Solubility

CP ceramics can dissolve in basic, neutral, or acid solutions, depending on their chemical composition. Particularly in acidic environments CP ceramics dissolve rapidly. Important for the dissolution process is the Ca/P ratio of the ceramic used. TCP (Ca/P <1.67) dissolves 12.3 times faster than HA (Ca/P = 1.7) in an acidic medium and 22.3 times faster than HA in a basic medium (Hyakuna *et al.* 2007). Other properties of the biomaterial, i.e., porosity, crystallinity, and impurities of the biomaterial can influence this process (Horner 2004).

The dissolution process results in an increase of the extracellular concentrations of calcium ($(Ca^{2+})_e$) and phosphate ($(PO_4^{3-})_e$). The high $(Ca^{2+})_e$ and $(PO_4^{3-})_e$ results in the precipitation of apatites on a substrate ceramic, forming a carbonate-apatite-crystal layer. The very strong interface between the material and bone is believed to be influenced by this crystal layer (Horner 2004). HA has a low dissolution rate which results in almost direct bonding with bone and tissue components. When degradation is extensive, as in the case of β-TCP, the dissolution/recrystallization layer is correspondingly wide (Bagambisa *et al.*1993).

3.2 Hydroxyapatite

Hydroxyapatite is a naturally occurring form of calcium apatite with the formula $Ca_5(PO_4)_3(OH)$, but is usually written $Ca_{10}(PO_4)_6(OH)_2$ to denote that the crystal unit cell comprises two molecules. It is the main mineral component of bone. Carbonated-calcium deficient hydroxyapatite is the main mineral of which dental enamel and dentin are comprised.

Highly crystallized HA tends to be stable *in vivo* and is resorbed at a very slow rate of 5% per year via osteoclast activity (Muralithran & Ramesh 2000). But more soluble forms of HA can be produced by reducing crystal size and adding impurities (Ducheyne & Qiu 1999) that would reduce its mechanical properties. HA is generally observed to be non-bioresorbable and therefore suitable for long-term surgical procedures. High porosity HA provides better chemical bonding at the implant-tissue interface and allows biological bonding through in-growth of the host tissues into the implant pores (Ducheyne & Qiu 1999;Ducheyne *et al.* 1978). However, high porosity can give rise to poor mechanical properties. Also HA is generally very brittle and hard, leading to difficulties in reshaping and handling during surgical operations (Cao & Hench 1996).

Stoichiometric synthetic HA ($Ca_{10}(PO_4)_6(OH)_2$), with a Ca/P atomic ratio of 1.67, was introduced as a bone-graft substitute because its formula is similar to that of the inorganic mineral phase of bone. Biological HA is calcium deficient and a carbonated apatite (Elliot 1994). The bonding mechanism of HA to bone, seems to be due to the attachment at the surface of the HA of osteogenically competent cells which differentiate into osteoblasts. A cellular bone matrix is then formed at the surface of the HA. An amorphous area is present between the surface and the bone tissue containing thin apatite crystals. As maturation occurs, this bonding zone shrinks and HA becomes attached to bone through a thin epitaxial layer, resulting in a strong interface with no layer of fibrous tissue interposed between the bone and HA (Hamadouche & Sedel 2000). Bone formation grows from the surface of the HA towards the centre of the pores (Hench & Wilson 1993).

Many researchers have observed that the mechanical strength and fracture toughness of HA ceramics can be improved by the use of different sintering techniques. These include; addition of a low melting secondary phase to achieve liquid phase sintering for better densification (Lopes *et al.* 1998) and (Santos *et al.* 1996); incorporation of sintering additives to enhance densification through grain boundary strengthening (Georgiou & Knowles 2001) and (Kalita *et al.* 2002); and use of nano-scale ceramic powders for better densification contributed by large surface area to volume ratios of nano-size powders. It is believed that nano-scale HA has the potential to revolutionize the field of biomedical science from bone regeneration to drug delivery. During the past 15 years, much attention has been given to nano-structured HA CP ceramic, with major research emphases of production of nano-scale powders to improve the mechanical as well as biological properties (Driessens *et al.* 2002).

Synthetic HA is limited in its use as a biomaterial, primarily due to its low load bearing capacity which can be illustrated by the relatively poor mechanical properties compared with bone (Rey & Freche 1991). However, improvements of its mechanical properties have been made with the inclusion of soluble phosphate based glasses (P_2O_5–CaO–Na_2O) (Hench & Wilson 1993). Phosphate glasses, when incorporated into HA, melt at a lower temperature compared with HA and can act to increase density by enhancing the sintering mechanisms which greatly enhances the mechanical properties. Furthermore, decomposition of HA into secondary phases, α- and β-TCP, can occur. This is related to the compositional effects, in particular the Ca/P ratio (Hench & Wilson 1993;Lopes *et al.* 1998). It can also be seen as a function of sintering temperature (Rey & Freche 1991).

The main disadvantages which have limited the clinical application of HA as a bone graft substitute are related to the brittle nature and poor tensile strength of the material. The existence of porosity in ceramics considerably affects the mechanical properties (Xu *et al.* 2001). The incorporation of glass in HA acts as a sintering aid, which enhances densification, and as a result reduces porosity. This occurs through a liquid phase sintering mechanism, which accelerates inter-particulate diffusion and bonding, thus causing elimination of porosity and shrinkage (Santos *et al.*1996). However, in this system, it is further complicated by the occurrence of decomposition and phase changes that can also have a detrimental or beneficial effect on the mechanical properties. Ultimately, both porosity and phase decomposition are influencing factors in the outcome of the mechanical properties.

Santos *et al.* (1996) concluded that HA undergoes considerable elimination of porosity during sintering, predominantly between 1200 °C and 1250 °C. However, the mechanical properties are still relatively poor. The addition of a glass as a sintering aid significantly improves the flexural bending strength. The majority of the enhancement comes from the decomposition of HA to β-TCP with an associated volume change, helping to improve the mechanical properties. At higher firing temperatures, the β-TCP inverts to the high temperature α-TCP form. A relatively small amount of α-TCP can be sustained in the composites. However, large percentages of glass can promote formation of significant amounts of α-TCP with a resultant decrease in flexural bend strength.

3.3 TCP

Tri-calcium phosphate (TCP) is thermodynamically stable only at elevated temperatures (1000–1500 °C) (Elliot 1994). Gibson proved β-TCP to be resorbable *in vivo* with new bone

growth replacing the implanted TCP (Gibson *et al*. 2000). Generally β-TCP is resorbed within 6 weeks after implantation (Spivak & Hasharoni 2001). β-TCP and α-TCP are the two forms of TCP that are known to exist, β-TCP transforms to α-TCP at around 1200 °C; the later phase is stable in the range of 700–1200 °C (Groot & Wolke 1990). However, α-TCP has received little importance in the biomedical field. The disadvantage for using α-TCP is its rapid resorption rate, which limits its usage as a biomaterial (Metsger *et al.*1999).

TCP would form apatite layer in body environment and has been used for bone repair in the form of ceramic blocks or granules. It is a weak bioceramic and thus cannot be used on its own as major load-bearing implants in the human body.

3.3.1 β–TCP

β-TCP, is a bioresorbable CP ceramic and is a promising material in the field of biomedical applications such as orthopaedics. It has also been observed to have significant biological affinity and activity and responds very well to the physiological environments. Because of its slow degradation characteristic, the porous β-TCP is regarded as an ideal material for bone substitutes that should degrade by advancing bone growth (Hench & Wilson 1993). These factors give β-TCP an advantage over other biomedical materials when it comes to resorbability and replacement of the implanted TCP *in vivo* by the new bone tissue (Gibson *et al.* 2000). Since it is well tolerated when implanted into bone β-TCP has great potential to act as a scaffold allowing bone regeneration and growth. X-ray diffraction patterns reveal that β-TCP has a pure hexagonal crystal structure. It is reported that the resorbability of β-TCP *in vivo* might be strongly related to the characterization and stability of the β-TCP structure (Okazaki & Sato 1990).

A number of synthesis methods have been used to produce β-TCP powders. The conventional methods include solid-state process (Bigi *et al.* 1997) and wet-chemical method (Liou & Chen 2002). The wet-chemical method gives Ca-deficient apatite ($Ca_9(HPO_4)(PO_4)_5(OH)$, CDHA) with the same molar ratio of Ca/P as that of TCP. It needs to be calcined above 700–800 °C to transform into β-TCP as shown by the following reaction:

$$Ca_9(HPO_4)(PO_4)_5(OH) \rightarrow 3Ca_3(PO_4)_2 + H_2O \quad \text{(equation 3.1)}$$

3.3.2 α–TCP

α-TCP has the same composition as β-TCP but is significantly more soluble (-logKsp for α-TCP = 25.5 compared to β-TCP = 29.5 in distilled water (Elliot 1994)). α-TCP is metastable at normal physiological temperatures (Jillavenkatesa & Condrate 1998), releasing almost 10 times more calcium than β-TCP under neutral pH conditions (Karlinsey et al. 2010). α-TCP hydrolyses to form a CDHA, this was first reported by Monma and Kanazawa in 1976. The same group later investigated the hydrolysis process as a means to form setting cement; however, they found that the hydrolysis reaction proceeded too slowly at a pH higher than 7.5 to allow setting in a clinically applicable time (Monma *et al.* 1984). Although α-TCP-water mixtures have been studied extensively for the last 20 years here is still a need for new alternatives to increase their injectability and create macropores.

3.4 BCP

The development of biphasic calcium phosphates (BCP) has drawn considerable attention, especially with HA-TCP. Although HA and TCP are similar in composition, they have very

different biological resorption rates; the dense HA ceramics are almost non-resorbable and bio-inert when implanted, whereas the porous β-TCP ceramic allow relatively rapid degradation following implantation. When used as a mixture, biodegradable HA-TCP graft material has the ability to dissolve, break down and allow new bone formation and remodelling required to attain optimal mechanical strength without hindrance. Several authors have produced ceramics using a combination of different phases, combining the properties (Jillavenkatesa & Condrate 1998;Kohri *et al.* 1993a;Kohri *et al.* 1993b;LeGeros 2002;Li *et al.* 2007;Ramay & Zhang 2004;Wang *et al.* 1998). Victoria and Gnanam reported the production of BCP by a precipitation technique using 1.0 M $Ca(OH)_2$ and H_3PO_4 (Victoria & Gnanam 2002). The HA and TCP ratio was found to be 70:30.

3.5 Commercially available CP ceramic materials

A great deal research has been focussed on the formulation CP ceramics in the past thirty years and as a consequence there are now several products commerciall available. **Table 3.3** illustrates many of these commercialised CP ceramic materials.

Table 3.3: Illustrates the commercialised CP ceramic materials on the market.

Material	Product Name	Company Name	Application	Studies
HA	Calcitite	Calcitek, USA	Dental, orthopaedics, ear surgery, maxillofacial: coatings for metal implants	Legeros *et al.*2003
	Osteograf/D	Sterio-Oss, USA	Mainly dental but also some orthopaedic	Legeros *et al.*2003
	Bioapatite	PRED, France	Dental, orthopaedics, ear surgery, maxillofacial: coatings for metal implants	Penel 1997, Andre-Frei *et al.* 2000, Hemmerle 1997
β-TCP	Synthograf	Synthograf, USA	Buccal defect, extraction site, internal or lateral sinus lift, crest augmentation and periodontal defects.	Chopra *et al.* 2007/ 2008; Schulze-Spate *et al.* 2008; Coelho *et al.* 2006
BCP	Triosit	Biomatlante, France	Large bony defects, periodontal defects, orthopaedic lesions, lumbar spine fusion, correction of scoliosis, and ophthalmic implants.	Ellinger *et al.* 1986; Nery *et al.* 1990/ 1992; Daculsi *et al.* 1990; Wykrota *et al.* 1998.
non-ceramic apatite	Osteogen	Biomet, Inc	Sinus lift, augmentation of tooth sockets, peri-implant alveolar defects, periapical, periodontal defects and femur, tibia, fibula, humerus, clavicle, ulna, radius.	Legeros et al.2003

3.6 Drawbacks of CP Ceramics

While a number of commercial CP ceramics are available, they generally have significant drawbacks, which has limited their clinical application and stopped them from replacing autograft tissue as the gold standard. Since consolidation into a monolith requires high temperature processing, preoperative knowledge of the bone defect site is required, precluding use for the repair of bone damage due to trauma. CP ceramics can be delivered as granules that can be pressed into a defect; however, migration from the site of implantation can lead to further complication. The requirement of a high temperature processing step also means that it is not possible to incorporate heat sensitive therapeutic molecules into the ceramic during manufacture. Densification of the ceramic during the sintering process results in changes in

the ceramic structure this mean that sintered CP ceramics do not closely resemble the calcium phosphate phases found in bone. Sintering results in solid state diffusion between the crystals comprising the cement matrix. While solid state diffusion results in an increase in strength, it also causes crystal growth which results in a significant reduction in specific surface area which can compromise biological integration. Calcium phosphate based cements were designed with the aim of meeting many of the shortcomings of calcium phosphate ceramics that are processed at high temperature. Following mixing, calcium phosphate cements are an injectable paste material used for filling cavities in bone. This mouldablilty allows the material to conform around irregular cavities and harden to form a matrix of hydroxyapatite or brushite. Setting of both materials results in little or no exotherm and since no the materials are not heat treated following compaction into the defect, they are microcrystalline and so more closely resemble the mineral phase of bone than sintered CP ceramics. Chapter four reviews these cements and their applications in greater detail.

Chapter Four

Calcium Phosphate Cements

Calcium phosphate ceramics, as mentioned in the previous chapter, are used in bone replacement applications, whereby the new bone tissue is able to colonize the implanted material (in macroporous foams). In the case of these porous implants, the interconnected porous structure allows the formation of bone tissue growth by osteoblasts that migrate into the structure. In the mid-1980's, a new calcium phosphate bone replacement material was reported (Brown & Chow 1985) that have the advantages of calcium phosphates, with the added advantage of a cement material. CPCs are formed by the combination of a solid powder phase, of calcium phosphate (s), and an aqueous solution.

4.1 Advantages of CPC's

In dentistry calcium phosphate cements play a secondary role at the moment, although they often have excellent bone repair properties (Sugama *et al.* 1992). The CPCs are able to activate the osteoclastic and osteoblastic functions of bone regeneration with the added advantage that these cells are able to modify the structure of the cement material so that in more closely resembles native bone. Moreover, they have the advantage over the bioceramics as they do not need to be delivered in prefabricated forms (calcium phosphate ceramics are commonly applied as granules or blocks), because these self-setting cements can be handled by the clinician in paste form and injected into bone cavities. CPCs can be formulated to be mouldable, injectable and thus allow complete filling of a cavity, *in situ*, within the operating theatre. Cements are of lower crystallinity than ceramics and therefore exhibit a comparatively higher specific surface area (cements – 100 m^2/g; ceramics – 1 m^2/g). CPCs

can produce brushite as the final product by a cement setting reaction; however, brushite cannot be sintered like other ceramics because brushite dehydrates at 50 ºC. For this reason heat sensitive therapeutic molecules can also be incorporated into the cement matrix, whereas, with ceramics the heat sensitive therapeutic molecules have to be incorporated after manufacture. Other benefits include; initial setting characteristics of the material which gives, in an acceptable clinical time, and suitable mechanical strength for a shorter tissue functional recovery.

Although there are numerous formulations of CPC, essentially there are only three different end products; apatite, brushite and amorphous calcium phosphate. The only study on amorphous calcium phosphate shows that the cement is rapidly converted into apatite (Driessens *et al*. 1996). For the purposes of these thesis, therefore two main types of cement end products are discussed; HA and brushite cements. Brushite based cements have been the focus of much research in the past decade (Bohner 2000a;Grover *et al.* 2003;Grover *et al.* 2006;J.Lu *et al.* 2002), as the importance of implant resorption has become more apparent.

This chapter presents a review of the calcium phosphate cements used for medical applications and also describes the setting, rheological and mechanical properties of HA and brushite cements and reviews current and future clinical applications.

4.2 Hydroxyapatite

4.2.1 Chemistry of setting reactions

HA setting cements are the most commonly researched CPC, due to HAs compositional resemblance to natural bone. In the last 30 years HA has moved from research to

commercialisation **(Table 4.1)**. The main types of HA based cement system are as follows; TTCP (tetracalcium phosphate; $Ca_4(PO_4)_2O$)/DCPA (monetite; $CaHPO_4$), α-TCP/DCPA, α-TCP/MCPM (monocalcium phosphate monohydrate; $CaH_2PO_4.H_2O$) and amorphous calcium phosphate cements, which are explored in this chapter.

TTCP/DCPA cement

The TTCP/DCPA cement is a derivative of Brown and Chow's original cement the in which an equimolar mixture of TTCP (basic) and DCPA (neutral) is combined with water to form apatite (slightly basic) cement paste (Brown & Chow 1986) that sets as:

$$Ca_4(PO_4)_2O + CaHPO_4 + H_2O \rightarrow Ca_5(PO_4)_3OH + H_2O \qquad \text{(equation 4.1)}$$

This reaction produces a stoichiometric hydroxyapatite (SHA) however, due to the unequal dissolution of the two phases it is thought that the cement actually sets to form a calcium deficient hydroxyapatite (CDHA) (Ishikawa *et al*. 1999) in accordance with equation 4.2:

$$3Ca_4(PO_4)_2O + 6CaHPO_4 \rightarrow 2\ Ca_9(HPO_4)(PO_4)_5OH + H_2O \qquad \text{(equation 4.2)}$$

From equations 4.1 and 4.2 it is very clear that there is no consumption of the liquid phase in these setting mechanisms; the presence of water is simply to allow the formation of a workable cement paste and aid ion transport. This "water-less" cement, as it is sometimes termed, can be of great advantage allowing the cement reactants to be sterilised as high as 300 ºC (Elliot 1994).

α-TCP/DCP cement

Based on the hydrolysis of α-TCP the formation of a CDHA was first reported in 1976 by Monma and Kanazawa, the reaction was considered to be far too slow for clinical situations.

This led to the addition of DCP, DCPD, PHA or sodium phosphate solution (Na_2HPO_4 or NaH_2PO_4) to improve reaction kinetics and provide for faster setting harder materials exhibiting setting times of less than 30 mins (Driessens *et al.* 1993a;Durucan & Brown 2000;Huisen & Brown 1998).

$3\ \alpha\text{-}Ca_3(PO_4)_2 + H_2O \rightarrow Ca_9(HPO_4)(PO_4)_5OH$ (equation 4.3)

The cement is a hydraulic cement system, which means that the HA only forms on consumption of water, unlike the TTCP/DCPA formulation. Hydraulic cements based on calcium phosphates offer the advantage of being freely mouldable and adaptable to bone defects.

α-TCP/MCPM cement

In 1995, Constantz *et al.* added calcium carbonate to CPC to alter the crystallite size of HA in the cement, by replacing PO_4^{3-} with CO_3^{2-}. This improved the degradation speed significantly, and results showed excellent clinical treatment effects in bone repair (Constantz *et al*. 1995a). The dry mixture of α-TCP, MCPM and calcium carbonate mixed with sodium phosphate solution resulted in the formation of a hardened matrix of Dahllite:

$Ca_{8.8}(HPO_4)_{0.7}(PO_4)_{4.5}(CO_3)_{0.7}(OH)_{1.3}$ (equation 4.4)

A study on the solubility and dissolution rates of various different commercially available HA (Norian CRS and Bonesource) demonstrated an increase in solubility with increasing ionic substitutions into the apatite lattice and decreasing crystallinity (Fulmer *et al.* 2002). The presence of carbonate ions in the lattice of HA have been shown to result in a reduction in crystallite size and an increase in the number of lattice defects.

Amorphous calcium phosphate cements

There is only one ACP-based bone cement currently on the market (Biobon in **Table 4.1**). This cement comprises a mixture of ACP (50wt%) and DCPD (50wt%) which is mixed with an appropriate amount of aqueous medium (deionised water or saline) with a liquid to solid ratio of 0.8 ml/g at room temperature (Tofighi *et al*. 2001). An injectable paste is obtained which sets in less than 20 min at 37 °C; hydrolysis of the ACP results in the formation of HA, as the end product. After hardening it is constituted of nanocrystalline apatite with crystal dimensions close to those of human bone. This cement setting reaction is endothermic; this means that the cement does not set until body temperatures are reached. This extends working time for the paste at room temperature and links setting to implantation; great advantages for this cement formulation. Several authors have experimented to modify formulations of this ACP-based cement, including additives with a view to improve and control other properties; in particular, setting time and injectability can be optimised for different requirements by controlling the amount and nature of additives (Wang *et al.* 2007a;Wang *et al.* 2006). Van den Vreken *et al.* studied the influence of ACP when added to two cement formulations: an α-TCP-based cement and a TTCP–MCPM-based cement and prepared pure ACP cement as a reference (Van den Vreken *et al*. 2010). The results demonstrated that the addition of ACP to the cement formulations led to a decrease in the crystallinity of the end product and was converted to a nanocrystalline CDHA. Addition of ACP to these two CPCs resulted in cements that exhibited good setting times, compressive strengths suitable for non-load-bearing applications and demonstrated good cell viability, making them suitable candidates for bone substitute materials.

4.2.2 Setting properties

CPC's must set slowly enough to provide sufficient time to a surgeon to perform implantation but fast enough to prevent delaying the operation. Good mechanical properties should be reached within minutes after initial setting (Bohner 2007). Gillmore needles have been used with success to measure the initial (*I*) and final (*F*) setting times of calcium orthophosphate cements (Driessens *et al.* 1993b). Two different needles are used to measure *I* and *F* setting times **(Appendix 1)**. The clinical meaning is that the cement paste should be implanted before time *I* and that the wound can be closed after time *F*. The cement should not be deformed between times *I* and *F* because in that stage of the setting process any deformation could induce cracks (Driessens *et al.* 1998). Setting times of HA have been reported to be in a range between 30 mins (Brown & Chow 1986) to 150 mins (Liu & Shen 1997); this is for the same cement system. However, setting times that exceed 30 mins are clinically limited; therefore, much work has been directed towards the use of additives as a means of reducing the setting times of these cements.

Accelerators

It was previously suggested that the presence of a crystal seed could reduce the setting time and increase the compressive strength, however Liu and Shen investigated the effect of crystal seeding on the hydration of CPC. They found that the setting time of the CPC with the addition of 5wt% low crystallinity hydroxyapatite (used as a crystal seed) was 7 min. This improvement in the setting time was due to HA serving as a substrate for heterogeneous nucleation which accelerated nucleation, this meant that the increasing quantity of crystal seeding lowered the setting time to a degree, although the extent at which the setting time was reduced lessened as the crystal seeding continued to increase (Liu & Shen 1997). However,

they found that the effect of the crystal seeding on the compressive strength of the cement was negative; reducing from 60 MPa to 44 MPa (10wt% HA). The acceleration of the nucleation in this reaction means that the growth is limited; this resulted in the formation of smaller sized and lower aspect ratio products. This production of many metastable small particles undergo dissolution-reprecipitation during hydration; these particles react and damage the microstructure, lowering the strength of the seeded cements (Liu & Shen 1997).

Yang *et al.* also found that the microstructure was affected by the seed crystals in the cement; the presence of the seed crystals (20wt% HA seed crystals) appeared to lengthen the HA crystals from "sub-micron" to 1-2 μm (Yang *et al.* 2002). This was suggested as the reason for the decrease in strength. Several other studies on crystal seeding demonstrate similar results; Brown *et al*. indicated that HA seeds accelerate the initial setting reactions but did not appear to have major long-term effects on the extent of reaction or on the microstructure (Brown & Fulmer 1991). Bermudez *et al.* found that the compressive strength of the CPC based on MCPM–CaO system initially increases with HA seeds content up to 8%, and then decreases (Bermudez *et al.* 1994a). However, for the α-TCP–MCPM–CaO system, they found that the cement setting time decreases with HA seeds content up to 3% and then increases (Bermudez *et al*. 1994b).

Phosphate Solutions

Another means of reducing the setting times of HA cements is the addition of sodium phosphate to the liquid phase. This addition of phosphate ions causes rapid supersaturation of the HA and causes rapid precipitation. Fernandez *et al.* refers to the effect of phosphate ions on the setting reaction as a "common ion effects" and reported a reduction in the final setting

times of the cement composed of α-TCP and DCP. Both cements exhibited the same common ion effect following the addition of 6wt% Na_2HPO_4 or $NaH_2PO_4.2H_2O$ (instead of water for making the cement pastes); where the setting times were reduced by a factor of 10. However, they found this lowered the strength of the cements; the addition of 4wt% Na_2HPO_4 formed α-TCP cement with 50% of the original compressive strength of the α-TCP cement made using water as the liquid phase. As means of comparison $CaCl_2$ was also used to reduce setting times; however, it was observed that no common ion effect occurred. This suggests that the reduction in setting time was attributed by the lowering of the pH of the cement mix, by the acidic phosphate salts (Fernandez *et al.* 1994).

Ishikawa *et al.* found that the setting time of a calcium phosphate cement consisting of TTCP and DCPA was reduced from 30 to 5 min by use of a cement liquid that contained a phosphate concentration of 0.25 mol/l or higher. The diametral tensile strength and conversion to HA during the first 3 h were also significantly increased by the phosphate (Ishikawa *et al.* 1995).

Effect of temperature

It has been demonstrated in various studies that temperature has a marked effect on the setting times of HA cements. An elevation in temperature from 21 ºC to 37 ºC can result in a three-fold reduction in setting times. This effect would be advantageous in clinical applications where the cement is handled at room temperature, giving the surgeon increased handling time with a reduced setting time implanted (*in situ*). This was explored by Driessens *et al.* when a cement of powder (P) is mixed with a liquid (L) at a ratio of 3.13 g/ml was produced; consisting of α-TCP (64wt%), DCP (27wt%) and HA (9wt%) and with a liquid component of

2.5wt% Na_2HPO_4. This exhibited setting times of approximately 30 mins at 20 ºC and 10 mins at 37 ºC, a significant decrease (Driessens *et al.* 2000).

4.2.3 Rheological properties

Injectability and cohesion are required for the successful *in vivo* introduction of CPC's. The cement paste is required to be injectable with low resistance; the powder–liquid phase must not separate during the injection process, which mainly depends on a suitable rheological property of CPC slurry. In order to prevent wash-out of the cement materials, viscosity modifying agents are often added to the cement formulation; this also reduces viscosity and minimises the invasive methods of cement application.

Cohesion promoters

The ability of a hydraulic paste to harden in an aqueous environment without releasing loose particles has been termed "cohesion" (Bohner *et al.* 2006). From the various parameters that may influence the cohesion of the CPC paste were identified both theoretically and tested using new methods. Their results suggested that the two better methods to increase the cohesion of a calcium phosphate paste are to decrease the average particle size of the paste constituents or in some cases to add a viscosity modifying agen such as xanthan.

An appropriate cohesion is said to be achieved when no disintegration of the cement paste is observed in the fluid. This can be accomplished by keeping a high viscosity for the cement paste or using cohesion promoters (e.g. 1% aqueous solution of sodium alginate (Alves *et al.* 2008;Bermudez *et al.* 1993)). Commercial cements such as, Norian SRS fulfils both criteria, but others don't necessarily fulfil any of these requirements. For example, BoneSource and

Cementek are not injectable and blood must be kept away from the implanting site until setting (Bohner 2000;Bohner 2001). Also, decohesion of the cement during mixing may lead to inflammatory reactions (Miyamot *et al.* 1999).

Injection of HA cements

Injectability is the ability to be extruded through the aperture of a hypodermic needle (e.g. 2 mm diameter and 10 cm length) and for certain applications injectability is a requirement. Usually, injectability of a cement paste varies inversely with its viscosity, the P:L ratio, as well as the time after starting the mixing of liquid and powder (Khairoun *et al.* 1998;Serraj *et al.* 2002). When put under pressure, some CPC's demonstrate demixing into a thin paste, which is extruded, and a thick mass, which remains inside the syringe; this is called filter-pressing. In the case of demixing, the exact composition of the extruded part of the paste becomes unknown. Moreover, due to a deviation from the initial P:L ratio, it becomes unclear whether the setting behaviour and the mechanical properties of the extruded part are still clinically acceptable. Therefore, a good cohesion of the paste is necessary in order to avoid these problems.

Two examples of workability-improvement agents, which are added to the powder of the cement, are polysaccharides and gelatine. Polysaccharides significantly increase the injectability (Lewis 2006) while gelatine was expected to increases the compressive strength and both initial and final setting times, these effects being attributed to a reduction in total porosity and achievement of a more compact microstructure (Bigi *et al.* 2004). Furthermore, gelatine is a commonly used polymer (Chang *et al.* 2003;Vandelli *et al.* 2004a;Watase &

Nishinari 1980), it is completely resorbable *in vivo*, and its presence in the cement gives a composite material where both the organic and the inorganic phases resemble those of bone.

Gbureck *et al.* enhanced the injectability of α-TCP-based cement, by adding several fine-particle-sized fillers, and demonstrated that the use of inert filler can yield significant viscosity reduction. In comparison, the use of tri-sodium citrate as a liquid phase only led to a slight decrease of the cement viscosity (Gbureck *et al.* 2005b). The study concluded that optimization of inter-particle spacing by using inert filler material can yield significant strength improvements and viscosity reduction.

4.2.4 Mechanical properties

During the setting reaction of the cement, calcium phosphate crystals grow and become partly interlocked, given the cement the characteristics of mechanical rigidity. As calcium phosphates are brittle, the compressive strength of a CPC is always greater than its tensile strength. Most CPC have a tensile strength of 1–10 MPa, whereas the compression strength varies between 10 and 100 MPa. The mechanical properties of a CPC depend on its composition. The main determining factor is the ratio between the amount of cement powder and mixing liquid. If this P:L ratio is large, the porosity of the CPC is low. As the mechanical properties decrease exponentially as porosity increases, low porosity always corresponds to high mechanical properties. As a rule of thumb, the tensile strength increases two-fold with a 10 vol% decrease in porosity. The mechanical properties reported by CPC manufacturers are never documented, so it is difficult to compare CPC.

Particle Size Distribution

The particle size distribution plays a crucial role in the mechanical properties of the cement by determining the minimal volume required to form workable cements and also affecting the rate and extent of the setting reaction. Some authors have studied the influence of the particle size of the reactants on the final mechanical properties of some cements, such as DCP-TTCP based cements or DCPD-TTCP based cements (Otsuka *et al*. 1995).

A study on the reaction kinetics and the underlying physico-chemical mechanisms responsible for the final structure and properties of the cement were investigated by Ginebra *et al.* The particle size of the powder phase is introduced as a variable, in order to determine its influence on the final structure of the cement at the micro and nano-scale range (Ginebra *et al.* 2004). It was concluded that the crystallite size of the final product can be strongly reduced by increasing the specific surface area of the starting powder; this tailors the developing calcium phosphate materials with structures at the micro and nano-scale levels.

Cement Stoichiometry

The alteration of the stoichiometry of the setting reaction can affect the mechanical properties of the cement when two different phases react. For example, the use of excess TTCP or DCPA in the reaction, results in a reduction of mechanical strength. When equimolar amounts of both TTCP and DCPA are mixed at P:L of 4 g/ml a cement exhibiting diametral strengths of 13 MPa were produced. In comparison, when TTCP and DCPA are mixed at molar ratios of 2.0 and 0.25 diametral strengths of 6 MPa are exhibited. This reduction in mechanical strengths is a result of a heterogeneous cement matrix caused by the reaction of unreacted material (Ishikawa *et al.* 1999).

Compaction

Reducing the relative porosity can improve the mechanical strength of the cement. Compaction (uni- or bi-axial) of the cement setting paste is one technique used to reduce the porosity. However, it is not known whether the compaction of the cement material will alter the specific surface area significantly or how the pore size distribution changes with the compaction pressure.

Ishikawa and Asaoka showed a linear relation between diametral tensile strength and porosity of CPC cement, where porosity was controlled by compaction pressure (up to 173 MPa). However, when compaction pressures above; 100 MPa were applied, little decrease in porosity was achieved, and diametral tensile strength was not significantly improved (Ishikawa & Asaoka 1995). Thereafter, Barralet *et al.* explored the effect of compaction pressures up to 106 MPa on the mechanical properties in compression and calculated the specific surface area of TTCP/DCPA cement (Barralet *et al.* 2002b). They concluded that the compaction pressure did not alter the specific surface area of the cement, which implies that the dissolution of TTCP/DCPA cement would not be affected by porosity changes induced by the compaction process.

Following this in 2003, Barralet *et al.* reported wet compressive strengths of 90 MPa made using sodium citrate as the liquid phase; the cement was manually compact, using finger pressure. The addition of sodium salts of α-hydroxy acids with more than one acid group to the liquid phase of apatitic cement improved the effectiveness of biaxial compaction (Barralet *et al.* 2003). By mechanical compaction, using pressures of 200 MPa, the compressive

strength of the final cement was increased to 180 MPa; comparable to the strength of cortical bone. This increase of strength widens the range of applications for such cements.

4.2.5 *In-vitro* ageing

In-vitro ageing is a means of initially investigating individual parameters that may affect the mechanical or degradation properties of the material *in-vivo*. The basic requirements that a synthetic bone replacement must possesses can be screened by means of *in vitro* studies.

Effect of ageing times

HA cement formulated by the mixture of an equimolar powder of TTCP and DCPA with water at P:L of 4 g/ml was aged by Ishikawa *et al.* in a dynamic flow system containing simulated blood plasma to investigate the surface changes that CPC's undergo in solutions that have electrolyte concentrations similar to that of human blood. The simulated blood plasma was comprised of; Na^{2+} (142 mmol/l), K^{+} (5 mmol/l), Ca^{2+} (2.5 mmol/l), HCO_3^{-} (4.2 mmol/l), Mg^{2+} (1.5 mmol/l), Cl^{-} (148.8 mmol/l), HPO_4^{2-} (1 mmol/l) (Ishikawa *et al*. 1994). It was determined that over the 20 week ageing study the sample had increased in mass by a factor of 0.5; this was due to the formation of HA on the surface of the cement. The benefit of this result was an increase in the diametral tensile strength, from 10 MPa at the start of the study, prior to ageing to 16 MPa after 20 weeks of ageing. Phase composition conveyed that the bulk composition remained unchanged; this meant the increase of strength was attributed by the precipitation of the HA layer. While the study was aimed to simulate human blood; this study did not completely meet the requirements of the conditions entirely. The simulated blood plasma composed of the ions listed above does not contain the protein constituents of blood which are known to inhibit the formation of HA on the surfaces of implants.

Solubility

HA is the least soluble calcium phosphate compound in physiological conditions (Nelson 1981). It is possible to create a lattice distortion by incorporating different ions into the crystal structure and thereby increasing the solubility. Some ionic substitutions such as carbonate have been shown to increase the solubility of apatites, while fluoride substitution into the apatite lattice decreases solubility. In the same way, the degree of crystallinity affects the solubility behaviour of apatites; highly crystalline apatites tend to be very insoluble, while poorly crystalline apatites have higher relative solubility (Bohner 2001). Stoichiometric HA was found to be the least soluble among the materials tested, compared to the non-stoichiometric precipitated apatite with high specific surface area and showed higher levels of calcium and phosphate release (Fulmer *et al.* 2002). Following this, Shellis and Wilson studied the apparent solubility distribution of hydroxyapatite at different pH values (Shellis & Wilson 2004); experiments were performed at pH 4.5, 5.0, and 5.5. Results showed a tendency to increase slightly with pH but in most cases the 95% confidence intervals overlapped, indicating a lack of statistical difference between values.

Chen *et al.* use the solid-titration method to investigate the solubility of HA, under the conditions of minimised excess solid, in order to clarify behaviour (Chen *et al.* 2004). The solubility for HA in KCl solution, in the absence of CO_2 obtained, differs considerably from the results of previous solubility studies. The increase in solubility due to CO_2 reported earlier was confirmed, while the effect of excess phosphate was found to be to increase the apparent solubility of HA, contrary to elementary mass-action expectations.

4.2.6 Clinical applications

Pre-clinical studies

Although there have been many commercialised products developed over the years, there still remains the need to formulate improved cement pastes. Taking this into consideration, there are few studies published on the *in vitro* cellular response to CPC's. However, there have been a large number of *in vivo* studies on the development and biological response to HA providing sufficient evidence to progress the development of these cement formulations to allow pre-clinical *in vivo* studies (Apelt *et al.* 2004;Barralet *et al.* 2004;Blokhuis *et al.* 2000;Bohner *et al.* 2005;Constantz *et al.*1995a;Devlin & Lieberman 2007;Frakenburg *et al.* 1998;G.Daculsi *et al.* 2004;Grynpas *et al.* 2002a;Joosten *et al.* 2004;Ohura *et al.* 1996;Kozloff *et al.* 2009;Kurashina *et al.* 1997;Munting *et al.* 1993;Penel *et al.* 1999;Regsegger & Laib 1998;Spivak & Hasharoni 2001;Taniwaki *et al.* 2003).

Commercial formulations

The first commercial CPC products were introduced over 15 years ago for the treatment of maxillo-facial defects (Kamerer *et al*. 1994) and of fracture defects (Constantz *et al*. 1995b). Since then, companies are establishing second-generation cements and are also expanding their range to fulfil the various requirements of clinical orthodontics and orthopaedics. Several *in vitro* studies with injectable CPC's show their feasibility and mechanical effectiveness. Animal studies confirm their osteoconductivity (Apelt *et al.* 2004;Chen *et al.* 2003;Horstmann *et al.* 2003;Iooss *et al.* 2001;Joosten *et al.* 2004;Kim *et al*. 2004;Mendez *et al.* 2004;Turner 2002). An example of these bioactive injectable cements is the commercially available self-hardening calcium phosphate composites, Norian® (Stanton *et al.* 2004), consisting of equimolar amounts of TTCP and DCPA, hardens when mixed with water and

forms a resorbable HA as the end-product. This material provides excellent mechanical properties and direct bone in-growth ability, but it set *in situ* after injection. **Table 4.1** elaborates further on the various commercialized HA cement products.

Table 4.1: Summarizes the commercialised apatite based cement products with their composition details (Bohner *et al.* 2005).

Company	Cement name	Components (Powder (P)/ Solution (S))
ETEX	α-BSM Embarc Biobon	P: ACP (50%), DCPD (50%) S: H2O (unbuffered saline solution)
Stryker-Leibinger Corp.	BoneSource	P: TetCP (73%), DCP (27%) S: H_2O, mixture of Na_2HPO_4 and NaH_2PO_4
Teknimed	Cementek®	P: α-TCP, TetCP, Na Glycerophosphate S: H_2O, $Ca(OH)_2$, H_3PO_4
	Cementek® LV	P: α-TCP, TetCP, Na Glycerophosphate, dimethylsiloxane S: H_2O, $Ca(OH)_2$, H_3PO_4
Biomet	Calcibon® (Biocement D)	P: α-TCP (61%), DCP (26%), CaCO3 (10%), PHA (3%) S: H_2O, Na_2HPO_4
	Mimix™	P: TetCP, α-TCP, $C_6H_5O_7Na_3{\cdot}2H_2O$ S: H_2O, $C_6H_8O_7$
Mitsubishi materials	Biopex®	P: α-TCP (75%), TetCP (20–18%), DCPD (5%), HA (0–2%) S: H_2O, sodium succinate (12–13%), sodium chondroitin sulphate (5–5.4%)
	Biopex®-R	P: α-TCP, TetCP, DCPD, HA, $Mg_3(PO_4)_2$, $NaHSO_3$ S: H_2O, sodium succinate, sodium chondroitin sulphate
Kyphon	KyphOs™	P: α-TCP (77%), $Mg_3(PO_4)_2$ (14%), $MgHPO_4$ (4.8%), $SrCO_3$ (3.6%) S: H_2O, $(NH_4)_2HPO_4$ (3.5 m)
Shanghai Rebone Biomaterials Co.	Rebone	P: TetCP, DCP S: H_2O
Synthes-Norian	Norian® SRS Norian® CRS	P: α-TCP (85%), $CaCO_3$ (12%) MCPM (3%) S: H_2O, Na_2HPO_4

4.3 Brushite

Dicalcium phosphate dihydrate (DCPD) is a mineral, formula $CaHPO_4 \cdot 2H_2O$ (brushite); a precursor of apatite formation. Brushite cements are in general weaker and more acidic than HA cements, however, their constituents are more soluble *in vivo* meaning that resorption may be aided by dissolution (Elliot 1994). Subsequently, research rapidly progresses to increase the mechanical properties, for example: strength, thus expanding prospective clinical application. Brushite cements are resorbed faster compared to HA cements (Nilsson *et al.* 2002) due to the fact that brushite is a meta-stable compound when used under physiological conditions (Vereecke & Lemaitre 1990). The transformation of brushite into apatite after implantation, resulting in an increase of the resorption time should be prevented by adding a magnesium salt of low solubility (Flautre *et al*. 1999).

4.3.1 Chemistry of setting reactions

Brushite cements typically set following the combination of an acidic aqueous source of phosphate ions such as MCPM or H_3PO_4 with β-TCP. The precipitation of brushite crystals is a result of a drop in the pH (lower than 4.2) of the cement slurry following mixing.

β-TCP-MCPM-H_2O cement

The first reported brushite cement by Lemaitre *et al.* (1987) is a product of β-TCP (slightly basic) reacted with MCPM (acidic) and water, to form DCPD (neutral). The MCPM can either be dissolved in the water prior to mixture with the β-TCP or may be combined with β-TCP prior to the water (Mirtchi *et al.* 1989).

$$\beta\text{-}Ca_3(PO_4)_2 + Ca(H_2PO_4)_2.H_2O + 7\ H_2O \rightarrow 4\ CaHPO_4.2H_2O \qquad \text{(equation 4.5)}$$

β-TCP-H_3PO_4-H_2O cement

The use of orthophosphoric acid to replace MCPM as the acid component in formulating brushite cements was demonstrated by Bohner *et al.* (1995).

$$\beta\text{-}Ca_3(PO_4)_2 + H_3PO_4 + 6\ H_2O \rightarrow 3\ CaHPO_4.2H_2O \qquad \text{(equation 4.6)}$$

Bohner *et al.* (1997) claimed that the cement produced posses several advantages when compared to that formed from β-TCP and MCPM, with simpler and faster preparation, easier control of the chemical composition and a relatively high tensile strength to the β-TCP and MCPM cement.

TTCP-CaO-MCPM cement

The acidic nature and rapid reactions of MCPM and H_3PO_4 brushite cements, the quantities of the cement components used are often non stoichiometric; resulting in the formation of a cement matrix consisting of a proportion of unreacted β-TCP. Constantz *et al.* practically produced a phase pure brushite matrix following the mixture of TTCP, MCPM and CaO with an undisclosed dilute solution (Constantz *et al*. 1998).

$$Ca_4(PO_4)_2O + CaO + Ca(H_2PO_4)_2.H_2O \rightarrow CaHPO_4.2H_2O \qquad \text{(equation 4.7)}$$

Nanocrystalline hydroxyapatite-H_3PO_4

Barralet *et al.* reported another brushite cement formation, which set following the mixture of nanocrystalline HA with OA (Barralet *et al.* 2004).

$$Ca_9(PO_4)_5(HPO_4)OH + H_3PO_4 + 17\ H_2O \rightarrow 9\ CaHPO_4.2H_2O \qquad \text{(equation 4.8)}$$

Nanocrystalline HA has a higher specific surface area than that of HA produced by thermal processes due to smaller crystal size and therefore has greater kinetic solubility; increasing the rate of dissolution such that cement formation may occur (Lilley *et al.* 2005). The two major advantages of this formulation, over the other brushite cements are that; (1) the Ca:P ratio of the HA may be lowered so that cement may be produced with lower volume of acidic components; and (2) the HA lattice can accommodate for various ion substitutions into the crystal lattice; leading to possible changes in properties of the set cements (Barralet *et al.* 2004).

4.3.2 Setting properties

Brushite cements possess extremely rapid setting times; Driessens *et al.* confirmed the nucleation and resulting growth of brushite crystals to be rapid with a pH range of 2-6.5 (Driessens *et al.* 1993b). The cement setting times seem to be approximately 1-2 mins (Bohner et al. 2000), which is evidently a limiting factor for clinical applications as it is not practical to leave the surgeon so little time to apply the mould the cement correctly. This has led much research in the investigation of various retardants to slow the setting reaction; added advantages of improving the mechanical properties of the cement also accompany many of these additives.

Retardants

From previous work it is evident that pyrophosphate ions are most effective at increasing the setting times, however, sulphate ions are can simultaneously increase setting times and tensile strength, combinations of both of these retarding agents have been used to control cement properties (Bohner 2000;Bohner *et al.* 2000). The results of the study by Bohner and his co-

workers, reiterates the fact that these ions are able to inhibit DCPD crystal growth. With the addition of tetrasodium pyrophosphate solution at 33 mM concentration they demonstrated a four-fold increase in the final setting time of the brushite cement. A similar effect of pyrophosphate ions was exposed by Mirtchi *et al.* when they used β-dicalcium pyrophosphate (DCPP), with a setting time 5 mins after the addition of DCPP (without DCPP the setting time was observed at 30 s) (Mirtchi *et al.* 1989). The use of calcium pyrophosphate salts was less effective than pyrophosphate solutions since DCPP is relatively insoluble, even at acidic pH values (Grover 2005). Although the addition of pyrophosphate ions retarded the setting reaction, there was no net gain in strength.

$Ca_3(PO_4)_2 + H_4P_2O_7 + 4\ H_2O \rightarrow CaHPO_4.2H_2O + Ca_2P_2O_7.2H_2O$ (equation 4.9)

Mirtchi *et al.* then went on to observe the effects of calcium sulphate hemihydrates (CSH); results exhibited setting times to increase to 7 mins (Mirtchi *et al.* 1989). Unlike the addition of pyrophosphate ions, the CSH not only improved the setting times but also enhanced the diametral tensile strength of the cement; from 1 MPa (without CSH) to 2.5 MPa (with 10 wt% CSH). This therefore meant that the cement paste produced demonstrate higher strengths and better handling times; the combination of which can widen the applications of such cements. More recently, Bohner *et al.* agreed and reported that the effect of the sulphate ions on the setting time is larger below a concentration of 0.1 M. Above this concentration, CSH crystals nucleate and act as nuclei for DCPD crystals, which are the normal product of the setting reaction. This decreases the setting time and decreases the DCPD crystal size, resulting in an increase of the tensile strength of the cement (Bohner 1996).

Barralet *et al.* reported a significant improvement of setting times of brushite cements consisting of equimolar amounts of β-TCP and MCPM with a liquid phase of 500 mM or 1 M solutions of trisodium citrate or citric acid as setting retardants, at P:L of 3.3, 4.0, 4.5 and 5 g/ml. Results exhibit an increase in *I* setting times to 8-12 mins (Barralet *et al.* 2004). This study demonstrated for the first time the use of ionic modification to produce a low viscosity brushite cement paste that was injectable through a hypodermic needle.

4.3.3 Rheological properties

Previous studies demonstrate the use of carboxylic acids and viscosity enhancing agents on the brushite cement cohesion (Alkhraisat *et al.* 2009;Alkhraisat *et al.* 2008a). The cements were prepared using a mixture of β-TCP and MCPM, whereas the liquid phase was formed by 0.5 M citric acid solution modified by the addition of hyaluronic acid of different molecular weights. It was found that medium and high molecular weight hyaluronic acid enhanced the cement cohesion and barely affects the cement mechanical properties. Therefore, hyaluronic acid could be applied efficiently to reduce brushite cement disintegration. However, concentrations would have to be at least 0.5 % w/v, any less and the efficiency to prevent the cement disintegration is compromised (Alkhraisat *et al.* 2009).

A more recent study by the same group reports the effect of silica gel on brushite cement cohesion. The cement was prepared using the same method but with the liquid phase comprised carboxylic acids silica gel. This cement presents a shorter final setting time, better cohesion and higher amount of unreacted β-TCP than the cement prepared without silica gel (Alkhraisat *et al.* 2010). The aim was to produce cement that does not disintegration easily. The simultaneous use of carboxylic acids and silica gel has resulted in shorter cement final

setting time values than those for carboxylic acids alone. These acids inhibit the growth of brushite crystals through the binding of calcium ions by carboxylic groups exposed on the brushite surface (Barralet *et al.* 2005). The addition of silica gel was highly efficient in preventing cement disintegration; this modification could widen their clinical application, by reducing surgery time and resisting disintegration.

4.3.4 Mechanical properties

Brushite cement is too weak to be used in load-bearing areas (Grover *et al*. 2005a) and many studies have been dedicated to improving the mechanical properties of the set cement. Retarding the brushite crystal growth rate results in smaller sized crystals allowing them to pack more closely together and improving the mechanical properties of brushite cements (Grover *et al.* 2005b). However, Barralet *et al.* mentions that the strength improvements made by the addition of organic/inorganic additives will be useful for an application of the cements in some load-bearing areas, for example in upper spine surgery (vertebroplasty) (Barralet *et al.* 2005).

Pyrophosphate ions, sulphate ions, citrate ions, pyrophosphoric acid and carboxylic acids, such as citric, tartaric and glycolic acids have been used to increase the cement setting time and improve its mechanical properties (Alkhraisat *et al.* 2008a;Alkhraisat *et al.* 2008b;Barralet *et al.* 2004;Bohner 1996;Bohner *et al.* 2000;Grover *et al.* 2006;Marino *et al.* 2007).

Without the addition of additives several authors have again manipulated the formulations of the brushite cements. In once such technique Gbureck *et al.* produced tailor-made brushite

blocks with good mechanical properties have been synthesized using a 3D printing technique. This new technique produced cements with compressive strengths of up to 8.7 MPa. A further strength improvement was to hardening of the samples in phosphoric acid for three one minute washes, this increased the strength to 22 MPa (Gbureck *et al.* 2007a); XRD was used to determine the phase composition of these samples. Results proved they mainly consisted of brushite with minor phases of unreacted TCP and a lesser amount of DCPA. More recently, Hofmann *et al.* developed brushite cements as strong as 52 MPa in compression by adjusting particle size and size distribution of the β-TCP and the MCPM powder reactants and also the citric acid concentration, resulting in a decrease of cement porosity to 11% (Hofmann *et al*. 2009). The cement paste exhibited setting times of 4.5 min, which gave a good workable property.

4.3.5 *In-vitro* ageing

The major advantage of brushite cements is the higher solubility under physiological conditions, such that brushite is dissolved at the implantation site more rapidly than HA materials. This property has been demonstrated *in vitro* (Grover *et al.* 2003;Xia *et al.* 2006). However, brushite is meta-stable and this means brushite undergoes hydrolysis to form a stable HA CPC. After completing an ageing study of brushite in PBS for over 19 days, Constantz *et al.* demonstrated by that the brushite had completely converted to HA (Constantz *et al.* 1998).

Studies have been published which have investigated the factors that influence the hydrolysis of brushite cements both *in vitro* (Grover *et al.* 2003) and *in vivo* (Apelt *et al.* 2004), including implant volume, liquid refreshment rate and media composition. The study by

Grover *et al.* has shown that the rate of mass loss from brushite cement and the formation of HA are affected strongly by the above mentioned factors; this in turn inhibited hydrolysis (Grover *et al.* 2003).

Dehydration of brushite

Brushite is a hydrated secondary calcium phosphate that upon heating undergoes a dehydration process at around 130 ºC accompanied with phase transformation to monetite (dicalcium phosphate anhydrous; DCPA) at 160 ºC followed by decomposition of DCPA to calcium pyrophosphate at 425 ºC. It was found that brushite dehydration and DCPA decomposition occurred at lower temperatures in cements set with phosphoric acid and water (Alkhraisat 2009). HA started to appear in water and phosphoric acid brushite cements earlier than in carboxylic acid brushite cements. Carboxylic acids are able to inhibit the formation of HA and it was proven that the addition of citric acid to β-TCP-MCPM mixtures also prevented the formation of monetite.

4.3.6 Clinical applications

Many *in vivo* studies (Alkhraisat 2009;Apelt *et al.* 2004;Bohner *et al.* 2005;Ohura *et al.* 1996;Marino *et al.* 2006;Munting *et al.* 1993;Penel *et al.* 1999;Theiss *et al.* 2005) have demonstrated varied results and authors report incomparable data. However, a general trend shows, using the same animal model, degradation rate decreases as sample size increases, along with the brushite hydrolysis to HA.

Commercial formulations

Brushite cements possess relatively poor mechanical properties, therefore limiting their clinical applications to non-load bearing bone repair or replacements. However, there have been several cases of commercialisation of the brushite cement for the non-load bearing market, which is summarized in **Table 4.2**.

Table 4.2: Summerizes the commercialised brushite based cement products (Bohner *et al.*2005).

Company	Cement name	Components (Powder (P)/ Solution (S))
Synthes-Norian	chronOS™ Inject	P: β-TCP (73%), MCPM (21%), $MgHPO_4 \cdot 3H_2O$ (5%), $MgSO_4$ (<1%), $Na_2H_2P_2O_7$ (<1%) S: H_2O, sodium hyaluronate (0.5%)
Kasios	Eurobone®	P: β-TCP (98%), $Na_4P_2O_7$ (2%) S: H_2O, H_3PO_4 (3.0 m), H_2SO_4 (0.1 m)
CalciphOs	VitalOs	Component 1: β-TCP (1.34 g), $Na_2H_2P_2O_7$ (0.025 g), H_2O, salts (0.05 m pH 7.4 PBS S) Component 2: MCPM (0.78 g), $CaSO_4 \cdot 2H_2O$ (0.39 g), H_2O, H_3PO_4 (0.05 m)

4.4 Conclusion

CPC formulations are extremely promising bone replacement materials, which can be applied via minimal invasive surgical methods. The use of CPC's has reduced infection rates and lessened the aggression (Legeros 1988). Another advantage of CPC's is that the product of the reaction, usually apatite, is obtained at low temperature (Hench 1998a). Therefore, it is much more similar to the biological HA than the HA prepared by the conventional high temperature sintering methods; it is non-stoichiometric, and it has a low crystallinity and a high specific surface area (Ginebra *et al.* 2004). These characteristics increase the reactivity and resorbability of these materials. This chapter has evaluated the various advantages and

disadvantages that surround the development of CPCs and highlighted the availability of the commercialized cement products. Research in the field of CPCs has been growing at a steady pace and will continue to do so until a satisfactory bone replacement material has been developed; fulfilling all of the ideal graft material properties mentioned in Chapter 2.

In the following experimental chapters, various material properties have been manipulated to meet these ideal material properties mentioned above. In chapter five we discuss the importance of producing monetite based cements by means of manipulating the existing brushite cement formulation. Chapter six discusses the importance of phase separation in order to produce self setting or "ready mixed" cement pastes. Following this the addition of antibiotics within the cement matrices and how this affects the mechanical and physical structure of the cements is investigated in chapter seven. Finally chapter eight will explores the degradation of the different cement formulations and how porosity affects the degradation and hydrolysis of cements.

Chapter Five

Formulation of a monetite based cement

5. 1 Introduction

Calcium phosphate cements (CPCs) typically harden following the combination of a powder and an aqueous liquid. The cement paste can initially adapt to the irregular defects (Carey *et al.* 2005), frequently encountered in orthopaedic and craniofacial surgery, and sets to form a hardened graft for the replacement of lost or damaged bone (Grover *et al.* 2005b). These CPCs may be compositionally similar to the mineral phase of bone, and have been shown to be non-cytotoxic, osteoconductive, (Kitsugi *et al.* 1993) and to some extent can be replaced by new bone (Chow 1988). Ripamonti has also reported that CPC materials may exhibit some osteoinductive activity (Ripamonti 1996).

5.1.1 Problems with calcium phosphate cements

Depending on the stoichiometry and pH of the cement slurry, CPCs can set to form a matrix consisting of hydroxyapatite ($Ca_{10}(PO_4)_6OH_2$; HA) at a pH value of >4.2 or brushite ($CaHPO_4.2H_2O$; DCPD) at a pH value of ≤4.2. HA has in the past attracted more research as it compositionally resembles bone mineral. Researchers have, however, demonstrated that highly crystalline HA is insoluble in physiological conditions (-log Ksp = 58.6 at 37 ºC (Grover *et al.* 2005b)) and is resorbed at only 5% per year via osteoclastic activity (Muralithran & Ramesh 2000). This means the HA cement can remain *in vivo* for a considerable period of time following implantation, posing a risk of catastrophic brittle failure (Bohner 2000c). More soluble forms of HA, however, can be produced by reducing crystal size (Ducheyne & Qiu 1999) and incorporating substitutions (e.g. Mg^{2+}, CO_3^{2-}) (Fulmer *et al.*

2002). Some authors have incorporated high volumes of porosity into HA, to improve bonding at the implant-tissue interface by allowing the in-growth of the host tissues into the implant pores (Ducheyne & Qiu 1999;Ducheyne *et al.* 1978), although this has resulted in poor mechanical properties until bone integration occurs (Grynpas *et al.* 2002b;Ryshkewitch 1953).

5.1.2 Possible solutions

To address this problem some researchers (Barralet *et al.* 2002c;Barralet *et al.* 2004;Gbureck *et al.* 2003;Gbureck *et al.* 2005c;Grover *et al.* 2003;Lu *et al.* 2002;Lemaitre *et al.* 1987) have begun to focus on the production and refinement of brushite cements. Brushite cements can be resorbed faster than HA cements (Nilsson *et al.* 2002) as brushite is a meta-stable compound when used under physiological conditions (Theiss *et al.* 2005). Brushite is a sparingly soluble calcium phosphate (-log Ksp = 6.63 at 37 ºC (Grover *et al.* 2005b)) therefore can be resorbed both by cell-mediated mechanisms (Xia *et al.* 2006) and dissolution, meaning that they are potentially fully resorbable in the body (Grover *et al.*2006).

Monetite is the anhydrous form of brushite, ($CaHPO_4$; DCPA) (Elliot 1994); synthesised in the same way as brushite by the simultaneous addition of the same phosphate and calcium solution to the same phosphate solution at a high temperatures (100 ºC), as opposed to ambient temperatures with brushite (Ma *et al.* 2006) or by the dehydration of brushite, as brushite can lose crystal water at high temperatures (>50 °C) (Klammert *et al.*). Although brushite can be resorbed more rapidly than apatite, hydrolysis occurs converting the meta-stable brushite into the very stable apatite (Grover *et al.* 2003). Recently, Gbureck *et al.* demonstrated that monetite ceramics showed a better degradation profile than brushite when

implanted intramuscularly in rats, even though monetite has a lower chemical solubility because the low-solubility apatite phase was not formed in the monetite bioceramic (Gbureck *et al.* 2007b). This was particularly surprising since monetite is less soluble than brushite in physiological conditions (-log Ksp = 7.02 at 37 ºC (Grover *et al.* 2005b)). On evaluation of the retrieved implants, there was no evidence for the formation of HA within the largely monetite matrix. One significant problem with the use of monetite as a bioceramic, however, is that to date there are no cement formulations that set directly to form monetite. Monetite, therefore, has to be produced by a process of cement casting and then high-temperature heat treatment (>100ºC) (Hsu *et al.* 1998), which means that preoperative knowledge of the grafting site is required and it is not possible to incorporate heat sensitive therapeutic molecules into the ceramic matrix. The reason that monetite is not formed in cement matrices is not because it is thermodynamically less stable than brushite, which is actually a less stable phase, but because the rate of brushite crystal formation is considerably higher than for monetite (Elliot 1994).

Therefore, the hypothesis is to prove if the reaction in equation 4.5 produces brushite cements then if the water component is limited we would assum that the reaxction would then result in a monetite cemnt. This would follow the same theory as the dehydration method used to produce monetite, without the high temperatures.

5.1.3 Aims

From the literature it is evident that the formation of a monetite cement, without the use of high temperatures (casting, sintering, etc.), may pose to be a difficult task. However, in this study we have manipulated the formulation of the traditional brushite cement system to

produce slow setting monetite cement. Using the MCPM-β-TCP formulation, the powder components remain the same, while the liquid phase is replaced by a non-aqueous liquid; thus limiting the water component. The slowing down of the cement reaction, by limiting the addition of water, will favour the production of monetite instead of brushite. The paste must exhibit minimal effect on the mechanical properties of the cement to allow clinical usage in orthopaedic and/or craniofacial surgeries.

5.2 Materials and Methods

5.2.1 Materials

β-TCP was synthesised by heating an equimolar mixture of calcium carbonate (Merck, Darmstadt, Germany) and dicalcium phosphate anhydrous ($CaHPO_4$, Mallinckrodt Baker, Griesham, Germany) at 1400 ºC for 14 h prior to quenching at room temperature. The resulting sinter cake was broken up using a pestle and mortar and then passed through a 160 μm sieve. The powder was then milled for a period of 24 h in a centrifugal ball mill (PM400 Retsch, Germany) using a zirconia container (110 mm diameter) and zirconia charges (10 mm diameter). Monolcalcium phosphate monohydrate ($Ca(H_2PO_4)_2.H_2O$; MCPM, Fluka, Sigma, Dorset, UK), monocalcium phosphate anhydrous ($Ca(H_2PO_4)_2$; MCPA, Sigma, Dorset, UK) glycerol (Analytic Reagent grade; Fisher Scientifics, UK), and sodium alginate (viscosity = 570 MPa/s; Protanal SF200, pharmaceutical grade; FMC BioPolymer, UK) were used as received from the suppliers without further modification.

5.2.2 Cement formulation

The cement powder was formed from an equimolar mixture of β-TCP and MCPM. The powder components were combined and the resulting powder was homogenised using a vortex mixer (Fisher brand, UK) for a period of 5 min. For the monetite cement, the liquid component was glycerol containing 2wt% sodium alginate and in the case of the control materials double distilled water (dH_2O) was used as the liquid component.

Samples were prepared by mixing the powder component with the liquid component at powder-to-liquid mass to volume ratio (P:L) of 3 g/mL. The powder and liquid of the cement paste were mixed using a spatula to form a paste that was placed into an open-ended rubber

mould of diameter 5 mm and depth 10 mm, the walls of the mould were perforated to allow liquid exchange between the samples and the environment. To induce setting, the samples were immersed in phosphate buffered saline (PBS; Sigma, Dorset, UK) at 37 ºC on an orbital shaker (HT Infors, Infors UK Ltd, Wigan, UK) at 50 rpm. In the case of the control material, the cement powder was mixed with dH_2O at a P: L of 3 g/mL and the resulting paste was cast into a PTFE split mould to produce samples of diameter 6 mm and height 12 mm.

5.2.3 Cement paste stability and setting

The washout resistance was tested by shaping the premixed CPC sample into a small sphere (~ 5 mm in diameter) by hand, and then immediately placing it in 5 ml of double distilled water (Takagi *et al.* 2003). Samples demonstrated washout resistance by maintaining their structural integrity after being fully immersed in PBS. The initial and final setting times of the cement were determined using the Gilmore needles. The cement was considered initially set when 35.9 g was loaded on to a needle with a tip diameter of 800 μm (300 KPa) failed to make a perceptible indentation on the surface of the cement. The time measured from the powder-liquid mixing to this point was used as the initial setting time for the specimen. The final setting time was determined in the same way except using a 5.3 MPa load.

5.2.4 Cement mechanical properties

All samples were tested wet following immersion in PBS at 37 ºC for 24 h. Prior to testing, geometrical measurements of the samples were made to allow the subsequent calculation of cement porosity using Archimedes principle. For compression testing, the cement cylinders were loaded parallel to the their long axes using a Universal testing machine (Lloyd, Southampton, UK) at a constant cross head displacement of 2 mm/min until failure occurred.

Cement fragments were collected and dried at 37 ºC for further characterisation. Platinum coated cement fracture surfaces were examined using a field emission gun scanning electron microscope (SEM) (JEOL, JSM-7000F. UK). To determine the influence of storage time on the compressive strength (CS) exhibited by the premixed cements, the cement pastes were sealed in a universal container and stored at 4 ºC for periods of 3, 7, 14, 28 and 90 days before being cast into moulds in ambient conditions and allowed to harden in PBS at 37 ºC.

5.2.5 Perfusion through the cement pastes

To understand the uptake of water by the samples during the setting reaction, the paste was immersed in an aqueous environment; the diffusion of methyl blue, through the cement paste was investigated. The paste was packed into rigid, clear plastic tubing of different lengths, 10, 15, 20, 25 and 30 mm; the diameter was constant at 8 mm and the wall thickness was 500 µm. One end of the tubing was sealed with Para film (Parafilm® M, Structure Probe, Inc. USA) to allow the methyl blue to enter through one way and the diffusion was only measured in one direction only. The samples were withdrawn from the solution daily and digital images were taken. Dye penetration was quantified using image analysis (Image J, 1.36b, Wayne Rasband, National Institute of Health, USA).

5.2.6 Cement composition

X-ray powder diffraction data were collected using CuKα1 radiation from a powder diffractometer (D5000, Siemens), aligned in transmission mode. The data set was collected from 5 º to 60 º 2θ with a step size of 0.05 º. A multiphase, whole pattern Rietveld analysis was used to determine the crystalline phase compositions of the samples.

To determine whether the cement setting is diffusion limited, a cement sample was dissected into several layers. The cement measured a total radius of 5 mm **(Figure 5.5A)**; sections were cut using a scalpel shaving off 1 mm through the lenth of the sample for each layer after which the cement layers were separately powdered and examined. Each layer was characterized using the X-ray diffractometer and Rietveld refinement, which were compared with control samples. Rietveld refinement is a technique devised for use in the characterization of crystalline materials. The neutron and x-ray diffraction of powder samples results in a pattern characterized by peaks in intensity at certain positions. The height, width and position of these peaks can be used to determine many aspects of the materials structure.

Comparisons between the groups were made by the analysis of variance using single factor ANOVA. Differences were determined statistically significant with $\rho < 0.05$. Data are expressed as mean ± SD.

5.3 Results

The results of the various studies are illustrated below. The initial study was carried out using the glycerol and alginate combination to make the cement paste, made up of the powder components of the traditional brushite cement. Following the initial study various other gelling agents were explored to improve the results and determine the reason for the slow setting reaction which favoured the formation of monetite cement as the final set cement product instead of brushite.

5.3.1 Slow setting monetite cement

Cement setting and stability in solution

The incorporation of glycerol and sodium alginate into the brushite cement pastes resulted in considerable increases in both the initial and final setting times exhibited by the cement pastes.

Table 5.1: The formulations, mechanical and setting properties of the CPCs investigated in this study.

Powder components	Liquid Component	Setting Times (min)		Compression Strength (MPa)	Porosity (%)
		Initial	Final		
β-TCP + MCPM	Water	0.48 ± 0.06	6.90 ± 1.66	15.6 ± 5.8	36
	Water + 2wt% Alginate	1.21 ± 0.74	7.00 ± 1.56	7.9 ± 2.3	45
	Glycerol + 2wt% Alginate	60.7 ± 8.63	1355 ± 105	8.6 ± 3.5	13

Following the mixture of the powder and liquid components, the β-TCP–MCPM cement paste exhibited an initial setting time of 0.5 ± 0.1 min and a final setting time of 6.9 ± 1.7 min **(Table 5.1)**. In comparison the β-TCP–MCPM cement paste combined with glycerol and sodium alginate exhibited an initial setting time of 60 min and a final setting time of 1355 min **(Table 5.1)**. Although this setting time would be considered too long for a non-modified cement system, no significant disintegration of the cement paste was noted on immersion in dH_2O **(Figure 5.1)** and the cement continued to harden once immersed. **Table 5.1** also shows a significant decrease in porosity with the addition of glycerol.

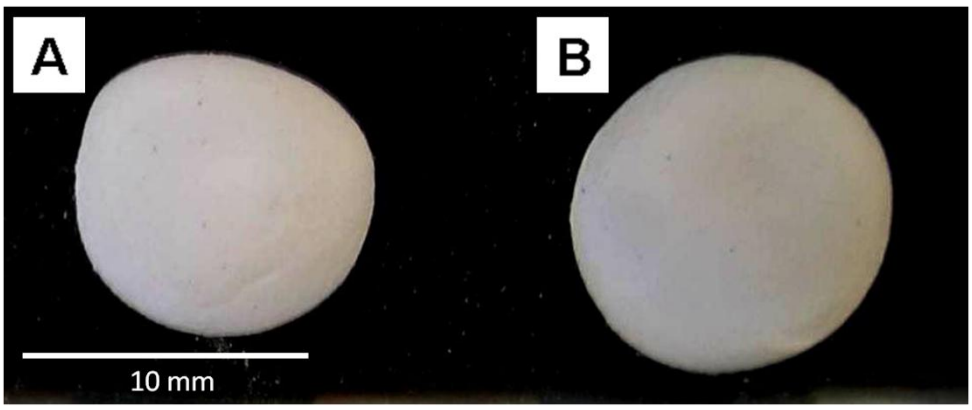

Figure 5.1: Image of spheres of the cement paste during immersion in PBS; (A) MCPM control cements (β-TCP + MCPM + water) and (B) MCPM cement paste (β-TCP + MCPM + glycerol). Images demonstrate the washout resistance of the paste formulations compared to the control samples; no visible degradation of the cement was evident.

To determine how the incorporation of sodium alginate and glycerol into the cement paste influenced cement microstructure, the cement fracture surfaces were evaluated using SEM. The control cement microstructure consisted predominantly of 'blade-like' crystals of approx. 50 µm length by 10 µm in width as widely reported in the literature **(Figure 5.2A)**. The addition of glycerol to the cement mix resulted in a significant change in microstructure, with the formation of irregular sub-micron crystals **(Figure 5.2B).**

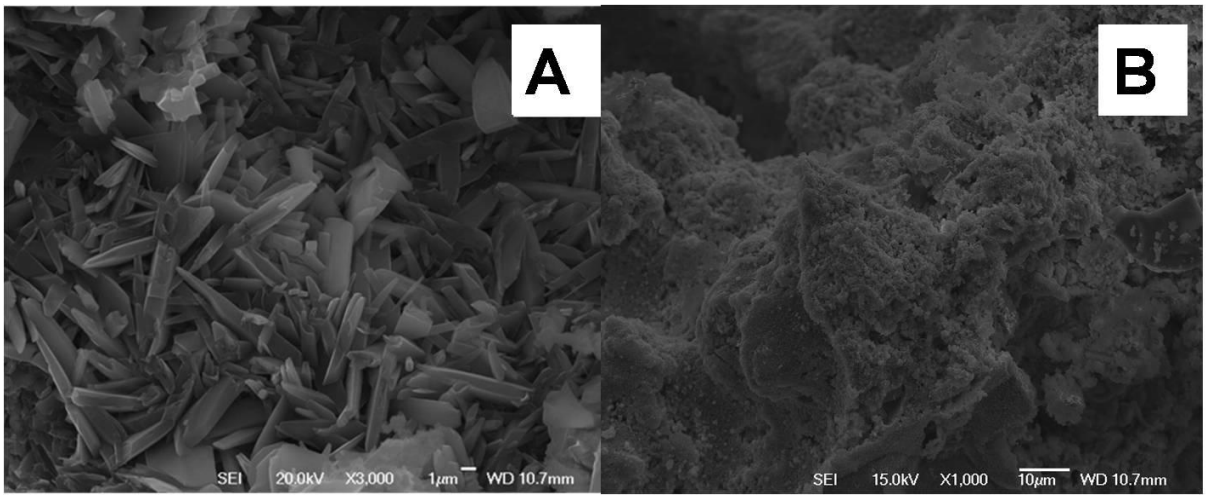

Figure 5.2: Scanning electron micrographs of cement fracture surfaces without (A) and with (B) the addition of sodium alginate and glycerol. The addition of the sodium alginate and glycerol resulted in a marked change in the morphology of the crystals within the cement matrix from predominantly blade-like to irregularly shape.

Mechanical properties with ageing cements

In order to determine the 'shelf-life' of the material, the sodium alginate and glycerol paste was stored for periods up to 90 days in a hermetically sealed container at 4 °C and was subsequently formed into cylindrical samples for testing in compression **(Figure 5.3)**. There was an initial statistically significant increase in the mean CS of the hardened materials up to 14 days of ageing from 8.6 ± 3.5 MPa to 13.2 ± 1.5 MPa ($p<0.05$), followed by a subsequent deterioration in compression strength ($p<0.01$) after 90 days of ageing (5.8 ± 0.7 MPa) **(Figure 5.3)**.

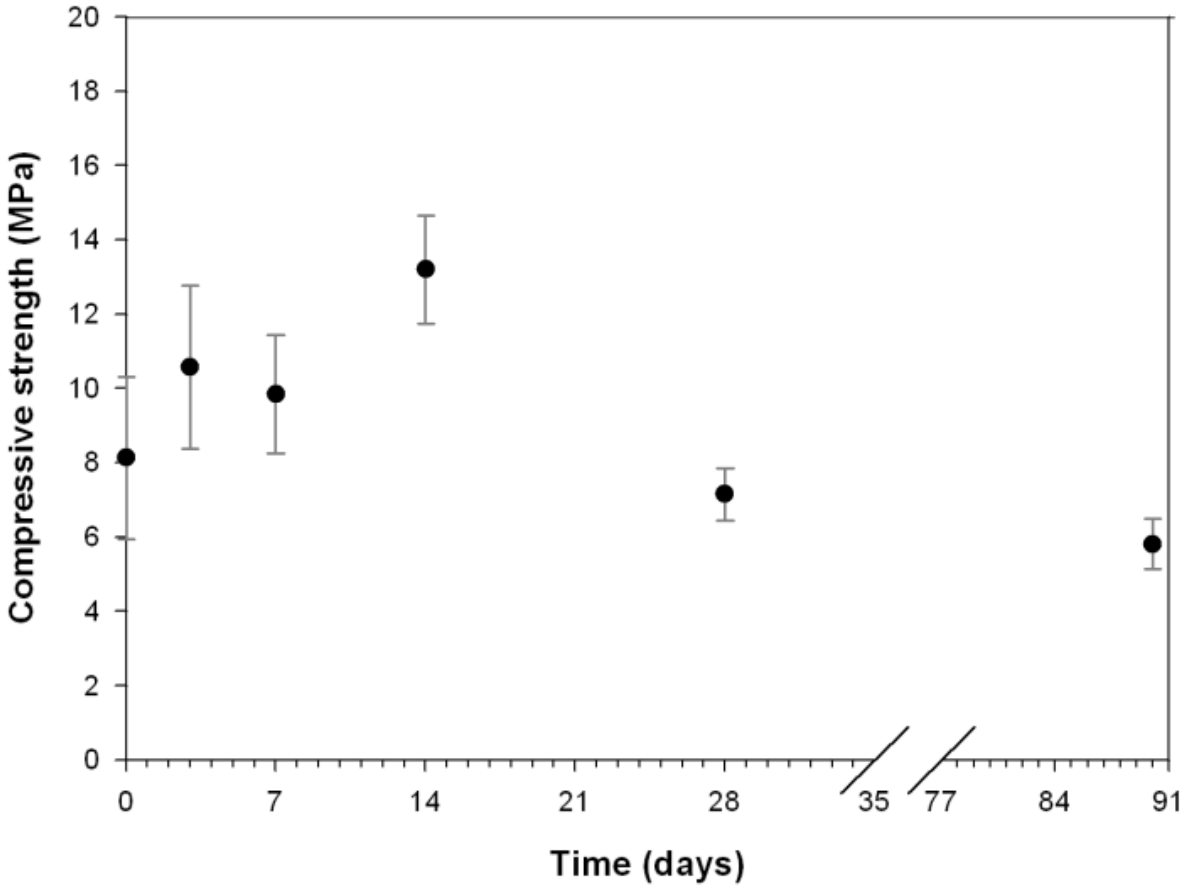

Figure 5.3: Effect of storage, of the paste formulation (at 4 ºC) prior to setting, on the compressive strengths exhibited by the hardened material.

The influence of ageing on the microstructure of the cement was determined using SEM **(Figures 5.4 A-F)**. The microstructure of the cement changed little throughout the study, and consisted at all timepoints of densley packed and irregularly shaped crystals. The crystals that formed the matrix of the cement contrasted significantly with those previously reported to form within the microstructure of monetite ceramics (Prado *et al.* 2001), which exhibit a plate-like structure of 400 nm in diameter. The storage of the cement paste in the sealed containers for 90 days did not seem to have a significant influence on the microstructure of the hardened material.

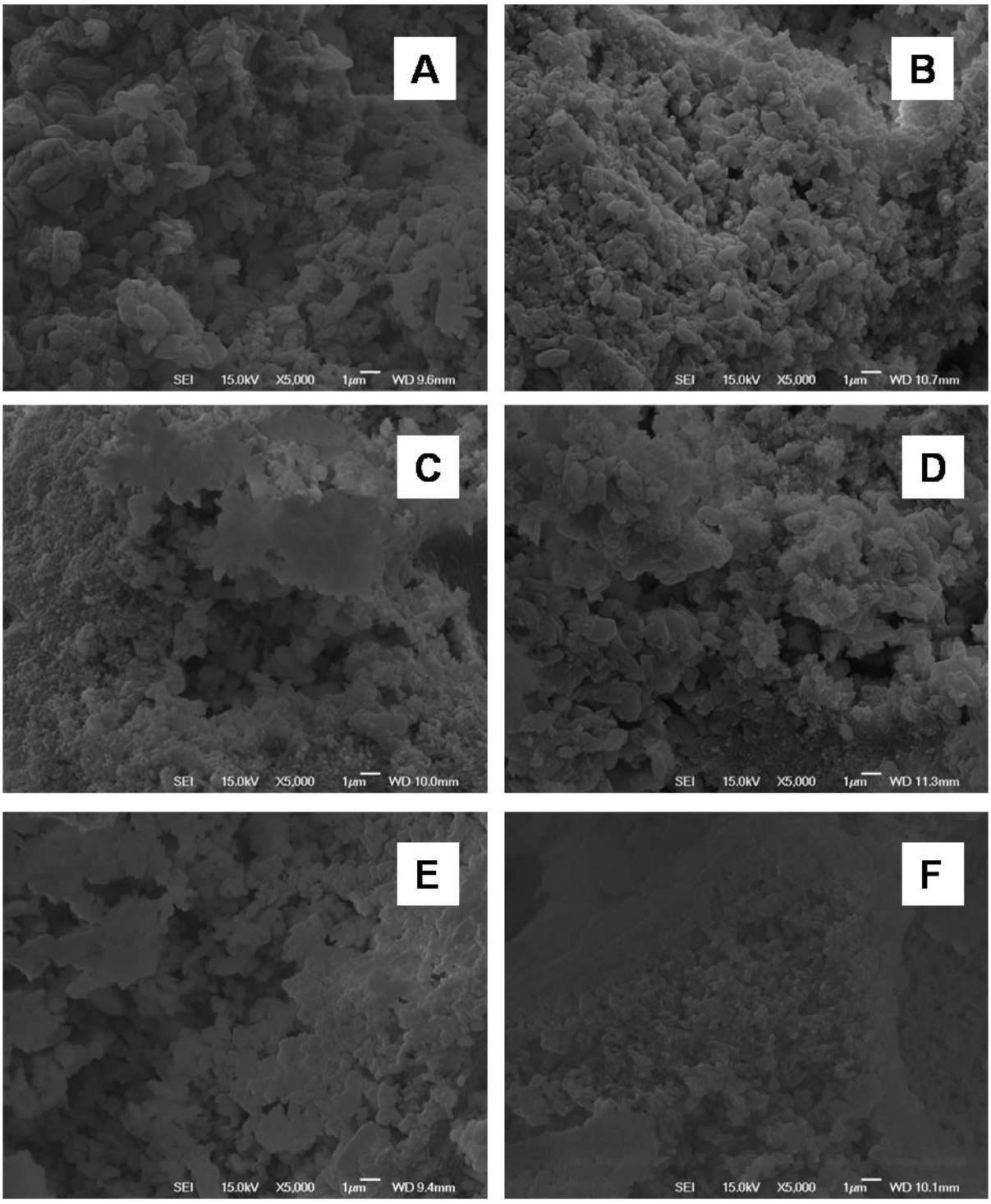

Figure 5.4: SEM micrographs show microstructure of the fractured surface of the aged cement samples. Samples were aged for 90 days in total; here we can see the minimal effect on the microstructure of the monetite cements over the period of time. Sample A illustrates the sample at day 0; sample B at day 3; sample C at day 7; sample D at day 14; sample E at day 28 and sample F at day 90.

Perfusion of the cement paste

Since hardening of the cement paste is dependent upon exchange of the glycerol in the paste with water, a cylinder of cement of diameter 10 mm was immersed in PBS for a period of 20 h in order to determine whether the reaction was diffusion limited.

The resulting hardened structure was dissected into layers of depth 1 mm **(Figure 5.5A)**. The phase composition of each layer was determined by means of Rietveld refinement phase analysis. Within the timeframe of the experiment there was little variation in the composition of the cement matrix, which in each case was formed principally of monetite **(Figure 5.5B).** There was a definite increase in the ratio of monetite to brushite toward the centre of the sample. Layer 1 for example consisted of 11 ± 2wt% brushite and 77 ± 2wt% monetite and layer 5 consisted of 2 ± 2wt% and 83 ± 2wt% of brushite and monetite, respectively.

In order to visualise the penetration of the sample by a liquid, cement cylinders were immersed in methylene blue. The only cement samples that were completely saturated with the methylene blue stain were the 10 mm and 15 mm samples, which became saturated after 4 and 9 days, respectively **(Figure 5.6)**. As the experiment proceeded, the rate of perfusion of the methylene blue through the cement matrix slowed significantly and complete penetration of the cement was not noted when the cement paste cylinder was of length >20 mm **(Figure 5.6A).** However, had the samples been left in the coloured solution for longer, the sample >20 mm would have also been fully saturated.

Although it is acknowledged that the molecular diameter of methylene blue is in the order of six times larger than water (1.35 nm compared with 2.75 Å) and hence may not be representative of water penetration, it is evident that cement setting significantly slows liquid penetration **(Figure 5.6B)** and therefore may place an upper limit on the maximum size of a paste-like cement material that requires water ingress for hardening to occur.

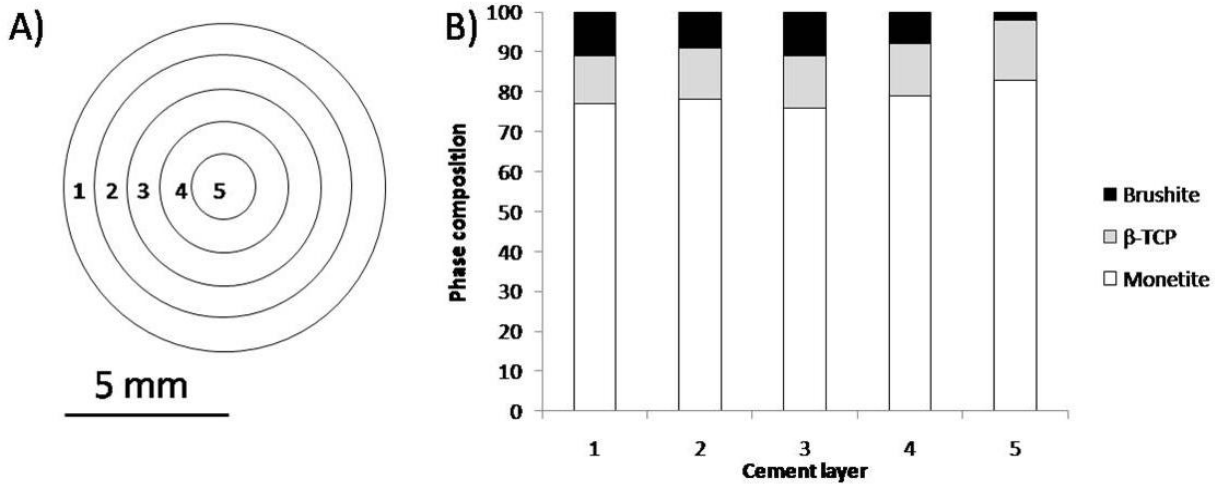

Figure 5.5: A schematic diagram illustrating the sections of cement dissected from the hardened cement cylinder (A) following immersion in PBS for a period of 20 h and the crystalline phase composition of each corresponding layer (B).

The results from **Figure 5.6A** and **B** suggest that during the setting reaction the outer layers of the sample set more rapidly than the inner most layers. X-ray diffraction **(Figure 5.7)** which determined the relative amount of β-TCP and MCPM converted to monetite in each layer was used to confirm this theory. **Figure 5.7** reveals the relationship between the layers and the relative conversion from β-TCP to monetite.

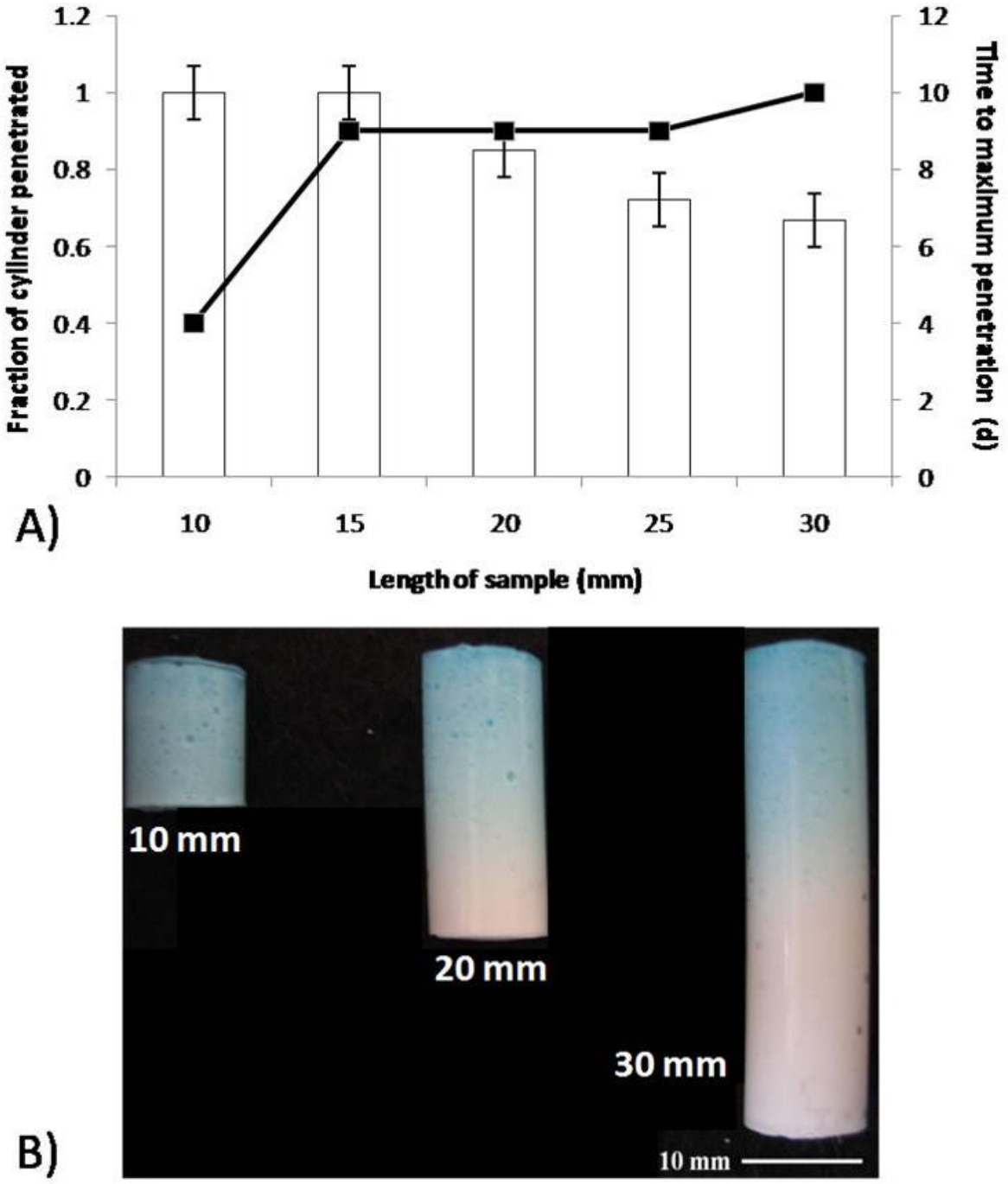

Figure 5.6: There was an upper limit on the distance that the methylene blue solution could perfuse the hardening cement paste, with samples of 10 and 15 mm in length being the only samples completely perfused (A), the rate of perfusion reduced significantly with time, showing that the cement hardening reaction provided a barrier to perfusion. B) Shows cement paste cylinders of 10, 20 and 30 mm of length following 9 days immersion in methylene blue solution.

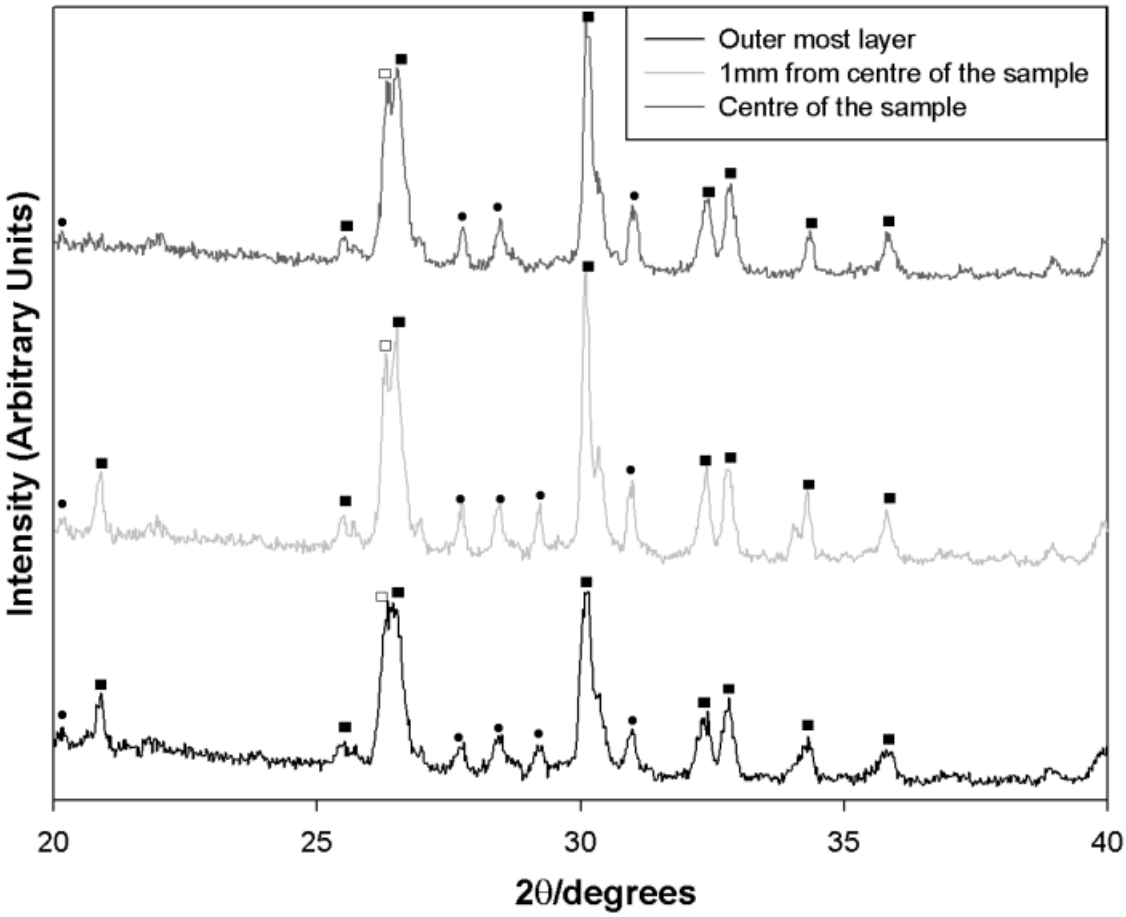

Figure 5.7: XRD results of the different layers of the cement paste sample. Layer 1 = outer most layer and layer 5 = inner most layer. The graph proves that the water-glycerol exchange is more efficient near the surface compared to the inner layer. The various peaks are indicative of the composition of the samples; ■ Monetite; ○ Brushite; ● β-tri-calcium phosphate (β-TCP); □ Monocalcium phosphate monohydrate (MCPM).

Cement composition

As expected the X-ray diffraction patterns of the control cements predominately consisting of brushite and some unreacted β-TCP **(Figure 5.8)**. After storage in paste form for 24 h at 4 °C, but prior to to immersion in PBS, the modified cement paste was shown to consist predominantly of crystalline β-TCP and MCPM. On immersion in PBS, this paste hardened to form a matrix that consisted of monetite and β-TCP alone. Relatively little brushite was detected within the hardened cement **(Figure 5.8)**.

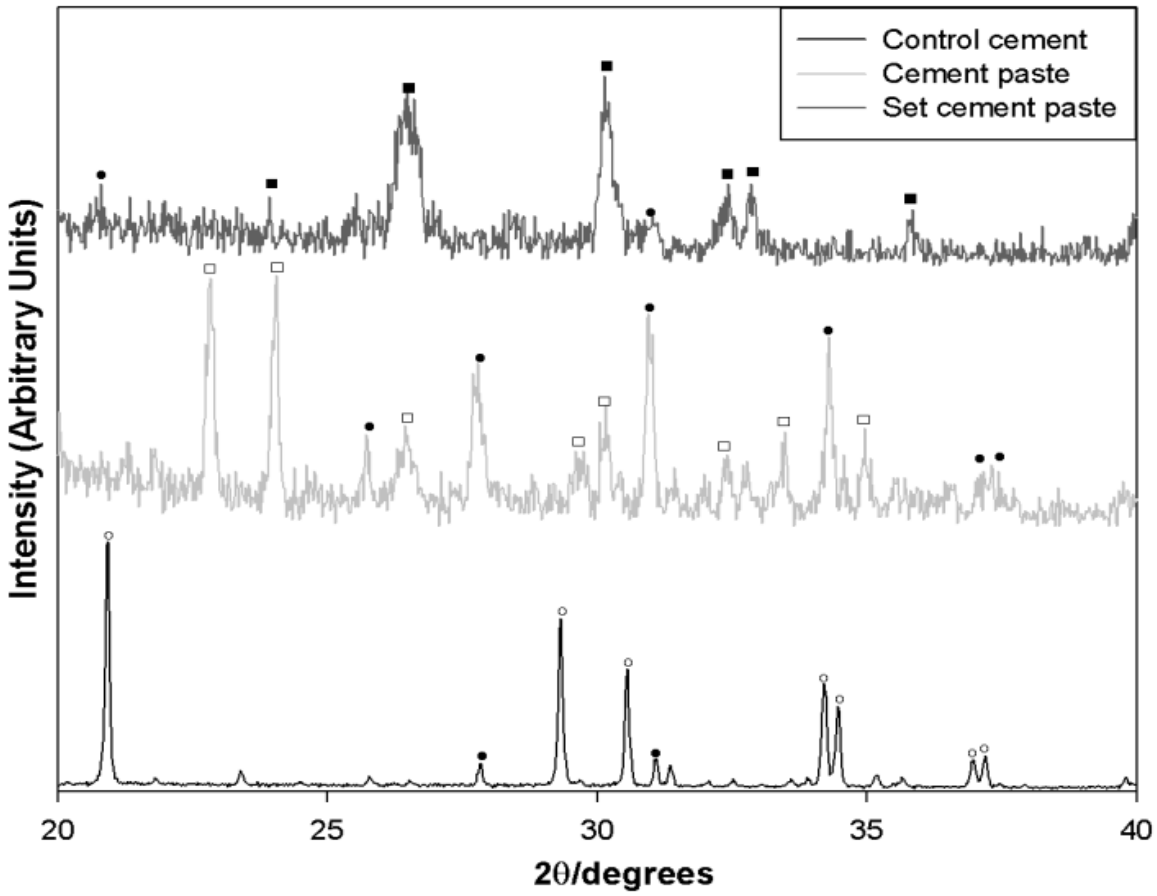

Figure 5.8: Compares the diffraction patterns of the MCPM control cement (β-TCP + MCPM + water) (bottom) with the paste formulation before (middle) and after (top) the cement paste has hardened. The various peaks are indicative of the composition of the samples; ■ Monetite; ○ Brushite; ● β-tri-calcium phosphate (β-TCP); □ Monocalcium phosphate monohydrate (MCPM).

To determine whether the formation of monetite was caused by the presence of alginate or glycerol within the cement paste, samples were formed using a range of sodium alginate concentrations between 0.2wt% and 2wt%, and a sample was made containing glycerol alone. There was little or no change in the relative intensity of the peaks indicative of monetite and β-TCP regardless of the quantity of sodium alginate present **(Figure 5.9)**, additionally, monetite was shown to form in the cement paste even without the addition of sodium alginate.

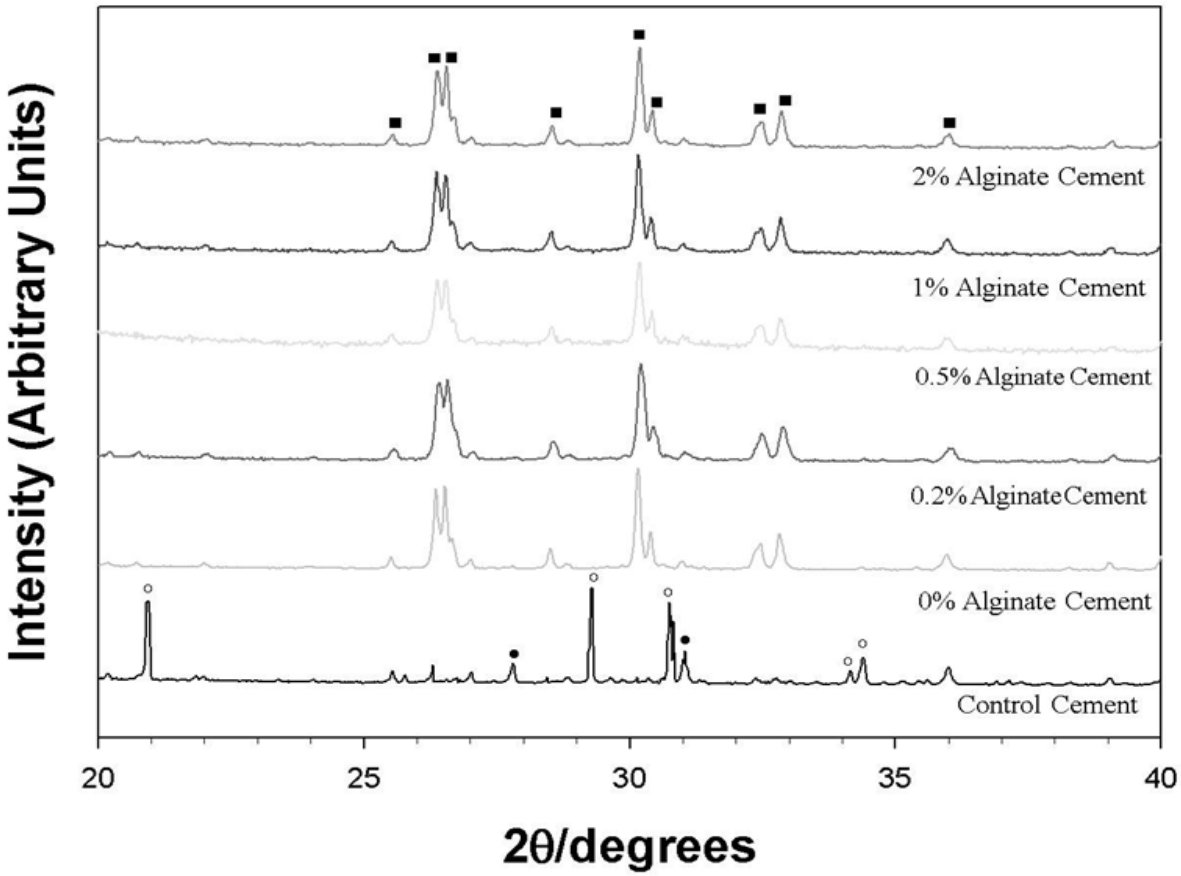

Figure 5.9: Compares the diffraction patterns of the MCPM paste formulation (made using glycerol and alginate) with varying amounts of alginate. The various peaks are indicative of the composition of the samples; ■ Monetite; ○ Brushite; ● β-tri-calcium phosphate (β-TCP); □ Monocalcium phosphate monohydrate (MCPM).

5.3.2 Comparing gelling agents

The initial study illustrates the use of alginate as the gelling agent and the results of these are found above, in section 5.3.1; the results highlight that the monetite cement is formed by slowing down the setting reaction, as the water component is limited. The cements demonstrated slow setting time then the control (brushite) cement and also lower compressive strengths. Consequently, a further study was undertaken to demonstrate whether a change in the gelling agent was a means of improved material properties. Various gelling agents are used in this study, for which more details can be found in **Appendix 2**.

Cement setting, stability and mechanical properties

The various different gelling agents were used in the formulation of the cement pastes and mechanically tested; the results are illustrated below in **Table 5.2**.

Table 5.2: The effect of the use of different gelling agents on the mechanical and setting properties of the CPCs investigated in this study.

Gelling agent	Setting Times (min)		Compression Strength (MPa)	Porosity (%)
	Initial	Final		
Alginate	60.8 ± 8.06	1355 ± 105	8.6 ± 3.0	13
Agarose	61.2 ± 8.04	1260 ± 156	8.1 ± 2.1	19
Carrageenan	62.7 ± 8.33	1280 ± 165	8.2 ± 2.1	20
Chitosan	64.5 ± 8.03	1440 ± 125	6.8 ± 3.2	28
Gellan gum	55.3 ± 8.23	1200 ± 60	9.3 ± 2.2	11
Gelatine	60.7 ± 8.63	1320 ± 90	8.6 ± 3.1	16

Figure 5.10 demonstrates that there is minimal effect when the gelling agent is varied on the average compression strengths of the cement paste formulations. The use of a gelling agent with the non-aqueous liquid has a significant effect on the compressive strength, as it is reduced by almost 50%, however, between the variations of the gelling agents there is no noticeable difference.

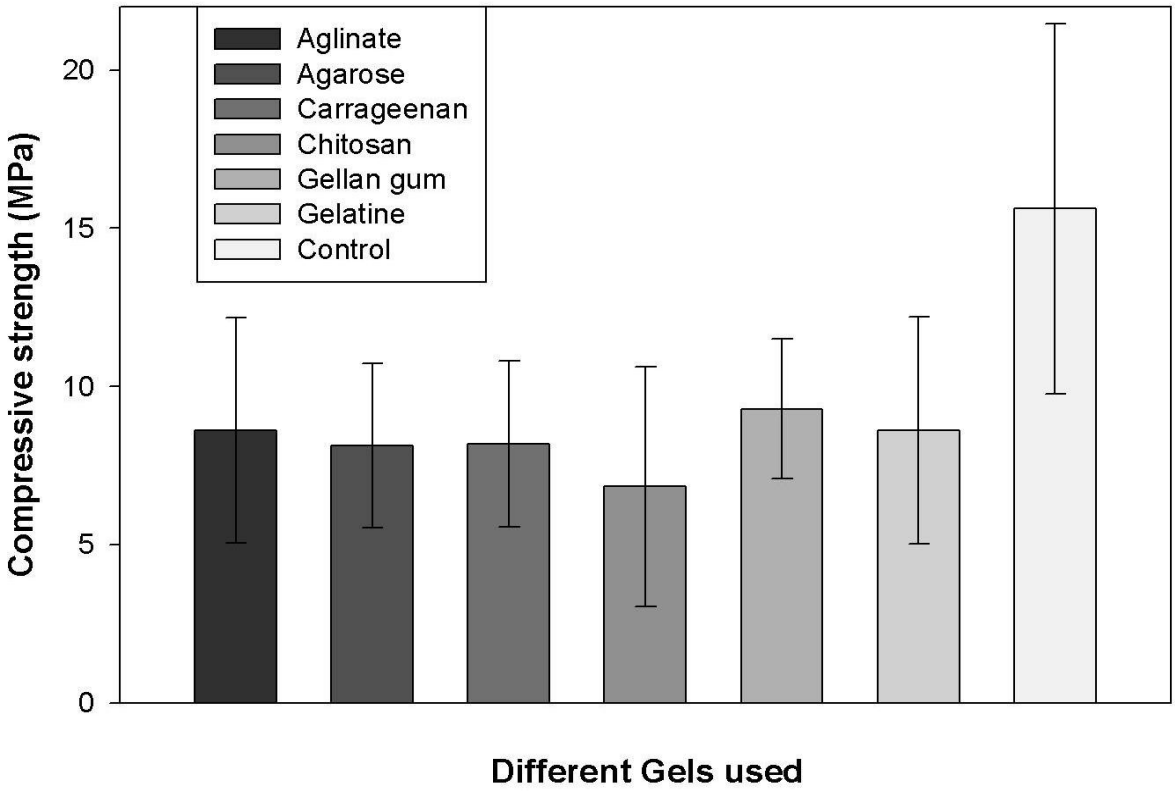

Figure 5.10: Effect of the variation in gelling agent of the paste formulation on the compressive strengths exhibited by the hardened material; all samples were prepared in the same manner.

Cement composition

The XRD pattern in **Figure 5.11** illustrates the difference in the composition of the each sample, in comparison to the control cement pattern (the pattern shown at the very bottom of the graph in Figure 5.18). The symbols suggest the presence of monetite and brushite in the set cement paste samples, compared to the control sample; which shows predominately brushite peaks only. Again the variation in the gelling agent used had no effect on the composition at a glance; further phase composition analysis will determine the exact quantities of the phases present in watch sample. The SEM images in Figure **5.12A–F**, suggest that there is no difference in morphology of the cements created using the various gelling agents.

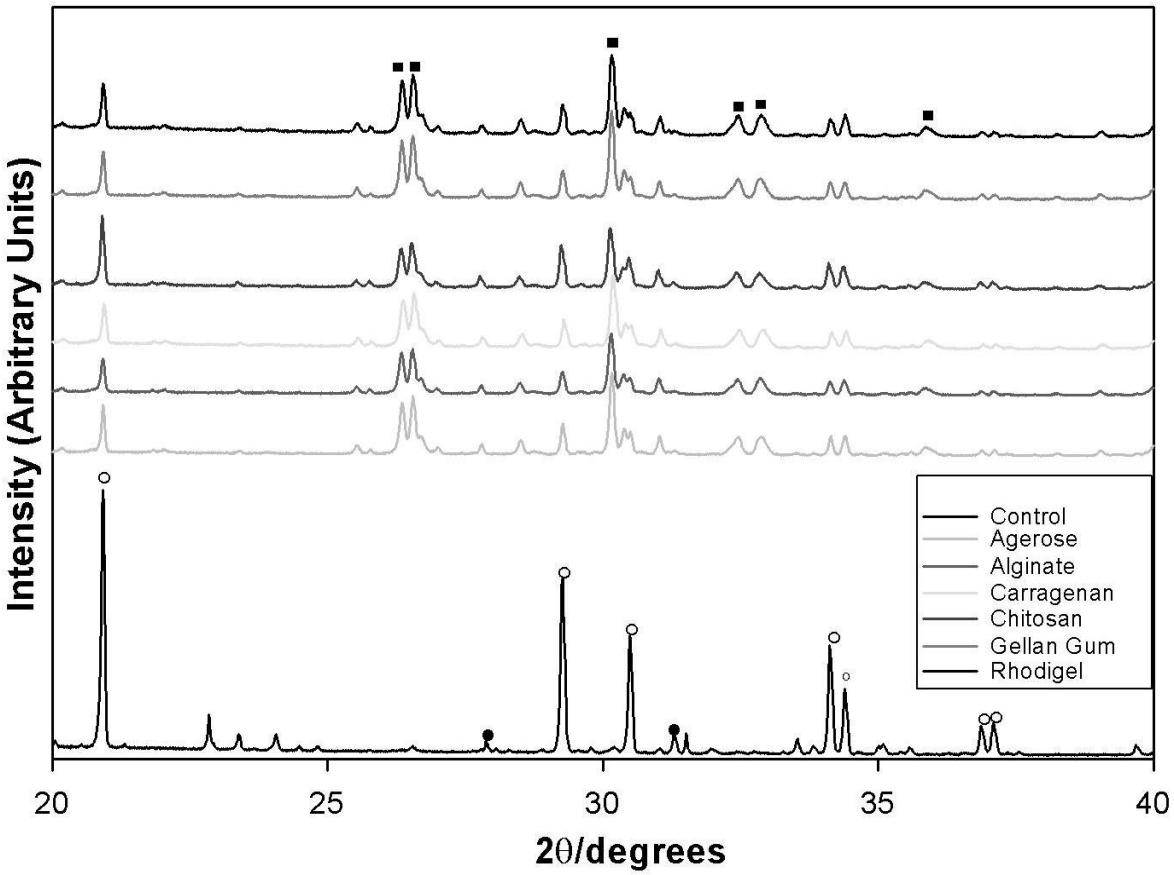

Figure 5.11: Compares the diffraction patterns of the MCPM control cement (β-TCP + MCPM + water) (bottom) with the paste formulation after the cement paste has hardened, using various different gelling agents. The various peaks are indicative of the composition of the samples; ■ Monetite; ○ Brushite; ● β-tri-calcium phosphate (β-TCP); □ Monocalcium phosphate monohydrate (MCPM).

Unlike the monetite shown in the above section 5.3.1, here in **Figure 5.12A–F**, the traditional monetite cement which forms plate-like crystals (Prado *et al.* 2001) can be seen. The flat plate-like structures are 1.0 μm in width and vary in length from 1.0 – 5.0 μm. Figures 6.10b, c and d, illustrate morphologies more like those demonstrated by brushite crystals, long flat needle-like structures (Grover 2005).

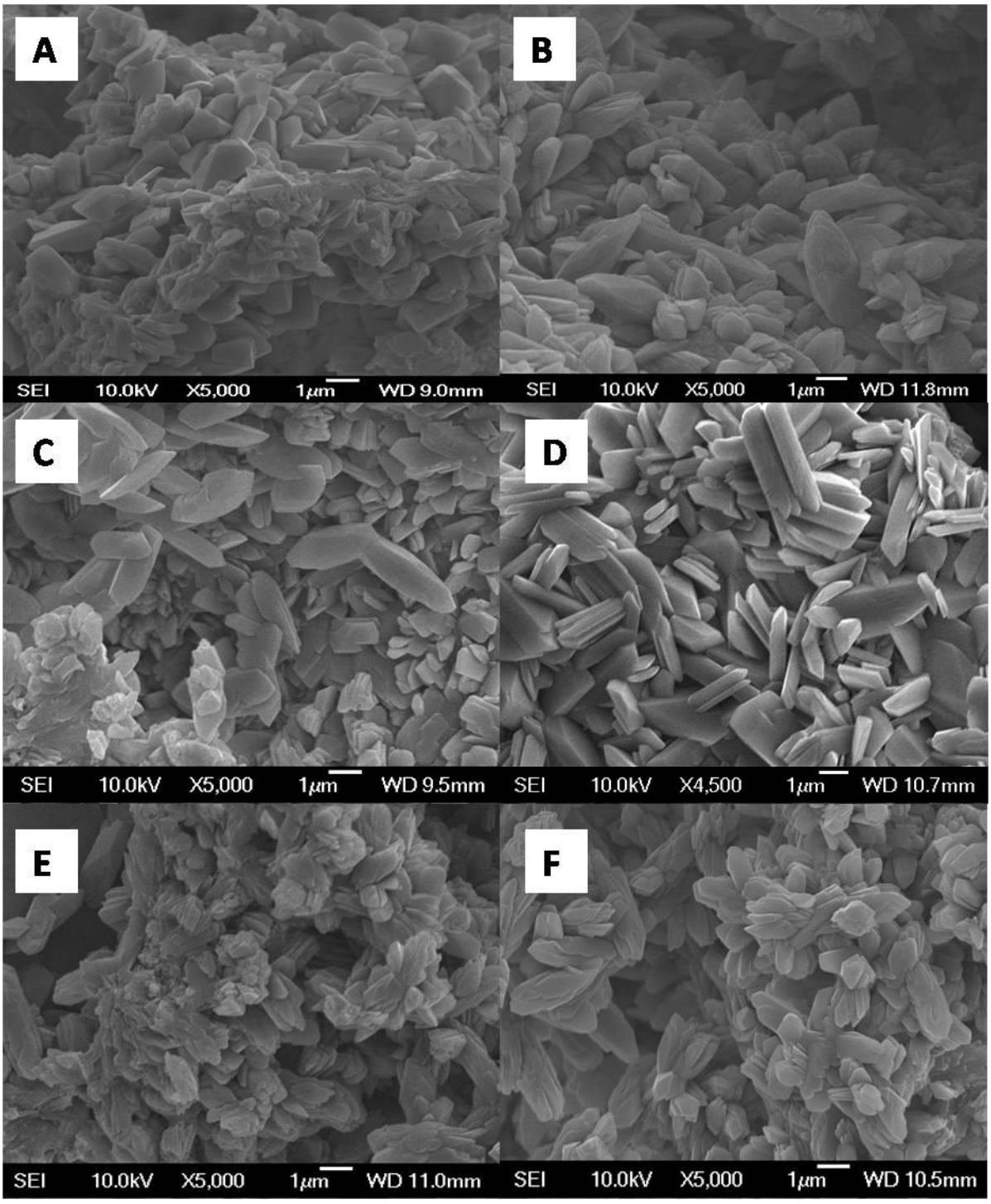

Figure 5.12: SEM micrographs show microstructure of the fractured surface of the different cement samples; each sample is composed using different gelling agent. Sample A illustrates the gelling agent Alginate; sample B uses Agarose; sample C uses Carrageenan; sample D uses Chitosan; sample E uses Gellan gum and sample F uses Gelatine. Here we can see the minimal effect on the microstructure of the monetite cements with varying the gelling agent.

5.4 Discussion

In the past ten years there has been a considerable change in the development of calcium phosphate based cement materials from those that set to form apatite, which exhibits limited resorption *in vivo* to those that set to form more soluble calcium phosphate phases such as brushite (Alkhraisat *et al.* 2008b;Gorst *et al.* 2006;Grover *et al.* 2003;Grover *et al.* 2006;Grover *et al.* 2008;Rousseau *et al.* 2002;Jinawath *et al.* 2001;Theiss *et al.* 2005). Due to the considerable refinements of brushite cement formulations they now exhibit a similar CS to that of apatite cements and can be delivered in a minimally invasive manner; their widespread use has been limited by a an unpredictable degradation rate, which may be influenced by implant location, composition or physical properties. The unpredictability of brushite cement degradation is as a result of the meta-stable nature of brushite, which when immersed in physiological solutions can hydrolyse to form apatite in accordance with Equation 5.1 (Bohner 2000).

$$5CaHPO_4.2H_2O \rightarrow Ca_5(PO_4)_3OH + 2H_3PO_4 + 9H_2O \qquad \text{(equation 5.1)}$$

Although several approaches have been investigated to prevent this phase transformation, none have been used in a commercially available material. Recently, Gbureck and co-workers demonstrated that the dehydrated form of brushite (monetite; $CaHPO_4$), is considerably more resistant to hydrolysis and hence may be more rapidly resorbed following implantation (Gbureck *et al.* 2007a).

To date, however, monetite ceramics can only be synthesised using elevated temperatures or by storing highly acidic brushite cement formulations at temperatures of >37 °C (Jinawath *et al.* 2001). The requirement of an additional processing stage means that

monetite ceramics cannot currently be delivered in cement form and hence suffer from many of the drawbacks associated with other bioceramics that are sintered prior to use, such as: difficulty to fit to irregular contours, requirement of preoperative knowledge of the defect and the requirement of a high temperature processing stage, which prevents the incorporation of temperature sensitive therapeutic molecules. Therefore, here for the first time we report the formation of a cement material that sets to form a matrix consisting of monetite without the requirement of an additional heating stage. The cement was formed by the addition of glycerol and sodium alginate to the cement mix rather than water alone.

The formation of monetite within the hardening cement material could be attributed to one of three factors: 1) The maintenance of a low pH value within the cement matrix; 2) The presence of sodium alginate preventing the incorporation of water into the brushite crystal; 3) A change in crystallisation kinetics to favour the formation of monetite rather than brushite. The control cement formulation hardened to form a matrix that consisted predominantly of brushite **(Figure 5.8)**, this suggestes that the formation of monetite within the cement matrix could not be attributed to the acidic nature of the cement matrix, that has previously been shown to result in monetite formation within brushite cements (Bohner *et al.* 2003).

It has previously been reported that the addition of sodium alginate to a precipitation reaction resulted in the precipitation of monetite, which increased in a monotonic manner with the addition of increasing quantities of the sodium alginate hydrocolloid (Lima *et al.* 2006). This change in composition was attributed to the ability of alginate to chelate calcium ions in the newly forming crystals and hence prevent the incorporation of layers

of water into the monetite crystal lattice. While this mechanism could go some way toward explaining the compositional changes that occured within the cement matrix, here we demonstrated that there was no relationship between the quantity of sodium alginate added to the cement mix and the amount of monetite forming within the cement matrix. Indeed, monetite formed within the cement matrix in the absence of sodium alginate **(Figure 5.9)**. This suggests that the addition of glycerol was critical to the formation of monetite within the cement. The presence of glycerol could have favoured the precipitation of monetite rather than brushite since mass transport throught the glycerol would have been hindered in comparison to water. As a consequence, the rate of crystal formation would have been reduced significantly **(Figure 5.2)**. Since brushite is actually less thermodynamically stable than monetite and forms only because its rate of crystallisation is an order of magnitude faster than monetite (3.32×10^{-4} mol DCPD min^{-1} m^{-2} (Elliot 1994)), reducing the rate of crystal formation within the cement so drastically could have favoured the formation of monetite within the cement rather than brushite. Indeed, the earliest report of purely synthesized monetite required that the precursor calcium nitrate and ammonium phosphate were adjusted to a pH value of 3 and then interdiffused through nitric acid prior to washing with acetone (Louati *et al.* 2005). The conditions in this study would have been very similar, with a low pH value within the cement paste and the limited interdiffusion of the reactants through the media.

The slow perfusion of liquid throught the cement paste was shown by the relatively slow penetration of methylene blue dye through the hardening material **(Figure 5.6)**. As setting proceeded, the rate at which dye penetration slowed significantly and in the case of cylinders of diameter 10 mm and length >10 mm, perfusion through the setting paste stopped

altogether. This suggests that with cementitious materials which require the exchange of water with a non-aqueous solvent such as glycerol, there is an upper limit to the size of implant that can be applied and will set to form a homogeneous matrix **(Figure 5.5)**. **Figure 5.7** shows that the inner most layers of the cement pastes have a relatively lower β-TCP to monetite conversion, compared to the outer most layers. This means that if the diffusion distance is kept small the setting time would be shorter and therefore, producing stronger cement. The formation of an implant that is homogeneous is particularly important to cement used for biomedical applications since a heterogeneous matrix results in the formation of a material with poor mechanical properties and a large proportion of unreacted acidic or basic compounds that could cause long-term complications *in vivo*. Efforts have previously been made to develop premixed cement pastes that set to form matrices of apatite (Carey *et al.* 2005;Takagi *et al.* 2003) or brushite (Han *et al.* 2009). While these studies demonstrated the efficacy of each premixed cement, none evaluated the homogeneity of the setting reaction throughout the matrix, and although Han *et al.* did report the formation of some monetite, it was as an impurity phase rather than the predominant product of the setting reaction. One reason for this could be that Han *et al.* used very small samples (diameter 6mm and height 3mm) and as such water penetration into the matrix would not have been limited by sample size **(Figure 5.6)**.

Han *et al.* also stated the importance of washout resistance of the cement material following implantation. Previously, Carey *et al.* observed that small particles of a TTCP-DCPA cement pastes elicited into the elute as the samples were setting even though the samples were not placed under agitation (Carey *et al.* 2005). The release of small debris could potentially cause a severe inflammatory response if implanted (Miyamoto *et al.*

1999). As such, sodium alginate has previously been incorporated into calcium phosphate cement to prevent the production such debris with significant success. The incorporation of sodium alginate here also prevented the generation of particulate material as a result of wash-out **(Figure 5.1)**. The setting times exhibited by the premixed cement material were considerably longer than for the control cement **(Table 5.1)**. While a final setting time of more than 20 h is inappropriate for traditional cement materials formed from the combination of a powder and liquid phase prior to implantation, in the case of this formulation where setting proceeded following immersion, the cement is not required to fully set before the surgeon closes the implant site.

The mechanical strength of any bioceramic cement is an important parameter as the cement requires having some load-bearing ability. The CS of monetite are demonstrated as 2.05 ± 0.2 MPa according to a recent study (Desai *et al.*2008), which is relevant for bone replacement as human trabecular bone has compressive strengths of 2–10 MPa. The CS results exhibited here **(Table 5.1** and **5.2)** are comparable to previous work with brushite cements (Charriere *et al.* 2001). Control cement exhibited 15.6 ± 5.8 MPa which reduced to 8.6 ± 3.5 MPa with the addition of the sodium alginate. **Figure 5.3** illustrates the changes in CS of the stored cement pastes over time; exhibiting initial average CS for MCPM was 8.1 ± 2.2 MPa. The data collected in this study shows that in the first 3 days the CS increased from 8.1 ± 2.2 MPa to 10.6 ± 2.0 MPa. There was a statistically insignificant decrease between day 3 and 7 (day 7 = 9.8 ± 1.6 MPa) and then an increasing to 13.2 ± 1.5 MPa. By 90 days the CS exhibited was 5.7 ± 0.7 MPa. This suggests that the CS decreases over time however after 3 months the CS was reduced by 38% of the initial CS measured and by 63% of the highest CS value of the monetite sample.

Further work was then undertaken to compare the use of various other gelling agents, such as Agarose, Chitosan (Carey *et al.* 2005). These gelling agents conveyed comparable results to that of Alginate. The gelling agents had average CSs from as low as 6.8 ± 3.2 MPa, using chitosan to 9.3 ± 2.2 MPa, and using gellan gun. There were several other gels which produce cements with compressive strengths around 8 MPa **(Table 5.2** and **Figure 5.10)**. The composition of the cement pastes when other gelling agents were used are illustrated in **Figure 5.11**. It is clear that the hardened cement pastes are composed predominately of monetite, with some peaks which represent brushite **(Figure 5.11)**. This means that limiting water component in this setting reaction is the key to the formation of monetite, and possibly where water in present in abundance there is a chance of brushite formation, hence there is the presence of both crystals in the final set cement paste. SEM micrographs **(Figure 5.19A–F)** show the typical structure of monetite cement, in the form of plate-like crystals (Prado *et al.* 2001). However, samples which may consist of some brushite are also demonstrated on the SEM micrographs; the presences of flat plate-like crystals and flat needle-like structures, representing monetite and brushite, respectively **(Figure 5.19A–F)**.

5.5 Conclusions

Here we have reported the first cement system that sets to form a matrix predominantly of monetite. The formation of monetite rather than brushite was attributed to the limited perfusion of the hardening cement paste with water during setting. Incomplete penetration of the cement by methylene blue has demonstrated the importance of sample volume on the formation of the set cement phase. i.e. too small volumes would set quickly and in the case of Han *et al*. produce a brushite phase as water is not limited sufficiently; large volumes, as demonstrated in this study, indicates that the perfusion will stop once this limit is reached.

Form this study; it was found that many different gelling agents can be used in the formulation of the paste cement. However, regardless of which gelling agent was used, the average material properties were similar. This indicates that the gelling agent is not the main influence of strength or structure here. The formation of monetite was possible due to the slowing down of the setting reaction, which was possible by limiting the water component.

Chapter Six

Controlled-setting cement pastes using polymer encapsulation

6.1 Introduction

In clinical situations, the surgeon's ability to accurately mix the cement and then to place the cement paste in the defect within the prescribed time is a critical factor in achieving optimum results (Takagi *et al.* 2003). The requirement for on-site powder–liquid mixing increases the surgical time (Carey *et al.* 2005). It may also result in insufficient and heterogeneous mixing thus compromising the implant strength, and inconsistencies between operators causing unpredictable variations in graft performance. Thus, it would be desirable to have a ready mixed cement paste that is stable in the package and hardens only after being placed in the defect.

One way to enable controlled setting would be to separate the cement components from one another in a polymeric micro-capsule that breaks down and releases a reactive component following the application of an appropriate stimulus. This section describes the use of an emulsion or double emulsion system to encapsulate orthophosphoric or pyrophosphoric acid and then incorporate the spheres into a ready-mixed paste consisting of β-TCP and water. The formed spheres were designed so that they would breakdown in response to pH, temperature (Eudragit) or the application of shear (poly(caprolactone)).

6.1.1. Microencapsulation

Microencapsulation is an extensively used technique to capsulate food flavourings (Kim *et al.* 1996), cosmetics (Miyazawa 2000), drugs (Mi *et al.* 2009;Sugawara *et al.* 1994;Wan *et al.*

1992), protein (Calvo 1997), antigens (Cleland 1998;Singh & O'Hagan 1998), cells (Mi 1999), and enzymes (Tiourina & Sukhorukov 2002). In biotechnology, microencapsulation of biologically active materials like living cells and enzymes may increase biological half-life. In the pharmaceutical industry, the reasons for microencapsulating a drug are to improve its stability, e.g. protection of vaccines from gastric acid, to reduce side effects or mask unpleasant taste, to reduce dosing frequency and total dosing amount, to obtain better pharmacological activity, and for sustained (long-lasting) release.

Microcapsules can be of the regular shape (e.g. spherical, tubular and oval) or irregular shape. The spherical form of microcapsules is the most common form in controlled release systems as release from a sphere should be more predictable than from an irregular shape. As illustrated in **Figure 6.1**, the typical forms of spherical microcapsules include matrix, single-wall (or single-layered), multi-wall (or multi-layered) and multi-core (Hua-Jiang Huang, Xiao Dong Chen, & Wei-Kang Yuan 2006). For easy administration of microencapsulated component, loaded microparticles can be further designed into tablets, capsules, and microparticle suspensions in a solution, which can be injected when their particle size is small enough.

The most common methods of microencapsulation are extrusion, solvent evaporation, phase separation, interfacial polymerization, spray drying and ionotropic gelation (Huang *et al.* 2006). Extrusion involves forming droplets by forcing a solution or suspension of active (core) material and wall material through a syringe, a coaxial needle or a nozzle (Breitenbach 2002); this is difficult for use in large-scale production, and the beads obtained are large. Spray drying has been widely utilized in the food industry. With the conventional spray

drying technique, the particles obtained can be small but the size distribution is very wide (Poncelet 1999). Interfacial polymerization always involves using many organic solvents and potentially cytotoxic wall materials (Ji *et al.* 2001).

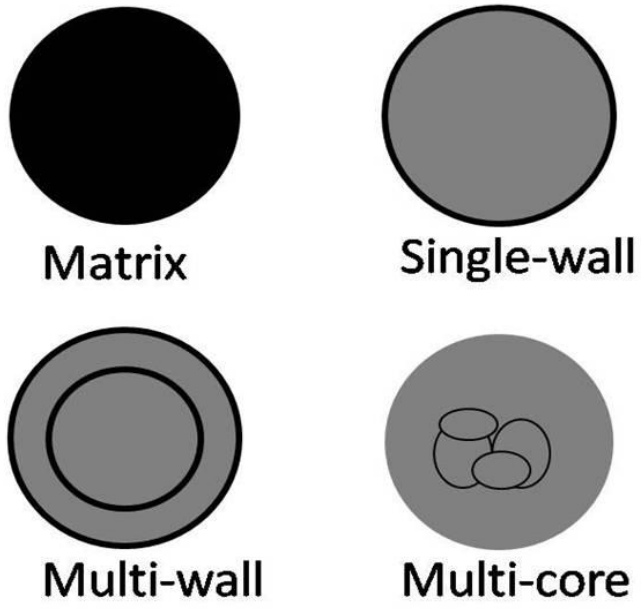

Figure 6.1: Typical forms of spherical microcapsules, which are made by various different methods, depending on the application. Matrix and single-wall are typically relatively easy to manufacture, compared to multi-wall and multi-core, which require more complex processing methods.

Solvent evaporation also involves using relatively more organic solvents. The substances encapsulated by these means may have more side effects after oral administration as they contain more non-biodegradable wall materials or residual solvents. Phase separation and ionotropic gelation involves less organic solvents, so substances microencapsulated pose less of a risk to the health of an individual exposed to them (Poncelet 1999). As emulsification appears to be a more straightforward way to obtain small droplets with relatively narrow size distribution, the following will focus on the emulsification based techniques, coupled with solvent evaporation, ionotropic gelation, phase separation and spray drying.

6.1.2 Emulsions

An emulsion is a mixture of two immiscible substances; one substance (the dispersed phase) is dispersed in the other (the continuous phase). Examples of emulsions include butter and margarine, espresso, mayonnaise, the photo-sensitive side of photographic film, and cutting fluid for metalworking. Emulsions tend to have a cloudy appearance, because the many phase interfaces (the boundary between the phases is called the interface) scatter light that passes through the emulsion (Chern 2006). Emulsions are unstable and do not form spontaneously; energy input through shaking, stirring, homogenizers, or spray processes are needed to form an emulsion. Over time, emulsions tend to revert to the stable state of oil separated from water (van der Graaf *et al.* 2005). Surface active substances (surfactants) can increase the kinetic stability of emulsions greatly so that, once formed, the emulsion does not change significantly over years of storage (Chern 2006).

Emulsions are part of a more general class of two-phase systems of matter called colloids. Although the terms colloid and emulsion are sometimes used interchangeably, emulsion tends to imply that both the dispersed and the continuous phase are liquid. There are three types of emulsion instability: flocculation, where the particles form clumps; creaming, where the particles concentrate towards the surface of the mixture while staying separated; and breaking, where the particles coalesce and form a layer of liquid (Antin & Salager 1986). Whether an emulsion turns into a water-in-oil emulsion or an oil-in-water emulsion depends on the volume fraction of both phases and on the type of emulsifier.

Double emulsions have significant promise for the production of multi-compartment microspheres. Although a certain measure of controlled instability is desired in some cases,

such as for a drug delivery systems, generally the stability of double emulsions is low and poorly controllable and therefore a main problem with regard to shelf life of a product (van der Graaf *et al.* 2005). The instability usually leads to a significant part of the internal phase being lost during the production of the double emulsion. A double emulsion is an emulsion in an emulsion; two main types of double emulsions can be distinguished: (1) water-in-oil-in-water (W/O/W) emulsions (Okochi & Nakano 2000), in which a W/O emulsion is dispersed as droplets in an aqueous phase, and (2) oil-in-water-in-oil (O/W/O) emulsions, in which an O/W emulsion is dispersed in an oil phase. W/O/W emulsions are more common than O/W/O emulsions. Double emulsions contain more interfaces and are even more thermodynamically unstable than single emulsions (Antin & Salager 1986).

The most important conventional emulsification devices are stirring apparatuses, rotor–stator systems and high-pressure homogenizers. Stirrers are the earliest type of equipment that has been used for emulsification. The dispersed phase is broken up by the shear stresses of the turbulence; the energy consumption is usually large. For the production of double emulsions, it is important not to use high-shear stresses to prevent disruption of the internal emulsions and coalescence with the external phase (van der Graaf *et al.* 2005).

6.1.3 Materials

Poly-caprolactone (PCL)

PCL is biodegradable polymer suitable for controlled release due to a high permeability (Wang *et al.* 2007b). Biodegradation of PCL is very slow in comparison to other polymers, so it is most suitable for long-term delivery extending over a period of more than one year meaning that it should retain ortho- and pyrophosphoric acid for long enough to allow for

manufacture, storage and delivery. A selection of drugs encapsulated in microspheres have exhibited a faster dissolution rate than pure drug due to an increase in surface porosity of microspheres (Kim *et al.* 2004). The release rate of drug from PCL depends on type of formulation, method of film preparation, PCL content, size and percent of drug loaded in the microcapsules (Miyai *et al*. 2008).

Eudragit®

Eudragit® polymers are copolymers derived from esters of acrylic and methacrylic acid, whose physicochemical properties are determined by the different functional groups attached to them **Figure 6.2** (Rohm Pharma 2003).

The two grades of Eudragit® used in this thesis were:

- Eudragit S100 is an anionic polymer of methacrylic acid and methacrylates with a -COOH group, which is designed to dissolve at pH values > 7.0 for release at the implantation site, usually for targeted delivery in the ileum between pH 6.0–7.5 (Li 2005;Zahirul *et al.* 2000).
- Eudragit RS has a low content in quaternary ammonium groups compared with other types of Eudragit (Rohm Pharma 2003). The ammonium groups, present as salts, make the polymer permeable under certain conditions. This property was utilised to make temperature sensitive polymer matrices (Fujimori *et al.* 2002).

Therefore, the hypothesis is to prove whether a novle CPC can be formulated that can set post operatively upon a change of environment, such as temperature or pH.

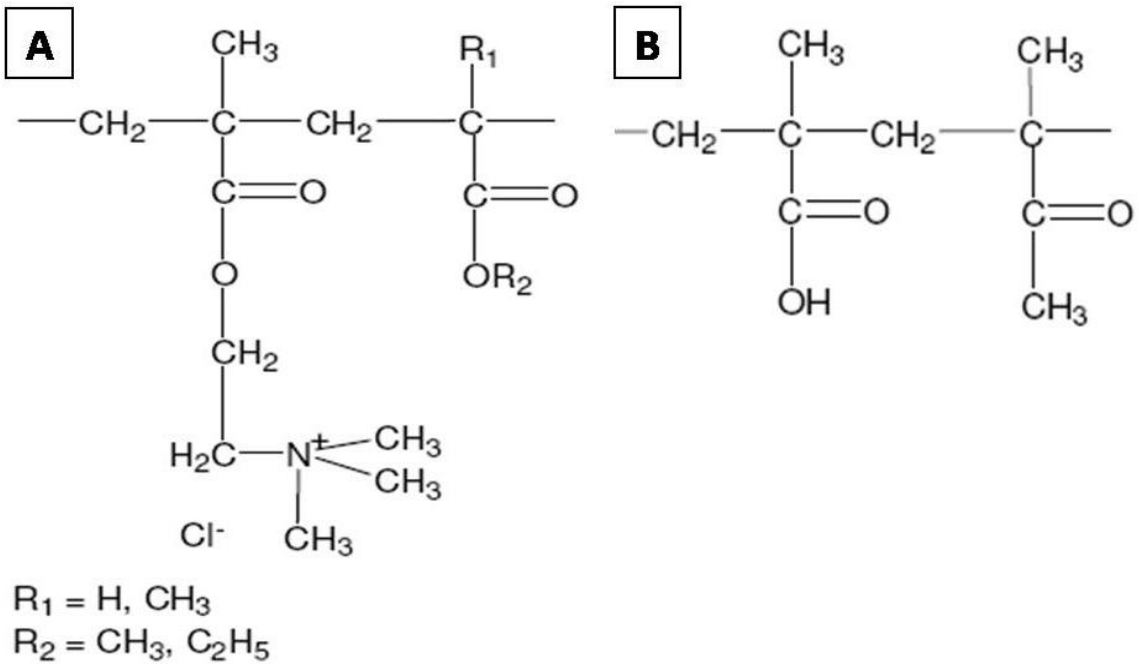

Figure 6.2: The chemical structures of Eudragit RS 100 (A) and Eudragit S100 (B) (Reproduced from (Rohm Pharma 2003)).

6.1.4 Aims

This chapter investigates the separation of the two cement components during the production, packaging, storage and transportation of the cement by using Eudragit® polymers, and demonstrate how the cement paste is able to set on demand when exposed to a change in temperature or pH.

The initial study involves the encapsulation of the traditional brushite cement by the formulation in Equation 4.6 (β-TCP-H_3PO_4-H_2O cement); this determined whether this method was viable. From these results, once the method of microsphere production had been refined the new modified brushite cement was tested; encapsulating pyrophosphoric acid (PPA) instead of H_3PO_4 (orthophosphoric acid, OA).

6.2 Materials and Methods

Eudragit® polymers are copolymers derived from esters of acrylic and methacrylic acid, whose physicochemical properties are determined by the different functional groups attached to them (Rohm Pharma Polymers, 2003). The two grades of Eudragit® used were; Eudragit S100 (pH sensitive) and Eudragit RS (thermo-sensitive).

6.2.1 Production of Microspheres

Most methods of producing microspheres are modifications of three basic techniques (Freitas *et al.* 2005); Solvent extraction/evaporation; Phase separation; Spray drying. Here solvent extraction evaporation methods have been used. The process consisted of four steps: (i) dissolution or dispersion of the substance to be encapsulated in an organic solvent containing the polymer (ii) emulsification of this organic phase in a second continuous phase immiscible with the first one (iii) solvent extraction into the continuous phase, and evaporation of the solvent, transforming the droplets into solid microspheres (iv) harvesting and drying (Freitas *et al.* 2005).

Eudragit®-PEG blend

Thermo-sensitive polymer matrices consisting of Eudragit® RS (Rohm Pharm, Darmstadt, Germany) and PEG 400 (polyethylene glycol with a low molecular weight) (Sigma Aldrich); polymers were produced by the solvent casting method (Fujimori *et al.* 2002). They were dissolved at 13% PEG to Eudragit® weight ratio in ethanol at 10 w/v% of total polymer concentration. Different amounts of 4 M orthophosphoric acid (0.5ml, 1ml, 1.5ml) were added to this polymer solution. This solution was then either cast into a rubber tube (10 mm diameter) cut in half along its length, or cast into Teflon coated dishes approximately 4 cm in

diameter. The solvent was allowed to evaporate at 40 °C for 48 h in an incubator (New Brunswick Scientific, U.S.A). The produced matrices were then removed and cut into 1 cm long pieces and stored in a silica gel desiccator.

Eudragit® S100

The pH threshold for Eudragit® S100 is 7.0; allowing 1 g of Eudragit® S100 to dissolve in 7 g methanol, ethanol, in aqueous isopropyl alcohol or acetone (containing approx. 3% water), as well as in 1 N sodium hydroxide to give clear to slightly cloudy solutions. Eudragit S100 microspheres where prepared by the solvent evaporation method in water-in-oil-in-water double emulsions. Eudragit S100 (600 mg) was dissolved in 10 ml of a mixed solvent system of dichloromethane (DCM)/ethanol/isopropyl alcohol in a ratio of 5:6:4 to form the organic phase (O). The internal aqueous phase (W1) was made up of 2ml, 1.5ml, 1ml and 0.5ml of 4M orthophosphoric acid along with polysorbate 20 (Sigma Aldrich) solutions (3% v/v). W1 was emulsified with the above organic phase for 2 minutes using an ultrasonic bath (Grant, XB6) in a 4 ºC ice bath which formed the primary emulsion (W1/O). The primary emulsion was added drop by drop using a syringe with a needle diameter of 0.45 mm to a 50 ml external aqueous phase (W2) of 2wt% PVA (polyvinyl alcohol) (MW 23,000-70,000, Sigma Aldrich) solution by using a high speed homogeniser (Silverson L4RT, England) at the speed of 2,000 rpm for 4 minutes to form a "multiple emulsion" (W1/O/W2). The resulting W1/O/W2 emulsion was stirred at room temperature overnight with a magnetic stirrer to evaporate the residual organic solvent. Samples were centrifuged (MSE High Speed 18, England) at 10,000g for 10 min and washed three times with distilled water to remove residual PVA. The microspheres were then resuspended in distilled water and freeze dried (Edwards, EF03) for 24 h. The final product was then stored in a desiccator at 4 ºC.

Eudragit® RL

Microspheres were prepared by the solvent evaporation method using an acetone/liquid paraffin system (Azarmi *et al.* 2002;Oth & Moδs 1989). Eudragit® RL (3 g) was dissolved in 27 ml of acetone using a magnetic stirrer. The PPA (1 g) and magnesium stearate (100 mg) were dispersed in the polymer solution. The resulting dispersion was then poured into a vessel of 1000 ml containing the mixture of 270 ml liquid paraffin and 30 ml n-hexane while stirring. A cylindrical vessel (10 cm inside diameter and 14 cm height) and a mechanical stirrer with a blade (6 cm diameter) were used. Stirring was continued for an hour, until the acetone evaporated completely. The polymer: acid ratio (3:1, w/w) and stirring rate (500 and 750 rpm) of the system were changed to obtain spherical particles. After evaporation of acetone, the microspheres formed were collected by filtration in a vacuum, washed 4–5 times with 50 ml n-hexane each and dried at room temperature for 24 h (**Figure 6.3**).

PCL microspheres

PCL microcapsules in this study were prepared using a simple emulsion solvent evaporation technique with a slight modification. The PCL (1.5 g) was dissolved in 50 ml dichloromethane, to which 1 ml of the PPA was added and stirred well; this formed the organic phase of the emulsion. This mixture was then emulsified into 500 ml of 2% w/v polyvinyl alcohol (PVA). The emulsion was placed under a high speed homogeniser (SILVERSON, machine serial No.V5100) for 3 min at 7,000 rpm. This emulsion was then magnetically stirred at 500 rpm followed by addition of 200 ml of distilled water, for 6 h, or until the dichloromethane had evaporated. This increased the diffusion of organic solvent into the external aqueous phase to promote microsphere hardening.

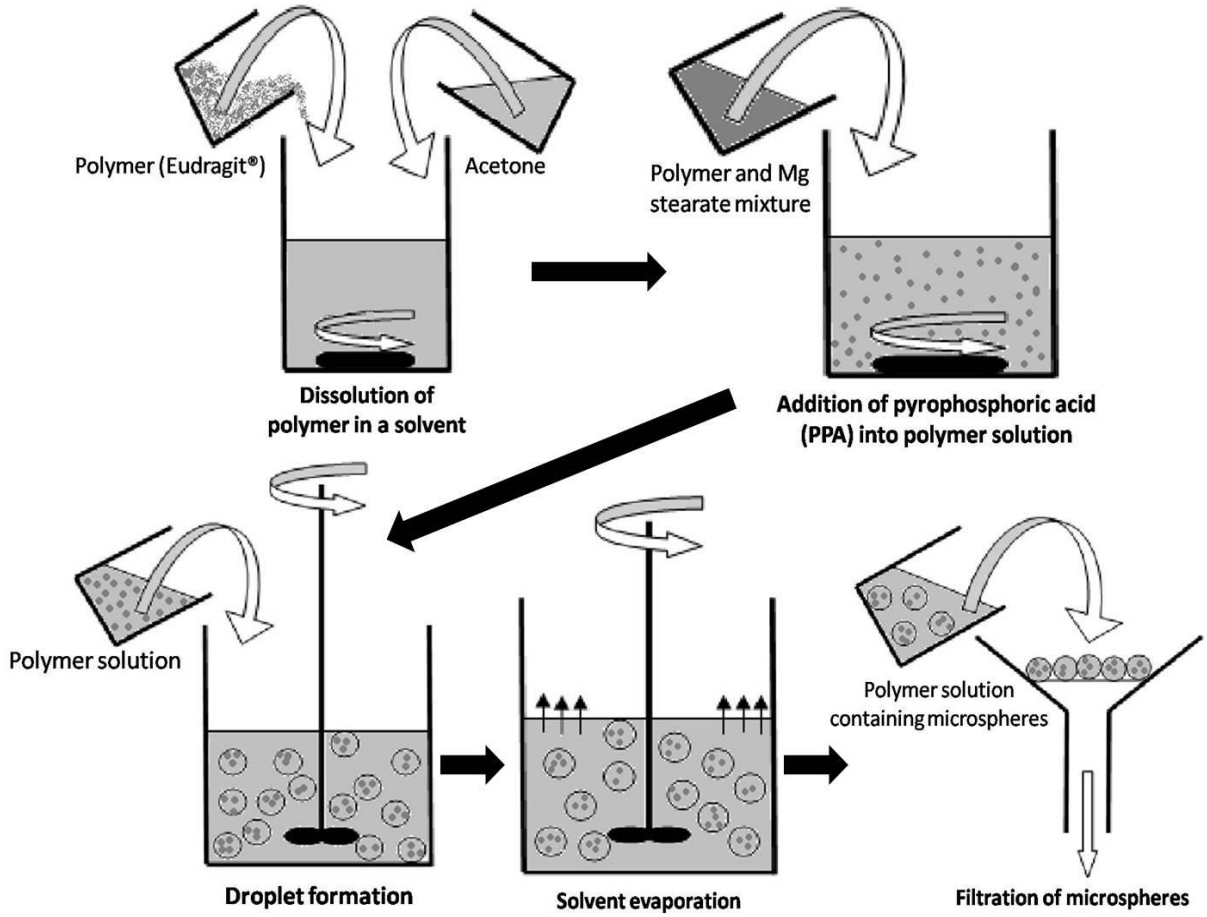

Figure 6.3: Illustration of the production of Microspheres by the solvent evaporation method using the acetone/liquid paraffin system (Azarmi *et al.* 2002;Oth & Moδs 1989).

After completion of solvent evaporation, the microspheres were collected by centrifugation, at 2,500 rpm for 10 minutes. The solutions were evenly distributed into the centrifuge tubes and the excess solution was discarded, then the microspheres were washed out using distilled water about 3-4 times each, this ensured that the PVA has been washed off the surface of the microspheres. The samples were collected and freeze dried and stored between 10-15 ºC. Microspheres dried at room temperature were then weighed and the yield was calculated using equation 6.1:

$$\%\, Yield = \frac{The\ amount\ of\ microspheres\ obtained\ (g)}{the\ theoretical\ amount\ of\ microspheres\ produced\ (g)} \times 100 \qquad \textbf{(}\text{equation 6.1)}$$

Table 6.1: The physicochemical properties of the poly(caprolactone) used in this study.

Grade of PCL	CAPA 2201	CAPA 6100
Structure	A standard grade liner polyester diol derived from caprolactone monomer terminated by primary hydroxyl groups	A high molecular weight liner polyester derived from caprolactone monomer
Physical Form	White waxy solid	White solid
Mean Molecular Weight	2000	10,000
Melting Point	40-50 ˚C	58-60 ˚C
Viscosity	480 mPa.s at 60 ˚C	9300 mPa.s at 100 ˚C
Solubility Parameter (δ)	9.34-9.43 $(cal/cm^3)^{1/2}$	9.34-9.43 $(cal/cm^3)^{1/2}$
Handling and Storage	Stored in air-tight containers	Packed in metal containers and stored in a dry place away from sources of heat.

6.2.2 Release study

The release of acid from both temperature-sensitive matrices and pH-responsive microspheres was detected and quantified using the same method. The encapsulated polymer (Eudragit (RL, S100 or E-PEG) or PCL) were weighed; half used as control. The encapsulated polymers were immersed in 200 ml of distilled water for the release. With the thermo-sensitive matrices half were placed in an incubator and the other half in a refrigerator for the control (at 4 ºC). A constant temperature of 37 ºC was maintained within the incubator for the thermo-sensitive matrices, and the control setup did not reach above 8 ºC in the refrigerator. For the pH-sensitive polymer matrixes, the control was kept at pH 4 and the rest was tested in a solution at pH 7. Thereafter, 300 µl of sample was collected every hour from both the experiment and the control for 7 h and was analysed for the presence of phosphate ions.

The technique that was used to quantify phosphate ion release was described by Chen *et al*. (Chen *et al.* 1956). Released solutions (300 µl) were mixed with 3.7 ml of distilled water and added to 4 ml of Reagent C. Reagent C was made by mixing 2 volumes of distilled water, 1 volume of 3 M sulphuric acid (Sigma Aldrich), 1 volume of 2.5% ammonium molybdate (Sigma Aldrich) solution and 1 volume of 10% ascorbic acid solution (Sigma Aldrich). The mixture of sample solution and Reagent C was kept at 37 °C in an incubator for 1.5–2 h, followed by the reading of the optical density which was measured at 620 nm using a spectrophotometer (Cecil CE 1020). The calibration curve for this experiment was made using different concentrations of a 2 M solution of potassium dihydrogen phosphate (Sigma Aldrich).

6.3 Results

6.3.1 Release from Eudragit microspheres

Various different combinations of Eudragit microspheres have been demonstrated in the literature; here we used two of the most common ones; temperature and pH sensitive, and also a mixed blend using other polymers.

Eudragit®-PEG blend (temperature sensitive)

The release of the encapsulated orthophosphoric acid (OA) from temperature sensitive 13% E-PEG matrices was investigated. Four batches of the matrix encapsulating 1 ml of a 4 M OA solution were made.

However, release studies were carried out on samples produced with OA as the encapsulation acid. **Figure 6.4** shows the percentage of the encapsulated acid released from the E-PEG matrix with respect to time. It can be seen that more than 90% of the encapsulated acid is released by the end of the seventh hour at 37 ºC while the control has released only around 15%. Also, the curve is indicative of a higher percentage of release in the first four h (releasing more than two-thirds of the encapsulated acid) than in the last 4 h of the experiments. This method was not used to produce cements with PPA as the samples produce were not microspheres; pellet-like rods were created. This method produced a sticky mixture that had to be poured into a mould and allow for the polymer blend to cure.

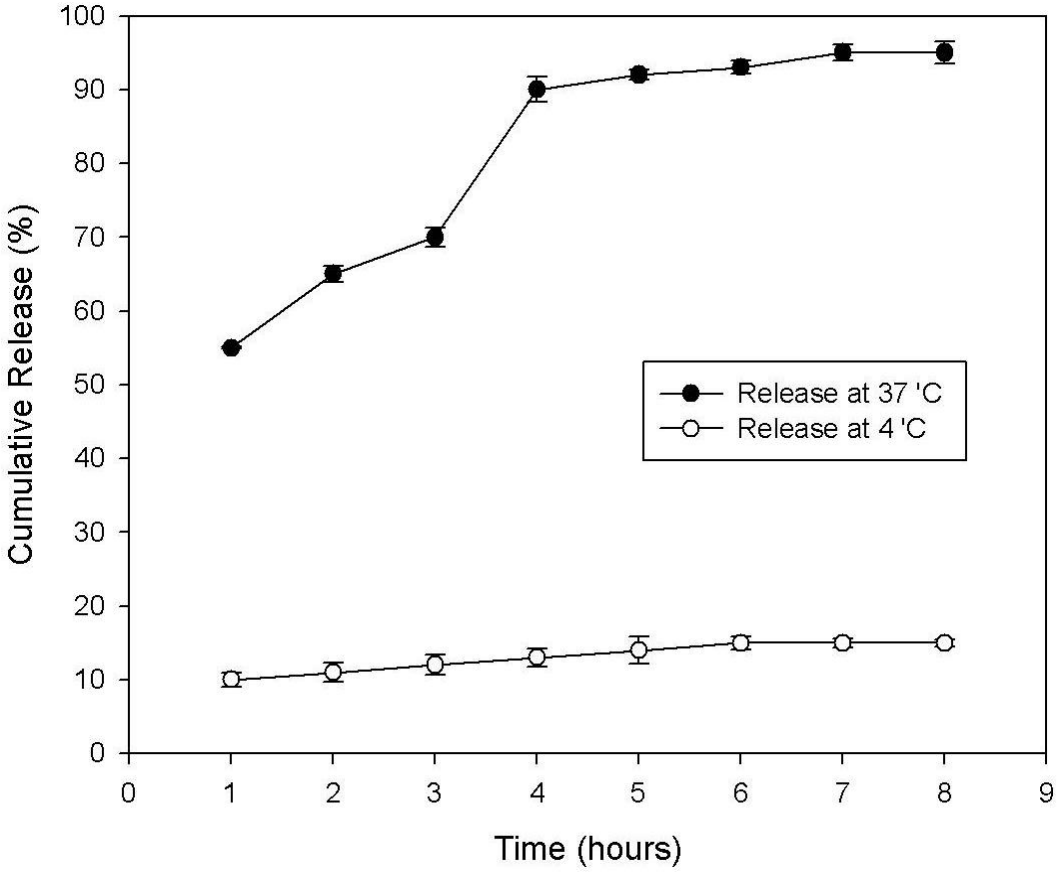

Figure 6.4: The graph illustrates the cumulative release, in percentage, of OA released against time in hours, over an 8 h period at the different temperatures; at 37 ºC the thermo-sensitive polymer releases the encapsulated content; at 4 ºC the content should remain encapsulated. The graph illustrates the mean values of the data points from all the batches produced (error bars are also indicated).

Eudragit® S100 (pH sensitive)

The average size of the microspheres prepared using the double emulsion technique (Jain *et al.* 2005) falls in the micron range, so scanning electron microscopy was used to observe them. The SEM micrographs clearly demonstrate the fragile nature of the microspheres **(Figure 6.5)**; majority of the spheres appear to be broken, even though samples were handled with care. The size of the microspheres can also be observed from the SEM and range between 10–200 µm; this variation may be due to the deficiency in controlling the stirring speed, which is the main factor influencing the particle size.

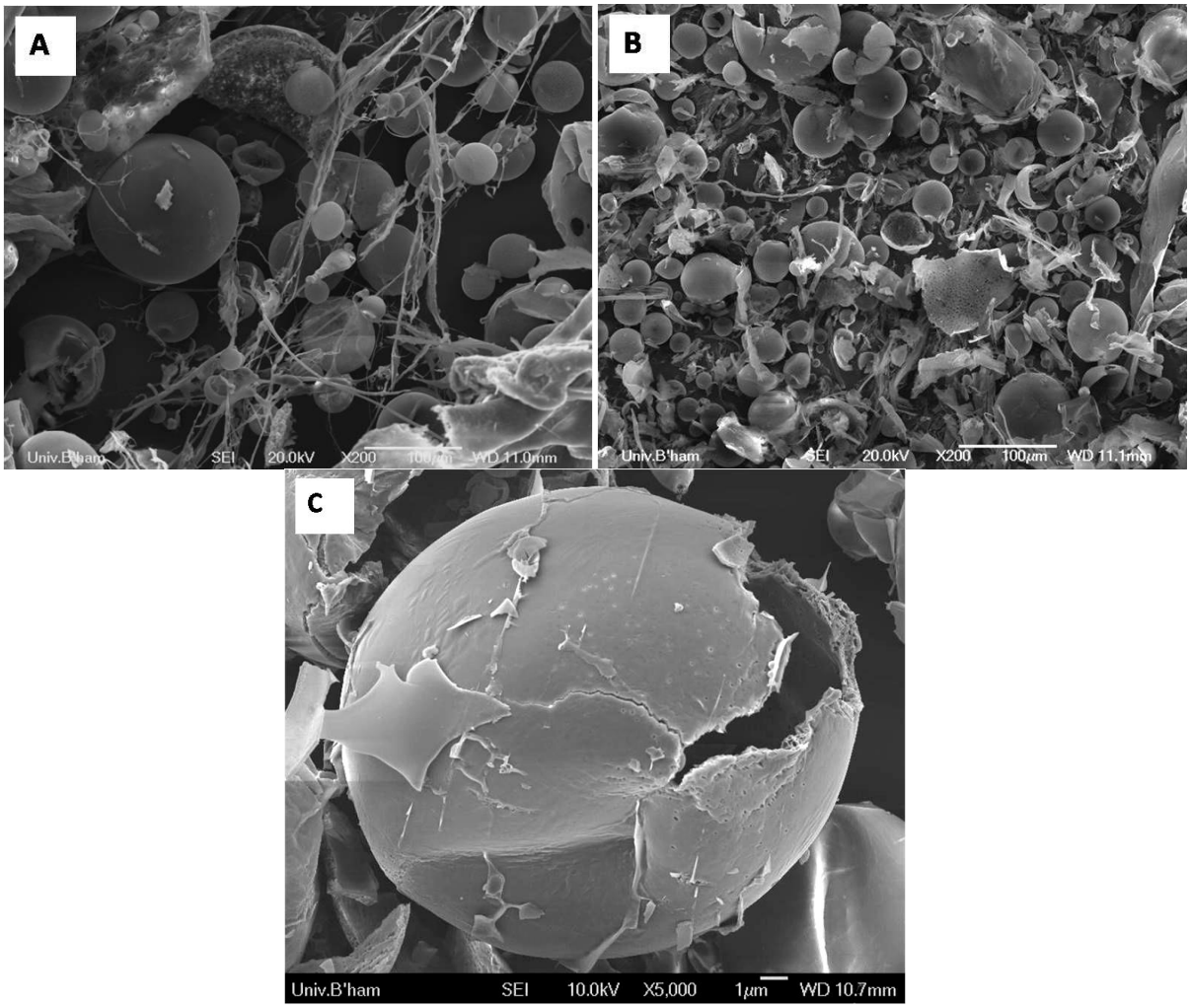

Figure 6.5: SEM micrographs of Eudragit S100 microspheres at 200 x magnifications (A) and (B). The morphology illustrated in the SEM micrographs clearly shows all of spheres to be broken. At 5,000 x magnifications (C) it can be seen that the microspheres do produce a hollow sphere, with a relatively smooth surface. Cracks or wrinkled-like surface of the microspheres may be attributed to the heat created by the high voltage of the electron beam.

An attempt was made to produce pH-sensitive Eudragit® S100 microspheres encapsulating OA. Four batches of microspheres, containing 2 ml, 1.5 ml, 1 ml and 0.5 ml of 4 M OA as their Internal Aqueous Phases (IAP) were prepared. The percentage of encapsulated OA released, assuming all the OA was encapsulated, is shown in **Figure 6.6.** It can be seen that no greater than 10% of the encapsulated acid maintained at pH 7–7.5 was released at the end of the 7 h period. This is likely to be because only a fraction of the acid was actually encapsulated, indicating that the technique used may not be the best for this application.

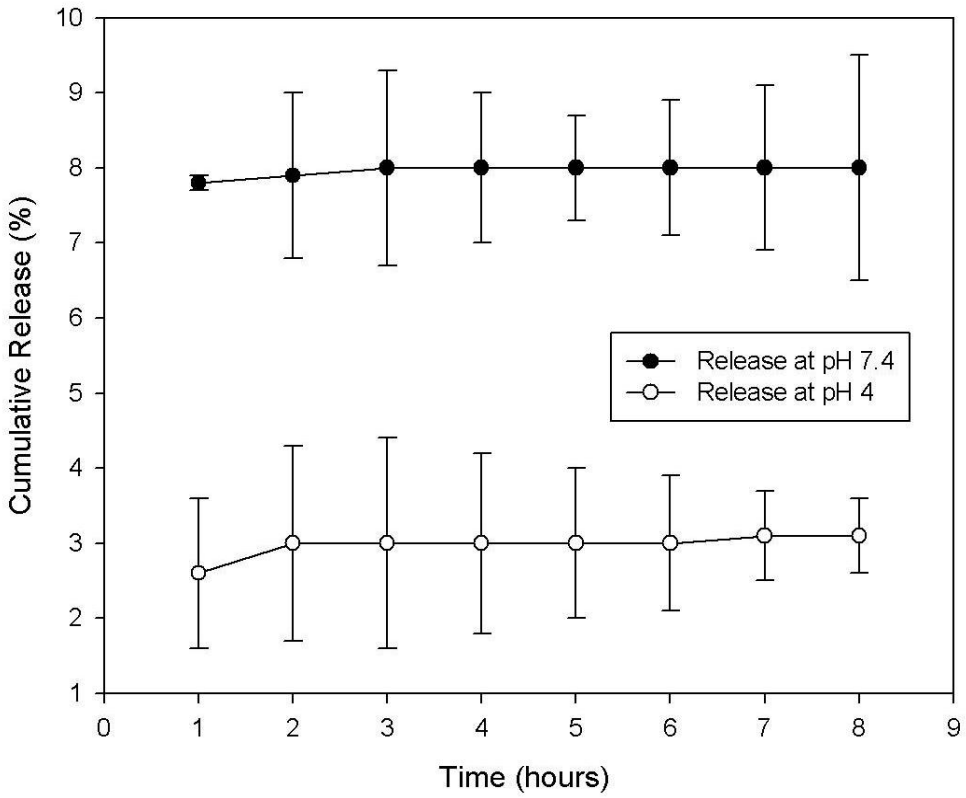

Figure 6.6: The graph illustrates the cumulative release, in percentage, of OA released against time in hours, over an 8 h period at the different pH; at pH7.4 the pH-sensitive polymer releases the encapsulated content; at pH 4 the content should remain encapsulated. The graph illustrates the mean values of the data points from all the batches produced (error bars are also indicated).

From previous investigations, it was clear that although the Eudragit S100 microspheres were manufactured using the double emulsion technique (Jain *et al.* 2005) **(Figure 6.5)**, they appeared to break very easily. Taking this into consideration a solvent evaporation method was used **(Figure 6.3)**. **Figure 6.7** shows that it was not possible to produce microspheres using this method.

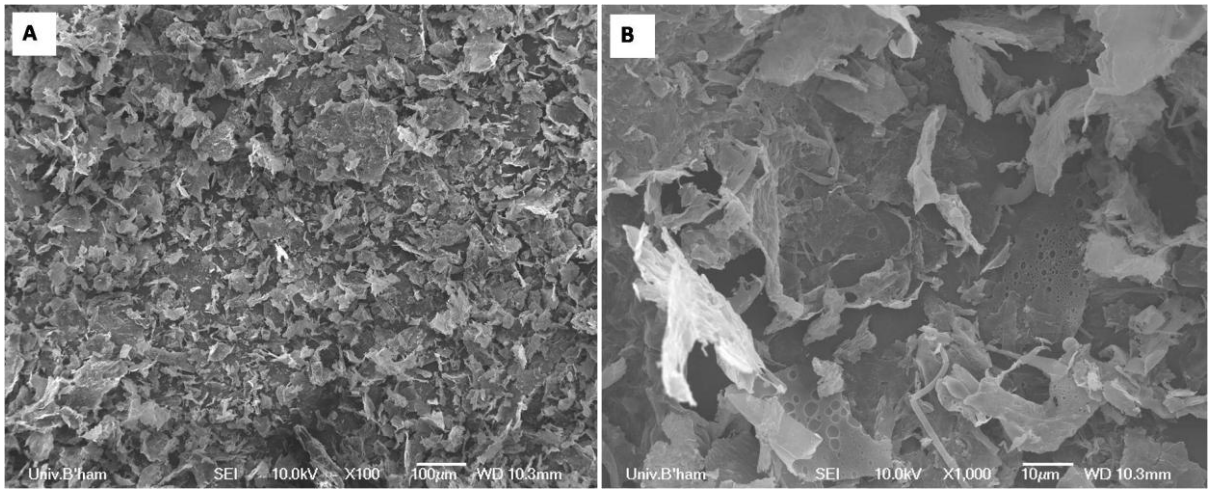

Figure 6.7: Eudragit S100 prepared by solvent evaporation method using acetone/liquid paraffin system **(Figure 6.3)**. The micrograph shows the fragments of the microspheres, the fluffy flake-like structure created by this method does not allow the encapsulation of OA (A) and PPA (B).

Subsequently as it can be seen from **Figure 6.8**, where both the release at pH 7 and pH 4 show similar release profiles, this method would clearly not be suitable for encapsulation of the OA and PPA. The Eudragit® S100 is unstable when formulated into microspheres with the solvent evaporation method using acetone/liquid paraffin system.

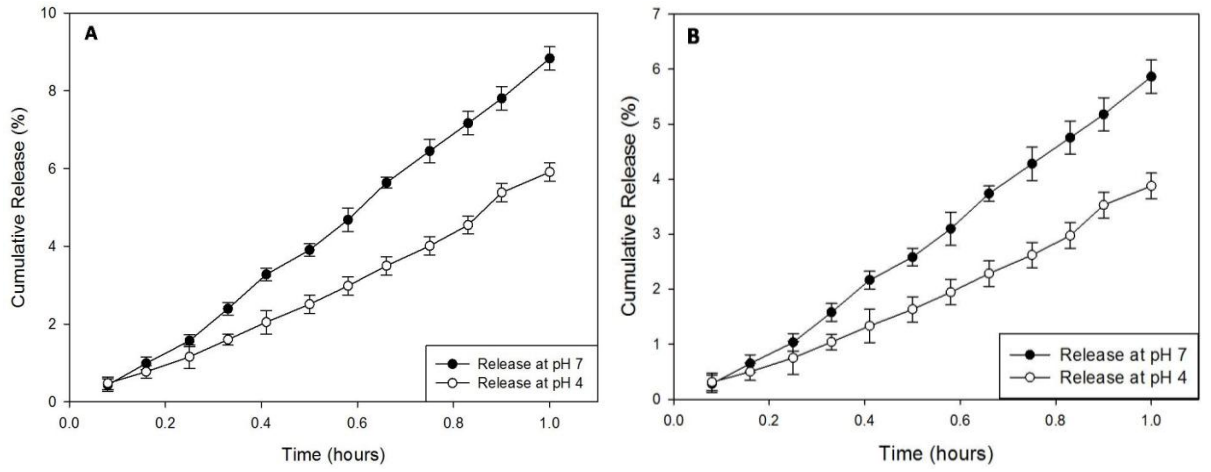

Figure 6.8: The graph illustrates the cumulative release in percentage of OA (A) and PPA (B) released against time in hours, at the different pHs; pH7 the pH-sensitive polymer releases the encapsulated content; at pH 4 the content should remain encapsulated, however results show total release of microsphere content. The graph illustrates the mean values of the data points from all the batches produced (error bars are also indicated). Eudragit S100 prepared by solvent evaporation method using acetone/liquid paraffin system **(Figure 6.3)**.

Eudragit® RL

Figures 6.9 illustrate the morphology of the microspheres produced using the solvent evaporation method. The microspheres were generally smooth, spherical and regular; however, they exhibited a wide particle size distribution from 10–150 μm in diameter, which may be due to a variation in flow during stirring. The microspheres also seem to be fused together in clumps. From **Figure 6.9B** it is clear that these clumps are bound together so if broken or separated it is likely to release the encapsulated content.

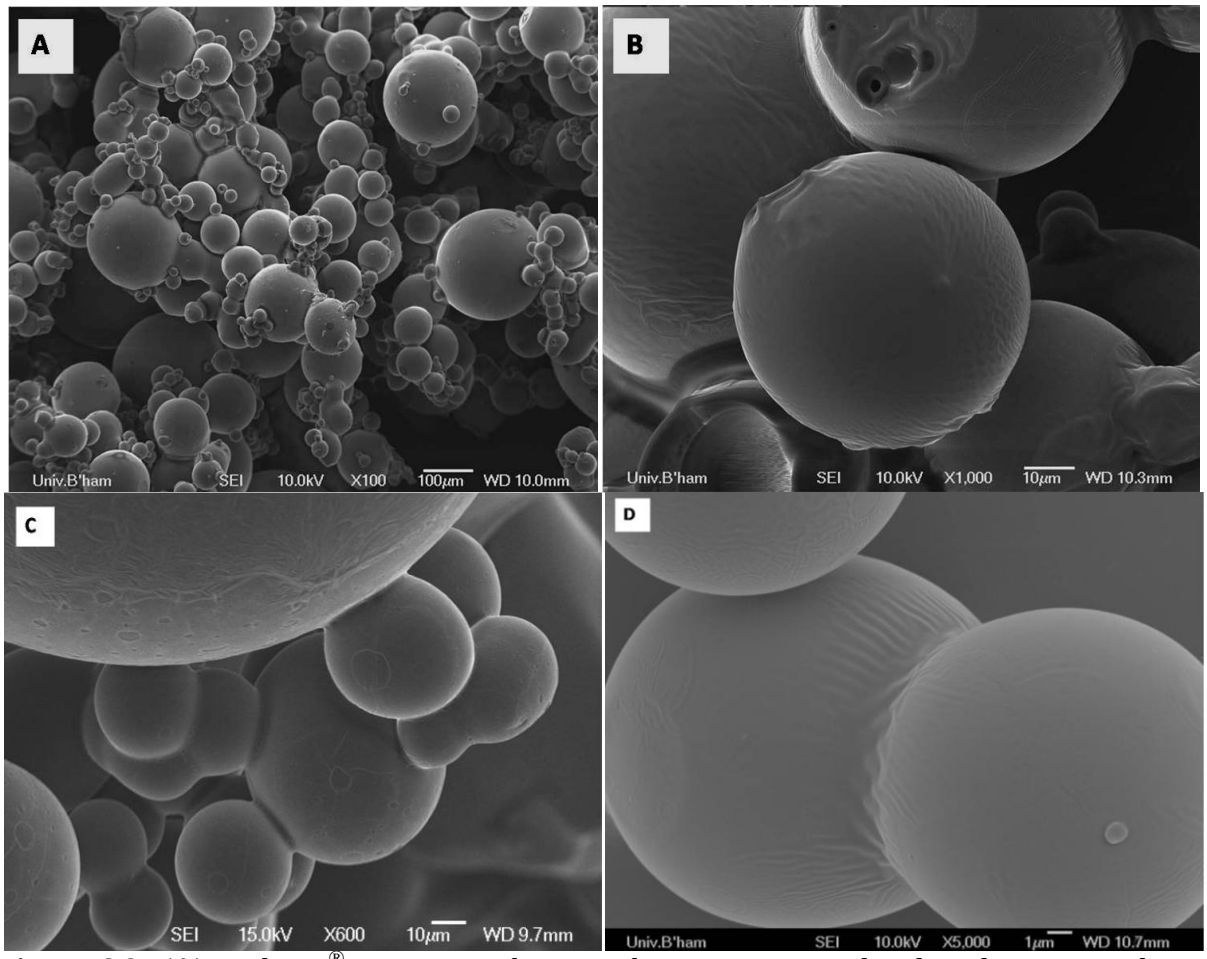

Figure 6.9: (A) Eudragit® RL microspheres without any encapsulated acids. Microspheres were prepared by solvent evaporation method using acetone/liquid paraffin system (**Figure 6.3**). (B) and (C) Higher magnification of the microspheres to emphasize the binding of the microspheres.

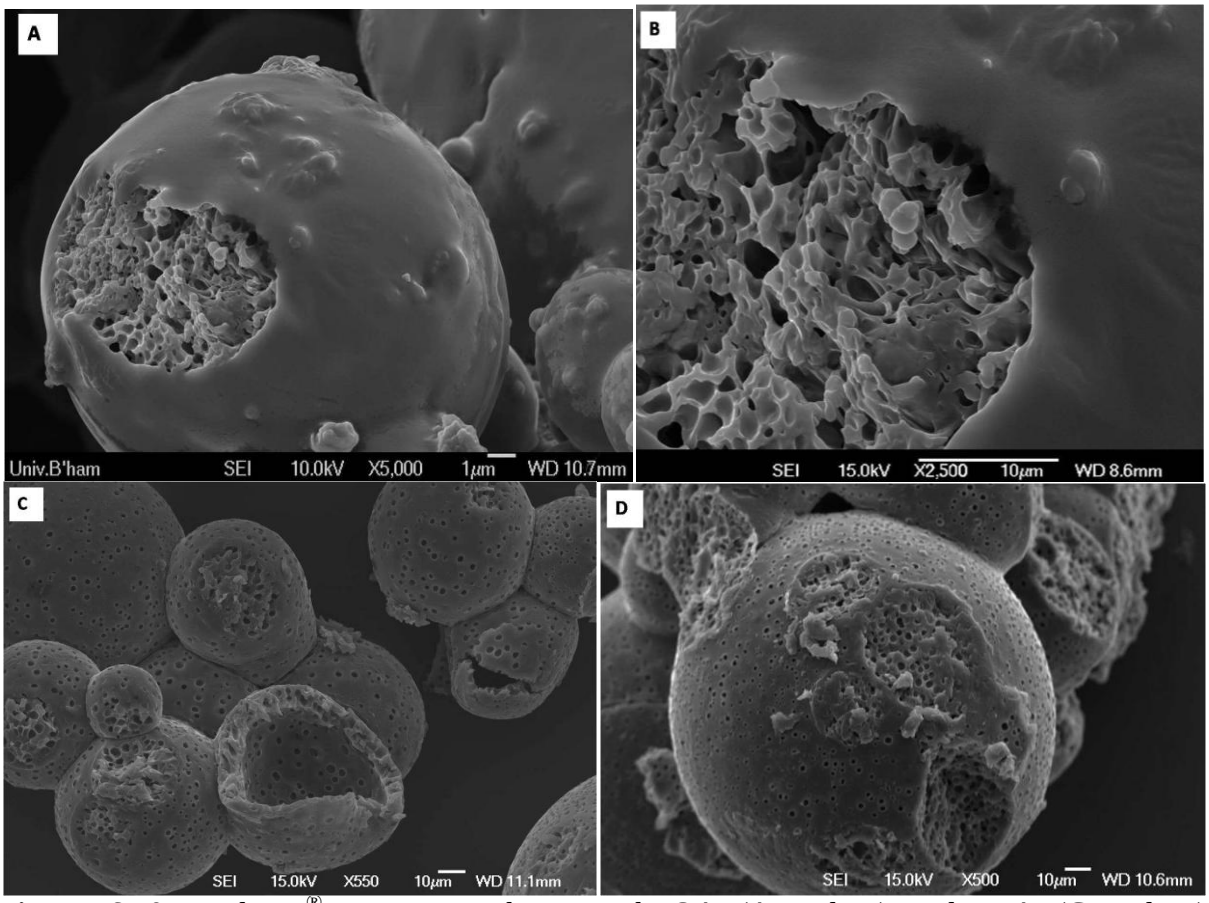

Figure 6.10: Eudragit® RL microspheres with OA (A and B) and PPA (C and D) encapsulated. Microspheres were prepared by solvent evaporation method (**Figure 6.3**). Micrographs show the difference in morphology of the two microspheres; with OA encapsulated the surface is smooth, with a porous interior structure; with the PPA the microspheres exhibited a porous surface, on closer inspection the interior was hollow or porous within the same batch.

Although from the study using Eudragit S100 microspheres it was apparent that majority of the microspheres produced were broken, however a small quantity of the samples were collected that had kept their structural integrity allowing the measure of the particle size distribution and compare with the Eudragit RL microspheres. Accordingly, **Figure 6.11** the particle size distribution of the microspheres was large ranging between 10 and 100 μm. The particle size distribution was not congruent with the previous observations made using SEM, suggesting that the particles were agglomerating in solution, this is also suggested by the

observed differences between the particle size distributions of different batches produced under the same conditions. When the homogeniser was set at speeds of less than 5,000 rpm, the spheres were not formed, illustrating the importance of effective force to create a stable emulsion.

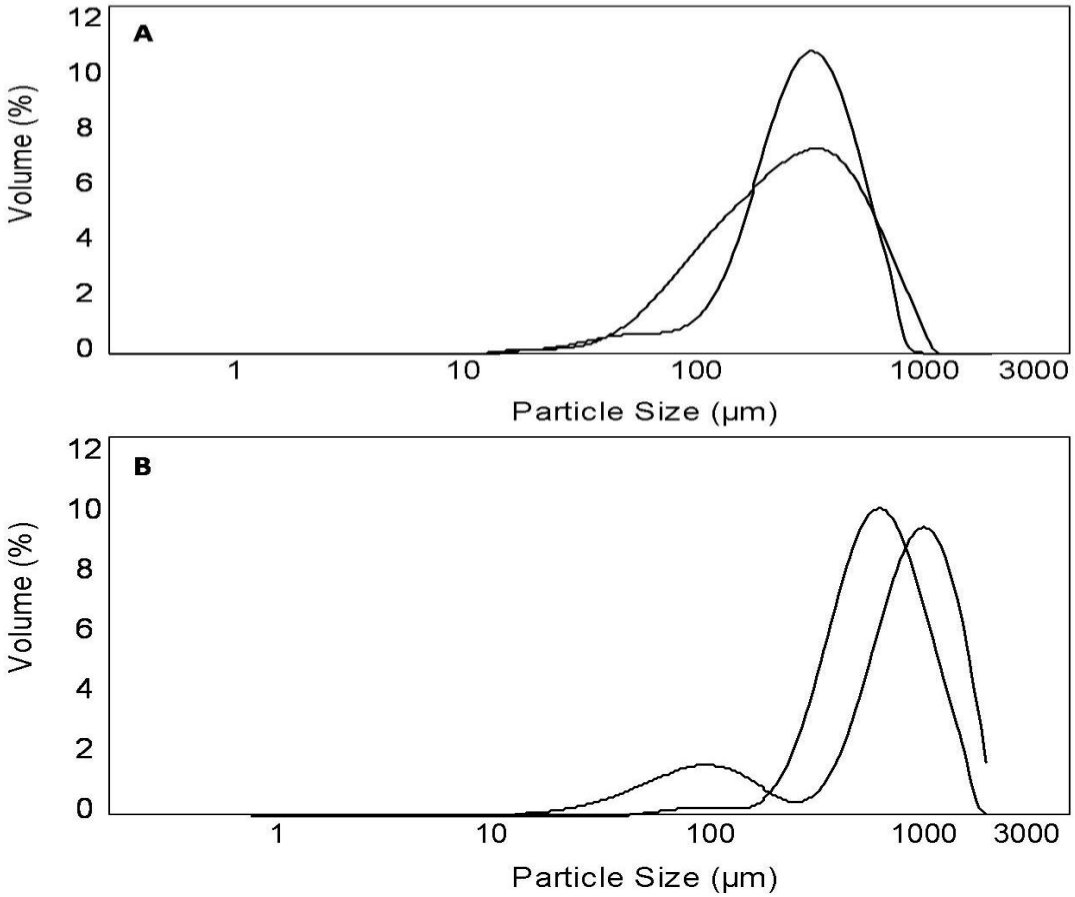

Figure 6.11: The graph illustrates the particle size distribution of the two microspheres produced; Eudragit S100 (A) and Eudragit RL (B), using the two different methods.

Release profiles for the microspheres producing using the solvent evaporation method using acetone/liquid paraffin system (**Figure 6.3**) are shown in **Figure 6.12.** The release was carried out over a 24 h period, to ensure maximum release was recorded; both phosphate and pyrophosphate release were calculated from the results and are illustrated in **Figure 6.12A**. The release from the control sample at 4 ºC was carried out for 8 h only; as no further release was measured after 3 h.

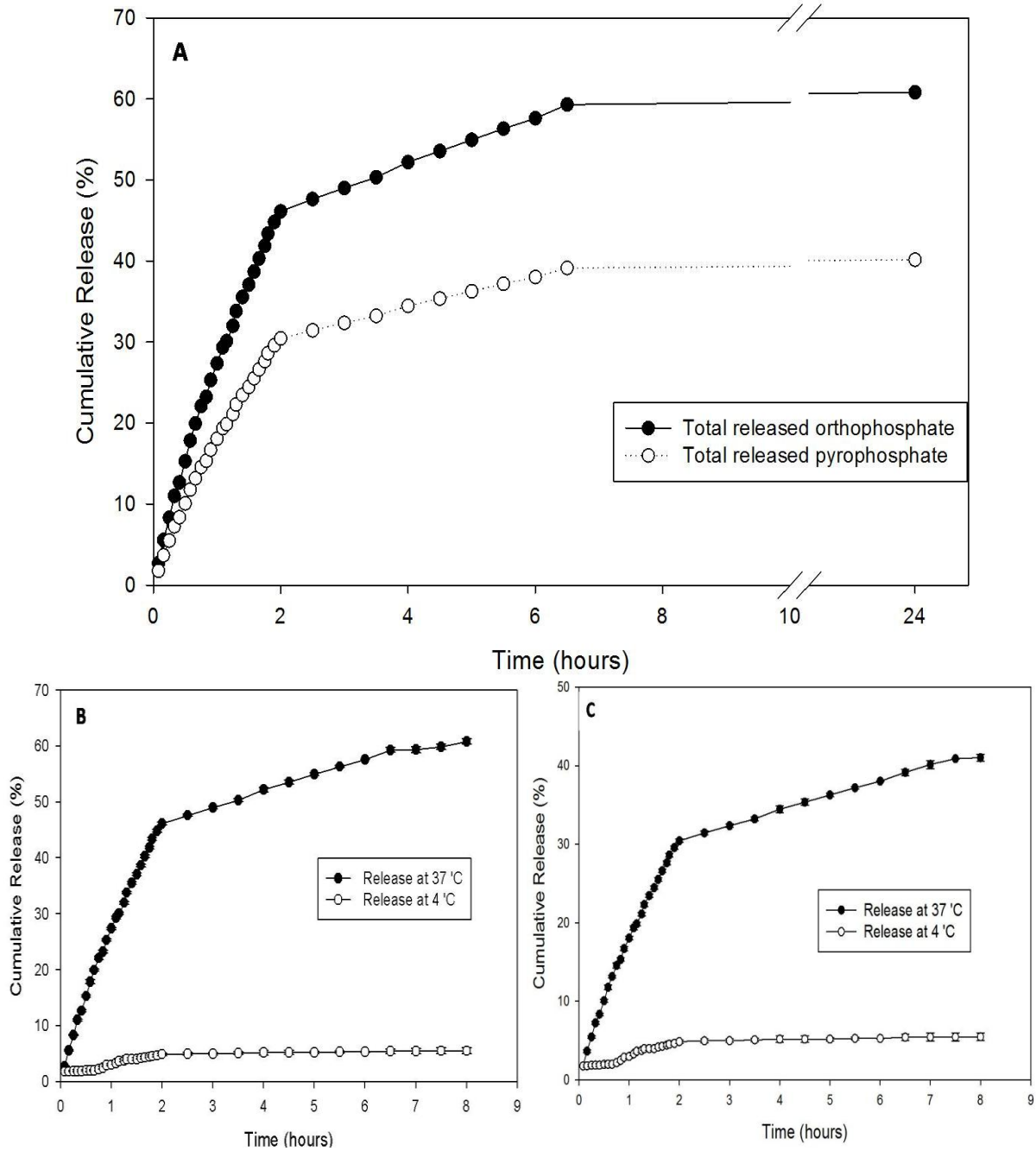

Figure 6.12: Illustrates the cumulative release (%) of OA and PPA over, (A) 24 h period at 37 ºC; (B) OA and (C) PPA release over an 8 h period at the different temperatures; 37 ºC the thermo-sensitive polymer releases the encapsulated content; at 4 ºC the content remain encapsulated. Illustrating the mean values of the data points from all the batches produced (error bars are also indicated).

It can be seen that the microspheres are releasing the phosphate steadily (**Figure 6.12**). The control (at 4 ºC), however, also shows a degree of release which could be attributed to the release of surface bound acid. The continued release suggests that the temperature of the distilled water, in which the microspheres release, may not have been low enough (may not have reached 4 ºC). This demonstrates that the thermo-sensitive Eudragit RL can be used to manufacture microspheres that are temperature sensitive.

Figure 6.13 demonstrates the effect of concentration of the acid on the conversion of β-TCP to brushite. It can be seen from the peak representing brushite that it increases in height with an increasing ratio of OA to β-TCP. This shows conclusively that the brushite crystals are formed within the cement mix. The peaks also confirm that the released acid is in fact OA, since no other component of the microsphere formulation can react with β-TCP to form brushite (Pflugrath 1999).

Microspheres were manufactured to encapsulate the acid component of the cement reactants; this was achieved and it was demonstrated that the release acid component was able to recreate the reaction with the cement powder components and form the cement matrix (**Figure 6.13**). Following this, the microspheres were mixed with the powder components and water at 37 ºC (using the Eudragit RL) to initialise the reaction. XRD patterns in **Figure 6.14** illustrate the resultant cement composition.

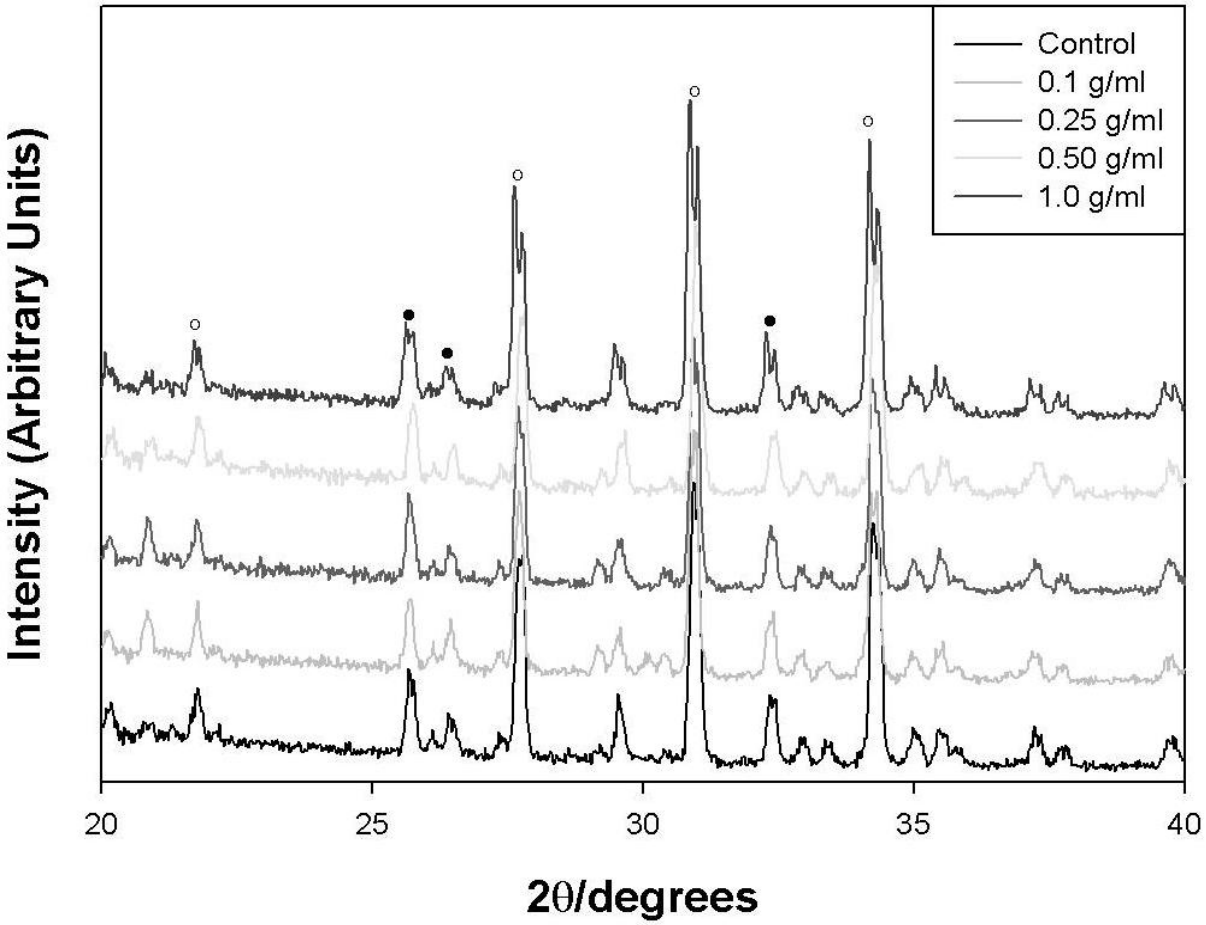

Figure 6.13: Compares the diffraction patterns of the control cement (β-TCP + OA+ water) with the varying concentrations of OA paste formulations using microspheres staggered on top. The various peaks are indicative of the composition of the samples; ○ Brushite; ● β-tri-calcium phosphate (β-TCP).

6.3.2 Cement composition

Once it was determined that Eudragit microspheres could be produced reproducibly; calculations using the stoichiometry equation determined the amount of microspheres are required to enable the powdered components to fully react to produce brushite cement. The correct amount of acid encapsulated Eudragit microspheres were then mixed with the β-TCP and placed in the incubator at 37 ºC overnight to allow the cement to harden. The set cements were then tested and compositions were compared to the control samples in the case of both OA and PPA cements.

The results from the XRD shown in **Figure 6.14** show the compositions of two cement formulations. The cements made using the microspheres to encapsulate the orthophosphoric acid and made without encapsulation formed brushite as the end product. The XRD patterns in **Figure 6.14A** exhibit very little change in composition, suggesting a complete reaction of β-TCP. Both the control pyrophosphate modified brushite cement, formed using a liquid phase of water and PPA, and the Eudragit pyrophosphate modified brushite cement, formed using the PPA component encapsulated within the microspheres, demonstrate that there is very little β-TCP remaining in the cement, suggesting almost complete reaction **(Figure 6.14B)**. Importantly, no MCPM was formed within the cement matrix, which can occur if the pH value of the cement paste drops significantly below pH 4.2 in localised regions within the cement paste. The apparent similarity in composition between the cement formed using the PPA free and encapsulated in Eudragit is very important as it demonstrates that the presence of the polymer has little or no influence on the final composition of the material.

SEM micrographs of the fracture surfaces of the Eudragit cement are shown in **Figure 6.15**. The micrographs show the effect of encapsulating the OA and PPA in the Eudragit microspheres instead of using it directly during mixing. The images illustrate the size and shapes of the brushite crystals; **Figure 6.15** confirms the composition of the cement produced due to the presence of blade-like crystals, representative of brushite. On examination at higher magnifications, the length of the blade-like structures ranged from 15–50 μm in length and from 2–10 μm in width.

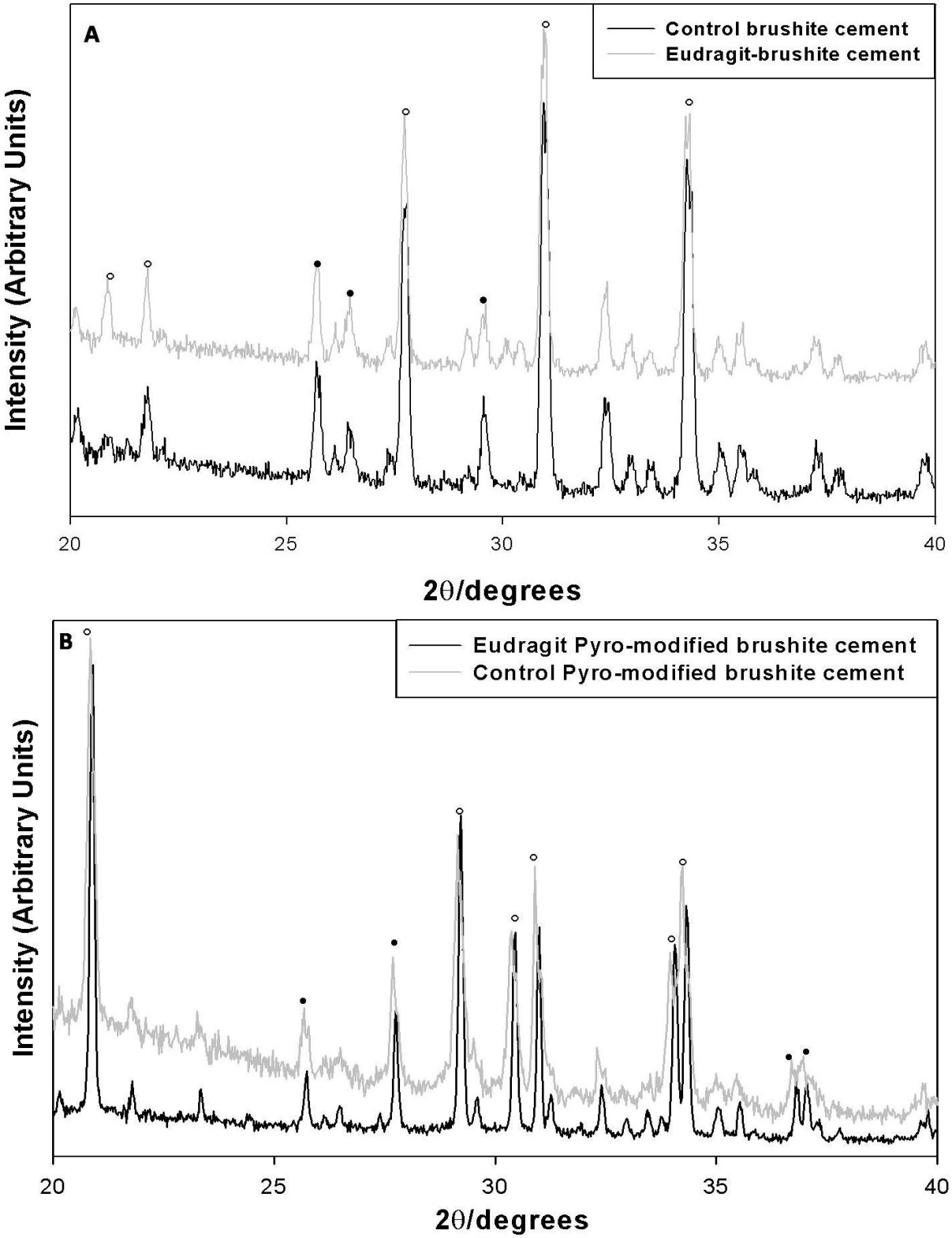

Figure 6.14: Compares the diffraction patterns of the control cement (β-TCP + OA (A) or PPA (B) + water) with the paste formulations using Eudragit RL microspheres with the encapsulated OA (A) or PPA (B). The various peaks are indicative of the composition of the samples; ○ Brushite; ● β-tri-calcium phosphate (β-TCP).

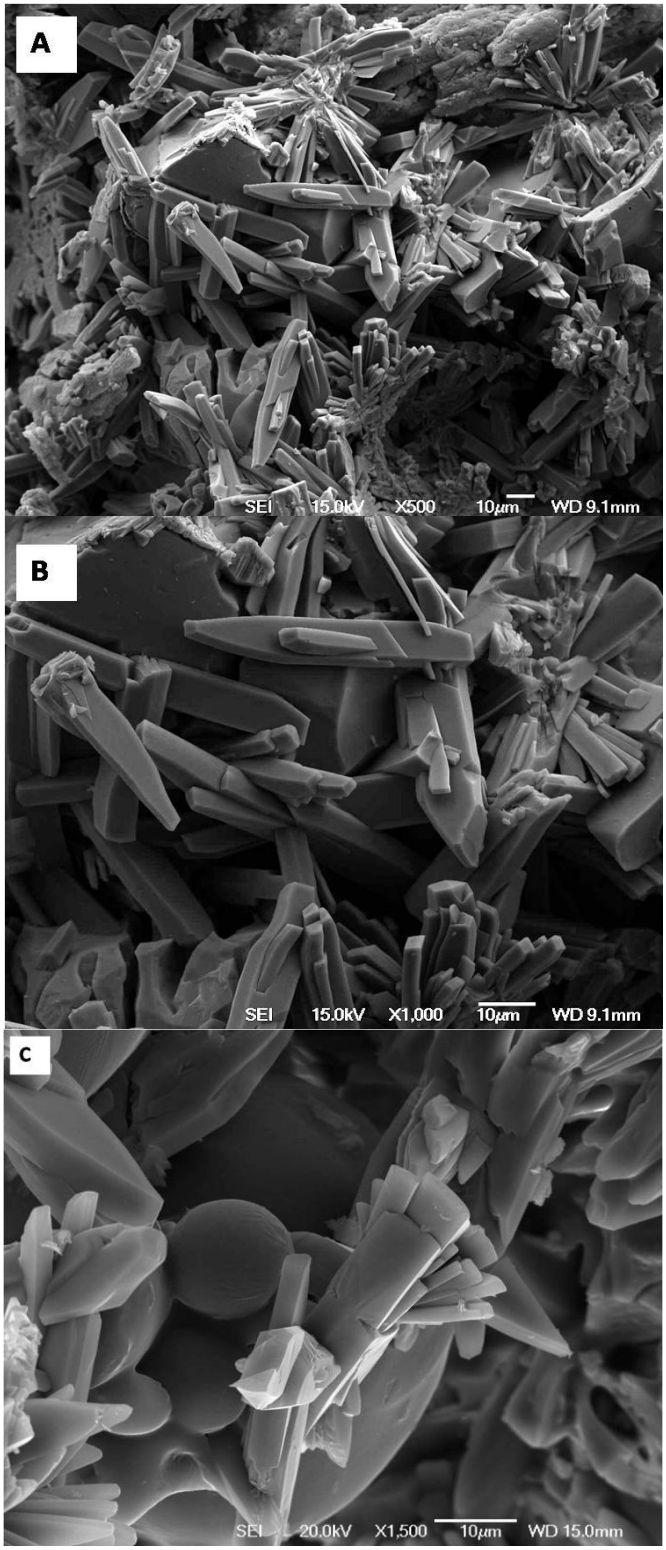

Figure 6.15: **(**A) SEM micrographs of the fracture surface of the set cement produced using Eudragit RL microspheres to encapsulate the OA component (500 X magnified); (B) A higher magnification (1,000 X) of the cements needle-like microstructure; and (C) the surface of the cement at 1,500 X magnifications that shows both brushite crystals and Eudragit RL microspheres. Eudragit® RL microspheres were prepared by solvent evaporation method using acetone/liquid paraffin system **(Figure 6.3)**.

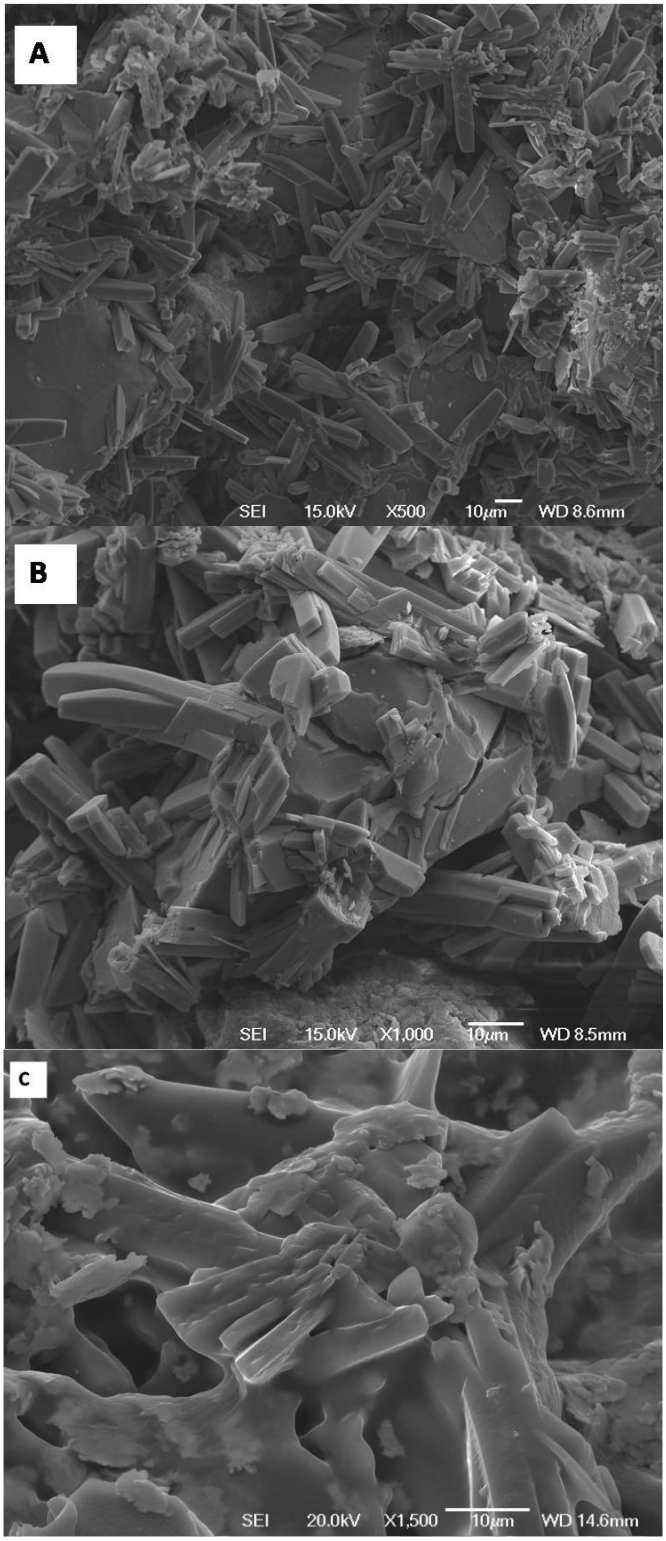

Figure 6.16: **(**A) SEM micrographs of the fracture surface of the set cement produced using Eudragit RL microspheres to encapsulate the PPA component (500 X magnified); (B) A higher magnification (1,000 X) of the cements needle-like microstructure; and (C) the surface of the cement at 1,500 X magnifications that shows both brushite crystals and Eudragit RL microspheres fused together; small amounts of degraded polymer is visible, which appears to be fusing the brushite crystal together in some areas. Eudragit® RL microspheres were prepared by solvent evaporation method using acetone/liquid paraffin system **(Figure 6.3)**.

6.3.3 Storage of microsphere-cement pastes

It is evident from **Figures 6.14–6.16** that the Eudragit encapsulated acid is able to be released, as a result of a change in surrounding conditions, and react with the powder component of the cement; forming a hardened brushite cement as the end product. The preservation of the paste-like nature of the material is shown in **Figure 6.17**.

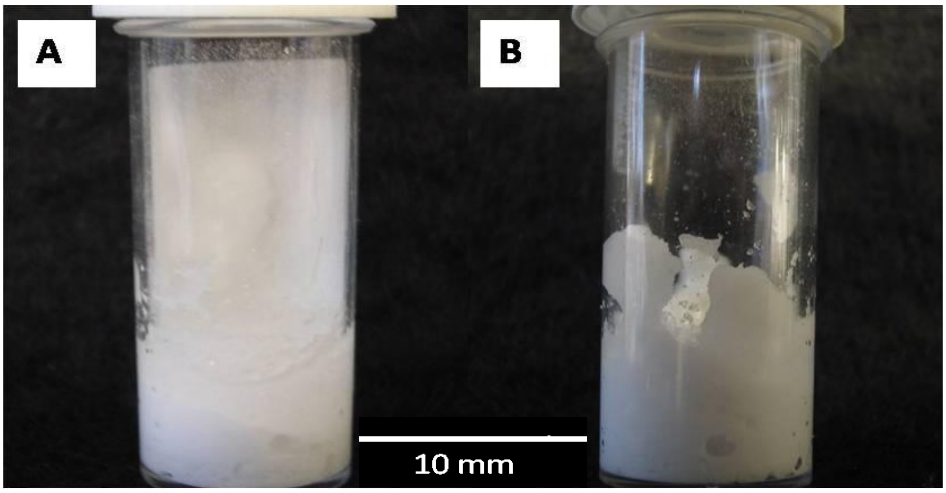

Figures 6.17: The images show the effect of storage at 4 ºC with the use of microspheres S100 (A) and RL100 (B).

The initial results were promising, illustrating that the cement paste could be stored without setting for 28 days **(Figure 6.17)**. The final samples were removed from storage at 4 ºC after 90 days appear to remain unset. However, when exposed to a change in temperature the microspheres released their content and allowed the cement paste to harden, producing set cement phase compositions comparable to the control samples **(Figure 6.18)**. The fact that the cement remains as a paste for such a long period in the sealed containers suggests that the microspheres have not 'leaked' their load of PPA into the cement paste. This confirms the efficacy of the temperature dependent materials on storing PPA in these conditions for an

extended period of time. Unfortunately, the materials produced using the pH responsive polymer hardened after only one day of storage at 4ºC, this excludes the further use of this system and consequently we are investigating other polymer (e.g. poly(caprolactone)) for the production of a 'shear-activated' cement system.

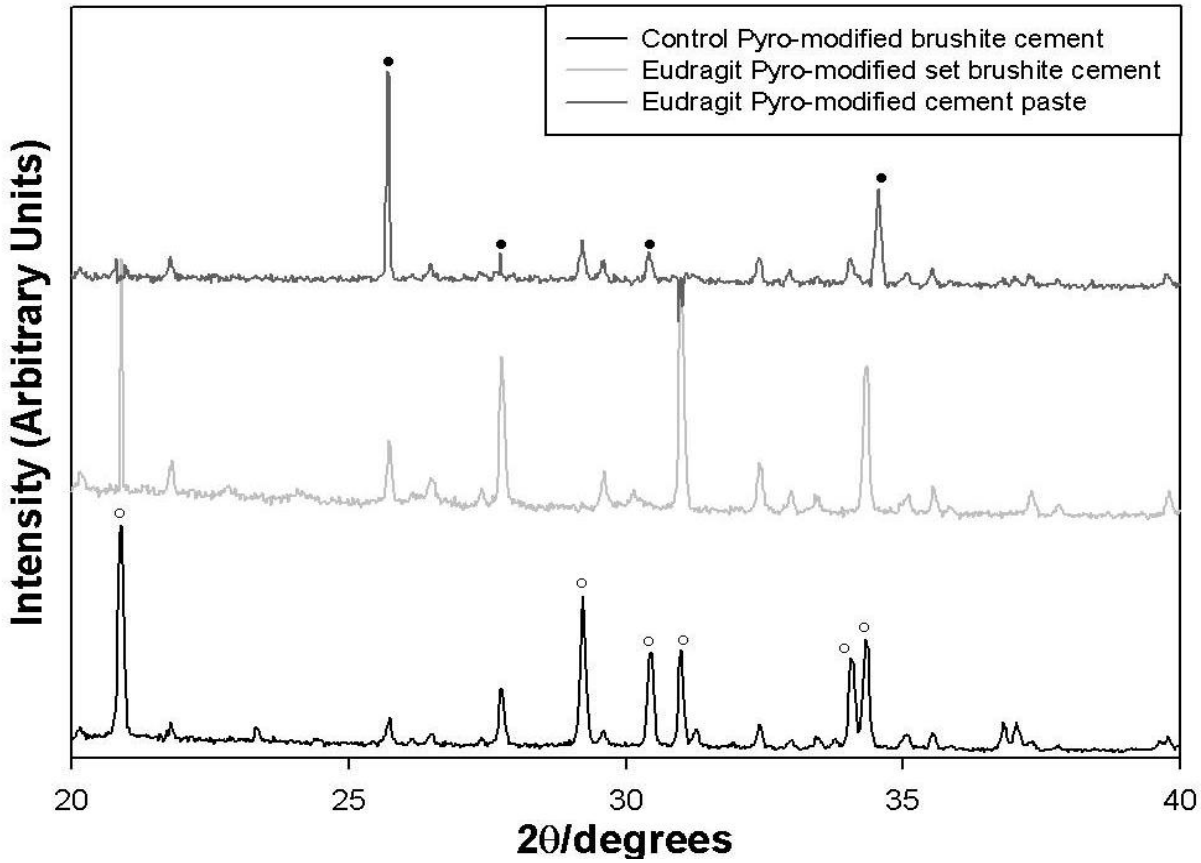

Figures 6.18: Illustrates that similarity in the composition of the control pyrophosphate modified brushite cement (bottom) and the Eudragit encapsulated PPA cement after being in storage at 4 ºC for 90 days then; heated to 37 ºC to allow hardening (middle) and without being exposed to a change in the environment to allow hardening (top). The various peaks are indicative of the composition of the samples; ○ Brushite; ● β-tri-calcium phosphate (β-TCP).

6.3.4 PCL microspheres

The results show that the PSD, again similar to the Eudragit microspheres, have a large range. The particles exhibit diameters from 0.4 μm to 3000 μm. Impeller speed did not influence the

mean particle size; the peaks were also broader as the speed was increased. ESEM images illustrate that the particles produced using the double emulsion method for PCL produced microspheres of diameter 0.5–1 µm; very small compared to Eudragit. Similar to Eudragit, there is a large variation in the size of the microspheres **(Figure 7.19)**. The EDS results in **Table 6.2** quantify the amount of the elements that are present in each spectrum, which relates to the box in **Figure 6.20**.

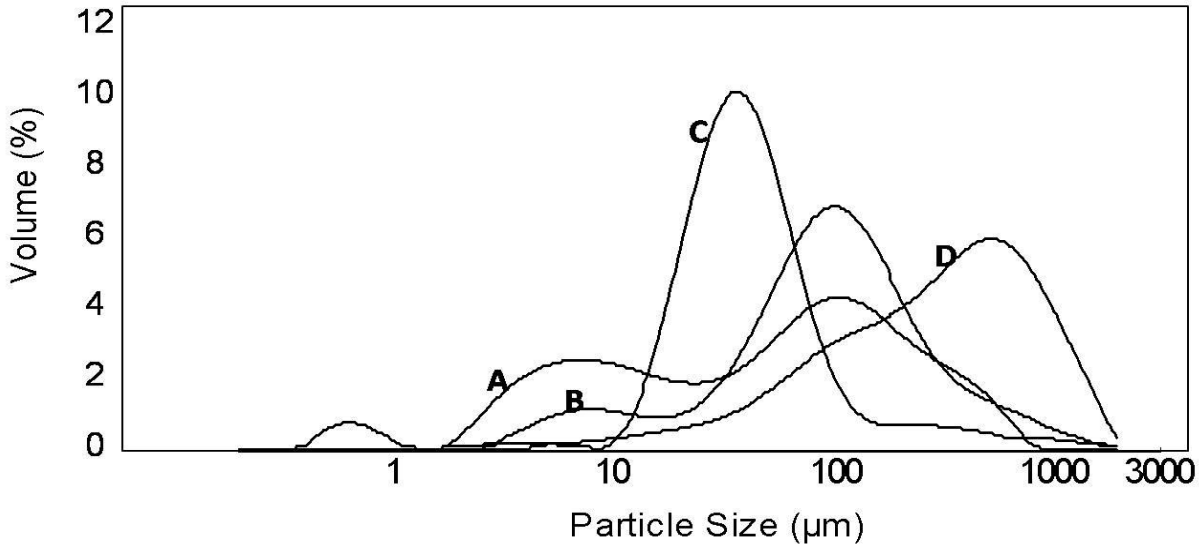

Figure 6.19: Shows the particle size distribution of the microspheres produced using PCL; the speed at which there were produced had a large effect on the PSD: 6,000 rpm (A); 3,000 rpm (B); 1,500 rpm (C); and 750 rpm (D).

Table 6.2: Shows EDS results of the microspheres produced using PCL, with the table which shows the elements present.

Spectrum 1			**Spectrum 3**		
Elements	**Weight %**	**Atomic %**	**Elements**	**Weight %**	**Atomic %**
C	76.01	80.34	C	87.16	89.26
P	25.60	20.31	P	15.16	11.65
O	-1.60	-0.66	O	-2.31	-0.92
Totals	100.00		**Totals**	100.00	

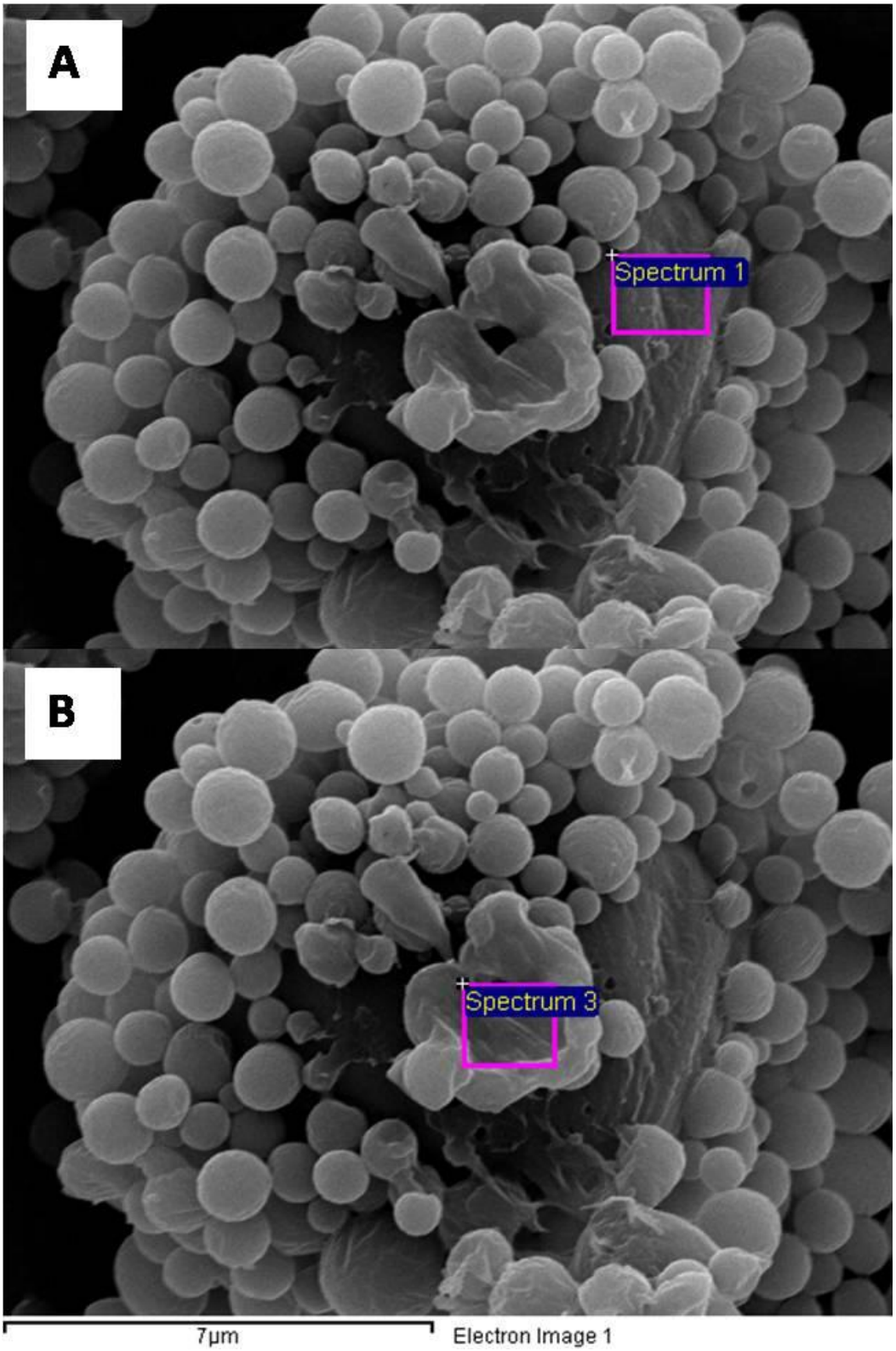

Figure 6.20: Shows the ESEM micrographs of the microspheres produced using PCL; (A) shows spectrum 1 – outer layer of the microsphere, (B) shows spectrum 2 – the inside of the microsphere, both relate to the EDS analysis in **Table 6.2**.

Here in **Figure 6.21** it is evident that the PCL microsphere released the encapsulated PPA without a stimulus. The PCL beads were dispersed into 37 ºC distilled water and elutes were taken every 10 minutes for a total of 90 minutes, the results demonstrate that PCL microspheres leak.

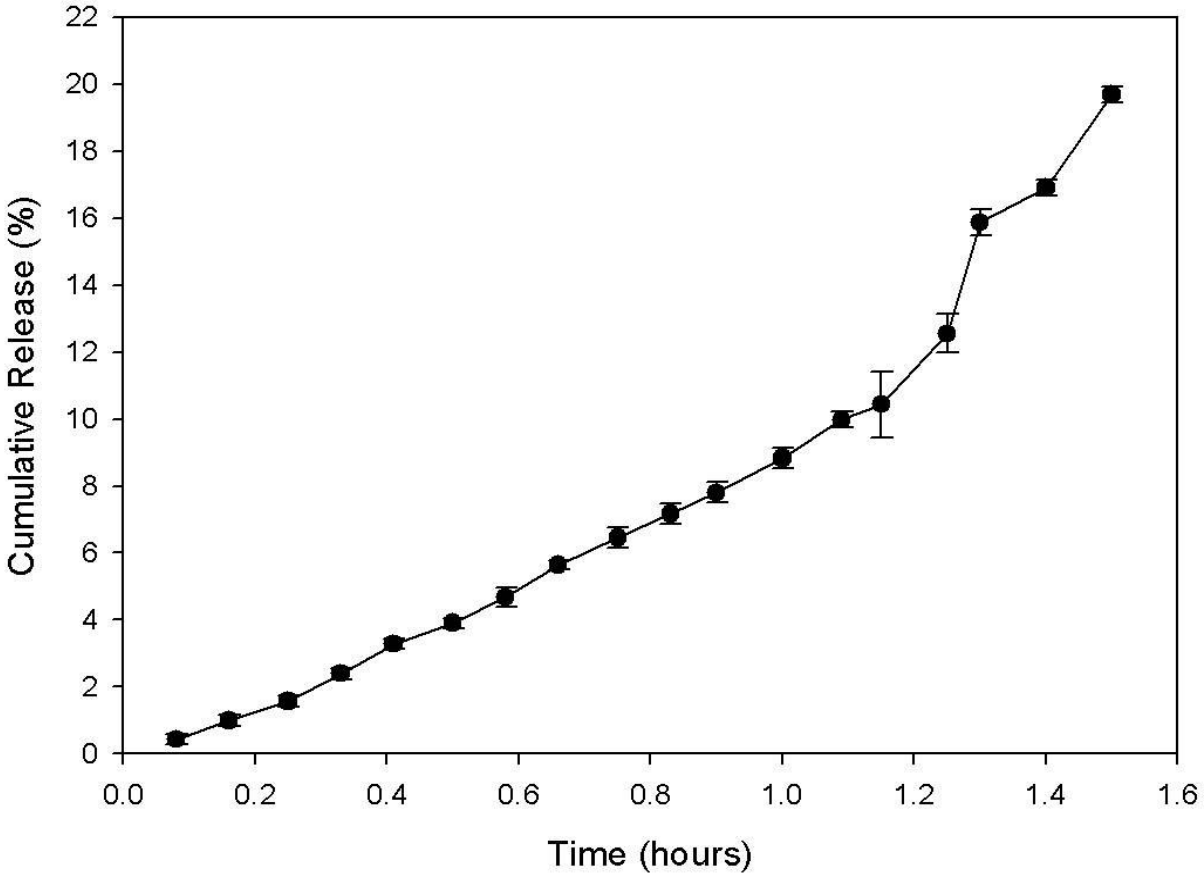

Figure 6.21: The graph illustrates the cumulative release, in percentage, of PPA released against time in hours, for a total of 2 h at room temperature of 22 ºC the content should remain encapsulated, however, here the contrary is demonstrated. The graph illustrates the mean values of the data points from all the batches produced (error bars are also indicated).

6.3.5 Mechanical properties of microsphere-cements

The resulting cements from the above successful cement formulations were compared to determine the most efficient method and polymer for the encapsulation of the acid component

of the cement. The results in **Figure 6.22** demonstrate that the strength of the cements produced is dependent on the speed of the homogeniser used. The slower the speed of the homogeniser the larger the microspheres, with more acid loaded, which mean the cement formulated is less porous as there is less degrading polymer.

From the results it is evident that the mechanical properties are directed related to the stirring rate. The faster the stirring rate the weaker the final cement is, due to the increased porosity. Microspheres produced at speeds of 6,000 rpm and mixed with the cement powders produce cements with strengths of 446 KPa and 403 KPa for Pyro and ortho brushite cements, respectively with similar porosity levels (16-17%). At the lower stirring speeds of 750 rpm (lowest speed the microspheres are able to be produced at) pyro brushite cement exhibits strengths of 767 KPa with porosities of 23%, whereas ortho brushite cements exhibit lower strengths of 662 KPa with higher porosities of 35%. This higher strength of the pyro cement may be attributed to the fusion of the brushite crystals with degrading Eudragit polymer **(Figure 6.16)**. In comparison **Figure 6.15** demonstrates the brushite crystals not fused together, and also shows the presents of the Eudragit polymer spheres between the brushite crystals, which may be the reason for the poor mechanical strengths.

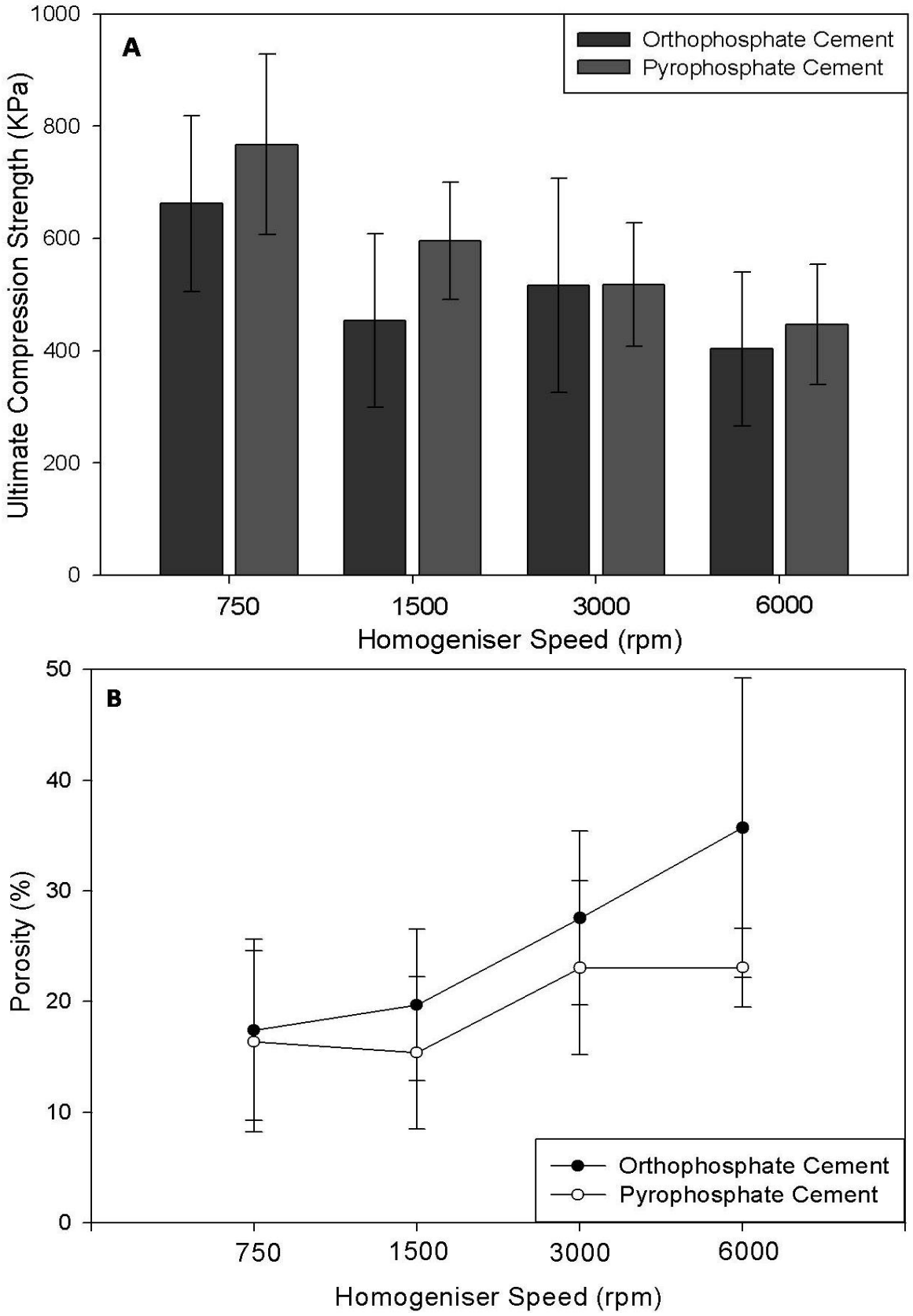

Figure 6.22: The graph illustrates the compressive strengths (A) of the cements compared to the relative porosities (B) at each homogeniser speed (750, 1500, 3000, 6000 rpm).

6.4 Discussion

Polymer matrices and microspheres were selected to be employed as temperature- and pH-sensitive encapsulation systems. Since there was no previously published work on the concept of using encapsulation techniques to delay CPC formation, different such methods were trialled during the first half of the project to see if the morphologies of the produced microspheres and matrices would be affected on encapsulating OA.

Eudragit®-PEG blend

The matrices, produced using a simple solvent casting technique had comparable morphologies to those obtained in previous studies (Fujimori *et al.* 2002) whose method was used in this work to encapsulate OA. The results of release studies carried out on temperature sensitive matrices have shown that there is a greater amount of the encapsulated OA released at around body temperature in contrast to the control (maintained at 4ºC), which released only small amounts of OA. As can be seen in **Figure 6.4**, during the first hour of the experiment an average of 50% of the encapsulated OA was released, while the control released only around 8%. In the second hour, close to 65% of the encapsulated amount was released in the experiment while the control released very little after the first hour. By 4 h of release, over 90% of the OA was released in the experiment while only a maximum of 15% was released in the control. After reaching a total release of over 90%, the curve plateaus showing on average greater than 95% release of the encapsulated amount by the end of the experiment. In contrast, the control curve, also demonstrated a plateau, but from the initial hour, shows only an average of 15% release by end.

The results obtained from these studies are similar to those obtained by Fujimori *et al* (2002) whose work involved quantifying the percentage of release of the drug acetaminophen from EPG matrices (Fujimori *et al.* 2002). They obtained an 80% release of a solution containing acetaminophen from 13% EPG matrices by end of a release study lasting 6 h. The cause of the much higher release of acid at 37 ºC could be attributed to the fact that 13% EPG matrices have a glass transition temperature at around that temperature making them more permeable than at 4 ºC. The results show in positive light that it would be possible to develop temperature-sensitive EPG matrices into an encapsulation system for use in CPC formulations. However, the morphology of these matrices would not be able to be incorporated within the cement components. Therefore, before they can be incorporated into a CPC formulation as a workable encapsulation system, they must be produced in micro-size. The formations of these micro-sized spheres were then carried out using different methods.

Eudragit® S100

The microspheres prepared by the double emulsion solvent evaporation method, using water-in-oil-in-water double emulsions (Jain *et al.* 2005), had regular morphologies, and were relatively spherical, as can be seen in the SEM pictures **Figure 6.5**. However, the microspheres appeared to be broken and damaged, therefore this was another method that was not of choice for producing microspheres for subsequent release studies. The release studies of pH-responsive microspheres have, contrary to expectation failed to show that a cement paste could be formulated without triggering setting and cement formation at a lower pH. It was found that in the first hour, there was a release of around 7% of the encapsulated amount in the experiment maintained at pH 7.4 (**Figure 6.6**). This was less than three times that of the control, which released in the same time, nearly 2.5% at pH 4; the low pH release also

demonstrated large errors (almost ± 1.0%). This shows that the microspheres are only slightly sensitive to pH, and that storing a cement mix at low pH such as 4 would result in conversion of at least half of the β-TCP into brushite. Furthermore the amount released did not increase by more than 1% in the following 6 h in both experimental and control release profiles. Therefore, not only was there an average release of only 7% of the entire encapsulated content of acid, but the microspheres did not show much sensitivity to pH. These results are in contrast to those obtained by Jain *et al.* (2005) who produced Eudragit S100 microspheres loaded with insulin, and obtained a release of nearly 50% by the end of a 6 h release study (Jain *et al.* 2005).

Two reasons could be attributed to the failure of the experiment with pH-responsive microspheres. One reason for the relatively poor pH-sensitivity seen in the control could be that not all of the acid was encapsulated within the microspheres. A considerable quantity of OA may have been deposited on the microsphere surface, thereby not releasing it as such, but washing off the surface attached acid, upon contact with water. Another reason could be that the microspheres incurred considerable damage during preparation since making double emulsions is a relatively complex procedure involving a high-shear homogenisation step and an extreme temperature freeze-drying step. The another method described previously (Haznedar & Dortunc 2004) was originally intended for the production of Eudragit RS; used on Eudragit S100 as an alternative. The method did not produced microspheres, instead clumps of highly irregular flake-like structures was formed, as apparent from SEM analysis **(Figure 6.7)**. The subsequent release profile of these polymer flakes was demonstrated in **Figure 6.8**; this was considered a failure. Again the flake-like structure probably bound much

of the acid on the surface, which washed off during the release study exhibiting release of phosphate regardless of a change in pH.

Eudragit® RL

The temperature sensitive microspheres were produced by a method (Azarmi *et al.* 2002) previously used for the encapsulation of drugs in to microspheres, such as insulin. The originally intended method for Eudragit® RS/RL polymers was used and produced regular bead like morphology. Initially, however, the microspheres were highly clumped together. Encapsulation was possible with the solvent evaporation method using the acetone/liquid paraffin system **(Figure 6.9–10)**. Consequently, the release profiles of these microspheres exhibited an initial burst and then plateaus after 60% of the total phosphate had been released (after 7 h). On comparing the control sample (at 4 ºC) to the increased temperature (37 ºC) sample release profile **(Figure 6.12)** it was obvious that this method was successful in producing a temperature sensitive microcapsule that would release on demand.

X-ray diffraction analysis was carried out on the cement mix obtained by mixing the released OA from the temperature-sensitive microspheres with increasing amounts of β-TCP. It showed that a small amount of the β-TCP was converted to brushite **(Figure 6.13)**. This was both conclusive evidence for cement formation as well as confirmation of the fact that the released content from the temperature-sensitive matrices was indeed OA and not any other substance. The reason for the small peaks representing brushite is likely due to the relatively small amounts of acid encapsulated (no more than 1 ml), and also due to dilution of OA samples when they were released (in 200 ml of water).

SEM micrographs of the fracture surfaces of the Eudragit cement are shown in **Figure 6.15**; the micrographs show the effect of encapsulating the PPA in the Eudragit microspheres instead of using it directly during mixing. The images illustrate the size and shapes of the brushite crystals which form blade-like crystals to indicate the presence of brushite. On examination at higher magnifications, the length of the blade-like structures ranged from 15–50 μm in length and from 2–10 μm in width. These sizes are consistent with the control pyrophosphate modified brushite cements made previously. **Figure 6.14** confirms the composition of the cement produced using XRD analysis which exhibits peaks for β-TCP and brushite. However, the presence of blade-like crystals in the pyro-modified brushite cement is not typical of the structure, as Grover *et al.* demonstrated the mixture of β-TCP-PPA-OA presented prismatic crystals 2–4 mm in length and 1–2 mm in width instead of the blade-like microstructure (Grover *et al.* 2005a). The presence of the brushite crystals here may be explained by the hydrolysis of the PPA to form OA. Grover *et al*. reported the presence of an unexpected amount of brushite in a study based on α-TCP-PPA-OA and suggested that when the cement is immersed in water, the P-O-P bond in a pyrophosphate ion could be hydrolyzed to form two orthophosphate ions, as shown in the equation 6.2, this may be the reason for the blade-like crystals present in the pyro-modified brushite cement:

$$H_4P_2O_7 + H_2O \rightarrow 2H_3PO_4 \qquad \text{(equation 6.2)}$$

Storage of microspheres

To determine the influence of storage time on the composition of the cement pastes formulated using microspheres, the cement powder and the microspheres were mixed using the quantities calculated from **Equation 6.1**, mixed with the adequate amount of distilled water and stored in a sealed universal container at 4 ºC for periods of 3, 7, 14, 28 and 90 days

before being cast into moulds in ambient conditions and allowed to harden in at various different conditions, as mentioned above. The initial results were promising; presenting the cement paste could be stored without setting for 28 days **(Figure 6.17)**. The final samples were removed from refrigeration after 90 days of storage and the consistency was analysed. The cement pastes that remain in a paste form, for such length of time, in the sealed containers suggests that the microspheres have not leaked their load of acid into the cement paste. This confirms the efficacy of the temperature dependent materials on storing the acid component in these conditions for an extended period of time. Unfortunately, the materials produced using the pH responsive polymer hardened after only one day of storage at 4 ºC therefore not useful for this investigation.

For the cement pastes that did not set, due the leakage of the microspheres, were then mixed under 37 ºC and allowed to set. This set cement was diffracted and results are explained using **Figure 6.18** show that brushite is the phase present in the final set cement, post hardening. It is also clear from the XRD patterns that the paste formulation remains as β-TCP and the acid kept separate from the powder not allowing the cement reactants to mix and set. The set cement consists predominately of brushite peaks with high intensities and a few, low intensity β-TCP peaks; comparable to control pyro-modified brushite cements.

PCL microspheres

As expected **Figure 6.19** shows that there is a variation in size with speed, as the speed was increased the microspheres reduced in size. However, as speed was increased, the microspheres exhibited a broader particle size distribution. This meant that the increase in speed was not stable, at lower speeds the microspheres seemed to be more stable, e.g. at

750rpm, the particle size distribution is of high intensity. The ESEM micrographs also confirm this results, **Figure 6.20** directly shows the variation in size. The spectrum boxes marked on the micrographs are analysed by the EDS and the results are shown in **Table 6.2.** The results quantify the elemental content of each spectrum taken; e.g. in spectrum 1 we expect to see the presences of everything that are components of the PCL microspheres only. From spectrum 2 we expected the same, however, with the presence of phosphorus which would indicate that the PPA was encapsulated. However, this was not the case. Both spectrums demonstrated no phosphorus presence. This could possibly be due to the small amount encapsulated or that the particular microsphere broken and analysed with the EDS was not recently broken. **Figure 6.21** illustrates the initial cumulative release of the acid released at room temperature (22 ºC); the content of the microsphere should remain encapsulated, however, it is the total opposite; total uncontrolled release was observed. The reason for this remains known; it may be due to the instability of the microspheres and the strength of the acid content.

Mechanical properties of the cements produced following the encapsulation of the acid component remains to be generally weak **(Figure 6.22)** compared to the control cements. This is no doubt due to the addition of the polymer microspheres that the acids were encapsulated in. At high speeds the microspheres produced were smaller; this means when mixed with the powder component of the cement matrix there is a higher ratio of polymeric material after release, due to the larger surface area in total. This in turn causes greater porosity in the hardened cement, as the polymer degrades and departs the cement matrix, leaving a highly porous scaffold. However, one method of overcoming this was to produce larger microspheres to maximise loading and minimise the polymer-to-cement ratio.

However, the continual production of larger microspheres can be difficult; microspheres were not easily fabricated below 750 rpm using the method by Azarmi *et al.*; although many methods suggest otherwise (Gao *et al.* 2006;Haznedar & Dortunc 2004;Kim *et al.* 2002;Sipos *et al.* 2005;Tamber *et al*. 2005;Wu *et al*. 2003). In the preparation of the microspheres, the selection of the appropriate solvent is of major importance. The ideal organic solvent has low toxicity and diffuses quickly into the external aqueous phase, thereby ensuring uniform solidification of the polymer. Rapid solidification of the globules is a key step, because this avoids coalescence of the droplets and drug outflow from them, especially at such low speeds. Acetonitrile, methanol, methyl ethyl ketone, acetone, ethyl acetate and also their mixtures are widely used as polymer carriers; these solvents are less toxic and their use can result in a slightly increased particle size (Ruan *et al.* 2002). Most of the research on polymer microsphere production is focussed around drug delivery, and optimising the encapsulation of drugs into the smallest particle size. However, here in this study we are looking at increasing at particle size to maximise the loading and minimising the amount of the polymer in the cement formulation. **Figures 6.22** demonstrate that producing larger microspheres can result in stronger cements, exhibiting 767 KPa at speeds of 750 rpm with an average porosity of 16% ($n = 3$). These cements demonstrated significantly greater strengths than the cements with microspheres produced at 6000 rpm ($\rho < 0.05$).

6.5 Conclusion

Using a Eudragit® RS-PEG 400 blend polymer, temperature-sensitive matrices were produced that successfully encapsulated OA. They were studied for release of the acid and it was found that almost all of it was released it at 37 ºC and only very little at 4 ºC showing the responsiveness of the matrices to different temperatures. X-ray diffraction then showed that the OA released from the polymer could cause hardening in the brushite cement.

The temperature-sensitive matrices can be tested further for increased capacity to encapsulate OA. When more information from different batches is available, the exact amount of polymer required to obtain a certain amount of brushite can be calculated and feasibility studies can be conducted for application *in vivo*. The temperature-sensitive matrices could be tested for the possibility of producing an injectable pre-mixed brushite CPC paste by mixing appropriate quantities of the ground or crushed OA-encapsulating matrices, β-TCP and water. Storing the paste at low temperatures such as 4 or 8 ºC would prevent the release of OA from within the polymer matrix and thus ensure that significant cement formation will only occur once implanted wherein the temperature of the CPC paste will be raised to around 37 ºC.

Chapter Seven

Calcium Phosphate Cements For Drug Delivery

7.1 Introduction

Postoperative infections are one of the largest problems associated with orthopaedic surgery and such infections often lead to severe pain, loss of bone tissue and possibly removal of implants, which requires secondary operations (Harris & Sledge 1990;Lew & Waldvogel 2004a;Ruchholtz *et al.* 2004). These orthopaedic-related infections are largely caused by Gram-positive bacteria such as *Staphylococcus aureus*, *epidermidis*, and *Streptococci* (Moojen *et al.* 2007). These bacteria are treated using various regimes of antibiotic administration and for this reason, an increasing number of these bacteria have become resistant to antibiotics. Especially methicillin-resistant *S. aureus*, which are commonly found in infections caused by orthopaedic surgery (Dion *et al.* 2005;Penner *et al.* 1996).

Often intramuscular or intravenous administration of an antibiotic does not allow sufficient concentrations of the drug to reach the area of infection, as blood circulation is limited and/or uncertain. Therefore, one current method of treatment is the localized delivery of antibiotics. One way of enabling localised delivery is to encapsulate the drug of choice into poly(methyl methacrylate) (PMMA) beads (Alt *et al.* 2004;Bohner *et al.* 1997), which are pressed into the defect or mixed with CPC (Itokazu *et al.* 1998). PMMA beads are, however, not resorbable (Penner *et al.* 1996) and require surgical removal after which they may be replaced either by new beads to prolong the antibiotic therapy or an alternative bone graft. Therefore, much research has focussed on the impregnation of antibiotics within resorbable materials such as CPCs (Anttipoika *et al.* 1990;Barralet *et al.* 2002a;Bohner *et al.* 1997;Dion *et al.* 2005;Frutos

et al. 2002;Ginebra *et al.* 2006;Jiang *et al.* 2008;Penner *et al.* 1996;Gitelis & Brebach 2002;Schnieders *et al.* 2006). The possibility to use CPCs, not only as bone substitutes, but also as carriers for local and controlled supply of drugs is very attractive. They have been used for the regeneration of bone defects caused by the resection of bone tumours, osteoporosis or osteomyelitis and can provide a prophylactic dose of antibiotics to prevent further infection. Unlike calcium phosphate ceramics employed as drug delivery systems, where the drugs are usually absorbed on the surface, in CPCs the drugs can be incorporated throughout the whole material volume, by adding them into one of the two cement phases, thus enabling more prolonged delivery of the therapeutic molecule of choice. Drugs can be introduced either in the liquid phase or in the powder phase of the CPC matrices. During cement setting, dissolution of calcium phosphates from the powder phase takes place, and it can be assumed that the drug is dispersed in the matrix formed by the set cement.

The hypothesis, therefore, must prove how CPC's can be formulated to exhibit properties of both a cement material scaffold and also is able to deliver antibiotics to the site of infection.

7.1.1 Aim

This chapter provides an insight in the application of CPC's as matrices for controlled drug release. Various formulations of the CPC's that have been previously studied are used here and have been manipulated by incorporating active molecules such as, Vancomycin Hydrochloride (VH) and Gentamicin Sulphate (GS). The principal objective of this investigation was to determine the effectiveness of the antibiotics which have been incorporated into the cement matrices by means of measuring the release and culturing microorganisms and determining inhibition zones.

7.2 Materials and Methods

7.2.1 Matrix preparation for CPC comparison study

The CPC's considered for the release study included two brushite cements and HA as a comparison. Firstly, HA cement consisted of an equimolar mixture of TTCP and DCPA which was mixed with water at a P: L of 3.5 g/mL. The setting reaction proceeded in accordance with Equation 7.1.

$$Ca_4(PO_4)_2O + CaHPO_4 + H_2O \rightarrow Ca_5(PO_4)_3OH + H_2O \qquad \text{(equation 7.1)}$$

The orthophosphate brushite cement consisted of β-TCP with a liquid component made up of 4 M orthophosphoric acid with 10 mM citric acid, as a retardant. The powder and liquid components were mixed at a P: L of 2.5 g/mL, the cement set in accordance with Equation 4.6. Finally, the pyrophosphate modified brushite cement consisted of β-TCP and a liquid mixture of distilled water combined with PPA with a water-to-PPA ratio of 1.37:1, both phases were mixed together at a P: L of 2.5 g/mL, and hardened in accordance with Equation 4.9. The VH (Sigma–Adrich, St. Louis, MO) was mixed with the cement powder at a concentration of 50 mg/g, prior to combination with the liquid phases in each case. All the cement matrices were poured into a PTFE split mould to produce set cylindrical samples of 12 mm (height) by 6 mm (diameter) and samples were allowed to harden for a period of 24 h in ambient conditions before further study.

7.2.2 Sample Elution

The CPC samples were immersed in 5 mL of pH 7.4 PBS stirred at 100 rpm and incubated at 37 °C. At regular time intervals 5 mL was withdrawn from each sample and assayed for

GS/VH content by a colourimetric method. Antibiotic release was monitored by measuring the absorbance of the elution medium at 280 nm and 246 nm (for VH and GS, respectively) using a UV–visible spectrophotometer (UVIKON 922, Northstar Scientific, Potton, UK). Antibiotic concentrations were determined from the average of three absorbance readings using corresponding calibration curves (Appendix 3).

7.2.3 Microbiological activity assay

Staphylococcus aureus (ATCC 25923, NCIMB, Aberdeen,UK) and *Staphylococcus epidermidis* (ATCC 12228, NCIMB, Aberdeen,UK) were aerobically cultured on nutrient agar plates, with antibiotic loaded CPC samples of known masses (approximately 2.0 g, 1.0 g, 0.5 g and 0.25 g) placed in the centre of each Petri dish for 24 h at 37 °C. The same was done for the samples used in the release experiment; this was thought to determine the potency of the cement samples following a release experiment lasting 24 days in total. The inhibition zones of the samples were determined by measuring the diameter of the inhibited area at three points. This zone also included the sample in the middle; the reason for this was that the samples varied in size. The effectiveness of the VH loaded cements was also measured by means of observing the broth culture turbidly with an inoculation of *S. aureus* (1×10^6 cfu/ mL) grown in Müeller Hinton broth for 24 h at 37 °C. A VH-containing sample was added into the Müeller-Hinton broth with *S. aureus* at a 1:1 ratio. A bijou containing 500 mL of Müeller-Hinton broth with *S. aureus* served as a positive control, and 500 mL of none inoculated Müeller-Hinton broth served as a negative control. All samples were incubated at 37 °C for 16–24 h. Antibacterial activity assays were conducted for both control calcium phosphate cements and calcium phosphate cements–loaded VH samples at each time point.

7.2.4 Mechanical Testing

The ultimate compressive strength (UCS) was measured using a Universal Testing Machine (Lloyd Instruments LTD, 6000R, Southampton, UK) at a crosshead speed of 2 mm/ min. The samples were tested before and after the 24 day release. Hardened cement samples were broken to provide fracture surfaces for observation, both before immersing in PBS to measure the release and after the release experiment had been terminated (after 24 days). The samples were coated with platinum before analysis in a field emission scanning electron microscope (SEM) (JEOL, JSM-7000F, UK).

7.2.5 Physicochemical characterisation

The crystalline compositions of the cement matrices were determined using XRD; Fourier transform infrared spectroscopy (FTIR) was also use to characterise the samples. The powdered samples were placed onto the diamond window on the stage of a smart orbit FTIR (NICOLET 380, Thermo Electron, Madison, WI), and the spectra were recorded at a resolution of 4 cm^{-1} and 32 scans. X-ray powder diffraction data were collected using CuKα1 radiation from a powder diffractometer (D5000, Siemens), aligned in transmission mode. The data set was collected from 5˚ to 60˚ 2θ with a step size of 0.05˚.

7.3 Results

Initial work carried out on the antibiotics VH and GS using characterisations methods, such as SEM, XRD and FTIR. This was to identify and characterise key properties the antibiotics prior to incorporation with the cement, to determine any factors which may influence the cement properties after mixing within the cement.

7.3.1 Comparison of CPCs

In the case of both the brushite cements, a burst release of VH was observed during the first 24 h of the stud **(Figure 7.1).** Following the initial burst, the rate of release reduced significantly, and after 11 days, both cements had released 75-80% of their loaded VH. In comparison the HA cements released only 20% of the VH within the first 24 hours, however, by day 4 the total percentage released increased to 40%, this trend continued until day 7 and carried on increasing until day 7 when the release reached 80%, after which it plateaued.

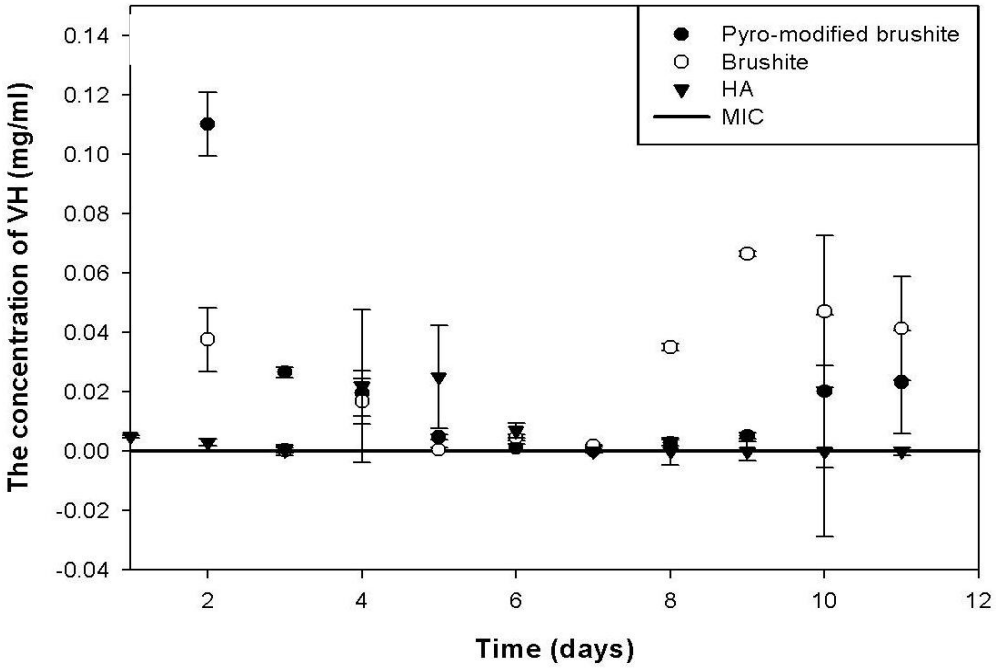

Figure 7.1: The concentration of the drug in the eluent per day, of VH from the three cement matrices; two brushite based cements are compared to the traditional HA cement, with the MIC line.

Figure 7.2 (A) illustrates the diameters of the inhibition zone formed around each cement sample when placed onto a culture of *S. aureus*. All the cement matrices exhibit similar inhibition zones ranging from 15–21 mm, interestingly, the HA cement not loaded with VH also demonstrates a bactericidal effect on the *S. aureus* comparable to that of the cements loaded with VH. The digital images in **Figure 7.2 (B)** give a visual representation of our findings.

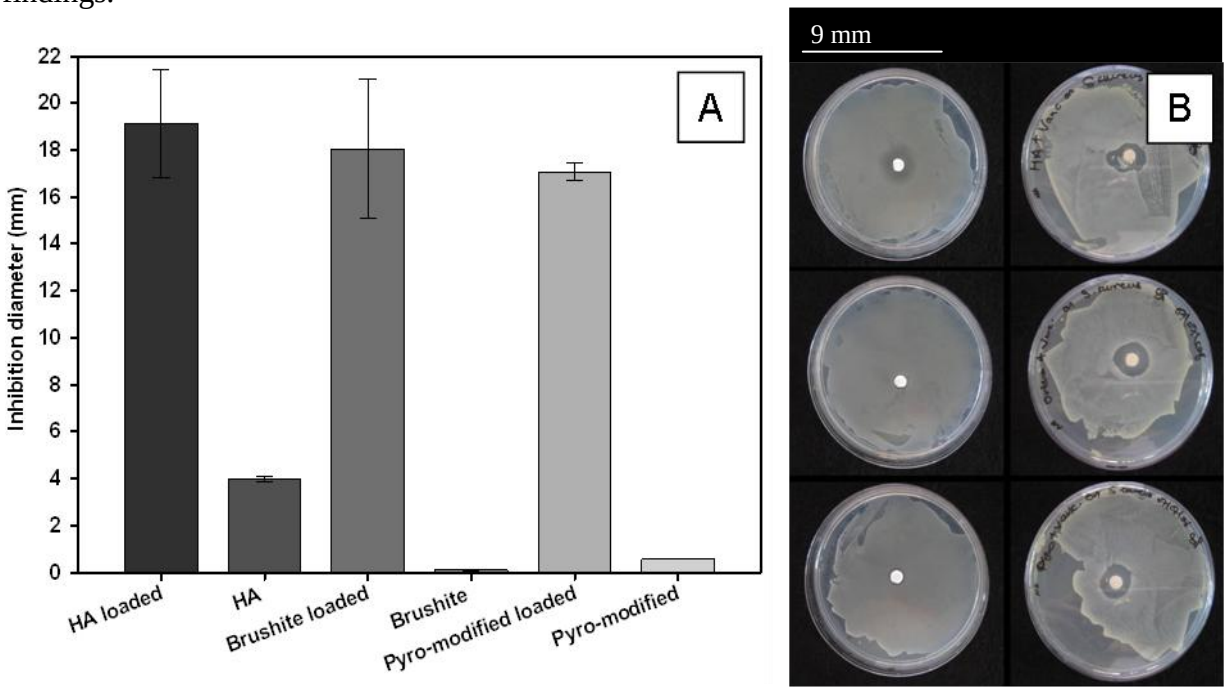

Figure 7.2: Illustration of the inhibition zone around the cements in both loaded and unloaded cement matrices (A); the digital images of the inhibition zones (B).

Table 7.1 shows the antimicrobial activities of the S. *aureus* in the broth; organisms were grown aerobically at an agitation of 100 spm at 37 °C, then VH eluted solutions were added to the broth dilutions. In the case of the two brushite based cements, sufficient antibiotic was released from the cement matrix to have an inhibitory effect on the S. *aureus* culture. On the other hand, the apatite cement did not release sufficient active drug to inhibit the growth of the organism.

Table 7.1: A summary of the results obtained from the antimicrobial assays performed using the VH eluted from each cement sample.

Cement formulations	*VH (mg/mL) Day 1*	*VH (mg/mL) Day 2*	*VH (mg/mL) Day 3*	*VH (mg/mL) Day 4*	*VH (mg/mL) Day 5*
Apatite cement (control)	0	0	0	0	0
Apatite cement loaded VH	3.43 e-3	5.51 e-3	5.59 e-3	9.23 e-3	0.02 ± 0.00
Ortho cement	0	0	0	0	0
Ortho cement loaded VH	1.17 ± 0.20	0.72 ± 0.10	0.44 ± 0.07	0.27 ± 0.05	0.19 ± 0.03
Pyro cement	0	0	0	0	0
Pyro cement loaded VH	1.25 ± 0.25	0.88 ± 0.08	0.60 ± 0.05	0.45 ± 0.08	0.35 ± 0.02

The microstructures exhibited by the brushite and HA based cements are shown in **Figure 7.3**. The brushite based cement material consisted of large plate-like crystal of 20 to 50 μm in length typical of a brushite cement microstructure. The HA based cement material was formed of submicron crystals that were considerably more densely packed than in the brushite cement.

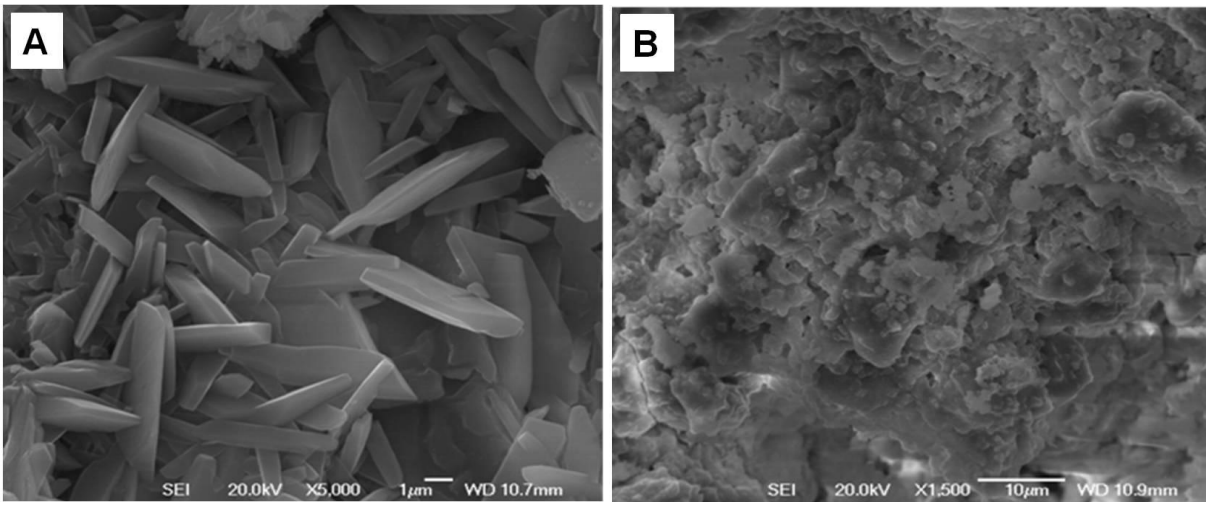

Figure 7.3: SEM images of the microstructure of (A) typical brushite structure, illustrates needle-like thin ling crystals and (B) HA cement, characterised by flat densely packed crystals.

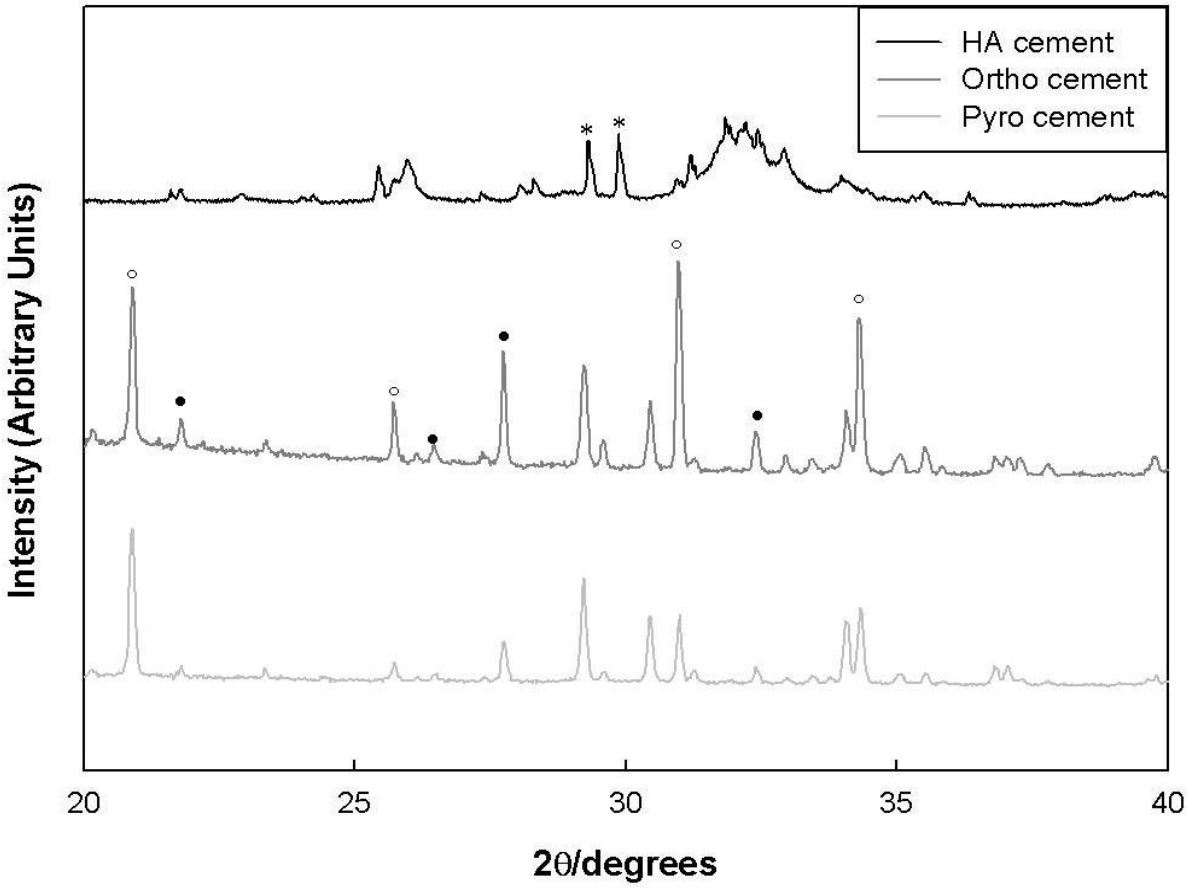

Figure 7.4: Compares the diffraction patterns of the samples as shown in the SEM micrographs of the various cement formulations. The various peaks are indicative of the composition of the samples; ○ Brushite; ● β-tri-calcium phosphate (β-TCP); * Tetracalcium phosphate (TTCP), which remained in small amount in the HA cement (at 28˚ and 29˚ 2θ).

The chemical characteristic of the cements were compared by XRD analysis **(Figure 7.4)**; the HA cement exhibited apatitic phases at approximately 32º 2θ and also exhibited some unreacted TTCP at 28˚ and 29˚ 2θ. The brushite phases were present in both orthophosphoric and pyrophosphoric brushite cements, with small amounts of unreacted β-TCP. FTIR was also used to characterise the cements **(Figure 7.5)**.

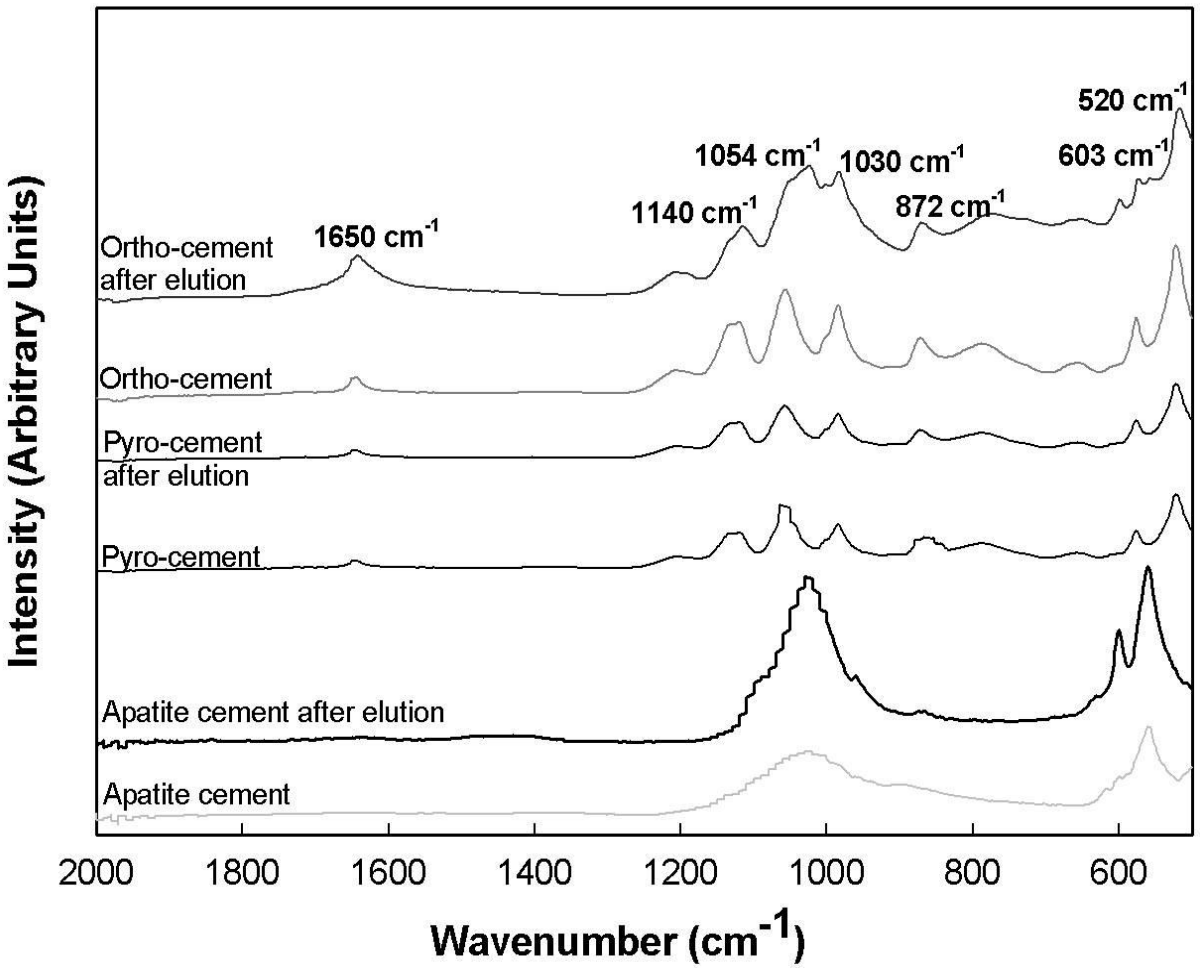

Figure 7.5: FTIR spectra of the apatite cement and brushite cements (both OA and PPA brushite cements). The spectra of all CaP based materials indicated the presence of phosphate groups at the range of 1070-1140 cm $^{-1}$. In addition, the peak at 872 cm $^{-1}$ of the brushite cements was indicative of the presence of HPO_4^{2-} groups.

7.3.2 Brushite cements

Cement setting times

The initial setting time for the control cements was 5 mins, as expected. The addition of GS reduced the setting time, but did not have a significant ($\rho \geq$ than 0.05) effect on the setting time. However, the addition of VH increased the setting time to a greater extent, as shown in **Table 7.2** and **7.3**.

Table 7.2: Compares the average setting times and the UCS (MPa) for the cements formulated using β-TCP + OA with the addition of antibiotics (GS and VH).

Cement formulations	*Average initial setting times (mins)*	*Average final setting times (mins)*	*Average UCS (MPa)*
β-TCP + OA (control)	3.55 ± 0.55	31.00 ± 1.56	38.72 ± 9.25
β-TCP + OA + GS	9.00 ± 1.16	78.00 ± 1.15	22.90 ± 4.04
β-TCP + OA + VH	11.00 ± 2.3	157.10 ± 20.5	11.88 ± 3.06

Table 7.3: Compares the average setting times and the UCS (MPa) for the cements formulated using β-TCP + PPA with the addition of antibiotics (GS and VH).

Cement formulations	*Average initial setting times (mins)*	*Average final setting times (mins)*	*Average UCS (MPa)*
β-TCP + PPA (control)	4.70 ± 1.64	10.20 ± 1.55	67.42 ± 25.60
β-TCP + PPA + GS	68.90 ± 8.88	88.10 ± 5.38	68.05 ± 16.50
β-TCP + PPA + VH	33.80 ± 1.75	88.80 ± 4.39	22.52 ± 13.70

Release of drugs

The concentration of the antibiotics, GS and VH released from the CPCs is shown in **Figure 7.6**, which illustrate the concentration of the released antibiotics from the CPC produced using of β-TCP + OA, over a period of 24 days. The concentration of VH initially released (with in 24 h) was somewhat higher than that of GS, at 8.5 mg/ mL in the first 24 h compared to 1 mg/ mL of GS. This may have been due to the poor washout resistance, as there was more visible degradation than the GS and control cements. The VH cement only increased a small amount thereafter, the highest concentration reached was 9.5 mg/ mL by 264 h.

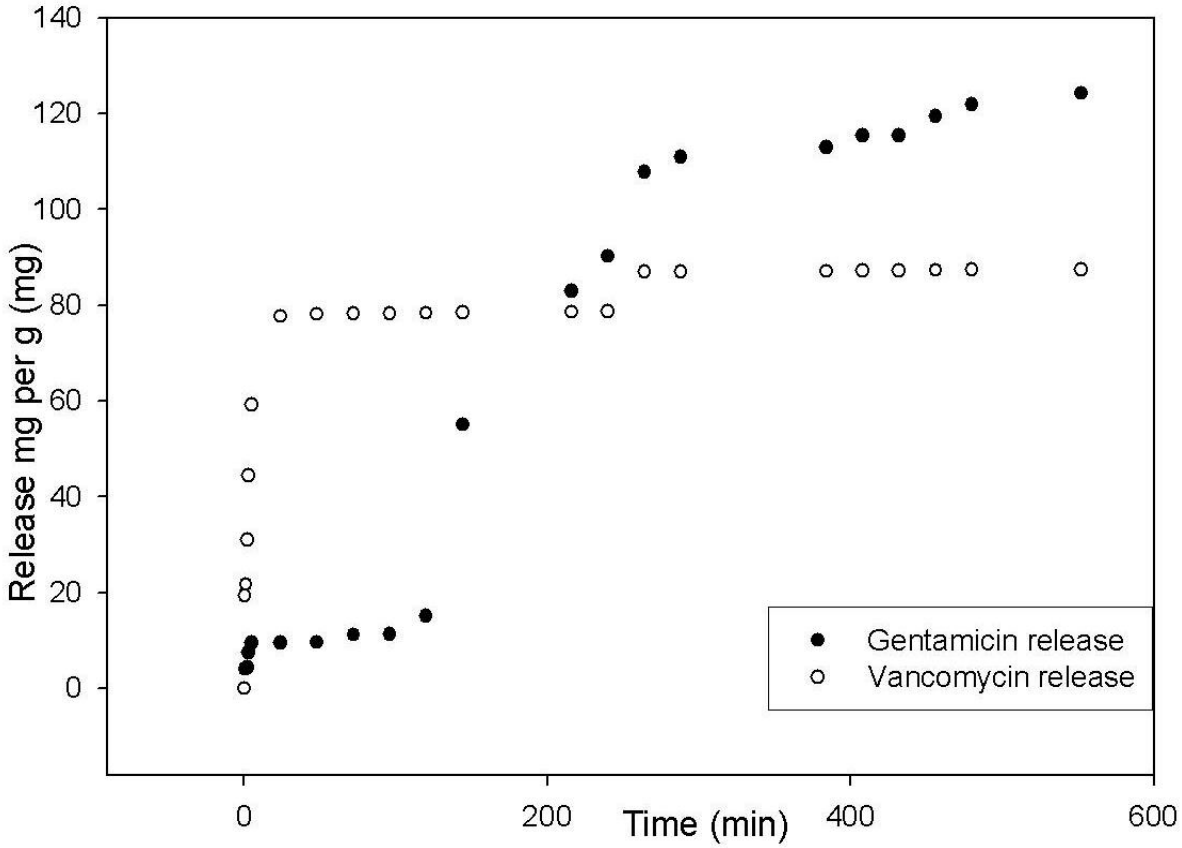

Figure 7.6: Illustrates the concentration of the antibiotic – gentamicin sulphate and vancomycin hydrochloride released from the β-TCP + OA cement, stored in PBS with at an agitation of 100 spm at 37 °C over a period of 24 days.

The concentration of the antibiotics, GS and VH released from the CPC produced using the same for the β-TCP + PPA cement is shown in **Figure 7.7**, over a period of 24 days; demonstrating an initial burst release which then plateaud very quickly. However, the amount released was very small (1.3 mg/ mL) with GS in the first 3 h compared to that released from the other cements. Once the release amount reached 1.9 mg/ mL by 96 h, the release rate decreased. The cement only released 0.06 mg/ mL from 96–288 h, after which not GS was released (10 days). VH shows a similar release pattern to that of GS; just releasing higher concentrations in the same time. The initial burst release took place within 18 h of immersion reaching 11 mg/ mL. The concentration reached 11.49 mg/ mL by 240 h (10 days), after which no more VH was released.

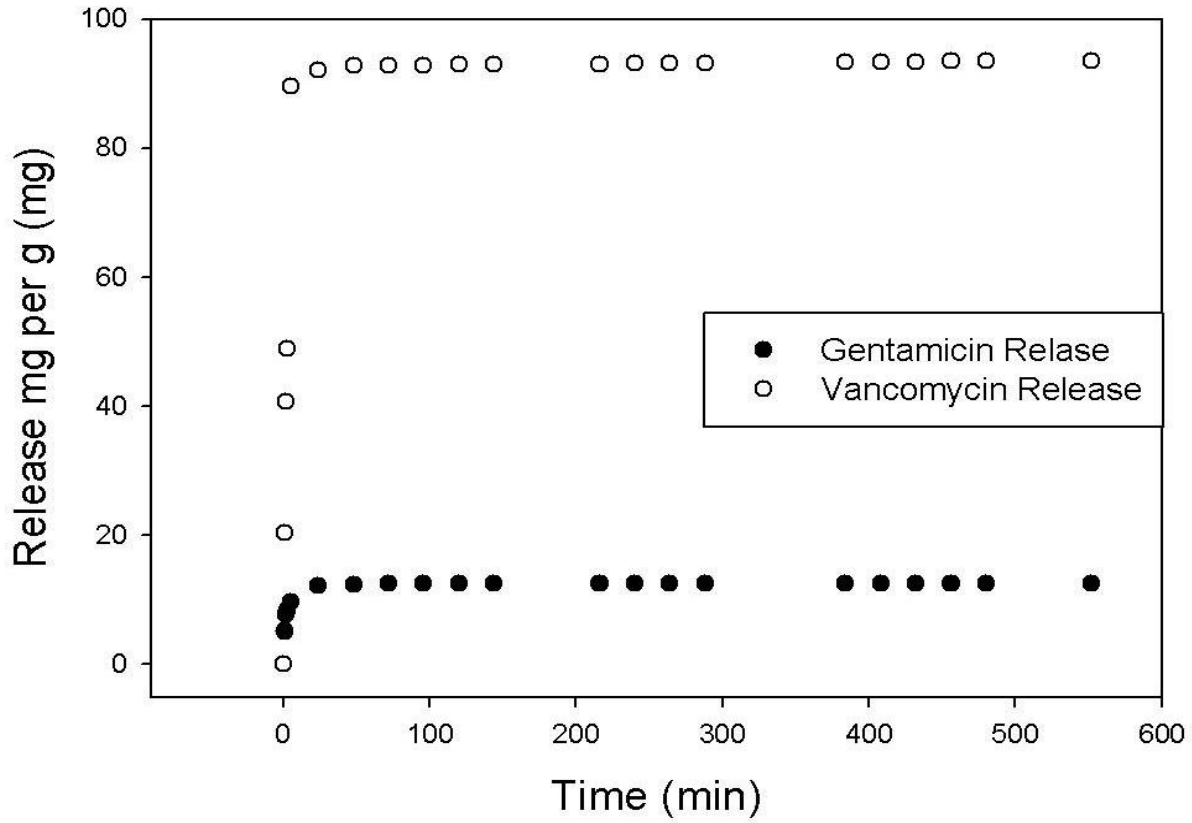

Figure 7.7: Illustrates the concentration of the antibiotic – gentamicin sulphate and vancomycin hydrochloride released from the β-TCP + PPA cement, stored in PBS with at an agitation of 100 spm at 37 °C over a period of 24 days.

Morphology of cements

SEM images **(Figures 7.8–7.13)** show the fracture surfaces of the cements before and after 24 days immersion in PBS. **Figure 7.10** shows the formation of needle like crystals of ~ 3–5 μm in length on the surface of the β-TCP once mixed with GS. The use of VH had a similar effect on the surface of β-TCP; however, the VH crystals were much larger in size (~ 10 μm) GS and also present large plate like structures.

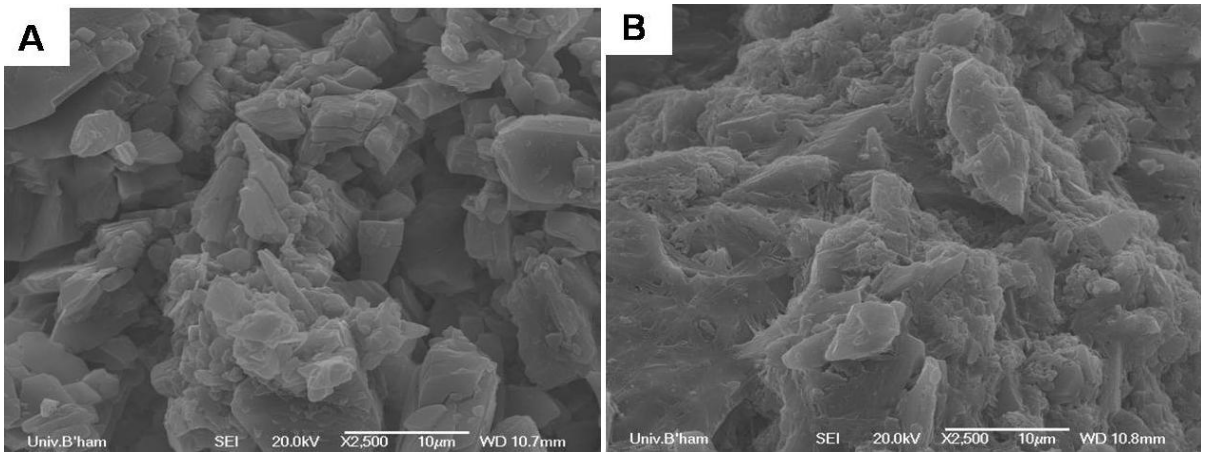

Figure 7.8: SEM images of the control OA cement sample; (A) illustrates small short brushite-like structure before and (B) demonstrates fused needle-like structures to create irregular globular structures, after being immersed in PBS for 24 days.

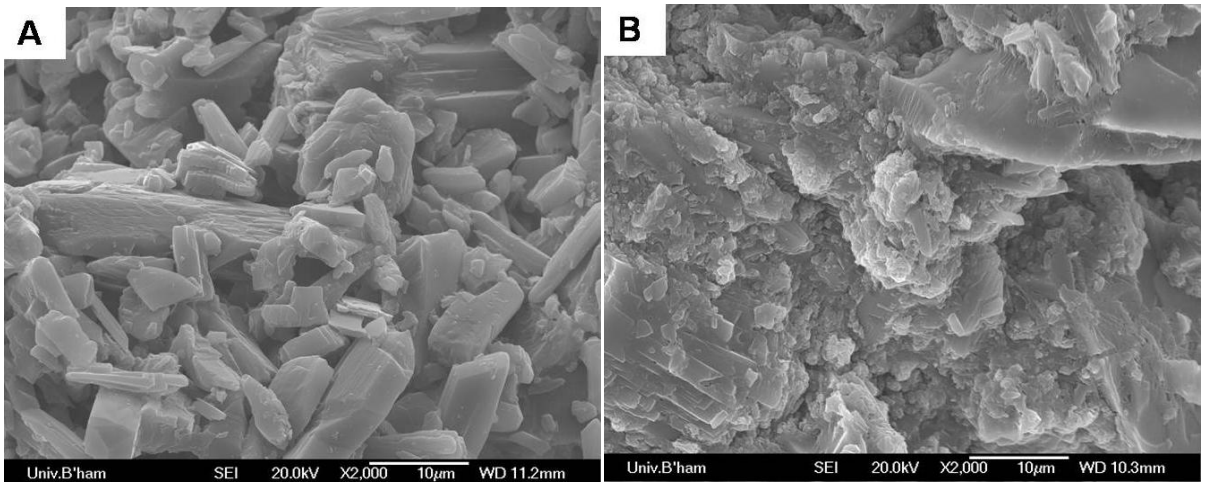

Figure 7.9: SEM images of the control PPA cement sample; (A) exhibits obvious needle-like structures indicating presence of brushite, before and (B) illustrates irregular globular structures, after being immersed in PBS for 24 h.

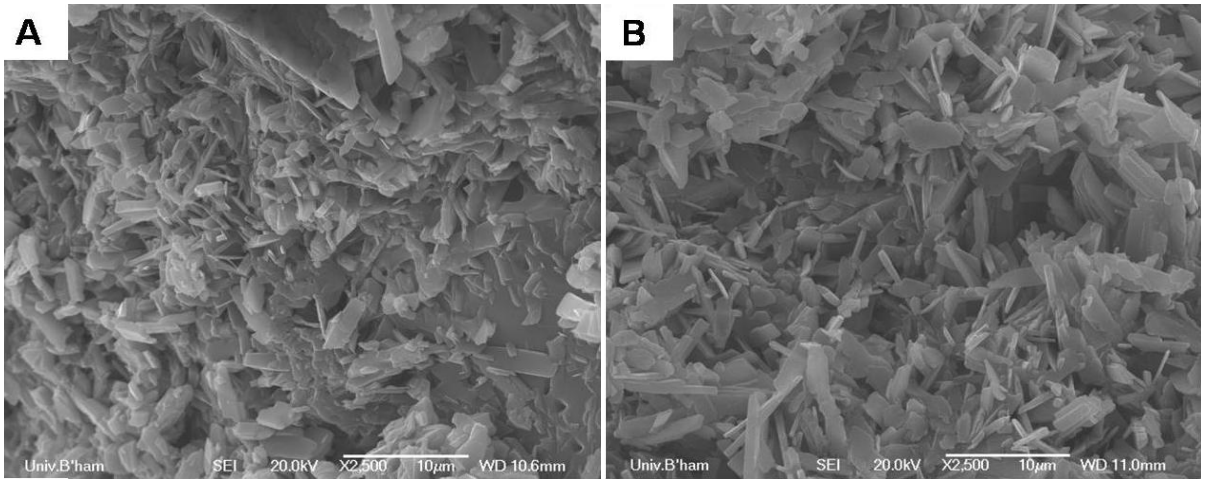

Figure 7.10: SEM images of the GS loaded OA cement sample; (A) before and (B) after being immersed in PBS for 24 days. Sharp defined fine need-like structures, 3–5 μm in length indicative of presence of brushite; no change in morphology indicated here.

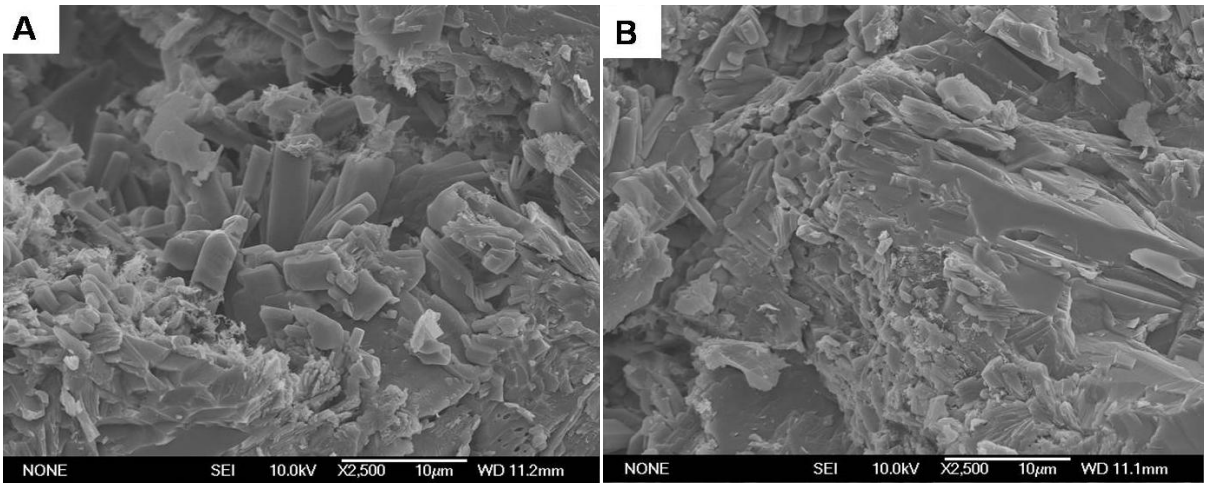

Figure 7.11: SEM images of the GS loaded PPA cement sample; (A) illustrates some brushite-like structure before and (B) demonstrates fused needle-like structures to create flat planes (10 μm in length), after being immersed in PBS for 24 days.

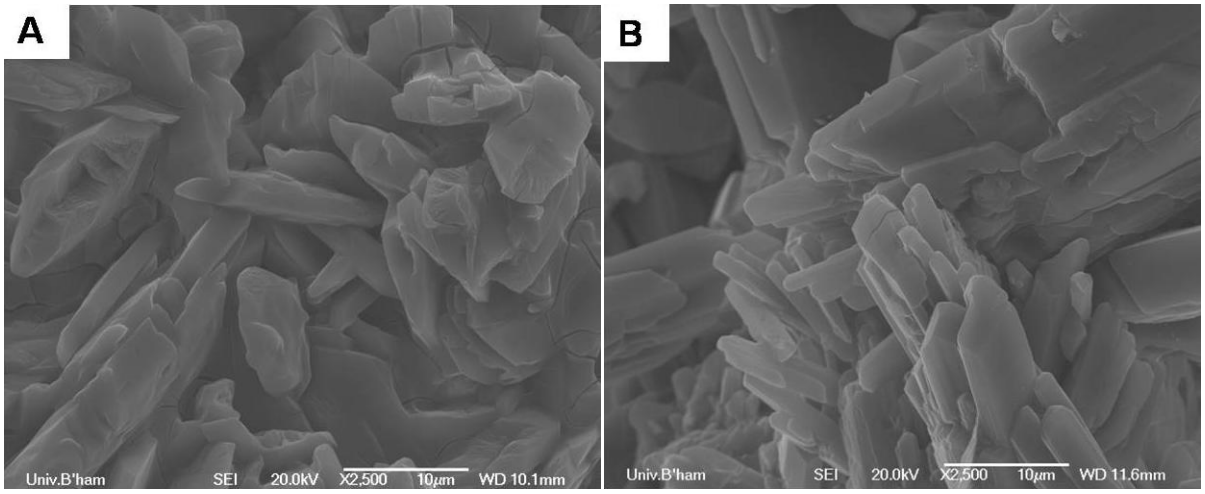

Figure 7.12: SEM images of the VH loaded OA cement sample, (A) before and (B) after being immersed in PBS for 24 days. Smooth flat plates over 10 μm in length; slightly needle-like indicating presence of brushite with larger crystals; no change in morphology indicated.

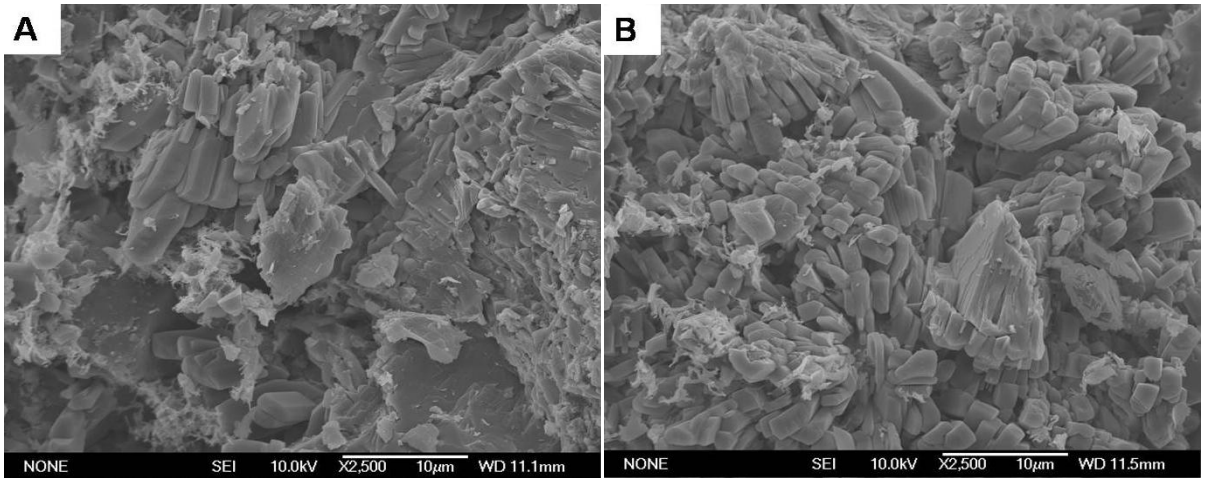

Figure 7.13: SEM images of the VH loaded PPA cement sample; (A) before and (B) after being immersed in PBS for 24 days. Sharp defined need-like structures, 3–7 μm in length indicative of presence of brushite; no change in morphology indicated here.

Inhibition of bacterial growth

Figure 7.14 and **7.15** compares the inhibition zones produced by the samples before and after the release experiment. Samples were aerobically cultured on *S. aureus* (ATCC 25923) over night at 37 °C. No valid inhibition zone measurements were obtained from the cultures with *S. epidermidis*, as the organism did not grow very well in the presence of the cements.

Results show that there was a significant (ρ < than 0.05) reduction in the inhibition zones produced before and after releasing of the antibiotics for 24 days with both cements. With OA cements, GS reduced from 18.5 mm to 3.1 mm and VH reduced from 16.6 mm to 2.5 mm. The control cement produced an inhibition zone, before and after the release but did not reduce significantly.

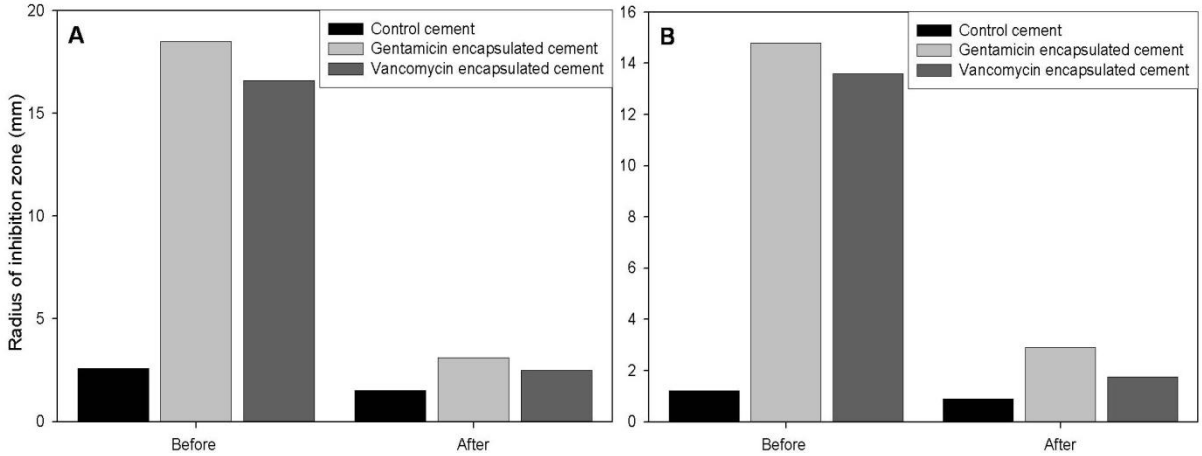

Figure 7.14: Average inhibition zones produced by OA cements grown on; *S. aureus* samples, after 48 h at 37 °C **(A)** and *S. epidermidis* samples, after 48 h at 37 °C **(B)**. The control cement illustrates some low antimicrobial activity.

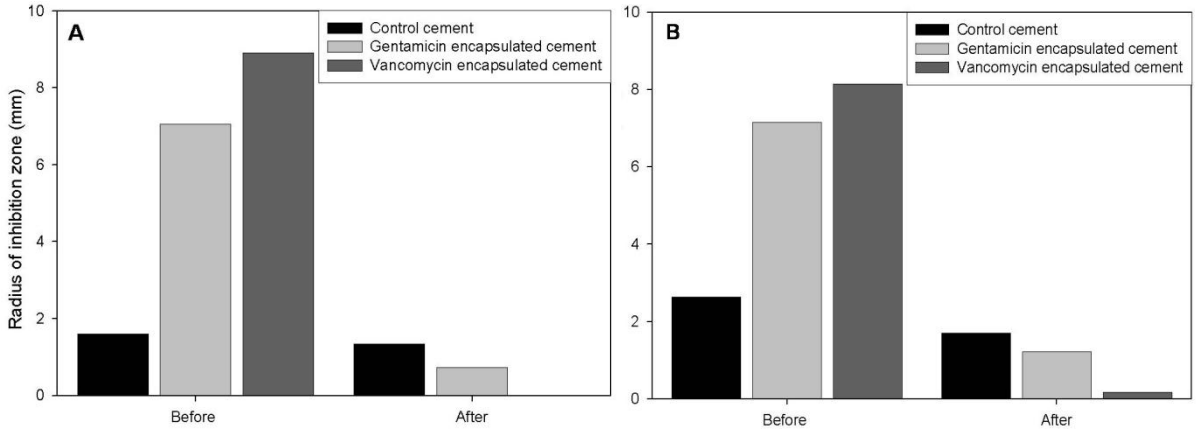

Figure 7.15: Average inhibition zones produced by PPA cements grown on; *S. aureus* samples, after 48 h at 37 °C (A), and (B) average inhibition zones of *S. epidermidis* samples, after 48 h at 37 °C. The control cement illustrates some low antimicrobial activity.

The PPA cement samples grown on *S. aureus* exhibited inhibition zones of 7.1 mm and 8.9 mm on average, after the encapsulation of GS and VH, respectively. After release experiments, the GS samples produced an inhibition zone 0.7 mm radius but the VH sample was unable to inhibit the growth of *S. aureus*. Growth on *S. epidermidis* follows the same pattern. The images in **Figures 7.16** and **7.17** illustrate the antimicrobial strength of the cements when loaded with GS (a), VH (b) and cements not loaded with any antibiotics (c) on a lawn of *S. aureus*; these results are represented quantitatively in **Figure 7.14** and **7.15**. The results show that the inhibition zones were significantly ($\rho < 0.05$) reduced in the control cements and the VH loaded cements after the release of the antibiotics.

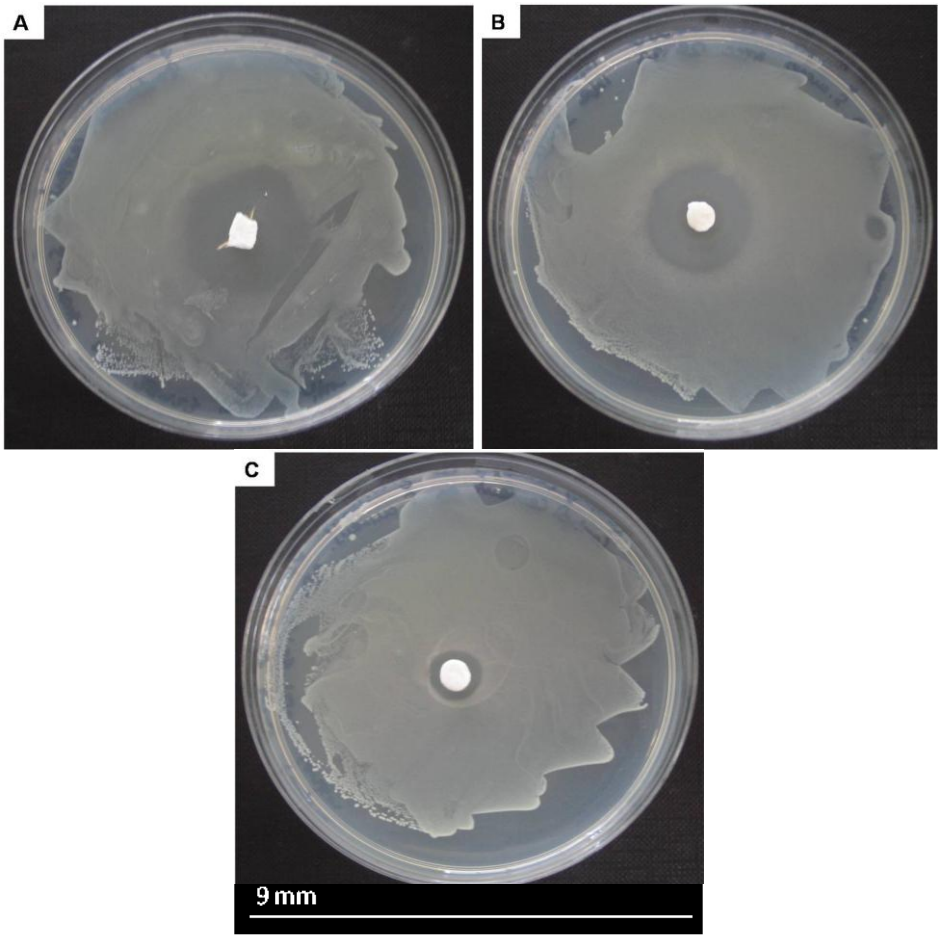

Figure 7.16: Images of the Inhibition Zones exhibited by GS **(A)** and VH **(B)** loaded OA cements compared with the inhibition zone produced by control OA cement **(C)**, which indicates that the control cement illustrates some low antimicrobial activity.

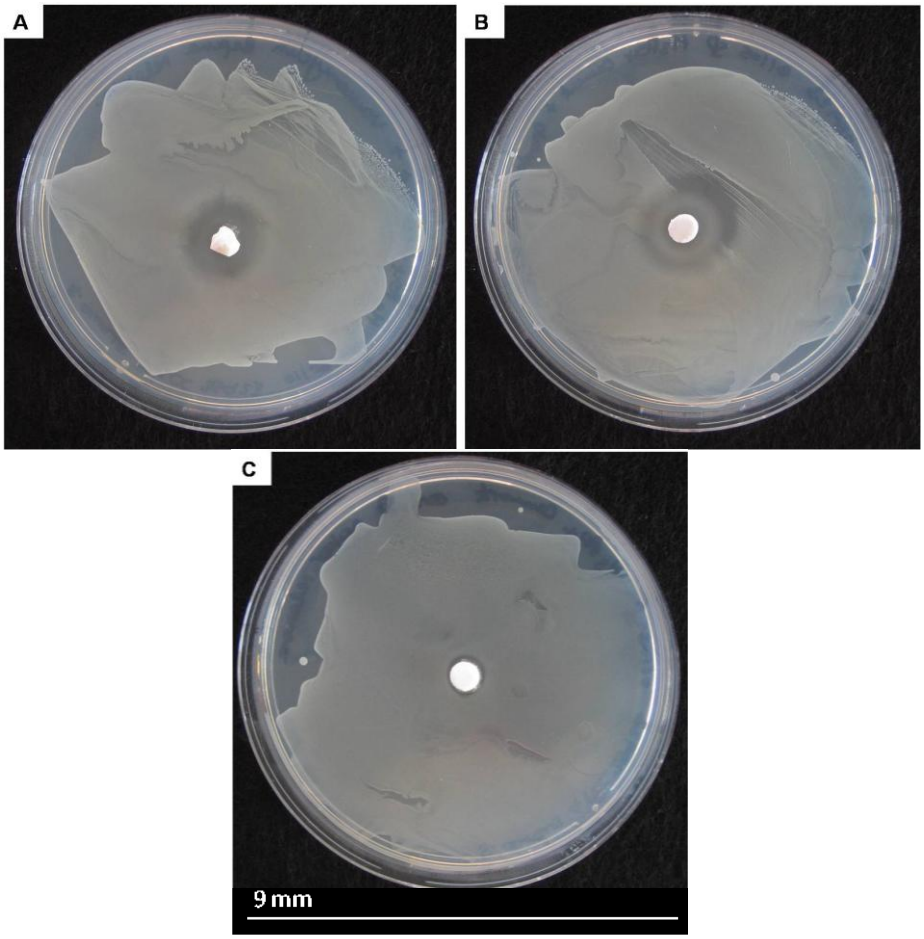

Figure 7.17: Images of the Inhibition Zones exhibited by GS **(A)** and VH **(B)** loaded PPA cements compared with the inhibition zone produced by control PPA cement **(C)**, which indicates that the control cement illustrates some low antimicrobial activity.

Figure 7.14–7.17 illustrates the inhibition zones of standard sample sizes made in a PTFE mould (diameter 12 mm and height 6 mm). However, although these samples have been compared in the figures the actual comparison of each antibiotic cannot be made, as the cement mass varies from one sample to another. To determine which antibiotic is better at inhibiting the growth of the bacteria the same mass of each sample was measured and used to compare the exhibited zone of inhibition (mm) with an increase in mass (g) **(Figure 7.18)**.

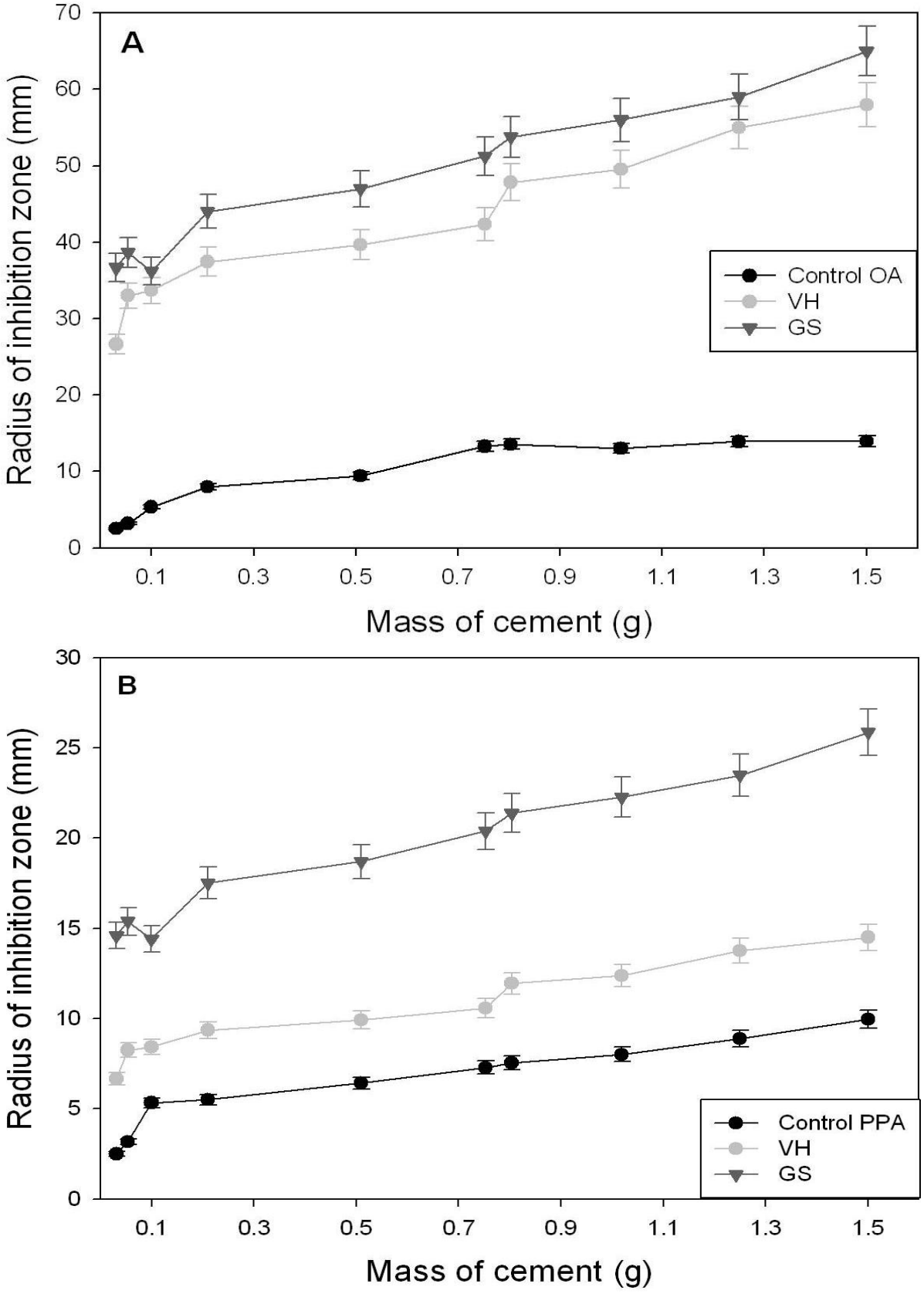

Figure 7.18: Inhibition Zones exhibited by the cements compared to the mass of cement samples placed in the centre of the lawn of culture; OA cement **(A)** and PPA cement **(B)**.

Compression strengths

The ultimate compression strengths of the cements reduced significantly ($\rho < 0.05$) after the release in the case of both cements. **Tables 7.4** show the effects of the addition of antibiotics.

Table 7.4: Average ultimate compression strengths of the cements before and after being placed in PBS for 24 days at an agitation of 100 spm at 37 °C.

	Average UCS (MPa)	
Cement formulation	*Before*	*After*
Control (β - TCP + OA)	38.72 ± 9.23	21.33 ± 5.34
Gentamicin (β - TCP + GS + OA)	22.90 ± 4.04	6.09 ± 1.77
Vancomycin (β - TCP + VH + OA)	11.88 ± 3.06	5.26 ± 3.41
Control (β - TCP + PPA)	67.42 ± 25.60	12.34 ± 4.80
Gentamicin (β - TCP + GS + PPA)	68.05 ± 16.50	8.27 ± 1.60
Vancomycin (β - TCP + VH + PPA)	22.52 ± 13.70	0.81 ± 0.70

7.4 Discussion

In the development of medical devices, there has been a growing need for materials that have antimicrobial properties in order to prevent infections (Christof *et al.* 2005). The gold standard treatment for the prevention of bone infections are PMMA beads (Kim *et al.* 2004) loaded with antibiotics, such as vancomycin (Shinsako *et al.* 2008) or gentamicin (Neut *et al.* 2001). These antibiotics are specifically used against *S. aureus* in the treatment of bone related infections such as osteomyelitis (Lew & Waldvogel 2004a). However, in order to achieve the desired antibacterial effect, it is necessary to supply a relatively high dose for example, 500 mg to 5 g (Korkusuz *et al.* 1993), which can lead to other complications. A local drug delivery system is advantageous because it is thought to decrease the systemic toxicity and it may also improve efficacy by delivering higher drug concentrations to infected bone (Frutos *et al.* 2002;Penner *et al.* 1996). The release of drugs from any drug delivery device depends on different factors such as the microstructure, the drug solubility, the type of bond between the drug and the matrix which holds it (Mathiowitz 1999), and the mechanism of degradation of the matrix (Ratner *et al.* 2004).

Calcium phosphate based materials such as HA, β-TCP, and brushite in particular, have shown promise in their ability to locally deliver a therapeutic dose of bactericidal drugs (Bohner *et al.* 1997;Dion *et al.* 2005). The reasons for this are owed to the ambient setting temperatures of these ceramics, which mean that active molecules can be incorporated into the matrices during manufacture; as a result the distribution of active molecules throughout the cement matrix is homogeneous. CPC's are also used as diffusion-controlled devices, where the drug is incorporated into a non-biodegradable matrix, through which it should diffuse. Although some CPCs are resorbable, in most of the CPC studied as drug-carriers, the

rate of matrix degradation is much lower than the rate of drug liberation. For that reason it is possible to assume that the drug release is mainly controlled by the process of diffusion through the cement matrix and not by the degradation of the same. Therefore, much research has been driven towards the impregnation of antibiotics within degradable materials such as CPC's (Anttipoika *et al.* 1990;Barralet *et al.* 2002a;Bohner *et al.* 1997;Dion *et al.* 2005;Frutos *et al.* 2002;Ginebra *et al.* 2006;Jiang *et al.* 2008;Penner *et al.* 1996;Gitelis & Brebach 2002;Schnieders *et al.* 2006).

Although, in most cases it can be considered that CPC do not degrade while drug is released, some authors have shown certain degree of degradation of CPC during drug liberation. For example, a study in Japan (Otsuka *et al.* 1997) showed an increase of porosity in a carbonated hydroxyapatite cement during the release of indomethacin, which was attributed to the cement degradation. In this case, the higher resorption rate of the cement was explained by the fact that the addition of different amounts of $NaHCO_3$ to TTCP/DCPD cement resulted in a carbonated apatite more soluble than the stoichiometric HA used in previous studies. Resorption of carbonated HA with time produced an increase of porosity, which increased the drug release rate (Chung & Park 2007). Consequently, if porosity does not remain constant, drug release kinetics does not follow Higuchi's law, and the drug diffusion through the CPC matrix is not the only mechanism which controls drug liberation. In any case, during release of drugs, the speed of resorption of the CPC matrix depends on various factors, such as chemical composition, microstructure and crystallinity of the cement. In the case of brushite cements, the degradation rate is much higher than that of apatite cements, and therefore is more important to consider these phenomena (Ginebra *et al.* 2006).

The setting reaction of the CPC can be affected or modified by introducing a drug either to the powder phase or to its liquid phase and, as a consequence, the physico-chemical (Ratier *et al.* 2001) and mechanical properties can change (Takechi *et al.* 1998). In general, in apatitic cements antibiotics tend to increase their setting times and reduce the mechanical strength. Takechi *et al*. studied the effect of incorporating flomoxef sodium in different concentrations (up to 10%) to the solid phase of cement formed by TTCP and DCPA. Since this antibiotic is very soluble, it was assumed that it dissolved fast in the cement liquid phase. The authors noticed a strong reduction of mechanical strength when the amount of antibiotic added increased. This decrease of mechanical strength was attributed to increased porosity and to some inhibition of the setting reaction, as suggested by the presence of certain amount of reactants when the antibiotic quantity increased. The drug release followed the kinetics typical for these types of materials, and after 72 h the total amount of liberated antibiotic was between 55% and 60%. In other cases, the modification of the CPC properties can be due to some chemical interactions between the antibiotic and the cement.

In comparison of the two main CPC's (brushite and HA) the results of this study reveal that HA exhibited different release kinetics compared to brushite cements **(Figure 7.1)**. HA rapidly released 90% of the encapsulated VH within 7 days, whereas, both the brushite cements steadily released the same amount over 11 days. Rapid release from both brushite cements suggests a link between the release profiles and the cement microstructure; both brushite cements follow a very close pattern with almost indistinguishable proportions of the VH released from the cement matrix at days 1 and day 11 **(Figure 7.1)**, respectively. This is highly likely since drugs are typically delivered from ceramic matrices by a process of simple diffusion. The HA cement had a slower initial release following a burst and plateaus by day

7, however, all the cements resulted with approximately 75% released by day 11. One explanation in the difference in release profiles may be the variation in microstructure **(Figure 7.2)**, which has an effect on the degradation of the cements (chapter 8 explains further). Additionally, the cement material contains a basic component (TTCP) that is likely to have caused transformation of the VH to its insoluble isoform, as a result inhibiting dissolution of the VH until the highly basic TTCP had either been reacted away or dissolved from the cement matrix. In addition, it is evident from the degradation study **(Chapter 8)** that there is a noticeable difference in the degradation of the cements with a difference in composition. The slower degradation of the HA may have provided an additional barrier to the release of VH from the cement matrix. As mentioned earlier, the residual unreacted TTCP (dissolution releasing of hydroxyl ions) may have been responsible for the bactericidal properties of the HA cement that was not loaded with VH **(Figure 7.2)**. Producing inhibition zone of comparable to the loaded HA cements; this mechanism has previously been exploited to develop antibacterial calcium phosphate cements from potassium substituted calcium phosphates (Gbureck *et al.* 2005a).

The antibiotic release kinetics of brushite cements, more resorbable than apatitic cements, was analysed by adding gentamicin sulphate both in powder form and as a solution (Bohner *et al.* 1997). The reactants used for the cement were MCPM and β-TCP. Once again the rheological and mechanical properties of the cement changed by antibiotic addition, but in the opposite direction of that reported by Takechi *et al.* They observed an increase of the setting time, which was initially too short, as well as an increase of mechanical strength, that was ascribed to the presence of sulphate ions in the antibiotic (Takechi *et al.* 1998).

The results illustrate the concentration of the released antibiotics (GS or VH) from the CPC produced using of β-TCP + OA **(Figure 7.6)** and β-TCP + PPA **(Figure 7.7)**, over a period of 24 days. The initial concentration of the released GS is lower than that of VH; within 24 h the cement releases 1 mg/ mL and releases 0.9 mg/ mL during the next 120 h. Thereafter a burst release occurs between 120–264 h. On the other hand, VH cements produced an initial burst release of 8.5 mg/ mL in the first 24 h, after which there was a very slow release for the next 24 days. The final concentration reached at the end of 24 days was 9.5 mg/ mL. In **Figure 7.7** the release from VH demonstrates an initial burst release. However, the amount released is very small (1.3 mg/ mL) compared to that released from the OA cement (12 mg/ mL). Release stopped after reaching 1.96 mg/ mL in 12 days. This could be due to the very slow degradation of the PPA cement *in vitro*. The GS release curve shows a similar pattern, with a burst release followed by no release after 10 days. However, the release concentration of VH is much higher (maximum released concentration = 11.49 mg/ mL). Both the cements demonstrated that after the first 10–15 days the cement stops releasing the antibiotics. The reason for the pause in release may be because the antibiotics on the surface of the cement samples have been released. Therefore, if the cement was left to degrade the antibiotic release would continue.

The control cement provided a weak antimicrobial potency with a maximum inhibition zone of 1.5 mm, with a sample mass of approximately 0.1 g **(Figure 7.16)**. The reason for this antimicrobial activity in the control cement originates from the release of hydroxyl ions which raise the pH value of the surrounding environment to approximately 12–12.5 (Gbureck *et al.* 2005a) after dissolution. This high pH value may destroy bacteria by damaging the cytoplasmic membrane and DNA and denaturing proteins. In contrast, the inhibition zones

around the GS and VH loaded cements were larger with values of approx. 44 mm and 37 mm, respectively. The antimicrobial potency of the GS containing cements had a significant difference ($\rho > 0.05$) after the sample was placed in solution to release antibiotics for 24 days. This means that the potency of the antibiotic reduces and antibiotics are eluted in the solutions during the release experiment. The compression results **(Table 7.4)** shows that the release has a significant effect ($\rho < 0.05$) on the UCS of the cements. Consequently, this means the addition of antibiotics reduces the strength, which may be due to the change in crystal structure or the dissolution of antibiotics to leave pores as shown in the SEM micrographs of brushite using OA and PPA **(Figure 7.8–7.13)**.

Although CPC's therapies show good results, a risk of establishing bacterial resistance due to low continual doses remains a threat (Durbhakula *et al*. 2004;Hendriks *et al*. 2004;Pitto & Spika 2004). In order to reduce the incidence of implant-associated infections, several biomaterial surface treatments have been proposed. One such study (Hamanishi *et al.* 1996) examined the incorporation of vancomycin to a CPC formed by TTCP and DCPD for treating osteomyelitis caused by MRSA. In an *in vitro* investigation they observed an effective release of vancomycin within 2 weeks, in the case of CPCs containing 1% vancomycin, and within 9 weeks for CPCs containing a higher content (5% vancomycin). In both cases, the released concentrations were higher than the effective concentration against different types of MRSA, which suggests that the dosage is high enough not to create bacterial resistance due to such treatment methods.

7.5 Conclusion

Incorporation of antibiotics within the cements has been demonstrated to release sufficient dosage, therefore reducing or even eliminating the risk of post-operative infections after major orthopaedic surgeries. We have demonstrated that VH can be delivered from brushite and HA cements, both the brushite matrices demonstrate similar release profiles. However, the HA cements damage the antibiotic effectiveness when VH was incorporated due to the high pH of TTCP; causing deamidation of VH. The release mechanism of VH from HA cements indicates more than one types of mechanism was involved.

Chapter Eight

Degradation of calcium phosphate cements

8.1 Introduction

Resorption of bone is a natural phenomenon that occurs during bone remodelling (details of the bone remodelling mechanisms are mentioned in Chapter 2). Ideally bone replacement materials should exhibit a similar resorption rate to natural bone, to ensure optimum osteoconduction and osteointegration once replaced with a synthetic material (Gupta *et al.* 2006). For this reason, much research has been driven towards alternative cements rather than HA; as HA is almost insoluble in physiological conditions, which means slow resorption rates. This in turn may eventually lead to catastrophic brittle failure.

8.1.1 Problems with CPC's

There are a number of problems associated with the use of calcium phosphate bone cements such as a very low resorption rate. There is some *in vivo* evidence to suggest that dissolution and cell mediated resorption occurs initially, it then slows down, as a result the cement may be stable for over 12 months after implantation (Legeros 1993). Previous work suggest that liquid to cement volume ratio (LCVR) does have an effect on the dissolution of the cements, higher LCVR allows more dissolution (Grover *et al*. 2006). Several other studies also show how the resorption of the various cements vary (Bohner & Baumgart 2004;Grover *et al.* 2006;Theiss *et al.* 2005); these studies all demonstrate that the more recently researched brushite cement exhibits faster resorption, compared to the traditional HA cement (Nilsson *et al.* 2002), this is due to the fact that brushite is sparingly soluble in physiological conditions. However, the transformation of brushite into apatite after implantation, results in an increase

of the resorption time (Constanz *et al.* 1998). This can be prevented by adding a magnesium salt of low solubility (Rousseau *et al.* 2003;Rousseau *et al*. 2002), they concluded that the presence of Mg in brushite cements affected their working characteristics significantly. Setting times, ultimate degree of conversion and mechanical performances were all altered as a result of the addition of magnesium phosphate. These effects depend largely on the nature of hydro-soluble polymers dissolved in the mixing liquid; specific interactions were suggested to exist between magnesium and hyaluronic acid.

8.1.2 Macroporosity of CPC's

Previous studies have shown that macropores can be introduced into cement by mixing the CPC with a pore-making agent that will be removed later. The pore-making agents that have been used by other researchers include hydrophobic liquid (Bohner 2000), degradable organic particles (Link *et al.* 2006), and $NaHCO_3$ (del Real *et al*. 2002). However, it is hard to control the particle or liquid drop size of these pore-making agents, consequently, making it difficult to manage the pore size of the macroporous cement; so the alginate beads were given more attention. The size of alginate beads can be controlled by using different needle size's, when produced using a needle technique. Alginate is the most frequently used polysaccharide system for protein encapsulation as it is readily available and inexpensive (details on structure and properties are found in Appendix 2). Sodium alginate hydrogels are widely used as thickeners in the food industry and in biotechnological applications, including cell encapsulation, protein delivery, and tissue engineering (Alves *et al.* 2008;Chan *et al.* 2002; Lima *et al.* 2006;Ishikawa *et al.* 1996;Serge *et al.* 2009). Moreover, sodium alginate microspheres were shown to exhibit bioadhesive properties, which can be exploited for site-specific drug delivery to mucosal tissues (Salgado *et al.* 2004).

The hypothesis must prove that CPC structure can be modified to allow the degradation to be controlled; this in turn should allow the brushite cement to chemically remain as brushite and not hydrolyse to HA.

8.1.3 Aim

CPC's have been widely used as a bone tissue engineering scaffold material due to its excellent osteoconductivity, however, *in vivo* resorption and tissue in growth is slow. To address these issues, calcium alginate beads can be introduced, which will create macroporosity in the system. The goal of this study was to investigate the handling properties and degradation characteristics of calcium phosphate cement containing calcium alginate beads. Alginate beads are non-toxic and very simple to make and the size of the alginate beads can be controlled by choosing the appropriate needle size. An in vitro degradation study was carried out in which cylindrical scaffolds were placed in PBS. Samples were assayed on mass, compression strength, and morphology; this study focuses on the effects of porosity on degradation. To enhance the rate of the degradation different amounts of calcium alginate beads were incorporated within the matrix. Micro CT was used to visually determine the effects and changes in porosity and pore size during degradation.

An *in vitro* ageing experiment in simulated physiological conditions (using PBS and serum) has been undertaken, with the aim of understanding the long term *in vivo* degradation of pyrophosphate modified brushite cements. The main purpose of this investigation was to monitor the degradation of the CPC in different solutions.

8.2 Methods and Materials

8.2.1 Materials

Calcium chloride dihydrate, tri-sodium citrate, ethanol, orthophosphoric acid and acetic acid were purchased from Fisher (Loughborough, UK), citric acid from BDH Laboratory Supplies (Poole, England), and sodium alginate, low-viscosity (3.7 mPas of 1% solution) alginate powder and high-viscosity (824 mPas of 1% solution) alginate powder from Sigma (UK). CPC's were synthesized in the laboratory.

8.2.2 Calcium phosphate cement synthesis

β-Tricalcium phosphate (β-TCP) was synthesized by heating a mixture of $CaCO_3$ (Merck, Germany) and $CaHPO_4$ (Mallinckrodt-Backer, Germany) to 1050 ºC for 24 h followed with quenching to room temperature in a desiccator. In this reaction the theoretical calcium to phosphate ratio (Ca: P) is 1.5. The sintered cake was crushed and passed through a 355 µm sieve. The purity of the solid phase was then detected by X-ray diffraction (XRD; D5000, Siemens, Munich, Germany).

8.2.3 Preparation of calcium-alginate beads

A calcium chloride solution of 100 mM and a sodium alginate solution of 2% w/v were prepared in distilled water. The cross-linked alginate beads were prepared by the 'drop wise' addition of 20 mL of sodium alginate solution into 100 mL of calcium chloride solution through steel hypodermic needles with different internal size such as 19, 21, 25 and 26 gauges, while being stirred. The beads were kept in calcium chloride solution for 2 h to allow hardening, and then separated from the solution by a funnel before washing with 600 µM calcium chloride. The beads were stored in the 600 µM calcium chloride at 4 ºC **(Figure 8.1)**.

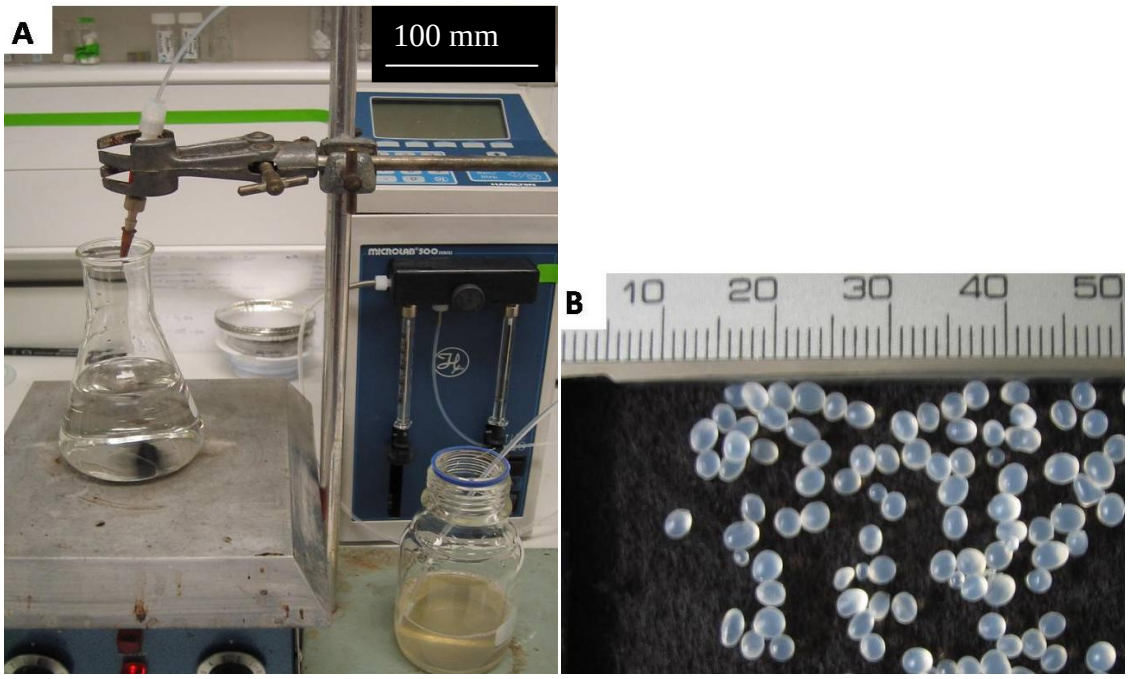

Figure 8.1: Illustrates the set-up of the set up of the calcium alginate bead production by means of a digital image. The smaller image on the bottom left indicates the final alginate product. The alginate beads are dried and separated by size, due the variance in the production (obvious non-homogenous bead production).

8.2.4 Macroporous cement

Orthophosphate brushite cement

A 4.5 M orthophosphoric acid solution containing citric acid at a concentration of 250 mM was prepared for mixture with the synthesized cement powder. A cylindrical tube of height to diameter aspect ratio 2:1 was prepared as a mould to form a cylindrical structure of porous cement. The beads were mixed with the cement powder, the cement: bead (C: B) mass ratios were ∞, 4, 2.3, 1.5 and 1. The samples were packed them into the prepared tubes and allowed to harden at 37 ºC for 12 h. Once removed from the moulds the beads were dissolved to be the porous cement structure by using a 10 mM tri-sodium citrate solution for 5 h on the shaker (100 rev/ min, 25 ºC, 86 Gallenkamp, Serial No. 5A 2658, cooled orbital incubator). Then the wet porous cement scaffolds remained at 37 ºC for an additional 12 h.

Pyrophosphate brushite cement

The pyrophosphate modified brushite cements were produced as described in chapter 6, however, with the addition of the calcium alginate beads to the powdered component (β-TCP). The different beads to cement ratios investigated were ∞, 4, 2.3, 1.5 and 1; and the P: L ratios of the paste were 2 g/ml. The cement samples were casted into rubber moulds with fixed height and diameter (ratio is 2:1). The cement filled moulds were then left in the incubators at 37 ºC for 12 h. After the 12 h, the samples were taken out of the moulds and then immersed into 10 mM tri-sodium citrate solution at 100 rpm at 37 ºC. This allowed the beads to be dissolved, leaving porous samples, which were then placed into the incubator at 37 ºC for an additional 12 h.

8.2.5 Mechanical studies

The compressive strength of the cements was determined using A Lloyd Material Testing Machine (Lloyd Instruments, 6000R, UK) was employed with a load cell of 30 kN to compress on the samples, with a cross-head displacement rate of 1 mm/min.

8.2.6 Characterization of macroporous cement scaffold

Measurements of diameter of the beads were calculated using digital images; a large batch of beads (30–50) were analysed using an image analysis software package (Image J 1.36b, National Institute of Health, USA).

Porosity

The different porosities in the cements could be observed by using computer micro-tomography (Micro CT; Skyscan 1072, Skyscan, Belgium) at the source of 100 kV/98 µA.

Micro CT has been previously proved to be a useful method to examine the microstructure in tissue engineering. The samples were set by the programme 'SKYSCAN-1172' and obtain the images with a cross-section pixel size of 8.468179 µm, Optical Axis line was 518. The scanning speed was set to 0.9 º/step of total 180 º rotation angle. It allows a complete reconstruction of a 3D object from a series of cross-sectional 2D images. The Micro CT software produced results of the pore sizes and percentage of porosity of the samples.

Phase composition

XRD (D5000, Siemans, Munich, Germany) was employed to determine the degree of reaction. Diffraction data was collected for 2θ ranging from 10 ° to 50 ° with a step size of 0.02 ° and a normalized count time of 0.3 s/step. The whole pattern analysis was employed to determine the crystalline phase compositions. The detection was carried out on cements incorporating 1 ± 0.83 mm alginate beads incorporated in brushite cement with C: B = ∞ and C: B = 1.

8.2.7 Degradation

The degradation study is based on the mass loss of the cement. The pyrophosphoric modified brushite cement samples are made using the same method as in previous work; β-TCP mixed with pyrophosphoric acid (PPA) and distilled water. The dry, hardened samples were then immersed in 20 ml PBS solution (at pH 7.4). The PBS solution was refreshed three times a week to simulate the dynamic environment of an implanted sample. The degradation is measured by mass lost in weight of the samples. At all allocated time points the samples were imaged with the use of the Micro CT.

8.3 Results

8.3.1 Comparing CPC degradation

In this initial study we compare the degradation properties of both commonly used CPC's; HA and brushite using these as comparisons for the recently developed pyrophosphate modified brushite cement (**Figure 8.2).** It is obvious from this study that HA exhibits slower degradation then brushite cements which conforms to previous research; and therefore HA is used as a means of comparison in this study to determine the relative degree of degradation.

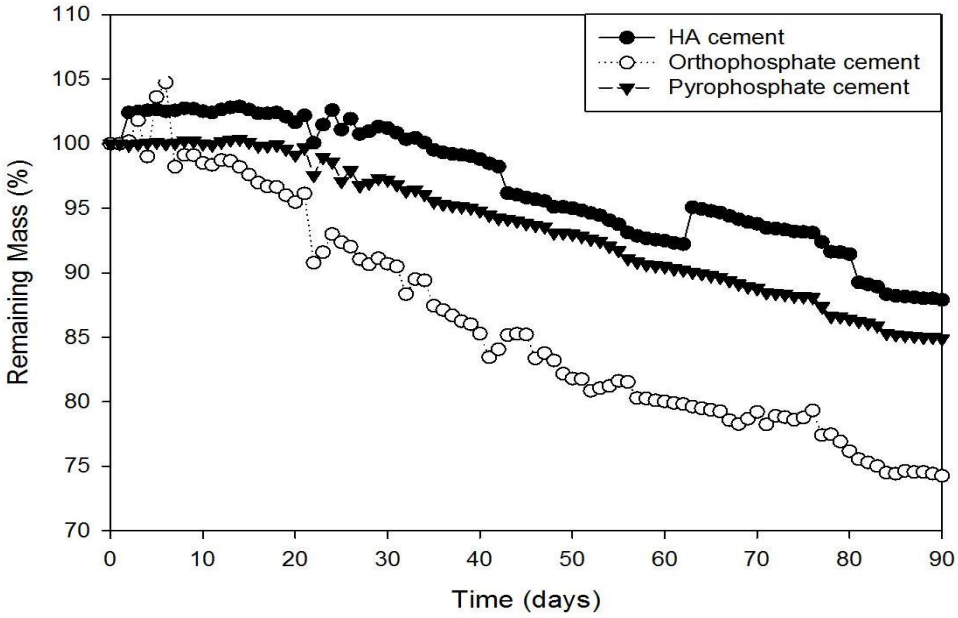

Figure 8.2: Graphs illustrate the degradation of cements over a period of 90 days. Two brushite cements were compared to the HA cement.

The HA cement demonstrated an initial increase in mass by day 2 of immersion in PBS, this may be due to the porous nature of the cement, which may have absorbed much of the PBS within the pores, demonstrating a mass increase upon measuring, as this was also apparent in the orthophosphate cement to a greater extent due to the larger amount of porosity **(Figure 8.3)**. However, the orthophosphate cement was exhibited a drop in mass of almost over 2wt% by day 7 and then steadily degraded over the 90 days to a final mass reduction of over 25wt%.

HA exhibited a reduction in mass of 10wt% over the same length of time and also demonstrated at various time points a gain in mass. In the case of the pyrophosphate cement there was a steady reduction in the mass of the cement throughout the 90 days of immersion in PBS with the cement losing approximately 15wt% of mass in this period of time. No obvious mass gain was noted; however interestingly there was a discrepancy in the results between days 20–27, where the results demonstrate an unstable degradation of the mass of all three samples. As this inconsistency with obvious for all three samples there may have been a malfunction or an irregularity of the equipment used to calculate the mass.

The SEM micrographs illustrate the microstructure of the cement samples **(Figure 8.3)**; HA demonstrates a smooth and fine fracture surface, with small globular structures of 1–2 μm, this may be the reason for the high relative porosity. Brushite cements demonstrate needle-like surfaces of 5–7 μm in length and approximately 1 μm in width, which is typical of brushite cement. Pyrophosphate modified brushite cement samples demonstrate similar needle-like structures with greater thickness (2–3 μm in width) packed around irregular particles of 1–2 μm; not typical of this cement, as previously suggested this may be attributed to the hydrolysis of the pyrophosphate to orthophosphate. **Table 8.1** indicates the key material properties to allow caparison of the samples.

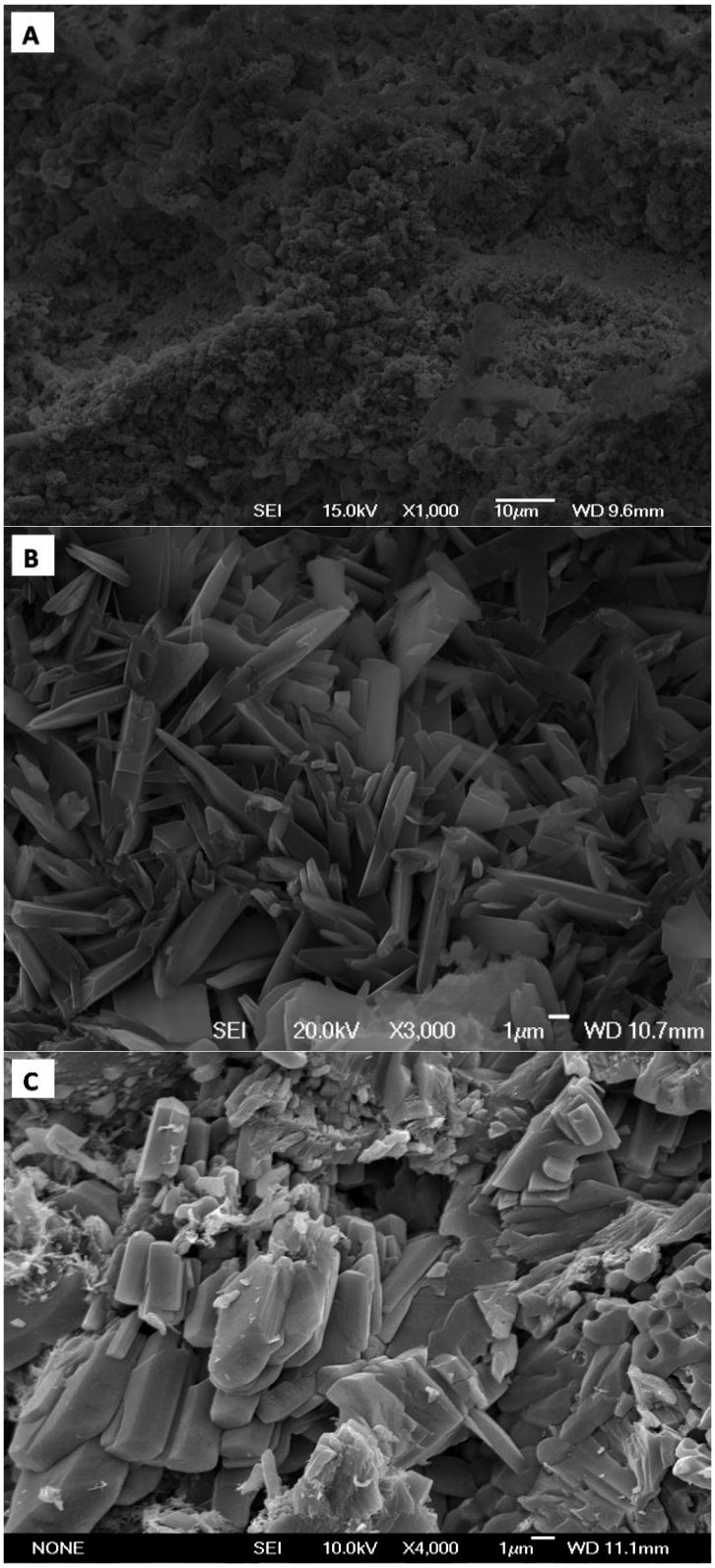

Figure 8.3: SEM micrographs illustrate the microstructure of the cements investigated; HA cement (A), orthophosphate brushite cement (B) and pyrophosphate brushite cement (C).

Table 8.1: Summarises the key properties of the cements; HA cement, orthophosphate brushite cement and pyrophosphate brushite cement. Comparing the porosity with the strength of the cements and how this affects the degradation rate.

Cement	Setting times (min)		Compression strength (MPa)	Specific surface area (m2g-1)	Relative porosity (%)
	Initial	Final			
HA	1.5 ± 0.30	6.0 ± 1.20	41.2 ± 8.70	17.4 ± 2.6	43 ± 2
Orthophosphate	3.5 ± 0.55	31 ± 1.56	38.7 ± 9.23	10.3 ± 1.5	36 ±7
Pyrophosphate	4.7 ± 1.64	10 ± 1.55	67.4 ± 25.6	14.2 ± 2.3	24 ± 3

8.3.2 Addition of macroporosity

In chapter 4 discussed the chemistry of the CPC's in detail and mentions that depending on the stoichiometry and pH of the cement slurry CPCs can set to form a matrix consisting of HA (pH value of >4.2) or brushite (pH value of ≤4.2). Due to the long term stability of HA, brushite (a sparingly soluble CPC) is considered as an alternative. However as studies has shown brushite can hydrolyse to HA. Here we use a method of incorporating macroporosity to overcome such long term stability and hydrolysis, by increasing the rate of cement degradation.

The incorporation of the calcium alginate beads (1.1 ± 0.2 mm in diameter) into the cement paste resulted in the formation of macroporosity in the cement without significantly influencing the cement setting reaction **(Table 8.2)**. In the absence of the beads (cement: bead ∞) the porosity contained within the pure cement was 25% and this increased with the addition of calcium alginate beads to a maximum of 57% at a cement: bead ratio of 1 **(Figure 8.4)**. The combination of calcium alginate beads even at a cement: bead ratio of six resulted in a reduction in compression strength from 48 ± 12 MPa with the addition of no beads to 12

± 1 MPa **(Figure 8.4)**. When the cement was mixed with the calcium alginate beads at a cement: bead ratio of 1 the cement exhibited a compression strength of 4 ± 0.2 MPa.

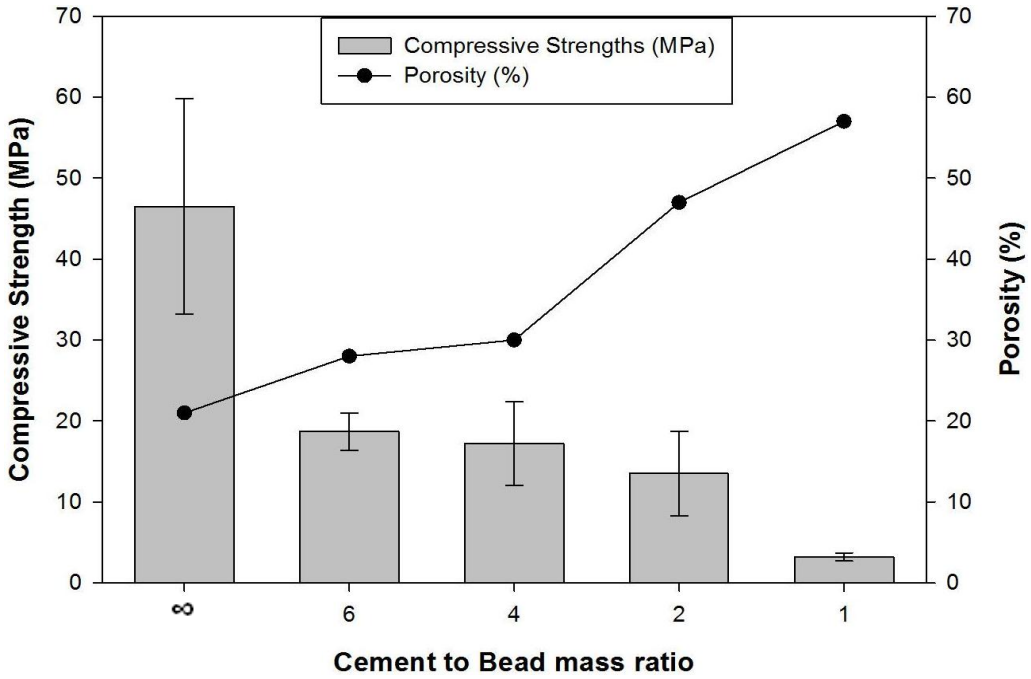

Figure 8.4: The influence of cement:bead mass ratio on the porosity contained within brushite cement and the compression strength exhibited by the hardened material.

The degradation profiles of the macroporous and non-macroporous brushite cements aged in PBS are shown in **Figure 8.5**. In the case of the non-macroporous brushite cement there was a steady reduction in the mass of the cement during the first 14 days of immersion in PBS with the cement losing approximately 10wt% of its mass in this time. After 14 days of ageing the rate at which the cement lost mass reduced significantly so that following 28 days of ageing the cement lost only a further 2wt% of its original mass. The macroporous brushite cement, in contrast, lost mass at a steady rate throughout the study so that after 28 days the cement had lost 60wt% of its original mass **(Figure 8.5)**.

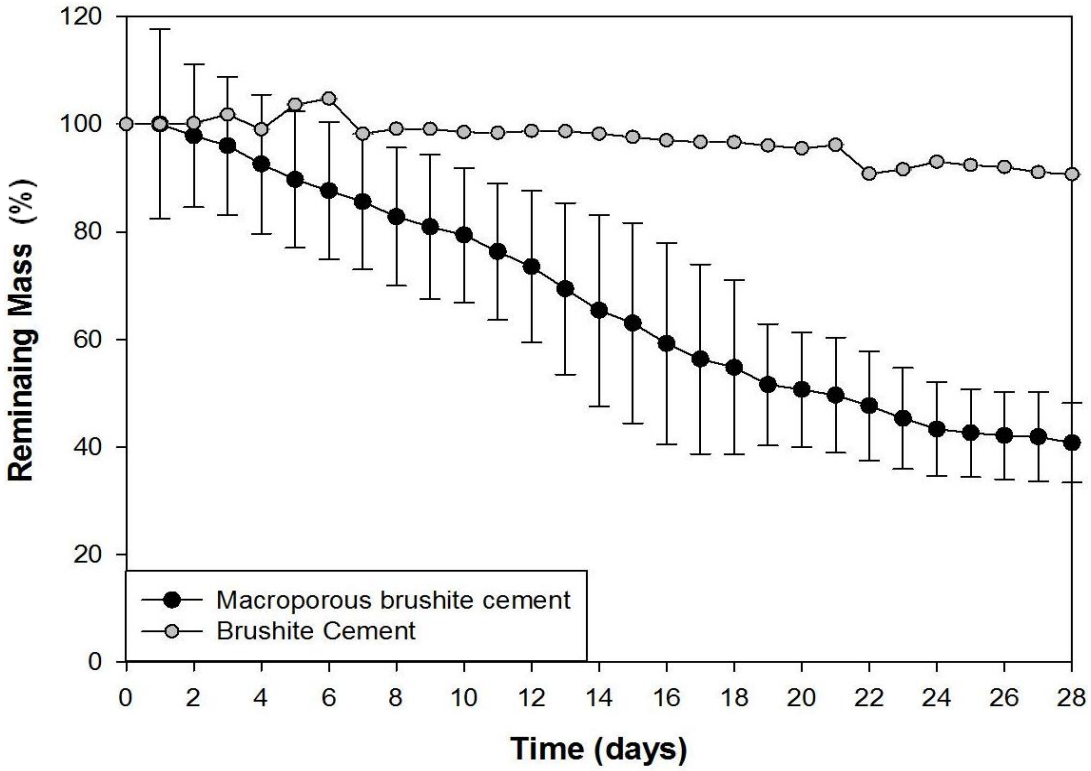

Figure 8.5: Illustrates the degradation profiles of macroporous and non-macroporous brushite cements.

There was a steady reduction in the proportion of the cement formed from brushite, after a period of 14 days of ageing HA was detected in the cement matrix **(Table 8.2)**, which corresponded to the reduction in the rate at which mass was lost from the cement material. In the case of the macroporous brushite cement aged in identical conditions, HA was not formed at any point during the study and interestingly, following 14 days of ageing, neither brushite nor HA was detected in the cement matrix **(Table 8.2)**. **Figure 8.6** demonstrates clearly that the phase composition prior to ageing of the brushite cement does not change with the addition of the alginate beads; XRD patterns are almost identical.

Table 8.2: Compares the composition of the macroporous brushite and non-macroporous brushite cement following immersion in daily refreshed PBS.

Time (days)	Composition (wt%)					
	Macroporous brushite			Brushite		
	Brushite	B-TCP	HA	Brushite	B-TCP	HA
0	33	67	0	34	66	0
7	24	76	0	28	72	0
14	0	100	0	80	8	12

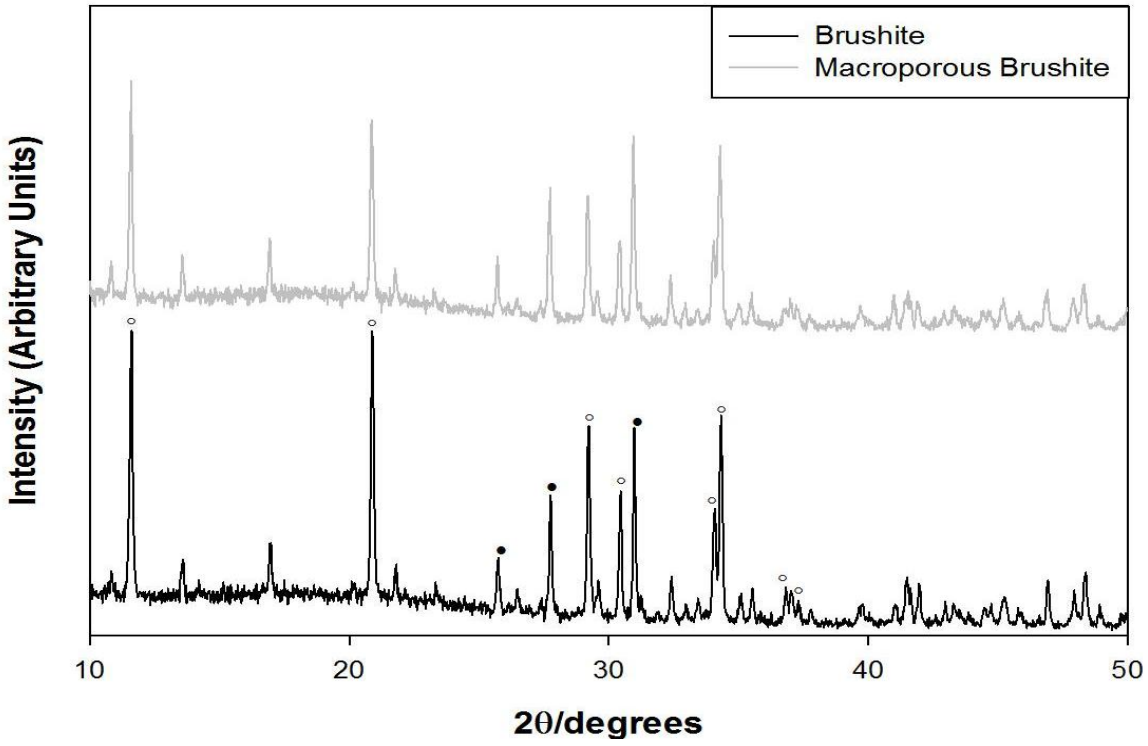

Figure 8.6: Compares the diffraction patterns of the control brushite cement (bottom) with and macroporous brushite cement (top). The various peaks are indicative of the composition of the samples; ○ Brushite; ● β-tri-calcium phosphate (β-TCP).

Following this different amounts of porosity were then added to the cement; 0, 20, 30, 40 and 50% porosity samples were produced. The amount of porosity was referenced to the amount of beads added to the cement powder, for example, if cement powder to bead ratio was 1:1

then the cement sample was considered to be 50%. This was the maximum amount of beads that could be added to produce a set cement scaffold. **Figure 8.7** illustrates the degradation of the various samples, which were ages over 90 days. Porosity was not able to be artificially added to the pyrophosphate brushite cement in the same manner as the beads did not mix homogeneously throughout the cement sample; beads were mixed, however during the setting reaction the beads where pushed to the top end of the mould. This may have been due to the density of the beads compared with the cement.

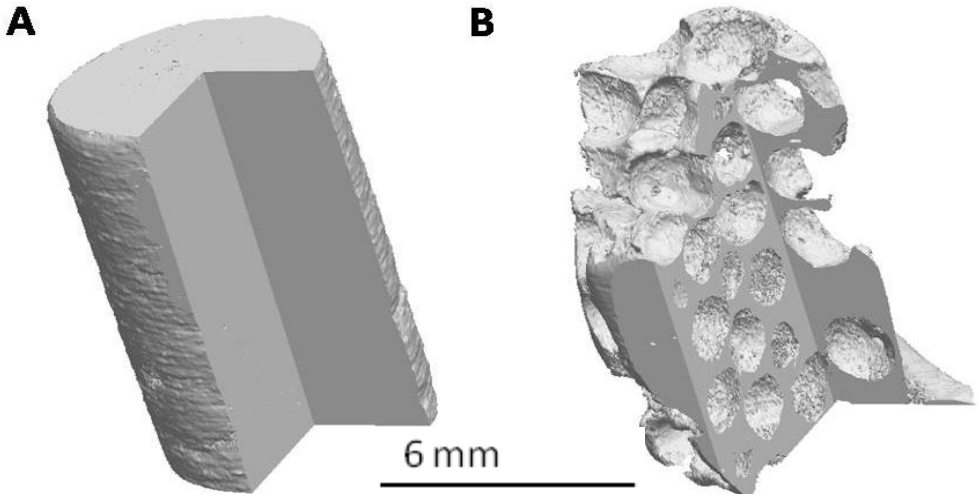

Figure 8.7: A 3D reconstruction of the control brushite cement (A) and macroporous brushite cement (B) with 50% beads.

8.3.3 Long term degradation of brushite cements

Long term degradation of orthophosphate cement samples with macroporosity of 20, 30, 40 and 50% beads are illustrated in **Figure 8.8**. The sample with 0% beads refers to the non porous cement. The degradation results clearly demonstrate the effect of the addition of porosity in the cement slurry. The results indicate that with the addition of 20 and 30% of beads of the total mass of the cement powder the cement degradation does not vary significantly. However, with the addition of over 40% of beads the degradation rate changes significantly ($\rho < 0.05$). The results from **Figure 8.9** demonstrates the results of compression

strengths of samples at the various time points after being allowed to degrade for a maximum period of 730 days (note that no results are exhibited for beyond day 365 due to lack of structural form).

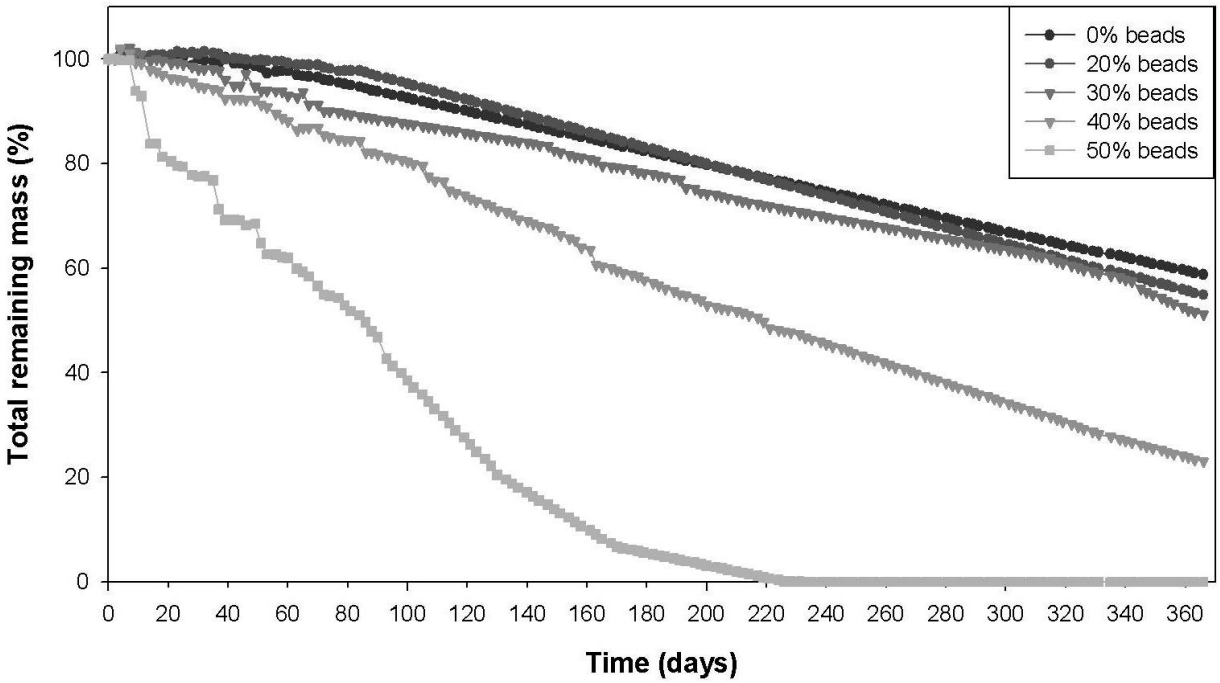

Figure 8.8: Graphs illustrate the degradation of cements over a period of 730 days. No results were recorded for day 545 and 730, as the samples had degraded too far to be measured using the same conditions; most samples beyond days 365 remained in particulate form.

The samples of PPA cement was degraded in two different solutions to demonstrate a biological environment serum was used and compared to the generic PBS solution used for the results in this chapter. It is clear from the results that serum aids the rate of degradation, however, **Figure 8.10** also exhibits a larger standard deviation for the samples degraded in serum, especially as the samples are aged for longer periods of time.

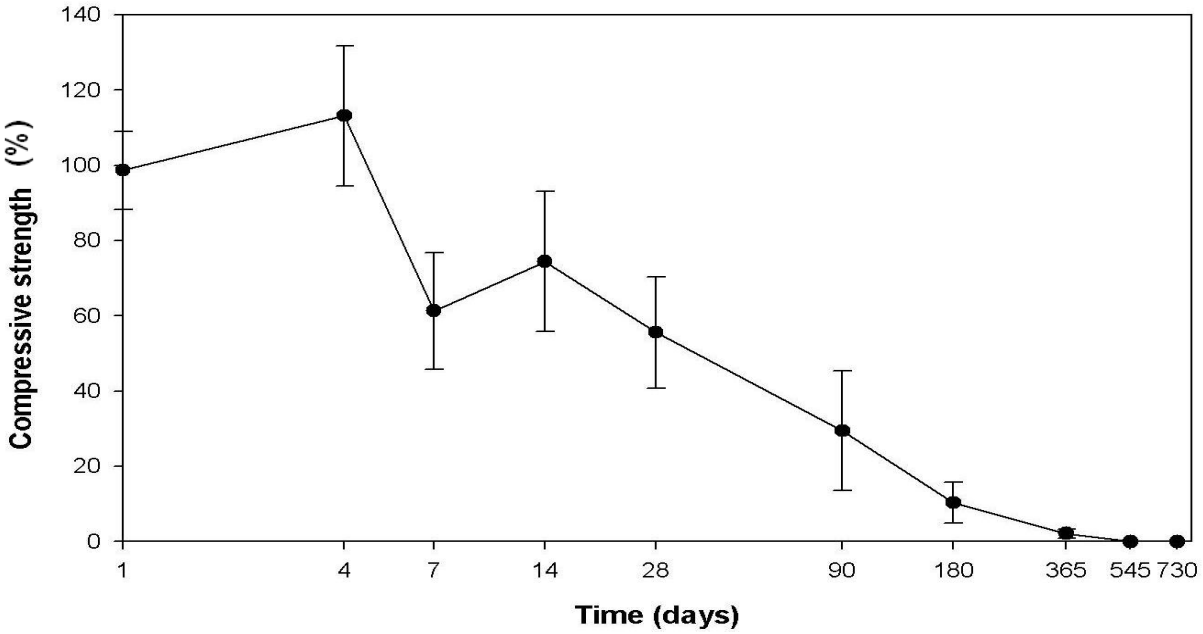

Figure 8.9: Graphs illustrate the degradation of the non porous orthophosphate brushite cements over a period of 730 days (2 years). The graph is plotted using common logs to allow a clear view of the compressive strengths over this long period of time (n = 6). No results were recorded for day 545 and 730, as the samples had degraded too far to be measured using the same conditions; most samples beyond days 365 remained in particulate form.

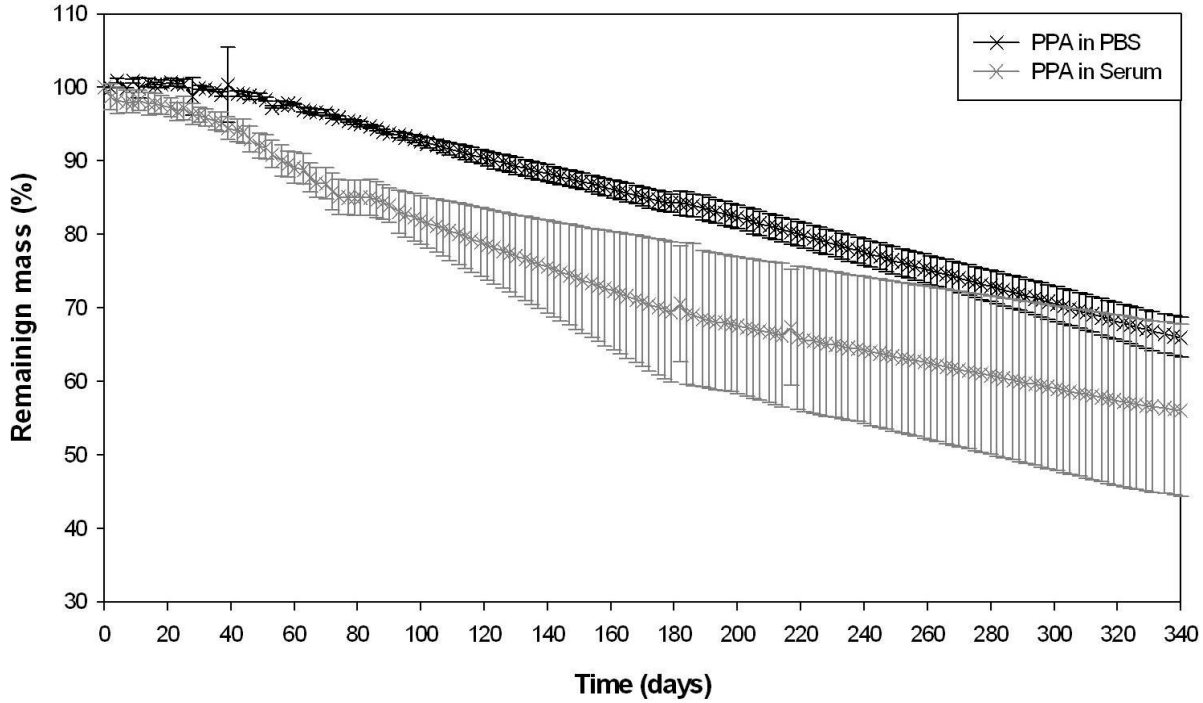

Figure 8.10: Graphs illustrate the degradation of cements over a period of 730 days. No results were recorded beyond day 340 (545 and 730), as the samples had degraded too far to be measured using the same conditions; most samples beyond days 365 remained in particulate form. Black plots demonstrate the PPA cement in PBS and the grey plot illustrates the degradation of PPA in serum solution.

8.4 Discussion

Brushite cements have considerable promise as new bone replacement materials as they are more soluble than HA in physiological conditions and could therefore be more rapidly resorbed than HA based materials *in vivo*. Although more soluble than HA cements, brushite is metastable and can hydrolyse to form HA which results in a reduction of pH at the implant site (equation 8.1) and ultimately results in the long term stability of the material (Fulmer & Brown 1998). A key factor affecting the dissolution of brushite is the concentration of calcium ions; an increase in concentrations results in a decrease in the rate of brushite dissolution (Kumar *et al.* 1999). This factor is directly connected to the method of ageing experiment; whether the ageing method is dynamic or static the resulting mass loss will differ due to the saturation of the ageing medium. The PBS used, here in this chapter, as an ageing medium contained no calcium ions. Consequently once the cement was immersed in the ageing solution, brushite dissolution began and an increase in calcium and phosphate ion concentration, as a result slowing the rate of dissolution. Therefore, to maintain a higher rate of dissolution the PBS ageing medium needs to be refreshed daily (using a dynamic ageing method).

A number of studies have been undertaken to elucidate the factors that can affect the hydrolysis reaction including, implant volume, media refreshment rate and media composition (Grover *et al.* 2006).

$$3\ CaHPO_4.2H_2O + 2\ Ca^{2+} \rightarrow Ca_5(PO_4)_3OH + 5H_2O + 3\ H^+ \qquad \text{(equation 8.1)}$$

Some authors have attempted to prevent this reaction from occurring by the incorporation of salts capable of preventing hydroxyapatite formation including magnesium phosphates and

calcium pyrophosphate into the cement (Grover *et al*. 2003). In this study, it has been demonstrated that the hydrolysis of the brushite can also be influenced by the porosity of the cement material. By increasing the rate of brushite dissolution, it is possible to prevent HA formation from occurring, thereby allowing continued degradation of the material. The more rapid dissolution of brushite from the cement may be due to the improved mass transport away from the cement in the presence of a network of macropores.

This study was undertaken to explore the effects of porosity on the degradation patterns and relationships of calcium phosphate cements. Here, in this study a novel idea was discovered to manipulate the degradation of these cements by introducing sodium alginate beads. The alginate beads manufactured by the needle technique using a simple process produced sizes 1-2 mm in diameter; these beads leave a suitable pore sizes for cell to be cultured in. Having analysed the cement produced by the formulation C: B = 2, the pore size was measured and was found to be near enough the same size as the diameter of the alginate beads, before addition. Interestingly, the macroporous cement consisted only of β-TCP by the end of the study. This is interesting as brushite is widely thought of as the phase that effectively binds the cement together. It is possible that another amorphous or poorly crystalline phase is present in the cement which cannot be detected using X-ray diffraction.

Figure 8.7 illustrates the three dimensional Micro CT images of the brushite cement sample, which demonstrates the effect of the addition of beads to the porosity of the samples. As the sample is aged, the highly soluble brushite cement is degraded and the pores are seen to increase in size over time. New pores are also formed as the sample is aged, this could be the weakening or expanding of an adjacent pore wall due to dissolution. This is exhibited in

Figure 8.8, which shows the degradation rates of several samples of different porosities. Collective with **Figure 8.9** the effect of this porosity on the compressive strength of the samples is, as expected, decreasing with time. This evidently suggests that the cement porosity can be manipulated to control the degradation of the implant for a wider application.

8.5 Conclusion

The new method to manufacture the macroporous cement has been exposed here in this study and this method possesses many advantages. The procedure is easy to reproduce just at room temperature, reducing manufacturing costs. The macropores are fabricated by mixing the non-toxic sodium alginate beads with the brushite cement; this enables pore size to be easily controlled within the cement by using different sizes of the beads. The pore sizes created in the cement does not affect the porosity significantly, but the samples that possessed a large pore size were stronger than those with a smaller pore sizes. The strengths of the macroporous CPC cement were generally low compared to dense cements; however, these macroporous cement can be applied in the bone tissue engineering. The degradation rate can be controlled by different porosities through using different amount of beads.

Chapter Nine

Thesis conclusions

Calcium phosphate cements have been investigated for several decades and here in this study we have manipulated the formulations to produce various ideas for the development of and enhancement of the material properties of CPC's.

9.1 Formulation of Monetite cement

We have reported the formulation of the first cement system that sets to form a matrix that is formed predominantly of monetite. The formation of monetite rather than brushite was attributed to the limited perfusion of the hardening cement paste with water during setting. Incomplete penetration of the cement by methylene blue has demonstrated the importance of sample volume on the formation of the set cement phase. i.e. too small volumes would set quickly, and in the case of Han *et al.* produce a brushite phase as water is not limited sufficiently; large volumes, as demonstrated in this study, indicates that the perfusion will stop once this limit is reached.

9.2 Controlled setting paste cement formulations

For good bone healing initial stabilisation is a prime factor. Injectable bone substitutes are good alternatives to allografts and calcium phosphate blocks because they may exactly fill the defect shape. Another important advantage with injectable calcium phosphate bone substitutes is their resorption rate. Since a material is unable to adapt, proliferate and remodel according to its' own overall biomechanical situation it is of great interest for most applications to replace the material within years. These ready mixed CPCs: (1) avoid the powder–liquid mixing in surgery thus cutting down the surgical time; (2) allow the paste to be

mixed in advance under controlled conditions therefore avoiding inadequate and inhomogeneous mixing; (3) will not harden in the package or in a syringe, and will harden rapidly in aqueous environment; and (4) eliminate the requirement for the surgeon to mix and finish the placement into the defect within a set time before the paste hardens. They may also allow for the pre-processing of the cement paste using processes such as high-shear mixing improving mechanical performance.

The cement paste formulations here have shown to be very promising; the results are evident of the successful use of the Eudragit microspheres to encapsulate PPA, which are then used to formulate the cement that has also shown to harden to form brushite. Future work will seek to evaluate the mechanical and setting characteristics of the pyrophosphate based cement formed using Eudragit comparing them with those exhibited by the non-encapsulated PPA. The cement pastes produced using the microencapsulation technique allow setting when the cement paste is exposed to a change in conditions. This is only true for the temperature sensitive microcapsules, as the pH sensitive microcapsules leak their load of PPA in a short period of time. To overcome this issue, the use of shear forces as a means to initiate the reaction as opposed to temperature or pH was investigated, though, the results were disappointing. The PCL microspheres were unable to carry the phosphorus; the ESEM spectrums demonstrated no phosphorus presence. This could possibly be due to the small amount encapsulated.

9.3 Calcium phosphate cements as drug delivery matrices

Incorporation of antibiotics within the cements has been demonstrated to burst release. The results conclude that the addition of GS allows better conservation of the original cement

strength compared to the addition of VH. Therefore, GS incorporated cements are suitable form of supplying drugs to areas where intravenous drug delivery is unsuitable or incapable of reaching the infected site. We also demonstrated, from another study, that sufficient VH can be delivered from three distinct CPC matrices at sufficient concentrations to exceed the MIC for *S. aureus* for 168 h. Importantly, the pH in the ceramic matrix during processing is a very important consideration in the effectiveness of the released drug against the bacteria. The findings of this study illustrate the importance of evaluating the antibacterial efficacy of drugs loaded into material for *in vivo* drug release, rather than simply monitoring release.

9.4 Degradation of calcium phosphate cements

Degradation of the cements does depend on the composition as is evident from the results. From the studies here has confirmed the literature that HA is more stable *in vitro* than brushite. The hydrolysis of brushite in calcium phosphate cement can be influenced by the porosity of the implant. By manipulating implant porosity through the addition of calcium alginate beads to the brushite cement during mixing, it may be possible to effectively tailoring the rate of *in vivo* degradation rate in clinical applications. We have demonstrated that the addition of porosity within the cement matrices it is feasible to regulate the cement scaffold's degradation rates. However, this study also found that the size of the beads does not have a substantial effect on the degradation. The data collected, does suggest that there is a relationship between the degradation patterns and the rate of degradation.

Chapter Ten

Future work

10.1 Formulation of Monetite cement

We have demonstrated that many different gelling agents can be used to add viscosity to the non-aqueous liquid used for the formulation of the monetite cements. However, we have only used one such non-aqueous liquid (glycerol); the use of other possibilities can open this novel idea to a vast range of applications. Several other possible non-aqueous liquids that may be considered:

- Propylene glycol (1,2-propanediol or propane-1,2-diol) - used in food, medicine, pharmaceuticals, emulsification agent, moisturizer in medicines, cosmetics, food, toothpaste, mouth wash, and tobacco products.
- Ethylene glycol (ethane-1,2-diol) - used in chilled water air conditioning systems.
- Triethylene glycol (TEG, or triglycol) - used by the oil and gas industry to "dehydrate" natural gas.
- Diethylene glycol (DEG) - a component brake fluid, lubricants, wallpaper strippers, artificial fog solutions, and heating/cooling fuel.
- Silicone oils - primary uses are as lubricants or hydraulic fluids.

The use of acceleration agents within the formulation and the effects of these on the phase composition would be interesting to study. In this study we have demonstrated that the setting of the monetite paste cement varies between 15–20 h, an accelerating agent would reduce that time dramatically. Following this *in vivo* studies into the compatibility of the

cement with cell adhesion and growth is an additional work that would require an in depth investigation; following some of the work on additives, mentioned in chapter 4.

10.2 Controlled setting paste cements using microspheres

Working on the formulation of this investigation and deriving methods to optimise the loading of the microspheres to get maximum acid to polymer ratio. Investigations on blend polymers and various other degradable polymer materials can be utilised for the manufacture of such capsules. Also the use of liposomes as an alternative to polymers would widen the applications of such technologies.

10.3 Drug delivery

Using the CPC as drug delivery matrix for a large range of antibiotics and selecting the optimum drugs for this versatile delivery matrix. These methods of incorporating drugs into cements can be used for commercial products such as, dental cements, root canal filling materials, etc.

10.4 CPC degradation studies

Continuing long term degradation studies to determine the effects of different environments would be the next stage of this investigation. Formulating a continuous degradation unit, in which the sample can remain and measurements of loss of mass and dimensions can be made without altering the surrounds and affecting the experimental conditions.

Chapter Eleven

Appendices

Appendix 1 Methods of Cement Characterisation 198

1.1 Cements characteristics 198
1.1.1 Setting characterisation 198
1.1.2 Mechanical characterisation 200
1.1.3 Porosity characterisation 201
1.1.4 Compositional characterisation 206
1.2 Cement reactant characteristics 209
1.2.1 Particle size 209

Appendix 2 The use of gelling agents for medical research 215

2.1 Non-aqueous liquids 215
2.1.1 Glycerol 215
2.2 Gelling agents 216
2.2.1 Alginate 217
2.2.2 Agerose 219
2.2.3 Carrageenan 219
2.2.4 Chitosan 221
2.2.5 Gellan Gum 222
2.2.6 Hyaluronic acid 222
2.2.7 Gelatine 223
2.2.8 HPMC 224

Appendix 3 Experimental data 225

Appendix 4 Publications 226

Appendix One

Methods of Cement Characterisation

Material characterisation is an important part of development for a new material. Characterisation aids the comparison of materials and establishes area's where improvements can be made to existing materials; increased osteointegration and osteoconduction, higher strengths, better handling and improved outcomes.

1.1 Cement characteristics

Cement materials are constantly developing; materials characterisation is a means of standardising and comparing each material to maximise its potential. When developing bone replacement materials the characteristics are comparable to natural bone; material characterisation allows quantification of the various parameters. In this thesis we take HA characteristics as a means of comparison, as HA is commercially available for clinical use.

1.1.1 Setting characterisation

Calcium orthophosphates which either can be formed by precipitation at room or body temperatures are formulations of cements containing at least one or more acidic components and one or more basic components which react when the powder is mixed with water. Several combinations of reactants are possible in the systems of calcium phosphates and even combinations with calcium phosphates containing sodium, potassium, magnesium, zinc, carbonate or chloride are thought to be useful. In addition, other compounds can be added as accelerators or retarders of the setting reaction or as promoters of bone in-growth.

The Gilmore needle technique

Gillmore Needles is an American Standard Test Method (ASTM C266−89) (ASTM 1993), used for the determination of the setting times for hydraulic-cement pastes. The Gillmore Needles instrument consists of two different needles: one with a weight of 113 g ± 0.5 g and a tip diameter of 2.12 mm ± 0.05 mm giving a static pressure of 0.3 MPa used for the initial setting time and the other one with a weight of 453.6 ± 0.5 g and a tip diameter of 1.06 ± 0.05 mm giving a static pressure of 5 MPa used for the final setting time. The setting times were measured by applying the weight to the surface of a cement cylinder held in a ring (cement parameters: 16mm diameter, 8mm height) at 30 second intervals and left for 10 seconds. The initial setting time is the time required for the test specimen to bear the initial Gillmore needle without leaving an impression on the surface, while the time required for the test specimen to bear the final Gillmore needle without leaving any mark is the final setting time.

The practical value of the initial setting time is that it defines the time during which the material must not be manipulated to avoid the solid structure, which is being formed during the setting, being destroyed (Driessens *et al.* 1993b). The practical value of the final setting time is that the material now has hardened, but maximum strength for some materials has not been achieved. In a study where over 100 formulations were tested on their ability to set upon mixing with water (Driessens *et al.* 1993b), the initial and final setting times were measured with Gilmore needles. The Gillmore needles technique is operator dependent, many researchers have reported varying final setting times for the same commercial cements (Grover *et al.* 2005b). For this reason interpretation of literature that quotes the setting times using the Gillmore technique must be considered subjectively.

1.1.2 Mechanical characterisation

In weight bearing structures such as the human skeleton, every newly developed biomaterial needs to be mechanically tested to ensure its functionality, consistency and reliability. For bio-cements, measurement of their multiaxial mechanical properties is more difficult, given that their behaviour depends heavily on the microstructural defects associated with the manufacturing process (Charriere *et al.* 2001). When bone is loaded, it undergoes a deformation; the amount of deformation is quantified by the amount of strain. Strain is defined as a change in length per unit of length (van Eijden 2000). This deformation cause's tension to occur in the bone tissue; quantified by the amount of stress, which is defined as force per unit area. The stress can be classified as compressive, tensile, or shear depending on how the load is applied.

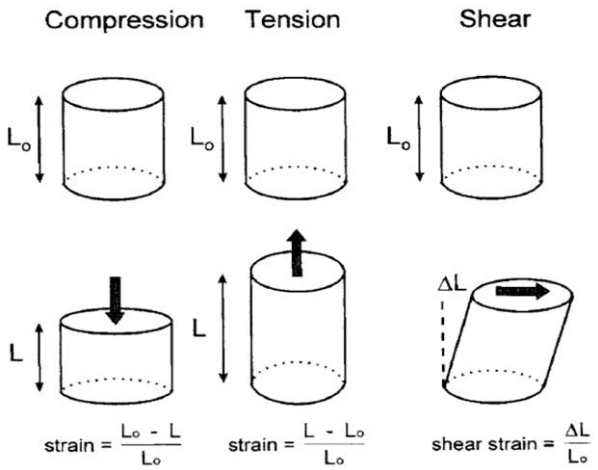

Figure A1.1: Illustration of the different types of strain for three forms of stress; compression, tension, and shear (van Eijden 2000).

Strength is a critically important mechanical feature of a bone replacement material. The yield strength is defined as the stress at the yield point, beyond which deformation causes tissue damage (van Eijden 2000). Beyond the yield point, the bone replacement tissue will not return to its original shape when the load is released. The ultimate strength is the

maximally sustainable stress; the breaking strength is the stress at which the material will break. The value of the ultimate strength of bone depends on the type of stress; typically bone is weaker in shear and in tension than in compression (van Eijden 2000). Brittleness is characterized by strongly differing tensile and compressive strengths, appreciable size effect, and high scatter of test data (Hoffman 1967).

Compressive strength

The mechanical properties of the bone substitutes were defined by compression testing. The samples used for the compression test should be cylindrical with the height-to-diameter ratio (H/D) equal to 2, to avoid bending. Samples were compressed at 1 mm per minute along their long axis until failure. Load and actuator displacement were recorded at a rate of 0.2 kHz and stored. The maximum load was used to calculate the compressive strength. The compressive strength is a measure of the maximum compressive force the material can withstand per unit area. During compression (**Figure A.2**) the compressive forces (C) generate tensile forces (T) in the centre of the specimen acting perpendicular to the vertical axis. These forces will tear the sample apart when the strength limit of the material is exceeded.

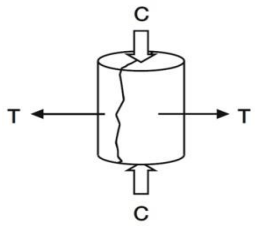

Figure A1.2: Compression Testing: the compressive forces (C) generate tensile forces (T) in the centre of the specimen acting perpendicular to the vertical axis.

1.1.3 Porosity characterisation

Surface area and porosity are important parameters regarding applications and performance of many materials; porosity has a marked influence on the mechanical properties of the material.

With regards to pore there are three main different types of pores: Micropores < 2.0 μm; Mesopores 2.0–50 μm; and Macropores > 50 μm (Thielmann & Burnett 2000). In order to gain a better understanding of how different pores can affect product properties knowledge of the pore size distribution is required. A standard method for the determination of micro- and mesopores size distributions is volumetric nitrogen adsorption measurements at 77 K (Murray *et al.* 1999). Macroporosity is not measurable by gas sorption and is usually obtained from mercury porosimetry (Portsmouth & Gladden 1991). An alternative to nitrogen adsorption at 77 K is dynamic sorption at ambient conditions using non-polar organic vapours. This approach has several benefits, especially for organic solids such as pharmaceutical and food materials (Thielmann & Burnett 2000).

Mercury porosimeter

Mercury intrusion porosimetry (MIP) is based on the principle that a non-wetting liquid (one having a contact angle greater than 90°) will only intrude capillaries under pressure (Abell *et al.* 1999). The relationship between the pressure and capillary diameter is described as;

$$P = -4\gamma\cos\theta / d \qquad \text{(equation A.1)}$$

where P is the pressure; g is the surface tension of the liquid; q is the contact angle of the liquid and d is the diameter of the capillary.

Mercury must be forced using pressure into the pores of a material. The pore size distribution is determined from the volume intruded at each pressure increment. Total porosity is determined from the total volume intruded. The MIP technique is widely used because of its ease and simplicity. However, it does not measure the true distribution of sizes for pore

geometries found in cement-based materials (Chatzis & Dullien 2005). For these systems, large internal pores are accessible by very narrow throats. The MIP technique misrepresents the size of these pores as having the diameter of their throats. Mercury intrusion is a penetration process, whereas nitrogen desorption is a phase equilibrium process. Consequently, the mercury intrusion curve measures the accessibility of the pore network to a meniscus of a particular size (Androutsopoulos & Mann 1979). The conventional nitrogen desorption isotherm is time-consuming to measure, typically taking from 6 to 12 h depending on the sample (Murray *et al.* 1999). Therefore it would be convenient to acquire the same structural data using a quicker and simpler technique. A possible alternative to the desorption isotherm is the mercury intrusion curve, which can typically be measured in about 1 h.

Calculation of density

According to Archimedes Principle when an object is immersed in a fluid, the fluid exerts on the object a force whose magnitude is equal to the weight of the displaced fluid and whose direction is opposite the force of gravity (Hughes 2006). Consider the specific case of an object suspended from a string while being immersed in a container of water.

Helium Pycnometer measures the density or more accurately the volume of solids, be they regularly shaped, porous or non-porous, monolithic, powdered, granular or in some way comminuted, employing some method of gas displacement and the volume to pressure relationship known as Boyle's Law. The Helium pycnometer works by the Archimedes' principle; consisting of two chambers, one to hold the sample and a second chamber of fixed, known internal volume. The device additionally comprises a valve to admit a gas under pressure to one of the chambers, a pressure measuring device connected to the first chamber, a

pathway connecting the two chambers, and a vent from one of the chambers. The working equation of a Helium pycnometer where the sample chamber is pressurized first is as follows;

$$V_s = V_c + V_r / 1 - (P_1/P_2) \qquad \text{(equation A.2)}$$

where V_s is the sample volume, V_c is the volume of the empty sample chamber (cell), V_r is the volume of the reference volume, P_1 is the first pressure and P_2 is the second pressure after expansion of the gas into the combined volumes of sample chamber and reference chamber.

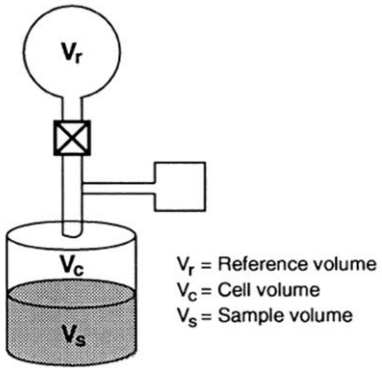

Figure A1.3: The Helium Pycnometer; automatic density analyzer that performs volume and density measurements.

DVS

Dynamic vapour sorption (DVS) is a well-established method for the determination of vapour sorption isotherms. The DVS-1 instrument, **Figure A.4** illustrates schematic diagram, used for these studies measures the uptake and loss of vapour gravimetrically using a Cahn D200 recording ultra-microbalance with a mass resolution of ± 0.1 μg. The high mass resolution and excellent baseline stability allow the instrument to measure the adsorption and desorption of very small amounts of probe molecule. The vapour partial pressure around the sample is controlled by mixing saturated and dry carrier gas streams using electronic mass flow controllers. The temperature is maintained constant ± 0.1 °C, by enclosing the entire system in a temperature-controlled incubator (Thielmann & Burnett 2000).

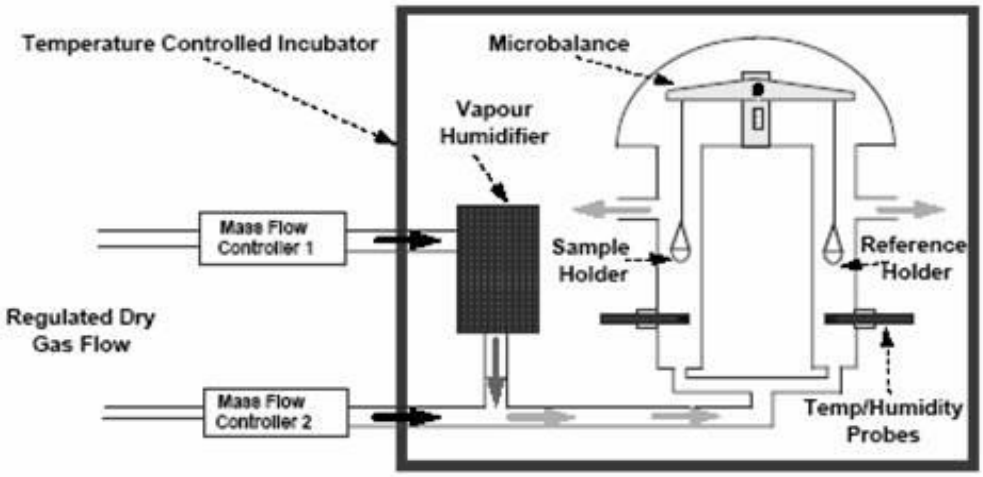

Figure A1.4: Schematic of Dynamic Vapour Sorption (Thielmann & Burnett 2000).

X-ray computed microtomography (Micro CT)

Conventional methods for evaluating osseointegration of tissue engineered scaffolds are based on 2D histological and radiographical techniques and in some cases mechanical testing. To further the development of optimal scaffold architectures and to characterise precisely the growth of bone into scaffolds a fast and non-destructive technique to measure the 3D properties of scaffold composites during growth is required. More recently, micro CT has been applied in bone engineering studies (Verna *et al.* 2002). In Micro CT analyses, it is crucial that the scan data is to be processed by the built-in programs of the microtomographic scanner used (Skyscan). The 3D reconstruction works by firstly creating a series of images of the sample using a 2-dimensional x-ray detector and an electronic x-ray source.

This method allows the investigation of the interconnectivity of the pores within a scaffold structure in a more quantitative manner then the traditional estimations made using SEM and other imaging techniques. This non-invasive techniques, allow non-destructive visualization, reconstruction and quantification in 3D with minimal sample preparation. Many researchers have found the use of Micro CT to be an improvement in the study of bone degeneration and

disease, especially when analysing the morphology of the trabeculae (Gielkens *et al.* 2008;Parkinson & Sasov 2008;Regsegger & Laib 1998;Tuan & Hutmacher 2005).

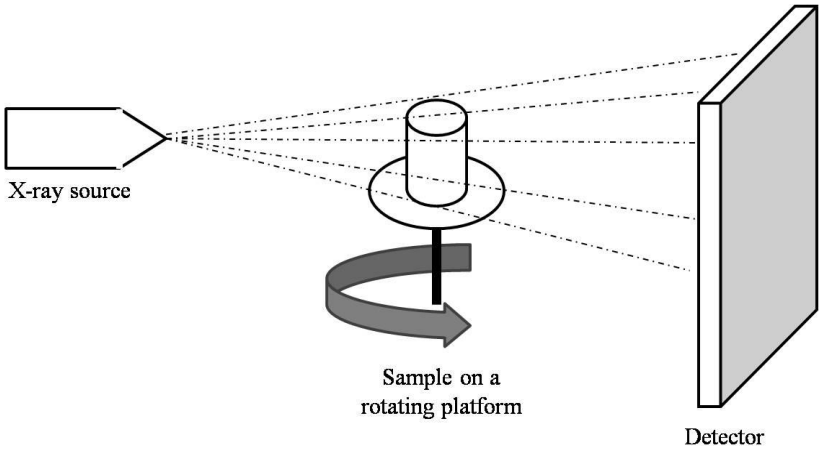

Figure A1.5: Schematic of the set up of the Micro CT. The sample is placed on a rotating platform; rotation angles can be set to sample specification. As the sample rotates an image is stored for 3D reconstruction using analysis software.

1.1.4 Compositional characterisation

Solid matter can be described as: amorphous, where the atoms are arranged in a random way similar to the disorder we find in a liquid; glasses are amorphous materials, or crystalline, where the atoms are arranged in a regular pattern, and there is as smallest volume element that by repetition in three dimensions describes the crystal.

XRD

X-Ray diffraction is used to identify the chemical composition of a crystalline phase. When a narrow beam of monochromatic X-rays penetrates the face of a crystal, diffraction will occur (**Figure A.6**). The condition of the diffracted beam is unique for every mineral and given by a relationship called the Bragg equation or the Bragg's law. Crystalline materials of high symmetry tend to give strong patterns with high and narrow peaks, while materials of lower crystal symmetry give weaker patterns with wider and lower peaks (Pflugrath 1999). XRD

was performed on the initial powder components, the cement during hardening and the end product. XRD patterns of the samples were recorded by step scanning using a microprocessor controlled diffractometer system (Siemens D500, Siemens AG, Munich, Germany) with a Ni-filter for the Kα of the Cu. The step scanning was performed with an integration time of 3 sec. at intervals of 0.05º (2θ).

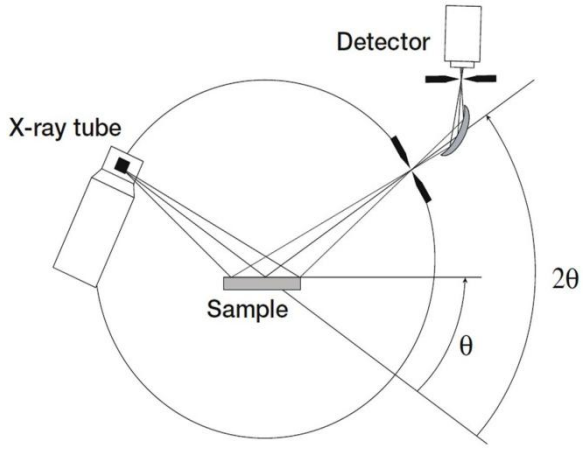

Figure A1.6: X-ray diffraction. A beam of monochromatic X-rays penetrates the crystals of the sample and diffracts to produce a pattern unique to the crystal phases present.

Rietveld refinement method

The Rietveld method allows precise quantitative phase analysis of building materials (Walentaa & Füllmannb 2004). A consistent, accurate and very reproducible method to quantify the relative phase abundances in cement materials is to use XRD in combination with the Rietveld method. This analysis is a powerful method for the determination of quantitative phase amounts in multiple phase mixtures.

The Rietveld method was developed by Hugo M. Rietveld in 1969 (Rietveld 1969) to refine neutron diffraction data. The principal of the method is that the intensities calculated from a model of the crystalline structure are fitted to the observed X-ray powder pattern by a least squares refinement. This is done by varying the parameters of the crystal structures and of the

peak profiles to minimise the difference between observed and calculated powder patterns (Walentaa & Füllmannb 2004). As the whole powder pattern is taken into consideration problems of peak overlap are minimised and accurate quantitative analyses can be obtained. To verify the precision and accuracy of the method it is therefore necessary to compare the results with alternative analysis methods. Detailed information of the theory and mathematics of the Rietveld method have been translated by many authors (Albinati & Willis 2004;G.Walentaa & T.Füllmannb 2004;Young *et al.* 1977).

Fourier Transform Infrared (FTIR)

FTIR Spectroscopy is an analysis technique that provides information about the chemical bonding or molecular structure of materials, whether organic or inorganic. It is used to analyse and identify unknown materials present in a specimen. The technique works on the principle that bonds and groups of bonds vibrate at characteristic frequencies. A molecule that is exposed to infrared rays absorbs infrared energy at frequencies which are characteristic to that molecule. During FTIR analysis, a spot on the specimen is subjected to a modulated IR beam. The specimen's transmittance and reflectance of the infrared rays at different frequencies is translated into an IR absorption plot consisting of reverse peaks. The resulting FTIR spectral pattern is then analyzed and matched with known signatures of identified materials in the FTIR library.

FTIR is a quick and simple method of initially identifying unknown materials, no sample preparation is required and no special conditions are required for the FTIR; no need for a vacuum like SEM or EDX. FTIR analysis can be applied to minute quantities of materials, whether solid, liquid, or gaseous.

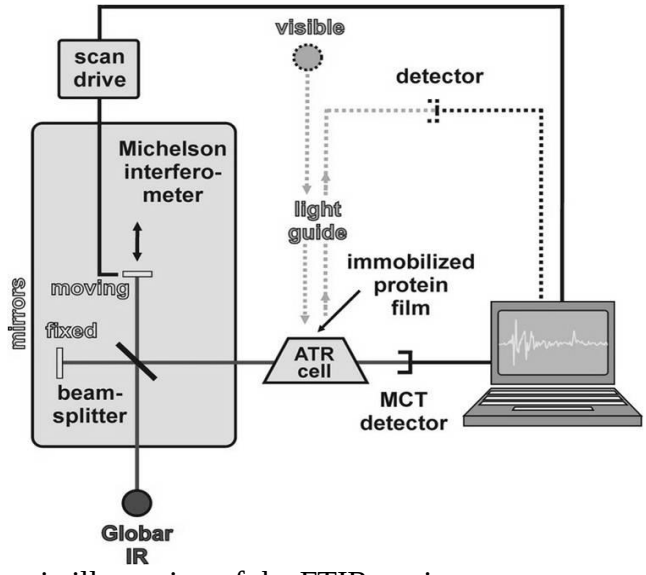

Figure A1.7: A schematic illustration of the FTIR equipment set-up.

1.2 Cement reactant characteristics

CPC reaction rates must be controlled; the CPC must react slowly enough to provide enough time to the surgeon for implantation, and fast enough to prevent delaying the operation (Bohner 2007). There are many factors that control the rate of reaction of a given chemical equation. Here we explore the effects of particle size on and the different methods used to determine the particle size of the powdered components and also the morphology of the end products.

1.2.1 Particle size

Particle size analysis and measurement is an important parameter across many industries for material analysis and characterization. The stability, chemical reactivity, opacity, flowability and material strength of many materials are affected by the size and characteristics of the particles within them. A number of different methods may be used to determine the particle size distribution of a powder; in this work only scanning electron microscopy (SEM) and laser diffraction methods were used.

Laser diffraction

In recent years particle sizing using the laser diffraction techniques has become the dominant method of choice. Laser diffraction units do not measure particle size distributions (PSD) but carry out light scattering experiments. The relationship between the light scattered by the particles and the final particle size distribution reported depends critically upon assumptions made about the optical properties of the material under study. Main advantages of the LD technique for PSD determinations include; short time of analysis (5–10 min per sample), high repeatability, and small sample size needed (≤1 g). The most important advantage is the wide range of size fractions into which the entire range of particle sizes can be divided, rather than an arbitrary division of the particles among a limited number of size fractions. This enables a more detailed data analysis and a simultaneous use of the same data sets for classification of the analyzed samples under different national classification systems (Eshel *et al*. 2004).

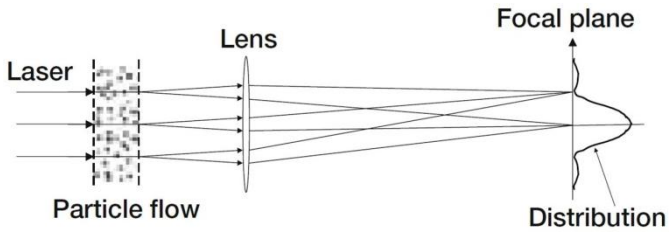

Figure A1.8: Laser diffraction for measurements of particle size distribution. A laser beam hits the particle flow and diffracts in angles inversely proportional to the particle sizes.

SEM

The SEM is an electron microscope that images the sample surface by scanning it with a high-energy beam of electrons in a raster scan pattern. The electrons interact with the atoms that make up the sample producing signals that contain information about the sample's surface topography, composition and other properties such as electrical conductivity.

The types of data signals produced by an SEM include; secondary electrons, back-scattered electrons (BSE), characteristic X-rays, light, specimen current and transmitted electrons. Secondary electron detectors are common in all SEMs, but it is rare that a single machine would have detectors for all possible signals. The signals result from interactions of the electron beam with atoms at or near the surface of the sample. In the most common or standard detection mode, secondary electron imaging or SEI, the SEM can produce very high-resolution images of a sample surface, revealing details about less than 1 to 5 nm in size. Due to the very narrow electron beam, SEM micrographs have a large depth of field yielding a characteristic 3D appearance useful for understanding the surface structure of a sample. The electron beam is thermionically emitted from an electron gun fitted with a tungsten filament cathode. Tungsten is normally used in thermionic electron guns because it has the highest melting point and lowest vapour pressure of all metals, thereby allowing it to be heated for electron emission, and because of its low cost.

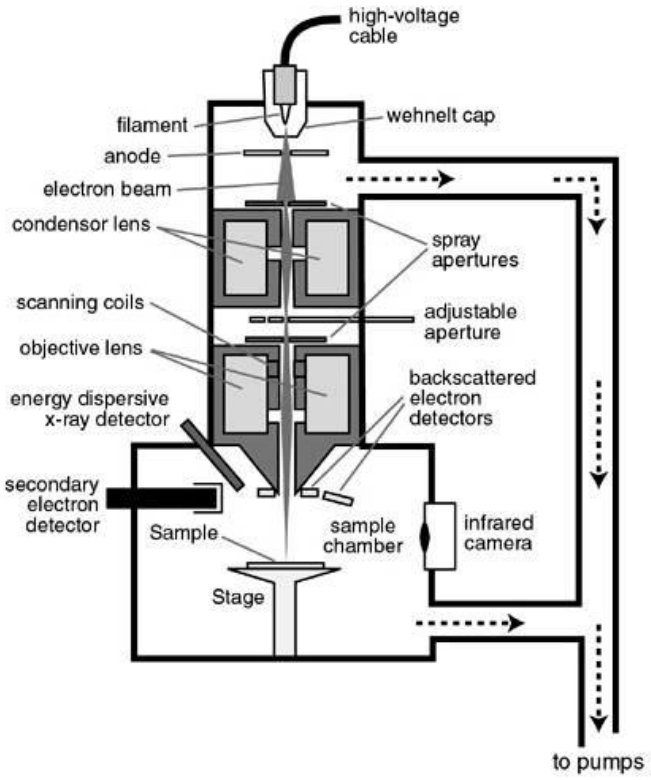

Figure A1.9: A schematic diagram of the SEM apparatus in a typical Joel 7000 SEM.

Appendix Two

Components of the monetite cements paste

Chapter 4 covered the key drawbacks of CPC's when used as bone replacement cements; one of which has been researched was the formulation of an alternative end product that had a suitable solubility, without the risk of hydrolysis to HA. Much research has covered this problem of hydrolysis of brushite to form HA. In chapter 5 we discussed a formulation of novel paste cements that set post operatively to form hardened monetite cement. This is the first of its kind at ambient conditions. Here we discuss the possible use of non-aqueous liquids and gelling agents which combine with the powdered components of the cement to produce a paste which is stable until it is immersed in an aqueous environment, whereby the setting reaction takes place.

2.1 Non-aqueous liquids

2.1.1 Glycerol

Glycerol, also well known as glycerin; is a colorless, odorless, hygroscopic, and sweet-tasting viscous liquid (McGraw-Hill 2009). Glycerol is a sugar alcohol and has three hydrophilic alcoholic hydroxyl groups (OH^-) that are responsible for its solubility in water; glycerol forms the backbone of triglycerides. Glycerol is completely soluble in water and alcohol but is only slightly soluble in many common solvents, such as ether, ethyl acetate, and dioxane. Its specific gravity is 1.262 at 25 °C (77 °F) referred to water at 25 °C, and its molecular weight is 92.09 (Lide 1994). It has a very low mammalian toxicity; therefore, glycerol has a wide range of applications in all industries, including the food and cosmetics industry to paint and lubrications.

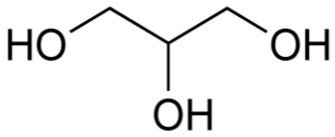

Figure A2.1: Chemical arrangement of Glycerol molecule with a parochial spatial arrangement of atoms (McGraw-Hill 2009).

Glycerol is used in nearly every industry. With dibasic acids which react to make the important class of products known as alkyd resins, which are widely used as coating and in paints (McGraw-Hill 2009). It is used in innumerable pharmaceutical and cosmetic preparations; it is an ingredient of many tinctures, elixirs, cough medicines, and anaesthetics; and it is a basic medium for toothpaste. In foods, it is an important moistening agent for baked goods and is added to candies and icings to prevent crystallization. It is used as a solvent and carrier for extracts and flavouring agents and as a solvent for food colours. Many specialized lubrication problems have been solved by using glycerol. Many millions of pounds are used each year to plasticise various materials (McGraw-Hill 2009).

2.2 Gelling agents

Gelling agents are materials used to thicken and stabilize liquid solutions. They dissolve in the liquid phase as a colloid mixture that forms an internal structure giving the resulting gel an appearance of a solid matter, while being mostly composed of a liquid, in turn thickening the solution. There are various types of materials used as gelling agents.

Polysaccharides are commonly used as polymer scaffolds in tissue engineering. The incorporation of these polymer scaffolds in tissue regeneration has been ongoing since the early 1980's (Yoon & Fisher 2006). Natural polymers are generally suitable to be used within the body as scaffolds and posses the ability to be degraded enzymatically. There are also

many disadvantages of using natural polymers, such as degradation rate and the lack of control of this property, the lifespan of the polymer *in vivo* may pose difficult to determine, and also the crucial property in this case, the mechanical strength, which can be reinforced using cross-linking.

Table A2.1: Properties of Degradable Natural Homopolymers that have been Utilization in the Fabrication of Tissue Engineering Scaffolds (Yoon & Fisher 2006).

Natural Polymer	Curing method	Primary degradation method	Primary degradation products
Alginate	Cross-linking	Alginate lyases	Mannuronic acid and Guluronic aicd
Agarose	Entanglement	Enzymatic agarases	Oligosaccharides
Carrageenan (Kappa)	Cross-linking	Enzymatic Kappaphycus alvarezii	B(1-3) linked and α(1-4) linked D-galactose
Chitosan	Cross-linking	Enzymatic chitosanase	Glucosamines
Hyaluronic acid	Entanglement	Enzymatic hyaluronidase	β(1-4) linked glucuronic aicd and glucosamine
Gelatine	Entanglement	Enzymatic collagenases	Various peptides depending on sequence

2.2.1 Alginate

Alginate is present in the cell walls of brown algae as the calcium, magnesium and sodium salts of alginic acid. The uses of alginates are based on three main properties (Fabia *et al.* 2005). The first is their ability, when dissolved in water, to thicken the resulting solution (more technically described as their ability to increase the viscosity of aqueous solutions). The second is their ability to form gels; gels form when a calcium salt is added to a solution of sodium alginate in water. The gel forms by chemical reaction, the calcium displaces the sodium from the alginate, holds the long alginate molecules together and a gel is the result.

No heat is required and the gels do not melt when heated. This is in contrast to the agar gels where the water must be heated to about 80 °C to dissolve the agar and the gel forms when cooled below about 40 °C. The third property of alginates is the ability to form films of sodium or calcium alginate and fibres of calcium alginates.

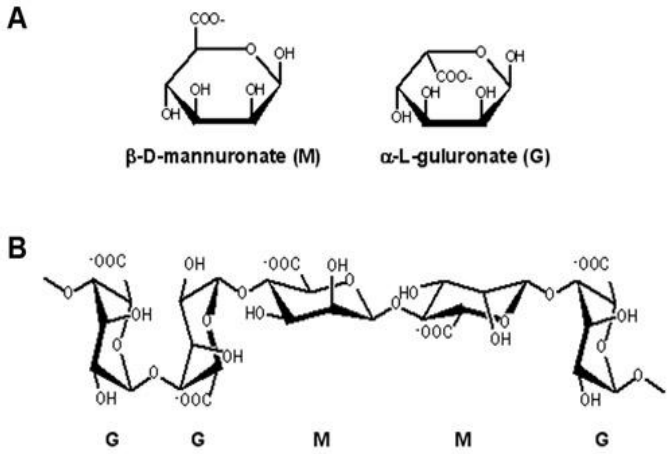

Figure A2.2: Structural illustration for alginates: (A) the monomers in alginate; (B) the alginate chain (Sriamornsak & Sungthongjeen 2007).

Alginate is used in the controlled release of medicinal drugs and other chemicals. In some applications, the active ingredient is placed in a calcium alginate bead and slowly released as the bead is exposed in the appropriate environment (Chan *et al.* 2002). More recently, oral controlled-release systems involving alginate microspheres, sometimes coated with chitosan to improve the mechanical strength, have been tested as a way of delivering various drugs (Pandey & Khuller 2004).

2.2.2 Agarose

Agarose is a linear polysaccharide extracted from marine red algae, and consists of β-1,3 linked D-galactose and α-1,4 linked 3,6-anhydro-αL-galactose residues. Sometimes, traces of sulphate groups can be present on the agarose chain, and may modify the gel properties (Normand *et al.* 2000).

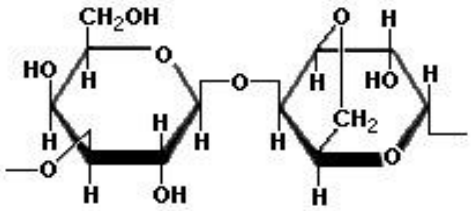

Figure A2.3: Structure of Agarose (Normand *et al.* 2000).

Agarose gel has been commonly used for the cell culture of cartilage and soft tissue and also been used as phantom material for material property characterization using image techniques due to its good elastic property and availability (Chen *et al.* 2004). For tissue culture systems, agarose hydrogels are widely investigated because they permit growth of cells and tissues in a three-dimensional suspension (Yoon & Fisher 2006). Agarose gels have been found to maintain chondrocytes, the predominant cell type in cartilage, in culture for several weeks and also, agarose hydrogels embedded with chondrocytes allow the expression of type II collagen and proteoglycans and results show promise for using agarose gels in cartilage repair (Yoon & Fisher 2006).

2.2.3 Carrageenan

Carrageenans are large, highly flexible molecules which curl forming helical structures. This gives them the ability to form a variety of different gels at room temperature. They are widely used in the food and other industries as thickening and stabilizing agents (Mangione *et al.* 2005). A particular advantage is that they are pseudoplastic, they are thin under shear stress and recover their viscosity once the stress is removed (Garcia & Ghaly 1996). This means that they are easy to pump but stiffen again afterwards. All carrageenans are high molecular weight polysaccharides (MacArtain *et al.* 2003). There are three main commercial classes of carrageenan:

- Kappa: strong, rigid gels. Gels with potassium ions, reacts with dairy proteins.
- Iota: soft gels. Gels with calcium ions.
- Lambda: Does not gel, used to thicken dairy products.

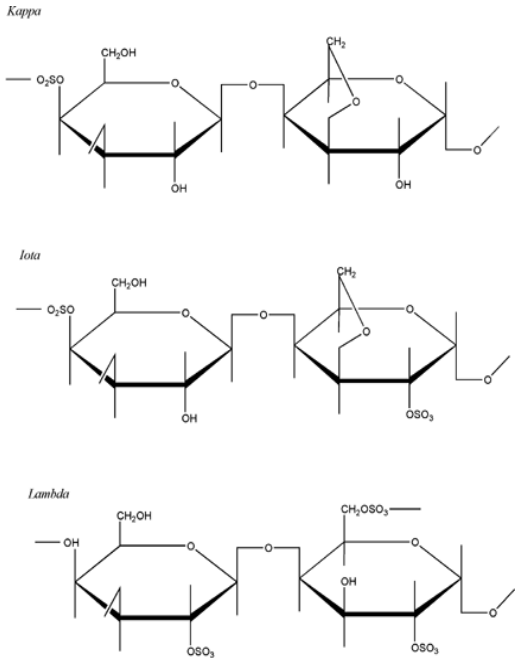

Figure A2.4: Schematic representation of the iota-carrageenan (top), kappa-carrageenan (middle), and lambda-carrageenan (bottom) (Serge *et al.*2009).

A recent publication (Borthakur *et al.* 2007) indicates that carrageenan induces inflammation in human intestinal epithelial cells. Consumption of carrageenan may have a role in intestinal inflammation and possibly inflammatory bowel disease, mutations of which are associated with genetic proclivity to Crohn's Disease.

2.2.4 Chitosan

Chitosan is a polysaccharide that is not only naturally abundant, but it is also non-toxic and biodegradable; as well as being a naturally regenerating resource (e.g., crab and shrimp shells) that can be further enhanced by artificial culturing. Made up of a linear polysaccharide (Yoon & Fisher 2006).

At the present, chitosan is the world's second most abundant polymer, following cellulose (Li *et al.* 1992). One of the most useful properties of chitosan is chelation whereby, chitosan can selectively bind desired materials such as cholesterol, fats, metal ions, proteins, and tumor cells (Hon & Tang 2000). Chelation has been applied to areas of food preparation, health care, water improvement, and pharmaceutics.

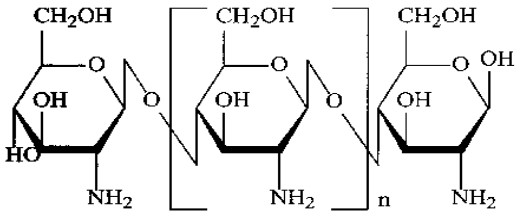

Figure A2.5: A schematic diagram of the chemical structure of Chitosan (http://170.107.206.70/drug_info/nmdrugprofiles/nutsupdrugs/chi_0067.shtml).

Chitosan haemostatic products have been shown to reduce blood loss in comparison to gauze dressings and increases patient survival (Pusateri *et al.* 2003). Chitosan also posses natural bactericide properties; a recent study demonstrates the antibacterial activity of chitosan was investigated by assessing the mortality rates of *Escherichia coli* and *Staphylococcus aureus* based on the extent of damaged or missing cell walls (Chung & Chen 2008).

2.2.5 Gellan Gum

Gellan gum is a water-soluble polysaccharide produced by *Sphingomonas elodea*, an aerobic gram-negative bacterium (Hamcerencu *et al*. 2008). The biopolymer gellan is a more recent addition to the family of microbial polysaccharides that is gaining much importance due to its novel property of forming thermo-reversible gels when heated and cooled (Jansson *et al.* 1983). As a food additive, gellan gum is used as a thickener, emulsifier, and stabilizer.

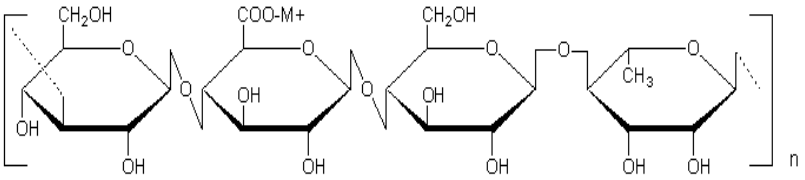

Figure A2.6: A schematic diagram of the chemical structure Gellan gum (http://commons.wikimedia.org/wiki/File:Gellan_gum_structure.png).

Gellan gum can be used to produce easy-to-swallow solid dosage forms, such as gels and coated tablets, and to modify the rate of release of active ingredients from tablets and capsules. Also, conveniently used for controlled or sustained release of various drugs (Paul *et al.* 1986) and also for microencapsulation preparation.

2.2.6 Hyaluronic acid

Hyaluronan, also called hyaluronic acid is a polymer of disaccharides (Yoon & Fisher 2006); found distributed throughout connective, epithelial, and neural tissues and forms in the plasma membrane instead of the Golgi and can be very large with its molecular weight often reaching the millions (Fraser *et al.* 2003). One of the chief components of the extracellular matrix, hyaluronan contributes significantly to cell proliferation and migration, and may also be involved in the progression of some malignant tumours.

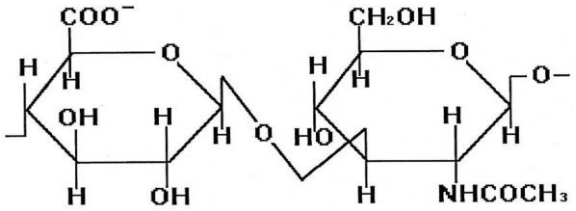

Figure A2.7: Hyaluronic Acid; D-glucuronic acid (left) and D-N-acetylglucosamine (right); (http://www.corgenixonline.com/ed_programs/Intro_to_HA.pdf).

More recently, many research groups have found that hyaluronan's properties for tissue engineering and regenerative medicine are significantly improved with cross-linking, producing a hydrogel (Shu *et al.* 2003).

2.2.7 Gelatine

Gelatine is a non-toxic, biodegradable, non-carcinogenetic, non-immunogenic and inexpensive natural polymer, which has been largely investigated for the preparation of nano- and micro- particles (Vandelli *et al.* 2004b). Gelatin is a protein produced by partial hydrolysis of collagen extracted from the bones, connective tissues, organs and some intestines of animals such as domesticated cattle, pigs, and horses.

Gelatine is soluble in aqueous solutions, gelling makes it possible for a product with a liquid structure to turn into one with a gel structure. The gel state looks similar to the solid state but differs by its instability; the gel is thermo-reversible. When a gelatin solution is cooled, the viscosity increases progressively and passes from a sol to a gel (Yoon & Fisher 2006). On the other hand, if the gel is heated, it dissolves and once again becomes a solution. Unlike most hydrocolloids of polysaccharide origin, gelatin gels independently of pH and without the need for other reactive agents. The sol/gel conversion is reversible and can be repeated, however, a succession of heating and cooling processes may cause gelatin to deteriorate to some extent. Due to this property, gelatin is often cross-linked to control drug release for the pharmaceutical industry and research (Vandelli *et al.* 2004c).

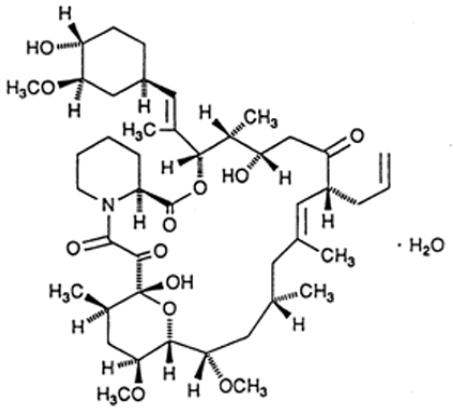

Figure A2.8: Gelatine (http://www.medsafe.govt.nz/Profs/datasheet/p/Prografcapinf.htm)

2.2.8 Hydroxypropyl methylcellulose (HPMC)

HPMC was petitioned as an ingredient of hard capsules used for encapsulating powdered herbs, used as an alternative to gelatine (animal based) capsules (National Organic Standards Board Technical Advisory Panel Review 2002). HPMC has many other uses as an emulsifier, thickening agent, stabilizer, gellant, and suspending agent. HPMC as a gelling agent can be mixed with the powder to improve the cohesiveness of the paste. The ratio of combined constituents is broad and the resulting paste can be formulated to control rather precisely the physical properties of the paste, including injectability, porosity and hardening time.

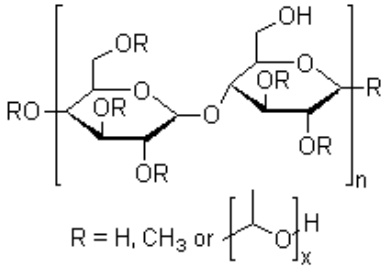

Figure A2.9: Structure of HPMC;
(http://images.chemnet.com/suppliers/chembase/190059_1.gif).

Appendix Three

Experimental data

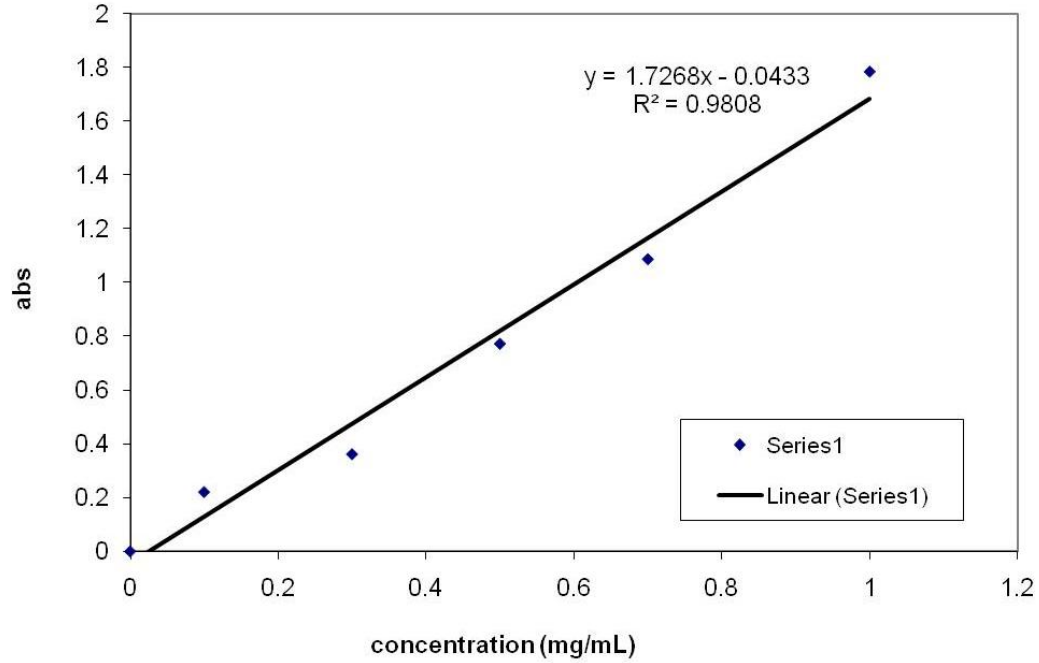

Figure A3.1: A calibration curve for Vancomycin Hydrochloride.

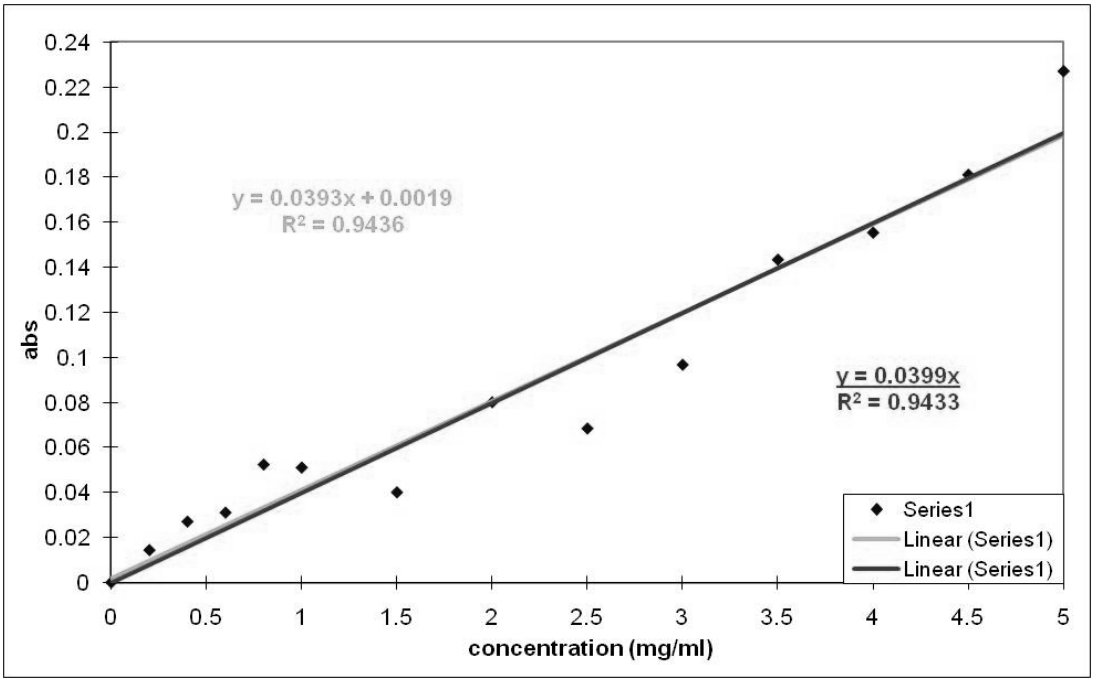

Figure A3.2: A calibration curve for Gentamicin Sulphate.

Appendix Four

Publications

L.M. Grover, **S.Patel**, Y. Hu, U. Gbureck and J.E. Barralet, Modifying brushite cement degradation using calcium alginate beads. *Key Engineering Materials Vols. 361-363 (2008) pp. 311-314* **224**

Peih-Jeng Jiang, **Sarika Patel**, Uwe Gbureck and Liam M Grover, A comparison of the efficacy of hydroxyapatite based cements and gels as drug delivery matrices. *Key Engineering Materials Vols. 361-363 (2008) pp. 327-330* **228**

Sarika Patel, Uwe Gbureck and Liam M Grover, The localised delivery of therapeutic molecules using calcium phosphate based biocements. *Extended Abstract: Cement and Concrete Science (2008) special cements and applications.* **232**

Elke Vorndran, Michael Klarner, Uwe Klammert, Liam M. Grover, **Sarika Patel**, Jake E. Barralet, Uwe Gbureck, 3D Powder Printing of ß-Tricalcium Phosphate Ceramics using different Strategies. *Advanced engineering materials Vol 10:12 (2008) pp. b67-b71* **237**

Peih-Jeng Jiang*, **Sarika Patel***, Uwe Gbureck, Ryan Caley and Liam M. Grover, (*equal contributions by authors) Comparing the efficacy of three bioceramic matrices for the release of vancomycin hydrochloride. *Journal of Biomedical Materials Research Part B: Applied Biomaterials Vols. 93B-1 (2009) pp. 51-58* **242**

Andrea Ewald, Daniel Hösel, **Sarika Patel**, Liam M. Grover, Jake E. Barralet, Uwe Gbureck, Silver doped calcium phosphate cements with antimicrobial activity. *Manuscript to be submitted in Journal of Pharmacy and Pharmacology (2009).* **250**

Sarika Patel, Uwe Gbureck, Serafim, Adrian J. Wright, Liam M.Grover, A monetite forming calcium phosphate cement. *Manuscript to be submitted in Journal of Materials Chemistry (2009).* **251**

Sarika Patel, Yanni Tan and Liam M. Grover, Synthesis and properties of macroporous brushite cements by introducing alginate beads. *Manuscript to be submitted in Advances in Applied Ceramics (2010).* **252**

Key Engineering Materials Vols. 361-363 (2008) pp. 311-314
online at http://www.scientific.net

Modifying brushite cement degradation using calcium alginate beads

L.M. Grover[1, a], S.Patel[1,b], Y. Hu[1], U. Gbureck[2,c] and J.E. Barralet[3,d]

[1]Department of Chemical Engineering, University of Birmingham, Birmingham, B15 2TT, UK.

[2]Department of Functional Materials in Medicine and Dentistry, University of Weurzburg, Wuerzburg, D-97070, Germany.

[3]Faculty of Dentistry, McGill University, Montreal, Quebec, H3A 2B2, Canada.

[a]l.m.grover@bham.ac.uk, [b] sxp244@bham.ac.uk, [c]uwe.gbureck@fmz.uni-wuerzburg.de, [d]jake.barralet@mcgill.ca

Keywords: calcium phosphate; cement; macroporous; alginate; degradation

Abstract. The hydrolysis of brushite in calcium phosphate cements to form hydroxyapatite is known to result in the long term stability of the material in the body. It has previously been established that this hydrolysis reaction can be influenced by implant volume, media refreshment rate and media composition. In this study, the effect of macroporosity on the rate of degradation of the material is investigated. Macroporosity was incorporated into the material using calcium alginate beads mixed into the cement paste. The inclusion of the calcium alginate beads did not influence the degree of conversion of the material and allowed the incorporation of porosity at up to maximum of 57%. The macroporosity weakened the cement matrix (from 46.5 to 3.2 MPa). When aged the brushite in the macroporous cement dissolved completely from the matrix resulting in a weight loss of 60wt% in a period of 28 days. This suggests that the controlled incorporation of calcium alginate beads into brushite cements *in vivo* can be used to control implant degradation rate.

Introduction

Depending on the stoichiometry and pH of the cement slurry, calcium phosphate cements (CPCs) can set to form a matrix consisting of hydroxyapatite ($Ca_{10}(PO_4)_6OH_2$; HA) at a pH value of >4.2 or brushite ($CaHPO_4.2H_2O$) at a pH value of ≤4.2. HA cements have typically attracted more research as they can set at or close to neutral pH and exhibit a composition similar to that of the mineral component of bone. Researchers have, however, demonstrated that HA cements can remain *in vivo* for a considerable period of time following implantation and therefore pose a risk of catastrophic brittle failure [1]. To address this problem some researchers have begun to focus on the production and refinement of brushite cements. Brushite is a sparingly soluble calcium phosphate in physiological conditions and therefore can be resorbed both by cell-mediated mechanisms [2] and dissolution, meaning that they are potentially fully resorbable in the body [3]. Brushite is, however, metastable in physiological conditions and can hydrolyse to form HA which has been shown to result in long-term implant stability [4]. Several studies have been published which have investigated the factors that influence the hydrolysis of brushite cements both *in vitro* [5] and *in vivo* [6], including implant volume, liquid refreshment rate and media composition [5]. In this study, the influence of implant porosity on the *in vitro* degradation of brushite cement was investigated. Porosity was varied by incorporating calcium alginate beads into the setting cement, which subsequently dissolved into the ageing medium, leaving a macroporous structure. Here we report the influence of porosity on the mechanical and *in vitro* degradation properties of a brushite cement system.

Materials and Methods

Cross-linked alginate beads were prepared by the 'drop-wise' addition of 20 mL of sodium alginate solution into 100 mL of calcium chloride solution through steel hypodermic needles of internal

Key Engineering Materials Vols. 361-363 (2008) pp. 327-330
online at http://www.scientific.net

A comparison of the efficacy of hydroxyapatite based cements and gels as drug delivery matrices

Peih-Jeng Jiang[1a], Sarika Patel[1b], Uwe Gbureck[2c] and Liam M Grover[1d]

[1]Chemical engineering, School of Engineering, University of Birmingham, B15 2TT

[2] Department of Functional Materials in Medicine and Dentistry, University of Wuerzburg, Wuerzburg, D-97070, Germany.

[a]pxj623@bham.ac.uk, [b]sxp244@adf.bham.ac.uk, uwe.gbureck@fmz.uni-wuerzburg.de[c], [d]l.m.grover@bham.ac.uk

Keywords: hydroxyapatite; drug delivery; cement; gel; calcium phosphate

Abstract. There is a current need for the localized delivery of antibiotics in order to treat implant based infections. In this study, the efficacy of hydroxyapatite (HA) gels, HA cements, and silica gels in the delivery of vancomycin have been investigated and compared. Vancomycin release was monitored at set time points using a UV/VIS spectrophotometer (288 nm). The activity of the vancomycin released from the cements and gels was assessed using an agar diffusion test with *Staphylococcus aureus*. Vancomycin was released rapidly from both HA matrices, and the silica gel in the first day of the experiment, but the release rate was slowed considerably after 3 days for the HA gels. Following ten days of aging, 70% of the vancomycin remained in the HA gel matrix and the quantity released from the gel was shown to retain its effectiveness against *Staphylococcus aureus*.

Introduction

Osteomyelitis is a bacterial infection of bone that can cause a loss of blood supply to the infected bone and can spread to adjacent tissues. For traditional treatment of osteomyelitis, surgery may be required along with the administration of antibiotics [1]. The delivery of antibiotics to the site of infection is useful to allow the prophylactic treatment of osteomyelitis [2]. It offers the delivery of effective concentrations of antibiotics to implant areas susceptible to infection. Currently, the localized delivery of antibiotics in the treatment of osteomyelitis is accomplied using poly(methylmethacrylate) (PMMA) beads as carriers for antibiotics such as gentamicin sulphate [3] or mixing bone cement with antibiotics encapsulated in PMMA [4]. However, because PMMA beads are not resorbable [5], they have to be surgically removed after a few months, after which they may be replaced either by new beads to prolong the antibiotic therapy or an alternative bone graft. In this study, biodegradable, and nontoxic bioceramics such as, HA gel [6] and HA cement [7] have been used for delivery of vancomycin. The effectiveness of the released vancomycin against *Staphylococcus aureus* was used to evaluate microbiological efficacy.

Materials and method

HA cements were formed by mixing equimolar amounts of tetracalcium phosphate (TTCP) and dicalcium phosphate anhydrous (DCPA) (Merck, Germany), combined with water at P: L ratio 4 g/ml. The liquid component of the cement contained 0.8 mg/mL vancomycin hydrochloride (Sigma Chemical Co., Germany). Once hardened, cement cylinders were immersed in 5 mL of distilled water at 37 °C. HA gels were formed as described by Barralet et al. [6]. The resulting suspension was filtered using a Büchner funnel to form a filter cake, the cake was combined with 20 mL of 0.8 mg/ mL vancomycin for 24 h at room temperature following which the suspension was refiltered. The filter cake loaded vancomycin was formed into pellets of 3 mm diameter and 10 mm height

The localised delivery of therapeutic molecules using calcium phosphate based biocements

Sarika Patel[1], Uwe Gbureck[2] and Liam M. Grover[1]*

[1] Chemical Engineering, School of Engineering, University of Birmingham, UK
[2]Department of Materials in Medicine and Dentistry,University of Wuerzburg, Germany

Address For Correspondence: Liam M. Grover, Chemcial Engineering, School of Engineering, The University of Birmingham, Edgbaston, Birmingham, B15 2TT, UK. Phone: +44-121-4143887Fax: +44-121-4145324E-Mail: L.M.Grover@bham.ac.uk

Extended Abstract: Cement and Concrete Science, University of Manchester, Manchester, 15-16th September 2008

Abstract

There is a current need for the localised delivery of antibiotics in order to treat implant based bacterial infections. Existing treatments use non-resorbable materials such as poly (methyl methacrylate) (PMMA) beads [1] loaded with antibiotics such as vancomycin hydrochloride (VH); unfortunately as they are not resorbable these beads require secondary surgery for removal [2]. Calcium phosphate cements (CPCs) have considerable potential for the localised delivery of drugs since they can be resorbed to some extent within the body [3], eliminating the need for a secondary surgical procedure. In this study, the efficacy of CPCs in the delivery of vancomycin hydrochloride (VH), a drug used in the treatment of osteomyelitis, has been investigated. VH release was monitored at set time points using a UV/VIS spectrophotometer (280 nm). The activity of the VH released from the cements was assessed using agar diffusion and broth dilution methods with *Staphylococcus aureus*.

Introduction

Osteomyelitis is a bacterial infection of bone that can cause necrosis due to a loss of blood supply to the infected tissue. The organism commonly isolated from all forms of osteomyelitis is *S. aureus* [4]; an anaerobic, gram-positive coccus, which can spread to surrounding tissue rapidly. Traditional treatments for osteomyelitis involve surgery, to remove the infected bone and the systemic administration of antibiotics [5], such as VH for a prolonged period of time. Intramuscular or intravenous administration of the antibiotic, however, does not allow sufficient concentrations of the drug to the local area as blood circulation is limited and often uncertain [6]. Currently, the localized delivery of antibiotics in the treatment of osteomyelitis is accomplished using poly(methyl methacrylate) (PMMA) beads as carriers for the drugs [1] or mixing CPC with antibiotics encapsulated in PMMA [7]. PMMA beads are, however, not resorbable [2] and require surgical removal after which they may be replaced either by new beads to prolong the antibiotic therapy or an alternative bone graft. In this study, three calcium phosphate based cement formulations [8] have been investigated for the delivery of VH. The effectiveness of the released VH against *S. aureus* was used to evaluate microbiological effectiveness of the released drug.

DOI: 10.1002/adem.200800179

3D Powder Printing of β-Tricalcium Phosphate Ceramics Using Different Strategies**

By *Elke Vorndran, Michael Klarner, Uwe Klammert, Liam M. Grover, Sarika Patel, Jake E. Barralet* and *Uwe Gbureck**

β-Tricalcium phosphate (β-TCP) is an osteoconductive and resorbable bone substitute material which is either applied as granules or a sintered monolithic body with defined shape.[1,2] Fabrication of the latter is done by slip casting,[3] isostatic pressing [4] and more recently by using rapid prototyping (RP) techniques.[5,6] Rapid prototyping is a technology where a near net shape three dimensional component is created by the layer by layer deposition of a material. One of the major advantages of RP methods, when compared with traditional ceramic processing methods, is that they allow the fabrication of patient specific implants from computer tomography (CT) data.[6] This is beneficial especially for large-size or geometrically complex defects since it is possible to produce implants with a high dimensional accuracy which guarantees optimal implant integration into the defect. Various RP techniques have been described in literature for the fabrication of calcium phosphate bioceramics, these methods can be divided into either direct or indirect techniques. The latter typically use wax or polymer structures which are produced by stereolithography and then infiltrated with a calcium phosphate slurry. After the slurry has hardened the inverse wax / polymer pattern is either dissolved at room temperature[7] or burned out during heat treatment[8,9] to leave the desired pore geometry. Direct RP techniques for bioceramic fabrication include selective laser sintering of polymer-modified ceramic powders,[10] computer aided design (CAD) guided fused deposition modelling[11] or 3D powder printing.[6] The latter uses organic or inorganic binders which are sprayed onto a flat powder bed and locally binds the ceramic particles due to adhesive forces or a hydraulic cement setting reaction. Subsequently a thin layer of powder is applied on top and the process is repeated resulting in a 3D set component. 3D powder printing is a commercially established process, using gypsum or starch powders for technical applications;[12,13] various groups have adapted the technique to other (bio)-material systems, e.g. polymers like polylactic acid (PLA) with chloroform[14] or a mixture of ethanol and acetone[15] were used as binder or calcium phosphate powders, used pure [16-18] or with polymeric additives,[19,20] combined with polymeric or acidic binder solutions. Most of these researchers dealt with the fabrication of insoluble hydroxyapatite implants. Inorganic binder solutions were used to allow hydraulic setting of the powder matrix as it is known from self setting calcium phosphate cements,[21,22] e.g. phosphoric acid solution which reacts with tricalcium phosphate powder to produce a matrix of dicalcium phosphate dihydrate ($CaHPO_4 \cdot 2H_2O$, DCPD, brushite) or citric acid in conjunction with tetracalcium phosphate ($Ca_4(PO_4)_2O$, TTCP) which forms calcium citrate complexes. Up to now only one manuscript has been published which describes the fabrication of porous β-TCP implants using 3D printing.[6] Although the authors reported the successful production of a clearly defined ceramic structure, an organic binder was used, which resulted in ceramics that exhibited relatively poor mechanical properties and were produced with a poor resolution.

The aim of the current work was to avoid these drawbacks by using an inorganic binder solution. Binding the powder through a hydraulic hardening process enabled, for the first time, the fabrication of phase pure β-TCP monoliths of defined macroporosity at high resolution by a cement setting

[*] *E. Vorndran, M. Klarner, Dr. U. Gbureck*
Department of Functional Materials in Medicine and Dentistry
University of Würzburg
D-97070 Würzburg, Germany
E-mail: uwe.gbureck@fmz.uni-wuerzburg.de
Dr. U. Klammert
Department of Cranio-Maxillo-Facial Surgery
University of Würzburg
D-97070 Würzburg, Germany
S. Patel, Dr. L. M. Grover
Department of Chemical Engineering
University of Birmingham
Edgbaston, Birmingham, B15 2TT, UK
Dr. J. E. Barralet
Faculty of Dentistry
McGill University
Montreal, Quebec,
3640 University Street, H 31 2BL, Canada

[**] *This study was financially supported by the Bavarian Government (Bavarian – Quebec grant No. 9.305 "Knochenimplantate") and the Deutsche Forschungsgemeinschaft (DFG Gb7/1-1). We acknowledge the provision of a Canada Research Chair and NSERC Discovery Grant (JEB).*

Comparing the Efficacy of Three Bioceramic Matrices for the Release of Vancomycin Hydrochloride

Peih-Jeng Jiang,[1]* Sarika Patel,[1]* Uwe Gbureck,[2] Ryan Caley,[1] Liam M. Grover[1]

[1] School of Chemical Engineering, University of Birmingham, Birmingham, B15 2TT, UK

[2] Department of Functional Materials in Medicine and Dentistry, University of Wuerzburg, Wuerzburg, D-97070, Germany

Received 8 January 2009; revised 26 June 2009; accepted 27 September 2009
Published online 18 December 2009 in Wiley InterScience (www.interscience.wiley.com). DOI: 10.1002/jbm.b.31557

Abstract: A number of calcium phosphate materials have been investigated as drug release matrices for the prophylactic treatment of implant-related osteomyelitis. However, some studies have shown the influence of processing on the efficacy of the delivered drug. The objective of this study was to evaluate the influence of pH during processing on the efficacy of vancomycin hydrochloride (VH) against *Staphylococcus aureus*. VH was loaded into a brushite cement ($CaHPO_4{\cdot}2H_2O$; pH 2.4); a hydroxyapatite cement ($Ca_{10}(PO_4)_6OH_2$; pH 9.4); and an apatite xerogel (pH 7.4). The pH of the material during processing had a significant influence on the mechanism of release from the cement. VH released from the apatite cement (pH 9.4) was not released in accordance with the Higuchi model. In addition to affecting release, the basic pH was shown to diminish the antibacterial potency of the released VH. Despite exceeding the minimum inhibitory concentration, the eluent from the apatite cement was ineffective against a culture of *S. aureus*. The findings of this study reinforce the importance of evaluating not only the release of the drug from the material matrix but also the antibacterial potency of the released drug. © 2009 Wiley Periodicals, Inc. J Biomed Mater Res Part B: Appl Biomater 93B: 51–58, 2010

Keywords: hydroxyapatite; drug delivery; cement; xerogel; brushite; vancomycin

INTRODUCTION

Bone-related infections, such as osteomyelitis, which causes a loss of blood supply to the infected bone and spreads to adjacent tissues, are complications associated with open fractures and the placement of implants. The treatment of osteomyelitis typically requires the removal of the injured tissue; however, bacteria are not thoroughly eradicated by debridement, and therefore, the systemic administration of an antibiotic may also be required.[1] Vancomycin hydrochloride (VH) is an antibiotic that is specifically used against *Staphylococcus aureus* in the treatment of bone-related infections. However, to achieve the desired antibacterial effect, it is necessary to supply a relatively high dose, for example, 500 mg to 5 g,[2–4] which can lead to both nephro- and ototoxicity.[5,6] A local drug delivery system is advantageous because it is thought to decrease the systemic toxicity and side effects of parenteral antibiotics, and it may also improve efficacy by delivering higher drug concentrations to the infected bone.[7,8]

Poly(methyl methacrylate) beads have previously been used for the local delivery of VH[9,10]; however, the highly exothermic setting reaction and nonresorbability of the material remain a problem.[11] Other resorbable materials have been evaluated for drug release, including plaster of Paris, fibrin, and poly(lactic acid).[12–14] The successful application of these materials would negate the need for a second clinical procedure. Calcium phosphate cements (CPCs) have also been evaluated for localized release of VH.[15–19] These materials are seen as advantageous because they exhibit a similar composition to the mineral component of bone and are already used widely for the replacement of hard tissues.[20–26] Calcium phosphate-based cements[27–30] are particularly desirable for the localized delivery of molecules because they are plastic following mixing and can be applied either as a mouldable paste or through a hypodermic needle.[31] Furthermore, they set with little or no exotherm and therefore can be used for the encapsulation of temperature-sensitive therapeutic molecules. As a result, some studies have reported the delivery of bone morphogenic proteins,[32] vascular endothelial growth factor,[33] and nanomicelles[34] from hardened cement matrices with significant success. Furthermore, a number of research groups have investigated the local delivery of antibacterial drugs such as VH from CPCs for the prophylactic treatment of

*These authors contribued equally to this work.

Correspondence to: L. M. Grover (e-mail: l.m.grover@bham.ac.uk)

Contract grant sponsors: Advantage West Midlands (AWM) and European Regional Development Fund (ERDF)

Silver doped calcium phosphate cements with antimicrobial activity

Andrea Ewald[1], Daniel Hösel[1], Sarika Patel[2], Liam M. Grover[2], Jake E. Barralet[3], Uwe Gbureck[1*]

[1]Department of Functional Materials in Medicine and Dentistry, University of Würzburg, D-97070 Würzburg, Germany
[2] School of Chemical Engineering, University of Birmingham, Edgbaston, UK, B15 2TT.
[3] Faculty of Dentistry, McGill University, Montreal, Quebec, Canada

*Corresponding author
Tel: + 49 931 201 73550 E-mail: uwe.gbureck@fmz.uni-wuerzburg.de

Abstract

There is a current need for the localised delivery of antibiotics in order to treat implant based bacterial infections. Existing treatments use non-resorbable materials such as poly (methyl methacrylate) (PMMA) beads (Bohner M, Lemaitre J, Van Landuyt P, Zambelli PY, Merkle HP, & Gander B 1997) loaded with antibiotics; unfortunately as they are not resorbable these beads require secondary surgery for removal (Penner, Masri, & Duncan 1996). Calcium phosphate cements (CPCs) have considerable potential for the localised delivery of drugs since they can be resorbed to some extent within the body (Xia, Grover, Huang, Adamopoulos, Gbureck, Triffitt, Shelton, & Barralet 2006), eliminating the need for a secondary surgical procedure. Both α- and ß-tricalcium phosphate (α- and ß-TCP) bone substitutes are osteoconductive and resorbable bone substitute materials. Therefore, in this study, the efficacy of, both hydroxyapatite (HA) and brushite, in the delivery of Silver ions (Ag^+), has been investigated. The activity of the Ag^+ released from the cements was assessed against the growth of both *Staphylococcus aureus* and *epidermidis*; the brushite cement exhibited excellent antibacterial properties and also showed an increase in compressive strengths of over 30% with the addition of Ag^+. Cellular interactions with the cements doped in Ag^+ were also investigated and demonstrated toxicity with high concentrations. In this study we have found that with a few changes in Ag^+ concentrations we can produce a fully resorable, osteoconductive bone replacement material that is combined with an antibacterial scaffold with controlled release over a period of time, which will inhibit bacterial infections such as osteomyelitis.

'A monetite forming calcium phosphate cement'

Sarika Patel [a], Uwe Gbureck [b], Adrian J. Wright [c], and Liam M. Grover*[a]

[a]School of Chemical Engineering, University of Birmingham, B15 2TT, UK.
[b]Department of Functional Materials in Medicine and Dentistry, University of Wuerzburg, D-97070, Germany.
[c]School of Chemistry, University of Birmingham, B15 2TT, UK

*corresponding author
E-mail: **l.m.grover@bham.ac.uk**
Tel: +44-121-414-3887
Fax: +44-121-414-5324

Abstract

Calcium phosphate cements (CPC'S) are used in the repair of craniofacial and orthopaedic defects. The majority of CPCs harden to form a matrix formed either of hydroxyapatite (HA; $Ca_{10}(PO_4)_6OH_2$) or brushite ($CaHPO_4.2H_2O$), depending upon the stoichiometry and pH value of the cement mix (Barralet, Lilley, Grover, Farrar, Ansell, & Gbureck 2004;Charriere, Terrazzoni, Pittet, Mordasini, Dutoit, Lemaitre, & Zysset 2001;Grover, Knowles, Fleming, & Barralet 2003;Hatim *et al*. 1998;Johnsson & Nancollas 1992). While historically the majority of research in this area has focussed on the development of HA based cements, much recent interest has been dedicated to the development of brushite based cements. This is because brushite is two orders of magnitude more soluble than HA and hence it has been reported to be more rapidly replaced by bone *in vivo* (Grover, Knowles, Fleming, & Barralet 2003). In some conditions, however, brushite hydrolyses to form a poorly crystalline apatite, which significantly slows the rate at which the material is replaced by bone. Recent work has shown that the dehydrated form of brushite (monetite – $CaHPO_4$) is considerably more resistant to hydrolysis than HA. To date, however, monetite can only be made through thermal dehydration of brushite at temperatures of greater than 100˚C or through the use of highly acidic cement mixes that would be inapproriate for use *in vivo* (Hsu, Chang, & Liu 1998). Here, a new cement formulation is reported that can be provided in paste form and following exchange of water with the aqueous milieu can set to form a matrix formed predominantly of monetite. The material exhibited a compressive strength of ~8 MPa and could be stored in paste form for a period of 90 days at 4˚C.

Keywords: Brushite, Monetite, Cement, Calcium, Phosphate, Alginate, Modification

Synthesis and properties of macroporous brushite cements by introducing alginate beads

Abstract

The objectives of this study were to synthesize the controllable degradation macroporous brushite cement by controlling the porosity using different size and amount of calcium alginate beads. And also the effect of cement:beads ratio on porosity and mechanical properties of macroporous cements were investigated. The *in vitro* degradation behaviour was performed by soaking the samples into the PBS solution for different periods of time. The weight of cements with lower porosity (0%) decreased much faster in the first 14 days than the last 14 days. The weight of cements with higher porosity (50%) decreased greatly and decreased more rapidly towards the end of the experiment. The weight of cements with intermediate porosity (30%), decreased constantly during the whole study. Compared with using different cross-linked hydrogels, the degradation speed of the cement cross-linked $CaCl_2$ was faster than that cross-linked with $MgCl_2$. This suggests that the alginate beads can be used to synthesize the macroporous cement and to control the porosity and the degradation rate.

Keywords: calcium phosphate cement, brushite, macroporous, degradation, alginate, tissue engineering

Chapter Twelve

References

- A.B.Abell, K.L.Willis, & D.A.Lange 1999, "Mercury Intrusion Porosimetry and Image Analysis of Cement-Based Materials", *Journal of Colloid and Interface Science*, vol. 221, pp. 39-44.

- ADA Division of Science 2002, *Bone-grafting materials: their uses, advantages and disadvantages* 133.

- Albinati, A. & Willis, B. 2004, "The Rietveld method," pp. 710-712.

- Alkhraisat, M. H., Rueda, C., Marino, F. T., Torres, J., Jerez, L. B., Gbureck, U., & Cabarcos, E. L. 2009, "The effect of hyaluronic acid on brushite cement cohesion", *Acta Biomaterialia*, vol. 5, no. 8, pp. 3150-3156.

- Alkhraisat, M. H., Marino, F. T., Retama, J. R., Jerez, L. B., & Lopez-Cabarcos, E. 2008a, "Beta-tricalcium phosphate release from brushite cement surface", *Journal of Biomedical Materials Research Part A*, vol. 84A, no. 3, pp. 710-717.

- Alkhraisat, M. H., Marino, F. T., Rodroguez, C. R., Jerez, L. B., & Cabarcos, E. L. p. 2008b, "Combined effect of strontium and pyrophosphate on the properties of brushite cements", *Acta Biomaterialia*, vol. 4, no. 3, pp. 664-670.

- Alkhraisat, M. H. 2009, *Bioactivity of calcium phosphate cements replace with strontium and Its Application in bone regeneration*, Doctoral.

- Alkhraisat, M. H., Rueda, C., Jerez, L. B., Tamimi Mari±o, F., Torres, J., Gbureck, U., & Lopez Cabarcos, E. 2010, "Effect of silica gel on the cohesion, properties and biological performance of brushite cement", *Acta Biomaterialia*, vol. 6, no. 1, pp. 257-265.

- Alt, V., Bechert, T., Steinr³cke, P., Wagener, M., Seidel, P., Dingeldein, E., Domann, E., & Schnettler, R. 2004, "An in vitro assessment of the antibacterial properties and cytotoxicity of nanoparticulate silver bone cement", *Biomaterials*, vol. 25, no. 18, pp. 4383-4391.

- Alves, H., dos Santos, L., & Bergmann, C. 2008, "Injectability evaluation of tricalcium phosphate bone cement", *Journal of Materials Science: Materials in Medicine*, vol. 19, no. 5, pp. 2241-2246.

- Amendola, A. & Stolley, M. P. 2009, "What Do We Really Know About Allografts?", *Clinics in Sports Medicine*, vol. 28, no. 2, pp. 215-222.

- Androutsopoulos, G. P. & Mann, R. 1979, "Evaluation of mercury porosimeter experiments using a network pore structure model", *Chemical Engineering Science*, vol. 34, no. 10, pp. 1203-1212.

- Antin, R. E. & Salager, J. L. 1986, "Emulsion instability in the three-phase behavior region of surfactant-alcohoi-oil-brine systems", *Journal of Colloid and Interface Science*, vol. 111, no. 1, pp. 54-59.

- Anttipoika, I., Josefsson, G., Konttinen, Y., Lidgren, L., Santavirta, S., & Sanzen, L. 1990, "Hip-Arthroplasty Infection - Current Concepts", *Acta Orthopaedica Scandinavica*, vol. 61, no. 2, pp. 163-169.

- Apelt, D., Theiss, F., El-Warrak, A. O., Zlinszky, K., Bettschart-Wolfisberger, R., Bohner, M., Matter, S., & Auer, J. A. 2004, "In vivo behavior of three different injectable hydraulic calcium phosphate cements", *Biomaterials*, vol. 25, no. 7-8, pp. 1439-1451.

- Arrington, E. D., Smith, W. J., Chambers, H. G., Bucknell, A. L., & Davino, N. A. 1996, "Complications of Iliac Crest Bone Graft Harvesting", *Clinical Orthopaedics and Related Research*, vol. 329.

- ASTM 1993, "Standard Test Method: ASTM C266-89. Time of Setting of Hydraulic Cement Paste by Gillmore Needles," in *Annual Book of ASTM Standards*, 04 edn, ASTM, ed., Philadelphia, p. 444.

- Augat, P. & Schorlemmer, S. 2006, "The role of cortical bone and its microstructure in bone strength", *Age and Ageing*, vol. 35, no. suppl_2, p. ii27-ii31.

- Azarmi, S., Farid, J., Nokhodchi, A., Bahari-Saravi, S. M., & Valizadeh, H. 2002, "Thermal treating as a tool for sustained release of indomethacin from Eudragit RS and RL matrices", *International Journal of Pharmaceutics*, vol. 246, no. 1-2, pp. 171-177.

- B.D.Ratner, A.S.Hoffman, F.J.Schoen, & J.E.Lemons 2004, "Biomaterials Science. An Introduction to Materials in Medicine," 2nd edn, Academic Press, San Diego, CA.

- B.L.Riggs, H.W.Wahner, E.Seeman, K.P.Offord, W.L.Dunn, R.B.Mazess, K.A.Johnson, & L.J.Melton 1982, "Changes in Bone Mineral Density of the Proximal Femur and Spine with Aging: Differences Between The Postmenopausal And Senile Osteoporosis Syndromes", *Journal of Clinical Investigation*, vol. 70, no. 4, pp. 716-723.

- Barralet, J. E., Tremayne, M., Lilley, K. J., & Gbureck, U. 2005, "Modification of Calcium Phosphate Cement with á-Hydroxy Acids and Their Salts", *Chemistry of Materials*, vol. 17, pp. 1313-1319.

- Barralet, J. E., Hofmann, M. P., Grover, L. M., & Gbureck, U. 2003, "High-Strength Apatitic Cement by Modification with -Hydroxy Acid Salts", *Advanced Materials*, vol. 15, no. 24, pp. 2091-2094.

- Barralet, J. E., Aldred, S., Wright, A. J., & Coombes, A. G. A. 2002a, "In vitro behavior of albumin-loaded carbonate hydroxyapatite gel", *Journal of Biomedical Materials Research*, vol. 60, no. 3, pp. 360-367.

- Barralet, J. E., Gaunt T, Wright AJ, Gibson IR, & Knowles JC 2002b, "Effect of porosity reduction by compaction on compressive strength and microstructure of calcium phosphate cement", *Journal of Biomedical Materials Research*, vol. 63, no. 1, pp. 1-9.

- Barralet, J. E., Grover, L., Gaunt, T., Wright, A. J., & Gibson, I. R. 2002c, "Preparation of macroporous calcium phosphate cement tissue engineering scaffold", *Biomaterials*, vol. 23, no. 15, pp. 3063-3072.

- Barralet, J. E., Grover, L. M., & Gbureck, U. 2004, "Ionic modification of calcium phosphate cement viscosity. Part II: hypodermic injection and strength improvement of brushite cement", *Biomaterials*, vol. 25, no. 11, pp. 2197-2203.

- Barralet, J. E., Lilley, K. J., Grover, L. M., Farrar, D. F., Ansell, C., & Gbureck, U. 2004, "Cements from nanocrystalline hydroxyapatite", *J.Mater.Sci.Mater.Med.*, vol. 15, no. 4, pp. 407-411.

- Beaman, F. D., Bancroft, L. W., Peterson, J. J., & Kransdorf, M. J. 2006, "Bone Graft Materials and Synthetic Substitutes", *Radiologic Clinics of North America*, vol. 44, no. 3, pp. 451-461.

- Bermudez, O., Boltong, M. G., Driessens, F. C. M., & Planell, J. A. 1993, "Compressive strength and diametral tensile strength of some calcium-orthophosphate cements: a pilot study", *Journal of Materials Science: Materials in Medicine*, vol. 4, no. 4, pp. 389-393.

- Bermudez, O., Boltong, M. G., Driessens, F. C. M., & Planell, J. A. 1994a, "Optimization of a calcium orthophosphate cement formulation occurring in the combination of monocalcium phosphate monohydrate with calcium oxide", *Journal of Materials Science: Materials in Medicine*, vol. 5, no. 2, pp. 67-71.

- Bermudez, O., Boltong, M. G., Driessens, F. C. M., & Planell, J. A. 1994b, "Development of some calcium phosphate cements from combinations of *á*-TCP, MCPM and CaO", *Journal of Materials Science: Materials in Medicine*, vol. 5, no. 3, pp. 160-163.

- Bigi, A., Bracci, B., & Panzavolta, S. 2004, "Effect of added gelatin on the properties of calcium phosphate cement", *Biomaterials*, vol. 25, no. 14, pp. 2893-2899.

- Bigi, A., Foresti, E., Gandolfi, M., Gazzano, M., & Roveri, N. 1997, "Isomorphous substitutions in [beta]-tricalcium phosphate: The different effects of zinc and strontium", *Journal of Inorganic Biochemistry*, vol. 66, no. 4, pp. 259-265.

- Blokhuis, T. J., Termaat, M. F., den Boer, F. C., Patka, P., Bakker, F. C., & Haarman, H. J. T. M. 2000, "Properties of calcium phosphate ceramics in relation to their in vivo behavior", *Journal of Trauma-Injury Infection and Critical Care*, vol. 48, no. 1, pp. 179-186.

- Bohner M 2007, "Reactivity of calcium phosphate cements", *Journal of Materials Chemistry*, vol. 17, no. 38, pp. 3980-3986.

- Bohner M, Lemaitre J, Van Landuyt P, Zambelli PY, Merkle HP, & Gander B 1997, "Gentamicin-loaded hydraulic calcium phosphate bone cement as antibiotic delivery system", *Journal of Pharmaceutical Sciences*, vol. 86, no. 5, pp. 565-572.

- Bohner M. 2000, "Calcium orthophosphates in medicine: from ceramics to calcium phosphate cements", *Injury*, vol. 31, no. 4, pp. 37-47.

- Bohner M., Gbureck U., & Barralet J.E. 2005, "Technological issues for the development of more efficient calcium phosphate bone cements: A critical assessment", *Biomaterials*, vol. 26, no. 33, pp. 6423-6429.

- Bohner M., Theiss, F., Apelt, D., Hirsiger, W., Houriet, R., Rizzoli, G., Gnos, E., Frei, C., Auer, J. A., & von Rechenberg, B. 2003, "Compositional changes of a dicalcium phosphate dihydrate cement after implantation in sheep", *Biomaterials*, vol. 24, no. 20, pp. 3463-3474.

- Bohner, M. 1996, "Effects of Sulfate, Pyrophosphate, and Citrate Ions on the Physicochemical Properties of Cements Made of b-Tricalcium Phosphate-Phosphoric Acid-Water Mixtures", *Journal of American ceramics socitety*, vol. 79, no. 6, pp. 1427-1434.

- Bohner, M., Doebelin, N., & Baround, G. 2006, "Theoretical and experimental approach to test the cohesion of calcium phosphate pastes", *European Cells and Materials*, vol. 12, pp. 26-35.

- Bohner, M. 2000b, "Calcium phosphate emulsions: possible applications", *Bioceramics*, vol. 192, no. 1, pp. 765-768.

- Bohner, M. 2000c, "Calcium orthophosphates in medicine: from ceramics to calcium phosphate cementsCalcium-orthophosphate in der medizin: von der keramik zu calciumphosphat-zementenDes orthophosphates de calcium en medecine: des ceramiques aux ciments phosphocalciquesLos ortofosfatos de calcio en medicina: de la ceramica a los cementos de fosfato de calcio", *Injury*, vol. 31, no. Supplement 4, p. D37-D47.

- Bohner, M. 2000a, "Calcium orthophosphates in medicine: from ceramics to calcium phosphate cementsCalcium-orthophosphate in der medizin: von der keramik zu calciumphosphat-zementenDes orthophosphates de calcium en medecine: des ceramiques aux ciments phosphocalciquesLos ortofosfatos de calcio en medicina: de la ceramica a los cementos de fosfato de calcio", *Injury*, vol. 31, no. Supplement 4, p. D37-D47.

- Bohner, M. 2001, "Physical and chemical aspects of calcium phosphates used in spinal surgery", *European Spine Journal*, vol. 10, no. 0, p. S114-S121.

- Bohner, M. & Baumgart, F. 2004, "Theoretical model to determine the effects of geometrical factors on the resorption of calcium phosphate bone substitutes", *Biomaterials*, vol. 25, no. 17, pp. 3569-3582.

- Bohner, M., Gbureck, U., & Barralet, J. E. 2005, "Technological issues for the development of more efficient calcium phosphate bone cements: A critical assessment", *Biomaterials*, vol. 26, no. 33, pp. 6423-6429.

- Bohner, M., Merkle, H. P., Landuyt, P. V., Trophardy, G., & Lemaitre, J. 2000, "Effect of several additives and their admixtures on the physico-chemical properties of a calcium phosphate cement", *Journal of Materials Science: Materials in Medicine*, vol. 11, no. 2, pp. 111-116.

- Borthakur, A., Bhattacharyya, S., Dudeja, P. K., & Tobacman, J. K. 2007, "Carrageenan induces interleukin-8 production through distinct Bcl10 pathway in normal human colonic epithelial cells", *AJP - Gastrointestinal and Liver Physiology*, vol. 292, no. 3, p. G829-G838.

- Breitenbach, J. 2002, "Melt extrusion: from process to drug delivery technology", *European Journal of Pharmaceutics and Biopharmaceutics*, vol. 54, no. 2, pp. 107-117.

- Brown W & Chow L 1985, *Dental restorative cement pastes.*, 4518430 (patent).

- Brown, P. W. & Fulmer, M. 1991, "Kinetics of Hydroxyapatite Formation at Low Temperature", *Journal of the American Ceramic Society*, vol. 74, no. 5, pp. 934-940.

- Brown, W. & Chow, L. 1985, *Dental restorative cement pastes.*, 4518430 (patent).

- Brown, W. & Chow, L. 1986, "A new calcium phosphate, water setting cement.", *Proceedings of The American Ceramic Society*, vol. In Brown PW. (ed.). Cements research progress., no. Ohio, pp. 352-379.

- Buddy D.Ratner 1996, *Biomaterials Science: An Introduction to Materials in Medicine*, 1st edn, Elsevier Science & Technology Books.

- C.Hamanishi, K.Kitamoto, S.Tanaka, M.Otsuka, Y.Doi, & T.Kitahashi 1996, "A self-setting TTCP-DCPD apatite cement for release of vancomycin", *Journal of Biomedical Materials Research Part B: Applied Biomaterials*, vol. 33, no. 3, pp. 139-143.

- Calvo, P. 1997, "Novel hydrophilic chitosan-polyethylene oxide nanoparticles as protein carriers.", *Journal of Applied Polymer Science*, vol. 63, no. 1, pp. 125-132.

- Cao, W. & Hench, L. L. 1996, "Bioactive materials", *Ceramics International*, vol. 22, no. 6, pp. 493-507.

- Carey, L. E., Xu, H. H. K., Simon, C. G., Takagi, S., & Chow, L. C. 2005, "Premixed rapid-setting calcium phosphate composites for bone repair", *Biomaterials*, vol. 26, no. 24, pp. 5002-5014.

- Carlalberta Verna, Michel Dalstra, Ulf M.E.Wikesjö, & Leonardo Trombell 2002, "Healing patterns in calvarial bone defects following guided bone regeneration in rats", *Journal Of Clinical Periodontology*, vol. 29, no. 9, pp. 865-870.

- Carter, D. R. & Hayes, W. C. 1977, "The compressive behavior of bone as a two-phase porous structure", *Journal of Bone and Joint Surgery*, vol. 59, no. 7, pp. 954-962.

- Chan, L. W., Lee, H. Y., & Heng, P. W. S. 2002, "Production of alginate microspheres by internal gelation using an emulsification method", *International Journal of Pharmaceutics*, vol. 242, no. 1-2, pp. 259-262.

- Chang, M. C., Ko, C. C., & Douglas, W. H. 2003, "Preparation of hydroxyapatite-gelatin nanocomposite", *Biomaterials*, vol. 24, no. 17, pp. 2853-2862.

- Charriere, E., Lemaitre, J., & Zysset, P. 2003, "Hydroxyapatite cement scaffolds with controlled macroporosity: fabrication protocol and mechanical properties", *Biomaterials*, vol. 24, no. 5, pp. 809-817.

- Charriere, E., Terrazzoni, S., Pittet, C., Mordasini, P., Dutoit, M., Lemaitre, J., & Zysset, P. 2001, "Mechanical characterization of brushite and hydroxyapatite cements", *Biomaterials*, vol. 22, no. 21, pp. 2937-2945.

- Chatzis, I. & Dullien, F. A. L. 2005, "Mercury porosimetry curves of sandstones. Mechanisms of mercury penetration and withdrawal", *Powder Technology*, vol. 29, no. 1, pp. 117-125.

- Chen PS, Toribara TY, & Warner H 1956, "Microdetermination of Phosphorus", *Anal Chem*, vol. 28, pp. 1756-1758.

- Chen, F., Mao, T., Tao, K., Chen, S., Ding, G., & Gu, X. 2003, "Injectable bone", *British Journal of Oral and Maxillofacial Surgery*, vol. 41, no. 4, pp. 240-243.

- Chen, Q., Suki, B., & An, K. N. 2004, "Dynamic Mechanical Properties of Agarose Gels Modeled by a Fractional Derivative Model", *Journal of Biomechanical Engineering*, vol. 126, no. 5, pp. 666-671.

- Chen, Z.-F., Darvell, B. W., & Leung, V. W. 2004, "Hydroxyapatite solubility in simple inorganic solutions", *Archives of Oral Biology*, vol. 49, no. 5, pp. 359-367.

- Chern, C. S. 2006, "Emulsion polymerization mechanisms and kinetics", *Progress in Polymer Science*, vol. 31, no. 5, pp. 443-486.

- Choi, K. & Goldstein, S. A. 1992, "A comparison of the fatigue behavior of human trabecular and cortical bone tissue", *Journal of Biomechanics*, vol. 25, no. 12, pp. 1371-1381.

- Choi, K., Kuhn, J. L., Ciarelli, M. J., & Goldstein, S. A. 1990, "The elastic moduli of human subchondral, trabecular, and cortical bone tissue and the size-dependency of cortical bone modulus", *Journal of Biomechanics*, vol. 23, no. 11, pp. 1103-1113.

- Chow, L. C. 1988, "Calcium Phosphate Materials:Reactor Response", *Advances in Dental Research*, vol. 2, no. 1, pp. 181-186.

- Christof, v. E., Bernd, J., Wolfgang, K., & Karsten, B. 2005, "Infections Associated with Medical Devices: Pathogenesis, Management and Prophylaxis", *Drugs*, vol. 65, pp. 179-214.

- Chung H.J & Park T.G 2007, "Surface engineered and drug releasing pre-fabricated scaffolds for tissue engineering", *Advanced Drug Delivery Reviews*, vol. 59, pp. 249-262.

- Chung, Y. C. & Chen, C. Y. 2008, "Antibacterial characteristics and activity of acid-soluble chitosan", *Bioresource Technology*, vol. 99, no. 8, pp. 2806-2814.

- Cleland, J. L. 1998, "Solvent evaporation processes for the production of controlled release biodegradable microsphere formulations for therapeutics and vaccines.", *Biotechnology Progress*, vol. 14, no. 1, pp. 102-107.

- Constantz, B. R., Barr, B. M., Ison, I. C., Fulmer, M. T., Baker, J., McKinney, L., Goodman, S. B., Gunasekaren, S., Delaney, D. C., Ross, J., & Poster, R. D. 1998, "Histological, chemical, and crystallographic analysis of four calcium phosphate cements in different rabbit osseous sites", *Journal of Biomedical Materials Research*, vol. 43, no. 4, pp. 451-461.

- Constantz, B. R., Ison, I. C., Fulmer, M. T., Poser, R. D., Smith, S. T., VanWagoner, M., Ross, J., Goldstein, S. A., Jupiter, J. B., & Rosenthal, D. I. 1995a, "Skeletal repair by in situ formation of the mineral phase of bone", *Science*, vol. 267, no. 5205, pp. 1796-1799.

- Constantz, B. R., Ison, I. C., Fulmer, M. T., Poster, R. D., Smith, S. T., VanWagoner, M., Ross, J., Goldstein, S. A., Jupiter, J. B., & Rosenthal, D. I. 1995b, "Skeletal Repair by in Situ Formation of the Mineral Phase of Bone", *Science*, vol. 267, no. 5205, pp. 1796-1799.

- Constanz, B. R., Ison, I. C., Fulmer, M. T., Fulmer, D., Poser, R. D., Smith, S. T., VanWagoner, M., Ross, J., Goldstein, S. A., Jupiter, J. B., & Rosenthal, D. I. 1998, "Histological, chemical, and crystallographic analysis of four calcium phosphate cements in different rabbit osseus sites", *Journal of Biomedical Materials Research Part B: Applied Biomaterials*, vol. 43, pp. 451-461.

- Cook, S., Baffes, G., Wolfe, M., Sampath, T., Rueger, D., & Whitecloud, T. 1994, "The effect of recombinant human osteogenic protein-1 on healing of large segmental bone defects", *Journal of Bone and Joint Surgery*, vol. 76A, no. 6, pp. 827-838.

- Cook, S., Salkeld, S., & Rueger, D. 1995, "Comparison of osteoinductive and osteoconductive biomaterials in healing large segmental bone defects", *American Academy of Orthopaedic Surgeons*, vol. 005.

- D.Buser, R.K.Schenk, S.Steinemann, J.P.Fiorellini, C.H.Fox, & H.Stich 1991, "Influence of surface characteristics on bone integration of titanium implants. A histomorphometric study in miniature pigs", *Journal of Biomedical Materials Research*, vol. 25, no. 7, pp. 889-902.

- D.S.Metsger, M.R.Rieger, & D.W.Foreman 1999, "Mechanical properties of", *Journal of Materials Science: Materials in Medicine*, vol. 10, no. 1, pp. 9-17.

- Daniel O.de Lima, Marcelo H.Prado da Silva, Jose B.de Campos, Alexandre M.Rossi, & Marisa M.Beppu 2006, "Influence of Alginate on Precipitation of Calcium Phosphates", *Key Engineering Marerials*, vol. 309-311, no. Bioceramics 18, pp. 195-198.

- David N.-S.Hon & Lie-Gui Tang 2000, "Chelation of chitosan derivatives with zinc ions. I. *O,N*-carboxymethyl chitosan", *Journal of Applied Polymer Science*, vol. 77, no. 10, pp. 2246-2253.

- De Long, W. G., Einhorn, T. A., Koval, K., McKee, M., Smith, W., Sanders, R., & Watson, T. 2007, "Bone Grafts and Bone Graft Substitutes in Orthopaedic Trauma Surgery. A Critical Analysis", *Journal of Bone and Joint Surgery*, vol. 89, no. 3, pp. 649-658.

- del Real, R. P., Wolke, J. G. C., Vallet-Regi M, & Jansen, J. A. 2002, "A new method to produce macropores in calcium phosphate cements", *Biomaterials*, vol. 23, no. 17, pp. 3673-3680.

- Desai, T. R., Bhaduri, S. B., & Tas, A. C. 2008, "A Self-Setting, Monetite ($CaHPO_4$) Cement for Skeletal Repair," 27 edn.

- Devlin, M. J. & Lieberman, D. E. 2007, "Variation in estradiol level affects cortical bone growth in response to mechanical loading in sheep", *Journal of Experimental Biology*, vol. 210, no. 4, pp. 602-613.

- Diana M.Yoon & John P.Fisher 2006, "Polymeric Scaffolds for Tissue Engineering Applications," in *The Biomedical Engineering Handbook: Tissue Engineering & Artificial Organs*, 3 edn, Joseph D.Bronzino, ed., Taylor & Francis Group, pp. 37-1-18.

- Dion, A., Langman, M., Hall, G., & Filiaggi, M. 2005, "Vancomycin release behaviour from amorphous calcium polyphosphate matrices intended for osteomyelitis treatment", *Biomaterials*, vol. 26, no. 35, pp. 7276-7285.

- Driessens, F., Planell, J., Boltong, M., Khairoun, I., & Ginebra, M. 1998, "Osteotransductive bone cements", *Proceedings of the Institution of Mechanical Engineers, Part H: Journal of Engineering in Medicine*, vol. 212, no. 6, pp. 427-435.

- Driessens, F. C. M., Boltong, M. G., Bermudez, O., Fernandez, E., Ginebra, M. P., & Planell, J. A. "Common ion effect on calcium phosphate cements", p. 30.

- Driessens, F. C. M., Boltong, M. G., Bermudez, O., & Planell, J. A. 1993b, "Formulation and setting times of some calcium orthophosphate cements: a pilot study", *Journal of Materials Science: Materials in Medicine*, vol. 4, no. 5, pp. 503-508.

- Driessens, F. C. M., Boltong, M. G., De Maeyer, E. A. P., Wenz, R., Nies, B., & Planell, J. A. 2002, "The Ca/P range of nanoapatitic calcium phosphate cements", *Biomaterials*, vol. 23, no. 19, pp. 4011-4017.

- Driessens, F. C. M., Boltong, M. G., Maeyer, E. A. P. D., Verbeeck, R. M. H., & Wenz, R. 2000, "Effect of temperature and immersion on the setting of some calcium phosphate cements", *Journal of Materials Science: Materials in Medicine*, vol. 11, no. 7, pp. 453-457.

- Driessens, F. C. M., De Maeyer, E. A. P., Fernandez, E., Boltong, M. G., Berger, G., Verbeeck, R. M. H., Ginebra, M. P., & Planell, J. A. 1996, "Amorphous calcium phosphate cements and their transformation into calcium deficient hydroxyapatite", *Bioceramics*, vol. 9, pp. 231-234.

- Ducheyne, P. & Qiu, Q. 1999, "Bioactive ceramics: the effect of surface reactivity on bone formation and bone cell function", *Biomaterials*, vol. 20, no. 23-24, pp. 2287-2303.

- Ducheyne, P., Aernoudt, E., De Meester, P., Martens, M., Mulier, J. C., & Van Leeuwen, D. 1978, "Factors governing the mechanical behavior of the implant-porous coating-trabecular bone interface", *Journal of Biomechanics*, vol. 11, no. 6-7, pp. 297-307.

- Durbhakula, S. M., Czajka, J., Fuchs, M. D., & Uhl, R. L. 2004, "Spacer endoprosthesis for the treatment of infected total hip arthroplasty", *J Arthroplasty*, vol. 19, no. 6, pp. 760-767.

- Durucan, C. & Brown, P. W. 2000, "[alpha]-Tricalcium phosphate hydrolysis to hydroxyapatite at and near physiological temperature", *Journal of Materials Science: Materials in Medicine*, vol. 11, no. 6, pp. 365-371.

- E.Caroline Victoria & F.D.Gnanam 2002, "Synthesis and Characterisation of Biphasic Calcium Phosohate", *Trends in Biomaterials & Artificial Organs*, vol. 16, no. 1, pp. 12-14.

- E.Mathiowitz 1999, "Encyclopaedia of Controlled Drug Delivery," E.Mathiowitz, ed., John Wiley and Sons, New York.

- Elliot, J. C. 1994, *Structure and Chemistry of the Apatites and Other Calcium Orthophosphates* ELSEVIER.

- Ellis, D. J. & O'Brien, M. E. 1974, "Osteomyelitis, iatrogenic osteolysis, pathologic fracture, and bone graft : Report of a case", *Oral Surgery, Oral Medicine, Oral Pathology*, vol. 37, no. 3, pp. 364-369.

- Emily Y.Ho 2005, *Engineering Bioactive Polymers for the Next Generation of Bone Repair*, PhD, Drexel University.

- Eshel, G., Levy, G. J., Mingelgrin, U., & Singer, M. J. 2004, "Critical Evaluation of the Use of Laser Diffraction for Particle-Size Distribution Analysis", *Soil Science Society of America Journal*, vol. 68, no. 3, pp. 736-743.

- F.B.Bagambisa, U.Joos, & W.Schilli 1993, "Mechanisms and structure of the bond between bone and hydroxyapatite ceramics", *Journal of Biomedical Materials Research*, vol. 27, no. 8, pp. 1047-1055.

- F.H.Martini 2001, *Fundamentals Of Anatomy And Physiology*, 5th edn, Prentice Hall College Div.

- Fernandez, E., Boltong, M. G., Ginebra, M. P., Berm·dez, O., Driessens, F. C. M., & Planell, J. A. 1994, "Common ion effect on some calcium phosphate cements", *Clinical Materials*, vol. 16, no. 2, pp. 99-103.

- Flautre, B., Delecourt, C., Blary, M.-C., Van Landuyt, P., Lemaitre, J., & Hardouin, P. 1999, "Volume effect on biological properties of a calcium phosphate hydraulic cement: experimental study in sheep", *Bone*, vol. 25, no. 2, Supplement 1, pp. 35S-39S.

- Frakenburg, E. P., Goldstein, S. A., Bauer, T. W., Harris, S. A., & Poser, R. D. 1998, "Biomechanical and Histological Evaluation of a Calcium Phosphate Cement", *Journal of Bone and Joint Surgery*, vol. 80, no. 8, pp. 1112-1124.

- Frank Thielmann & Daniel Burnett 2000, *Determination of Mesopore Size Distribution by Organic Vapour Sorption* Dynamic Vapour Sorption Application Note 38.

- Freitas, S., Merkle, H. P., & Gander, D. 2005, "Microencapsulation by solvent extraction/evaporation: reviewing the state of the art of microsphere preparation process technology.", *Journal of Controlled Release*, vol. 102, pp. 313-332.

- Friedlaender, G. E., Strong, D. M., Tomford, W. W., & Mankin, H. J. 1999, "Long-Term Follow-Up Of Patients With Osteochondral Allografts: A Correlation Between Immunologic Responses and Clinical Outcome", *Orthopedic Clinics of North America*, vol. 30, no. 4, pp. 583-588.

- Frutos, P., ez-Pena, E., Frutos, G., & Barrales-Rienda, J. M. 2002, "Release of gentamicin sulphate from a modified commercial bone cement. Effect of (2-hydroxyethyl methacrylate) comonomer and poly(N-vinyl-2-pyrrolidone) additive on release mechanism and kinetics", *Biomaterials*, vol. 23, no. 18, pp. 3787-3797.

- Fujimori J, Yonemochi E, Fukuoka E, & Terada K 2002, "Application of eudragit RS to thermo-sensitive drug delivery systems I. Thermo-sensitive drug release from acetaminophen matrix tablets consisting of eudragit RS/PEG 400 blend polymers", *Chem.Pharm.Bull.*, vol. 50, pp. 408-412.

- Fulmer, M. T., Ison, I. C., Hankermayer, C. R., Constantz, B. R., & Ross, J. 2002, "Measurements of the solubilities and dissolution rates of several hydroxyapatites", *Biomaterials*, vol. 23, no. 3, pp. 751-755.

- Fulmer, M. T. & Brown, P. W. 1998, "Hydrolysis of dicalcium phosphate dihydrate to hydroxyapatite", *Journal of Materials Science: Materials in Medicine*, vol. 9, no. 4, pp. 197-202.

- G.Daculsi, R.Z.LeGeros, E.Nery, K.Lynch, & B.Kerebel 2004, "Transformation of biphasic calcium phosphate ceramics *in vivo*: Ultrastructural and physicochemical characterization", *Journal of Biomedical Materials Research*, vol. 23, no. 8, pp. 883-894.

- G.Walentaa & T.Füllmannb 2004, "Advances In Quantitative Xrd Analysis For Clinker, Cements, And Cementitious Additions", *Advances in X-ray Analysis*, vol. 47, pp. 287-296.

- Gao, Y., Cui, F. d., Guan, Y., Yang, L., Wang, Y. s., & Zhang, L. n. 2006, "Preparation of roxithromycin-polymeric microspheres by the emulsion solvent diffusion method for taste masking", *International Journal of Pharmaceutics*, vol. 318, no. 1-2, pp. 62-69.

- Garcia, A. M. & Ghaly, E. S. 1996, "Preliminary spherical agglomerates of water soluble drug using natural polymer and cross-linking technique", *Journal of Controlled Release*, vol. 40, no. 3, pp. 179-186.

- Gbureck, U., Hölzel, T., Klammert, U., Würzler, K., Müller, F. A., & Barralet, J. E. 2007a, "Resorbable Dicalcium Phosphate Bone Substitutes Prepared by 3D Powder Printing", *Advanced Functional Materials*, vol. 17, no. 18, pp. 3940-3945.

- Gbureck, U., Hölzel, T., Klammert, U., Würzler, K., Müller, F. A., & Barralet, J. E. 2007b, "Resorbable Dicalcium Phosphate Bone Substitutes Prepared by 3D Powder Printing", *Advanced Functional Materials*, vol. 17, no. 18, pp. 3940-3945.

- Gbureck, U., Knappe, O., Grover, L. M., & Barralet, J. E. 2005a, "Antimicrobial potency of alkali ion substituted calcium phosphate cements", *Biomaterials*, vol. 26, no. 34, pp. 6880-6886.

- Gbureck, U., Spatz, K., Thull, R., & Barralet, J. E. 2005b, "Rheological enhancement of mechanically activated alpha-tricalcium phosphate cements", *Journal of Biomedical Materials Research Part B: Applied Biomaterials*, vol. 73B, no. 1, pp. 1-6.

- Gbureck, U., Dembski, S., Thull, R., & Barralet, J. E. 2005c, "Factors influencing calcium phosphate cement shelf-life", *Biomaterials*, vol. 26, no. 17, pp. 3691-3697.

- Gbureck, U., Grolms, O., Barralet, J. E., Grover, L. M., & Thull, R. 2003, "Mechanical activation and cement formation of beta-tricalcium phosphate", *Biomaterials*, vol. 24, no. 23, pp. 4123-4131.

- Georgiou, G. & Knowles, J. C. 2001, "Glass reinforced hydroxyapatite for hard tissue surgery--Part 1: mechanical properties", *Biomaterials*, vol. 22, no. 20, pp. 2811-2815.

- Giannoudis, P. V., Dinopoulos, H., & Tsiridis, E. 2005, "Bone substitutes: An update", *Injury*, vol. 36, no. 3, Supplement 1, p. S20-S27.

- Gielkens, P. F. M., Schortinghuis, J., de Jong, J. R., Huysmans, M. C., Leeuwen, M. B., Raghoebar, G. M., Bos, R. R. M., & Stegenga, B. 2008, "A comparison of micro-CT, microradiography and histomorphometry in bone research", *Archives of Oral Biology*, vol. 53, no. 6, pp. 558-566.

- Ginebra, M. P., Driessens, F. C. M., & Planell, J. A. 2004, "Effect of the particle size on the micro and nanostructural features of a calcium phosphate cement: a kinectic analysis", *Biomaterials*, vol. 25, no. 17, pp. 3453-3462.

- Ginebra, M. P., Traykova, T., & Planell, J. A. 2006, "Calcium phosphate cements as bone drug delivery systems: A review", *Journal of Controlled Release*, vol. 113, no. 2, pp. 102-110.

- Goldstein, S. A. 1987, "The mechanical properties of trabecular bone: Dependence on anatomic location and function", *Journal of Biomechanics*, vol. 20, no. 11-12, pp. 1055-1061.

- Gorst, N. J., Perrie, Y., Gbureck, U., Hutton, A. L., Hofmann, M. P., Grover, L. M., & Barralet, J. E. 2006, "Effects of fibre reinforcement on the mechanical properties of brushite cement", *Acta Biomater.*, vol. 2, no. 1, pp. 95-102.

- Grover, L. M. 2005, *Cold setting properties of calcium phosphate - pyrophosphoric acid - water mixtures.*, University of Birmingham, School of Dentistry.

- Grover, L. M., Gbureck, U., Wright, A. J., Tremayne, M., & Barralet, J. E. 2006, "Biologically mediated resorption of brushite cement in vitro", *Biomaterials*, vol. 27, no. 10, pp. 2178-2185.

- Grover, L. M., Gbureck, U., Wright, A. J., & Barralet, J. E. 2005a, "Cement formulations in the calcium phosphate H2O-H3PO4-H4P2O7 system", *Journal of the American Ceramic Society*, vol. 88, no. 11, pp. 3096-3103.

- Grover, L. M., Gbureck, U., Young, A. M., Wright, A. J., & Barralet, J. E. 2005b, "Temperature dependent setting kinetics and mechanical properties of beta-TCP-pyrophosphoric acid bone cement", *Journal of Materials Chemistry*, vol. 15, no. 46, pp. 4955-4962.

- Grover, L. M., Knowles, J. C., Fleming, G. J. P., & Barralet, J. E. 2003, "In vitro ageing of brushite calcium phosphate cement", *Biomaterials*, vol. 24, no. 23, pp. 4133-4141.

- Grover, L. M., Patel, S., Hu, Y., Gbureck, U., & Barralet, J. E. "Modifying Brushite Cement Degradation Using Calcium Alginate Beads", in *Biocermaics 20*, Trans Tech Publications, Switzerland, pp. 311-214.

- Grynpas, M. D., Pilliar, R. M., Kandel, R. A., Renlund, R., Filiaggi, M., & Dumitriu, M. 2002b, "Porous calcium polyphosphate scaffolds for bone substitute applications in vivo studies", *Biomaterials*, vol. 23, no. 9, pp. 2063-2070.

- Grynpas, M. D., Pilliar, R. M., Kandel, R. A., Renlund, R., Filiaggi, M., & Dumitriu, M. 2002a, "Porous calcium polyphosphate scaffolds for bone substitute applications in vivo studies", *Biomaterials*, vol. 23, no. 9, pp. 2063-2070.

- Guo, L. & Li, H. 2004, "Fabrication and characterization of thin nano-hydroxyapatite coatings on titanium", *Surface and Coatings Technology*, vol. 185, no. 2-3, pp. 268-274.

- Gupta, S., New, A. M. R., & Taylor, M. 2006, "Bone remodelling inside a cemented resurfaced femoral head", *Clinical Biomechanics*, vol. 21, no. 6, pp. 594-602.

- Gurevitch, O., Slavin, S., & Feldman, A. G. 2007, "Conversion of red bone marrow into yellow - Cause and mechanisms", *Medical Hypotheses*, vol. 69, no. 3, pp. 531-536.

- Hamcerencu, M., Desbrieres, J., Khoukh, A., Popa, M., & Riess, G. 2008, "Synthesis and characterization of new unsaturated esters of Gellan Gum", *Carbohydrate Polymers*, vol. 71, no. 1, pp. 92-100.

- Han, B., Ma, P. W., Zhang, L. L., Yin, Y. J., Yao, K. D., Zhang, F. J., Zhang, Y. D., Li, X. L., & Nie, W. 2009, "[beta]-TCP/MCPM-based premixed calcium phosphate cements", *Acta Biomaterialia*, vol. 5, no. 8, pp. 3165-3177.

- Harris, W. & Sledge, C. B. 1990, "Total hip and total knee replacement (Part II", *The New England Journal of Medicine*, vol. 323, pp. 801-807.

- Hatim, Z., Freche, M., Kheribech, A., & Lacout, J. L. 1998, "The setting mechanisms of a phosphocalcium biological cement", *Annales de Chimie Science des Materiaux*, vol. 23, no. 1-2, pp. 65-68.

- Haznedar, S. & Dortunc, B. 2004, "Preparation and in vitro evaluation of Eudragit microspheres containing acetazolamide", *International Journal of Pharmaceutics*, vol. 269, no. 1, pp. 131-140.

- Hendriks, J. G. E., van Horn, J. R., van der Mei, H. C., & Busscher, H. J. 2004, "Backgrounds of antibiotic-loaded bone cement and prosthesis-related infection", *Biomaterials*, vol. 25, no. 3, pp. 545-556.

- Hoffman, O. 1967, "The Brittle Strength of Orthotropic Materials", *Journal of Composite Materials*, vol. 1, no. 2, pp. 200-206.

- Hofmann, M. P., Mohammed, A. R., Perrie, Y., Gbureck, U., & Barralet, J. E. 2009, "High-strength resorbable brushite bone cement with controlled drug-releasing capabilities", *Acta Biomaterialia*, vol. In Press, Corrected Proof.

- Horner, J. H. 2004, "Bone structure and calcium metabolism", *Surgery (Oxford)*, vol. 22, no. 1, pp. 24a-24d.

- Horstmann, W. G., Verheyen, C. C. P. M., & Leemans, R. 2003, "An injectable calcium phosphate cement as a bone-graft substitute in the treatment of displaced lateral tibial plateau fractures", *Injury*, vol. 34, no. 2, pp. 141-144.

- Hsu, Y. S., Chang, E., & Liu, H. S. 1998, "Hydrothermally-grown monetite (CaHPO4) on hydroxyapatite", *Ceramics International*, vol. 24, no. 4, pp. 249-254.

- Hua-Jiang Huang, Xiao Dong Chen, & Wei-Kang Yuan 2006, "Microencapsulation Based on Emulsification for Producing Pharmaceutical Products - A Literature Review", *Developments in chemical engineering and material processing*, vol. 14, no. 3-4, pp. 515-544.

- Hyakuna K, Yamamuro T, Kotoura Y, Oka M, Nakamura T, Kitsugi T, Kokubo T, & Kushitani H 2007, "Surface reactions of calcium phosphate ceramics to various solutions.", *Journal of Biomedical Materials Research*, vol. 24, no. 4, pp. 471-488.

- I.R.Gibson, I.Rehman, S.M.Best, & W.Bonfield 2000, "Characterization of the transformation from calcium-deficient apatite to ß-tricalcium phosphate", *Journal of Materials Science: Materials in Medicine*, vol. 11, no. 12, pp. 799-804.

- Iooss, P., Le Ray, A.-M., Grimandi, G., Daculsi, G., & Merle, C. 2001, "A new injectable bone substitute combining poly([var epsilon]-caprolactone) microparticles with biphasic calcium phosphate granules", *Biomaterials*, vol. 22, no. 20, pp. 2785-2794.

- Ishikawa K, Takagi S, Chow LC, & Suzuki K 1999, "Reaction of calcium phosphates with different amounts of tetracalcium phosphate and dicalcium phosphate anhydrous", *Journal of Biomedical Materials Research*, vol. 46, pp. 504-510.

- Ishikawa, K. & Asaoka, K. 1995, "Estimation of ideal mechanical strength and critical porosity of calcium phosphate cement", *Journal of Biomedical Materials Research*, vol. 29, no. 12, pp. 1537-1543.

- Ishikawa, K., Miyamoto, Y., Takechi, M., Toh, T., Kon, M., Nagayama, M., & Asaoka, K. 1996, "Non-decay type fast-setting calcium phosphate cement: Hydroxyapatite putty containing an increased amount of sodium alginate", *Journal of Biomedical Materials Research Part B: Applied Biomaterials*, vol. 36, no. 3, pp. 393-399.

- Ishikawa, K., Takagi, S., Chow, L. C., & Ishikawa, Y. 1995, "Properties and mechanisms of fast-setting calcium phosphate cements", *Journal of Materials Science: Materials in Medicine*, vol. 6, no. 9, pp. 528-533.

- Ishikawa, K., Takagi, S., Chow, L. C., Ishikawa, Y., Eanes, E. D., & Asaoka, K. 1994, "Behavior of a calcium phosphate cement in simulated blood plasma in vitro", *Dental Materials*, vol. 10, no. 1, pp. 26-32.

- Itokazu, M., Wenyi, Y., Aoki, T., Ohara, A., & Kato, N. 1998, "Synthesis of antibiotic-loaded interporous hydroxyapatite blocks by vacuum method and in vitro drug release testing", *Biomaterials*, vol. 19, no. 7-9, pp. 817-819.

- J.D.Santos, P.L.Silva, J.C.Knowles, & F.J.Monteiro 1996, "Reinforcement of hydroxyapatite by adding P2O5-CaO glasses with Na2O, K2O and MgO", *Journal of Materials Science: Materials in Medicine*, vol. 7, no. 3, pp. 187-189.

- J.Fabia, Cz.Œlusarczyk, & A.Gawowski 2005, "Supermolecular structure of Alginate Fibres", *Fibres & Textiles in Eastern Europe.*, vol. 13, no. 5, pp. 114-117.

- J.L.Gilbert, J.M.Hasenwinkel, R.L.Wixson, & E.P.Lautenschlager 2000, "A theoretical and experimental analysis of polymerization shrinkage of bone cement: A potential major source of porosity", *Journal of Biomedical Materials Research*, vol. 52, no. 1, pp. 210-218.

- J.Lu, J.Dejou, G.Koubi, P.Hardouin, & J.Lemaitre 2002, "The biodegradation mechanism of calcium phosphate biomaterials in bone", *Journal of Biomedical Materials Research*, vol. 63, no. 4, pp. 408-412.

- Jain D, Panda A.K, & Majumbad D.K 2005, "Eudragit S100 entrapped insulin microspheres for iral delivery.", *AAPS Pharmaceutical Science Technology*, vol. 6, pp. 100-107.

- Jansson, P. E., Lindberg, B., & Sandford, P. A. 1983, "Structural studies of gellan gum, an extracellular polysaccharide elaborated by Pseudomonas elodea", *Carbohydrate Research*, vol. 124, no. 1, pp. 135-139.

- Jarcho, M. 1981, "Calcium-Phosphate Ceramics As Hard Tissue Prosthetics", *Clinical Orthopaedics and Related Research* no. 157, pp. 259-278.

- Ji, J., Childs, R. F., & Mehta, M. 2001, "Mathematical model for encapsulation by interfacial polymerization", *Journal of Membrane Science*, vol. 192, no. 1-2, pp. 55-70.

- Jillavenkatesa, A. & Condrate, R. A. 1998, "The Infrared and Raman Spectra of Tricalcium Phosphate", *Spectroscopy Letters: An International Journal for Rapid Communication*, vol. 31, no. 8, pp. 1619-1634.

- Johnsson, M. S. A. & Nancollas, G. H. 1992, "The Role of Brushite and Octacalcium Phosphate in Apatite Formation", *Critical Reviews in Oral Biology & Medicine*, vol. 3, no. 1, pp. 61-82.

- Jones, H. H., Priest, J. D., Hayes, W. C., Tichenor, C. C., & Nagel, D. A. 1977, "Humeral hypertrophy in response to exercise", *Journal of Bone and Joint Surgery*, vol. 59, no. 2, pp. 204-208.

- Joosten, U., Joist, A., Frebel, T., Brandt, B., Diederichs, S., & von Eiff, C. 2004, "Evaluation of an in situ setting injectable calcium phosphate as a new carrier material for gentamicin in the treatment of chronic osteomyelitis: Studies in vitro and in vivo", *Biomaterials*, vol. 25, no. 18, pp. 4287-4295.

- K.De Groot & J.G.C.Wolke 1990, *Chemistry of calcium phosphate bioceramics* CRC press, Boca Raton, FL.

- K.Ohura, M.Bohner, P.Hardouin, J.Lemaitre, G.Pasquier, & B.Flautre 1996, "Resorption of, and bone formation from, new *ß*-tricalcium phosphate–monocalcium phosphate cements: an in vivo study", *Journal of Biomedical Materials Research*, vol. 30, pp. 193-200.

- Kamerer, D. B., Hirsch, B. E., Snyderman, H., Costantino, P., & Friedman, C. D. 1994, "Hydroxyapatite cement: a new method for achieving watertight closure in transtemporal surgery.", *The American journal of otology*, vol. 15, no. 1, pp. 47-49.

- Karlinsey, R. L., Mackey, A. C., Walker, E. R., & Frederick, K. E. 2010, "Preparation, characterization and in vitro efficacy of an acid-modified [beta]-TCP material for dental hard-tissue remineralization", *Acta Biomaterialia*, vol. 6, no. 3, pp. 969-978.

- Katagiri, T. & Takahashi, N. 2002, "Regulatory mechanisms of osteoblast and osteoclast differentiation", *Oral Diseases*, vol. 8, no. 3, pp. 147-159.

- Keaveny, T. M., Morgan, E. F., Niebur, G. L., & Yeh, O. C. 2001, "Biomechanics Of Trabecular Bone", *Annual Review of Biomedical Engineering*, vol. 3, no. 1, pp. 307-333.

- Khairoun, I., Boltong, M. G., Driessens, F. C. M., & Planell, J. A. 1998, "Some factors controlling the injectability of calcium phosphate bone cements", *Journal of Materials Science: Materials in Medicine*, vol. 9, no. 8, pp. 425-428.

- Kim, B. K., Hwang S.J, Park J.B, & Park H.J 2002, "Preparation and characterization of drug-loaded polymethacrylate microspheres by an emulsion solvent evaporation method", *Journal of Microencapsulation*, vol. 19, no. 6, pp. 811-822.

- Kim, H. W., Knowles, J. C., & Kim, H. E. 2004, "Hydroxyapatite/poly([var epsilon]-caprolactone) composite coatings on hydroxyapatite porous bone scaffold for drug delivery", *Biomaterials*, vol. 25, no. 7-8, pp. 1279-1287.

- Kim, S. B., Kim, Y. J., Yoon, T. L., Park, S. A., Cho, I. H., Kim, E. J., Kim, I. A., & Shin, J. W. J. 2004, "The characteristics of a hydroxyapatite-chitosan-PMMA bone cement", *Biomaterials*, vol. 25, no. 26, pp. 5715-5723.

- Kim, Y. D., C.V.Morr, & T.W.Schenz 1996, "Microencapsulation properties of gum Arabic and several food proteins: Liquid orange oil emulsion particles.", *Journal of Agricultural and FoodChemistry*, vol. 44, no. 5, pp. 1305-1313.

- Kitsugi, T., Yamamuro, T., Nakamura, T., Kotani, S., Kokubo, T., & Takeuchi, H. 1993, "Four calcium phosphate ceramics as bone substitutes for non-weight-bearing", *Biomaterials*, vol. 14, no. 3, pp. 216-224.

- Klammert, U., Reuther, T., Jahn, C., Kraski, B., K³bler, A. C., & Gbureck, U. "Cytocompatibility of brushite and monetite cell culture scaffolds made by three-dimensional powder printing", *Acta Biomaterialia*, vol. In Press, Corrected Proof.

- Klawitter, J. J., Weinstein, A. M., & Peterson, L. J. 1977, "Fabrication and Characterization of Porous-Rooted Cobalt-Chromium-Molybdenum (Co-Cr-Mo) Alloy Dental Implants", *Journal of Dental Research*, vol. 56, no. 5, pp. 474-480.

- Kobayashi Y, T. N. 2003, "[Regulatory mechanism of bone resorption: roles of bone remodeling-regulatory cytokines 'osteokines' in osteoclast differentiation and function]", *Nippon Rinsho*, vol. 61, no. 2, pp. 200-206.

- Kodama, Y., Dimai, H. P., Wergedal, J., Sheng, M., Malpe, R., Kutilek, S., Beamer, W., Donahue, L. R., Rosen, C., Baylink, D. J., & Farley, J. 1999, "Cortical tibial bone volume

in two strains of mice: effects of sciatic neurectomy and genetic regulation of bone response to mechanical loading", *Bone*, vol. 25, no. 2, pp. 183-190.

- Kohri, M., Miki, K., Waite, D. E., Nakajima, H., & Okabe, T. 1993a, "In vitro stability of biphasic calcium phosphate ceramics", *Biomaterials*, vol. 14, no. 4, pp. 299-304.

- Kohri, M., Miki, K., Waite, D. E., Nakajima, H., & Okabe, T. 1993b, "In vitro stability of biphasic calcium phosphate ceramics", *Biomaterials*, vol. 14, no. 4, pp. 299-304.

- Korkusuz F, Uchida A, Shinto Y, Araki N, Inoue K, & Ono K. Experimental implant-related osteomyelitis treated by antibiotic-calcium hydroxyapatite ceramic composites. Journal of Bone and Joint Surgery 75B[111], 114. 1993.

- Kozloff, K. M., Quinti, L., Patntirapong, S., Hauschka, P. V., Tung, C. H., Weissleder, R., & Mahmood, U. 2009, "Non-invasive optical detection of cathepsin K-mediated fluorescence reveals osteoclast activity in vitro and in vivo", *Bone*, vol. 44, no. 2, pp. 190-198.

- Kurashina, K., Kurita, H., Hirano, M., Kotani, A., Klein, C. P. A. T., & de Groot, K. 1997, "In vivo study of calcium phosphate cements: implantation of an [alpha]-tricalcium phosphate/dicalcium phosphate dibasic/tetracalcium phosphate monoxide cement paste", *Biomaterials*, vol. 18, no. 7, pp. 539-543.

- L.L.Hench 1991, "Bioceramics: From Concept to Clinic", *Journal of American ceramics societty*, vol. 74, no. 7, pp. 1487-1510.

- L.L.Hench. Bioceramics. Journal of the American Ceramic Society 81[7], 1705-1727. 1998a.

- L.L.Hench 1998b, "Biomaterials: a forecast for the future", *Biomaterials*, vol. 19, no. 16, pp. 1419-1423.

- L.L.Hench & J.Wilson 1993, *An introduction to bioceramics* Singapore.

- Lee, A. J. C., Vangala, S., & Ling, R. S. M. 1976, "Fracture Of Acrylic Bone Cement", *The Lancet*, vol. 308, no. 7995, pp. 1142-1143.

- Lee, K., Jessop, H., Suswillo, R., Zaman, G., & Lanyon, L. 2003, "Endocrinology: Bone adaptation requires oestrogen receptor-[alpha]", *Nature*, vol. 424, no. 6947, p. 389.

- Legeros, R. Z. 1993, "Biodegradation and bioresorption of calcium phosphate ceramics", *Clinical Materials*, vol. 14, no. 1, pp. 65-88.

- Legeros, R. Z. 1988, "Calcium Phosphate Materials in Restorative Dentistry: a Review", *Advances in Dental Research*, vol. 2, no. 1, pp. 164-180.

- LeGeros, R. Z. 2002, "Properties of Osteoconductive Biomaterials: Calcium Phosphates", *Clinical Orthopaedics and Related Research*, vol. 395.

- Lemaitre J, Mirtchi AA, & Mortier A 1987, "Calcium phosphate cement for medical use: state of the art and perspectives of development.", *Silicates Industriels*, vol. 10, pp. 141-146.

- Lew, D. P. & Waldvogel, F. A. 2004a, "Osteomyelitis", *Lancet*, vol. 364, no. 9431, pp. 369-379.

- Lew, P. D. & Waldvogel, P. F. 2004b, "Osteomyelitis", *The Lancet*, vol. 364, no. 9431, pp. 369-379.

- Lewandrowski, K. U., Gresser, D., Wise, D. L., & Trantolo, D. J. 2000, "Bioresorbable bone graft substitutes of different osteoconductivities: a histologic evaluation of osteointegration of poly(propylene glycol-co-fumaric acid)-based cement implants in rats", *Biomaterials*, vol. 21, no. 8, pp. 757-764.

- Lewis, G. 2006, "Injectable bone cements for use in vertebroplasty and kyphoplasty: State-of-the-art review", *Journal of Biomedical Materials Research Part B: Applied Biomaterials*, vol. 76B, no. 2, pp. 456-468.

- Li, D. 2005, *Microencapsulation of proteins with Eudragit S100 polymer,* The University of Adelaide.

- Li, Q., Dunn, E. T., Grandmaison, E. W., & Goosen, M. F. A. 1992, "Applications and Properties of Chitosan", *Journal of Bioactive and Compatible Polymers*, vol. 7, no. 4, pp. 370-397.

- Li, Y., Weng, W., & Tam, K. C. 2007, "Novel highly biodegradable biphasic tricalcium phosphates composed of [alpha]-tricalcium phosphate and [beta]-tricalcium phosphate", *Acta Biomaterialia*, vol. 3, no. 2, pp. 251-254.

- Lide, D. R. 1994, *CRC Handbook of Data on Organic Compounds*, 3rd edn, CRC Press, Boca Raton, FL.

- Lilley, K. J., Gbureck, U., Wright, A. J., Farrar, D. F., & Barralet, J. E. 2005, "Cement from nanocrystalline hydroxyapatite: Effect of calcium phosphate ratio", *Journal of Materials Science-Materials in Medicine*, vol. 16, no. 12, pp. 1185-1190.

- Link, D. P., vad den Dolder, J., Jurgens, W., Wolke, J. G. C., & Jansen, J. A. 2006, "Mechanical evaluation of implanted calcium phosohate cements incorporated with PLGA microparticles", *Biomaterials*, vol. 27, no. 27, pp. 4941-4947.

- Liou, S. C. & Chen, S. Y. 2002, "Transformation mechanism of different chemically precipitated apatitic precursors into [beta]-tricalcium phosphate upon calcination", *Biomaterials*, vol. 23, no. 23, pp. 4541-4547.

- Liu, C. H. A. N. & Shen, W. E. I. 1997, "Effect of crystal seeding on the hydration of calcium phosphate cement", *Journal of Materials Science: Materials in Medicine*, vol. 8, no. 12, pp. 803-807.

- Liu, F., Malaval, L., & Aubin, J. E. 2003, "Global amplification polymerase chain reaction reveals novel transitional stages during osteoprogenitor differentiation", *Journal of Cell Science*, vol. 116, no. 9, pp. 1787-1796.

- Logeart-Avramoglou, D., Anagnostou, F., Bizios, R., & Petite, H. 2005, "Engineering bone: Challenges and obstacles", *Journal of Cellular and Molecular Medicine*, vol. 9, no. 1, pp. 72-84.

- Louati, B., Hlel, F., Guidara, K., & Gargouri, M. 2005, "Analysis of the effects of thermal treatments on CaHPO4 by 31P NMR spectroscopy", *Journal of Alloys and Compounds*, vol. 394, no. 1-2, pp. 13-18.

- M.A.K.Liebschner & M.A.Wettergreen 2003, "Optimization of Bone Scaffold Engineering for Load Bearing Applications," in *39*, II Bone edn, N.Ashammakhi & P.Ferretti, eds., p. -1.

- M.A.Lopes, J.D.Santos, F.J.Monteiro, & J.C.Knowles 1998, "Glass-reinforced hydroxyapatite: A comprehensive study of the effect of glass composition on the crystallography of the composite", *Journal of Biomedical Materials Research*, vol. 39, no. 2, pp. 244-251.

- M.Hamadouche & L.Sedel 2000, "Ceramics in Orthopaedics", *Journal of Bone and Joint Surgery (Br)*, vol. 82(B), no. 8, pp. 1095-1099.

- M.Nilsson, E.Fernandez, S.Sarda, L.Lidgren, & J.A.Planell 2002, "Characterization of a novel calcium phosphate/sulphate bone cement", *Journal of Biomedical Materials Research*, vol. 61, no. 4, pp. 600-607.

- M.Otsuka, Y.Matsuda, Z.Wang, J.L.Fox, & W.I.Higuchi 1997, "Effect of sodium bicarbonate amount on in vitro indomethacin release from self-setting carbonated-apatite cement", *Pharmaceutical Research*, vol. 14, no. 4, pp. 444-449.

- M.Takechi, Y.Miyamoto, K.Ishikawa, M.Nagayama, K.Asaoka, & K.Suzuki 1998, "Effects of added antibiotics on the basic properties of anti-washout-type fast-setting calcium phosphate cement", *Journal of Biomedical Materials Research*, vol. 39, no. 2, pp. 308-316.

- Ma, M. G., Zhu, Y. J., & Chang, J. 2006, "Monetite Formed in Mixed Solvents of Water and Ethylene Glycol and Its Transformation to Hydroxyapatite", *The Journal of Physical Chemistry B*, vol. 110, no. 29, pp. 14226-14230.

- MacArtain, P., Jacquier, J. C., & Dawson, K. A. 2003, "Physical characteristics of calcium induced [kappa]- carrageenan networks", *Carbohydrate Polymers*, vol. 53, no. 4, pp. 395-400.

- Mangione, M. R., Giacomazza, D., Bulone, D., Martorana, V., Cavallaro, G., & San Biagio, P. L. 2005, "K+ and Na+ effects on the gelation properties of [kappa]-Carrageenan", *Biophysical Chemistry*, vol. 113, no. 2, pp. 129-135.

- Marino, F. T., Torres, J., Hamdan, M., Rodriguez, C. R., & Lopez-Cabarcos, E. 2007, "Advantages of using glycolic acid as a retardant in a brushite forming cement", *Journal of Biomedical Materials Research Part B: Applied Biomaterials*, vol. 83B, no. 2, pp. 571-579.

- Marino, F. T., Torres, J., Tresguerres, I., Clemente, C., Lopez-Cabarcos, E., & Blanco, L. 2006, "Bone augmentation in rabbit calvariae: comparative study between Bio-Oss® and a novel ß-TCP/DCPD granulate", *Journal of Clincial Periodontology*, vol. 33, no. 12, pp. 922-928.

- McGraw-Hill 2009, *McGraw-Hill Encyclopedia of Science and Technology*, 5th edn, The McGraw-Hill Companies, Inc..

- Mendez, J. A., Fernandez, M., Gonzalez-Corchon, A., Salvado, M., Collia, F., de Pedro, J. A., Levenfeld, B. L., Lopez-Bravo, A., Vazquez, B., & San Roman, J. 2004, "Injectable self-curing bioactive acrylic-glass composites charged with specific anti-inflammatory/analgesic agent", *Biomaterials*, vol. 25, no. 12, pp. 2381-2392.

- Mi, F. L. 1999, "Porous chitosan microsphere for controlling the antigen release of Newcastle disease vaccine: preparation **of** antigen-adsorbed microsphere and in vitro release.", *Biomaterials*, vol. 20, no. 17, pp. 1603-1612.

- Mi, F. L., Sung, H. W., & Shyu, S. S. 2009, "Release of indomethacinfrom a novel chitosan microsphere prepared by naturally occurring crosslinker: examination of crosslinking and polycation-anionic drug interaction", *Journal of Applied Polymer Science*, vol. 81, pp. 1700-1711.

- Mirtchi, A., Lemaitre, J., & Hunting, E. 1989, "Calcium phosphate cements: action of setting regulators on the properties of the [beta]-tricalcium phosphate-monocalcium phosphate cements", *Biomaterials*, vol. 10, no. 9, pp. 634-638.

- Miyai, T., Ito, A., Tamazawa, G., Matsuno, T., Sogo, Y., Nakamura, C., Yamazaki, A., & Satoh, T. 2008, "Antibiotic-loaded poly-[epsilon]-caprolactone and porous [beta]-tricalcium phosphate composite for treating osteomyelitis", *Biomaterials*, vol. 29, no. 3, pp. 350-358.

- Miyamoto Y, Ishikawa K, Takechi M, Toh T, Yuasa T, Nagayama M, & Suzuki K 1999, "Histological and compositional evaluations of three types of calcium phosphate cements when implanted in subcutaneous tissue immediately after mixing", *Journal of Biomedical Materials Research*, vol. 48, pp. 36-42.

- Miyazawa, K. 2000, "Preparation of a new soft capsule for cosmetics", *Journal of Cosmetic Science*, vol. 51, no. 4, pp. 239-252.

- Moghimi, S. M. 1995, "Exploiting bone marrow microvascular structure for drug delivery and future therapies", *Advanced Drug Delivery Reviews*, vol. 17, no. 1, pp. 61-73.

- Moojen, D. J., Spijkers, S. N. M., Schot, C. S., Nijhof, M. W., Vogely, H. C., Fleer, A., Verbout, A. J., Castelein, R. M., Dhert, W. J. A., & Schouls, L. M. 2007, "Identification of Orthopaedic Infections Using Broad-Range Polymerase Chain Reaction and Reverse Line Blot Hybridization", *Journal of Bone and Joint Surgery*, vol. 89, no. 6, pp. 1298-1305.

- Munting, E., Mirtchi, A. A., & Lemaitre, J. 1993, "Bone repair of defects filled with a phosphocalcic hydraulic cement: an in vivo study", *Journal of Materials Science: Materials in Medicine*, vol. 4, no. 3, pp. 337-344.

- Muralithran, G. & Ramesh, S. 2000, "The effects of sintering temperature on the properties of hydroxyapatite", *Ceramics International*, vol. 26, no. 2, pp. 221-230.

- Murray, K. L., Seaton, N. A., & Day, M. A. 1999, "Use of Mercury Intrusion Data, Combined with Nitrogen Adsorption Measurements, as a Probe of Pore Network Connectivity", *Langmuir*, vol. 15, no. 23, pp. 8155-8160.

- Naomi Nishimura, Yasushi Taguchi, Takao Yamamuro, Takashi Nakamura, Tadashi Kokubo, & Satoru Yoshihara 1993, "A study of the bioactive bone cement-bone interface: Quantitative and histological evaluation", *Journal of Applied Biomaterials*, vol. 4, no. 1, pp. 29-38.

- Natali, A. N. & Meroi, E. A. 1989, "A review of the biomechanical properties of bone as a material", *Journal of Biomedical Engineering*, vol. 11, no. 4, pp. 266-276.

- National Organic Standards Board Technical Advisory Panel Review 2002, *Hydroxypropyl Methylcellulose*.

- Nelson, D. G. A. 1981, "The Influence of Carbonate on the Atomic Structure and Reactivity of Hydroxyapatite", *Journal of Dental Research*, vol. 60, no. 3_suppl, pp. 1621-1629.

- Neut, D., van de Belt, H., Stokroos, I., van Horn, J. R., van der Mei, H. C., & Busscher, H. J. 2001, "Biomaterial-associated infection of gentamicin-loaded PMMA beads in orthopaedic revision surgery", *Journal of Antimicrobial Chemotherapy*, vol. 47, no. 6, pp. 885-891.

- Normand, V., Lootens, D. L., Amici, E., Plucknett, K. P., & Aymard, P. 2000, "New Insight into Agarose Gel Mechanical Properties", *Biomacromolecules*, vol. 1, no. 4, pp. 730-738.

- O'Flaherty & Ellen J. 2000, "Modeling Normal Aging Bone Loss, with Consideration of Bone Loss in Osteoporosis", *Toxicological Sciences*, vol. 55, no. 1, pp. 171-188.

- Okazaki, M. & Sato, M. 1990, "Computer graphics of hydroxyapatite and [beta]-tricalcium phosphate", *Biomaterials*, vol. 11, no. 8, pp. 573-578.

- Okochi, H. & Nakano, M. 2000, "Preparation and evaluation of w/o/w type emulsions containing vancomycin", *Advanced Drug Delivery Reviews*, vol. 45, no. 1, pp. 5-26.

- Oth, M. P. & Moδs, A. J. 1989, "Sustained release solid dispersions of indomethacin with Eudragit RS and RL", *International Journal of Pharmaceutics*, vol. 55, no. 2-3, pp. 157-164.

- Otsuka, M., Matsuda, Y., Suwa, Y., Fox, J. L., & Higuchi, W. I. 1995, "Effect of particle size of metastable calcium phosphates on mechanical strength of a novel self-setting bioactive calcium phosphate cement", *Journal of Biomedical Materials Research*, vol. 29, no. 1, pp. 25-32.

- Pandey, R. & Khuller, G. K. 2004, "Chemotherapeutic potential of alginate-chitosan microspheres as anti-tubercular drug carriers", *Journal of Antimicrobial Chemotherapy*, vol. 53, no. 4, pp. 635-640.

- Parkinson, C. R. & Sasov, A. 2008, "High-resolution non-destructive 3D interrogation of dentin using X-ray nanotomography", *Dental Materials*, vol. 24, no. 6, pp. 773-777.

- Paul, F., Morin, A., & Monsan, P. 1986, "Microbial polysaccharides with actual potential industrial applications", *Biotechnology Advances*, vol. 4, no. 2, pp. 245-259.

- Peih-Jeng Jiang, Sarika Patel, Uwe Gbureck, & Liam M Grover "A comparison of the efficacy of hydroxyapatite based cements and gels as drug delivery matrices", in *Bioceramics 20*, pp. 327-330.

- Penel, G., Leroy, N., Van Landuyt, P., Flautre, B., Hardouin, P., Lemaεtre, J., & Leroy, G. 1999, "Raman microspectrometry studies of brushite cement: in vivo evolution in a sheep model", *Bone*, vol. 25, no. 2, Supplement 1, pp. 81S-84S.

- Penner, M. J., Masri, B. A., & Duncan, C. P. 1996, "Elution characteristics of vancomycin and tobramycin combined in acrylic bone--cement", *The Journal of Arthroplasty*, vol. 11, no. 8, pp. 939-944.

- Peter Patka, Henk J.Th.M.Haarman, & Maarten van der Elst 1995, "Bone substitution and bone repair in trauma surgery," in *Encyclopedic handbook of biomaterials and bioengineering*, 2 edn, Donald L Wise, ed., Marcel Dekker, New York, pp. 639-664.

- Petrakis, N. L. 1966, "Some physiological and developmental considerations of the temperature-gradient hypothesis of bone marrow distribution", *American Journal of Physical Anthropology*, vol. 25, no. 2, pp. 119-129.

- Pe´ter Sipos, Ildiko´ Cso´ka, Stane Src¡ic¡, Kla´ra Pintye-Ho´ di, & Istva´n Er+os 2005, "Influence of preparation conditions on the properties of Eudragit microspheres produced by a double emulsion method", *Drug Development Research*, vol. 64, no. 41, p. 54.

- Pflugrath J.W 1999, "The finer things in X-ray diffraction data collection", *Acta Crystallographica*, vol. D55, pp. 1718-1725.

- Pitto, R. P. & Spika, I. A. 2004, "Antibiotic-loaded bone cement spacers in two-stage management of infected total knee arthroplasty", *Int Orthop*, vol. 28, no. 3, pp. 129-133.

- Poncelet, D. 1999, "A physico-chemical approach to production of alginate beads by emulsffication-internal ionotropic gelation.", *Colloids and Surfaces a-Physicochernical andEngineering Aspects*, vol. 155, no. 2-3, pp. 171-176.

- Pornsak Sriamornsak & Srisagul Sungthongjeen 2007, "Modification of Theophylline Release With Alginate Gel Formed in Hard Capsules", *AAPS Pharmaceutical Science Technology*, vol. 8, no. 3, p. E1-E8.

- Portsmouth, R. L. & Gladden, L. F. 1991, "Determination of pore connectivity by mercury porosimetry", *Chemical Engineering Science*, vol. 46, no. 12, pp. 3023-3036.

- Prado Da Silva, M. H., Lima, J. H. C., Soares, G. A., Elias, C. N., de Andrade, M. C., Best, S. M., & Gibson, I. R. 2001, "Transformation of monetite to hydroxyapatite in bioactive coatings on titanium", *Surface and Coatings Technology*, vol. 137, no. 2-3, pp. 270-276.

- Pusateri, A. E., McCarthy, S. J., Gregory, K. W., Harris, R. A., Cardenas, L., McManus, A. T., & Goodwin, C. W. J. 2003, "Effect of a Chitosan-Based Hemostatic Dressing on Blood Loss and Survival in a Model of Severe Venous Hemorrhage and Hepatic Injury in Swine", *The Journal of Trauma*, vol. 54, no. 1.

- R.A.Young, P.E.Mackie, & R.B.von Dreele 1977, "Application of the pattern-fitting structure-refinement method of X-ray powder diffractometer patterns", *Journal of Applied Crystallography*, vol. 10, no. 4, pp. 262-269.

- R.E.Fraser, T.C.Laurent, & U.B.G.Laurent 2003, "Hyaluronan: its nature, distribution, functions and turnover", *Journal of Internal Medicine*, vol. 242, no. 1, pp. 27-33.

- R.P Dickenson, W.C Hutton, & J.R.R Stotf 1981, "Mechanical Properties of Bone in Osteoporosis", *The Journal Of Bone And Joint Surgery*, vol. 63 - B, no. 2, pp. 233-238.

- Raisz, L. G. 2005, "Pathogenesis of osteoporosis: concepts, conflicts, and prospects", *The Journal of Clinical Investigation*, vol. 115, no. 12, pp. 3318-3325.

- Ramakrishna, S., Mayer, J., Wintermantel, E., & Leong, K. W. 2001, "Biomedical applications of polymer-composite materials: a review", *Composites Science and Technology*, vol. 61, no. 9, pp. 1189-1224.

- Ramay, H. R. R. & Zhang, M. 2004, "Biphasic calcium phosphate nanocomposite porous scaffolds for load-bearing bone tissue engineering", *Biomaterials*, vol. 25, no. 21, pp. 5171-5180.

- Ratier, A., Gibson, I. R., Best, S. M., Freche, M., Lacout, J. L., & Rodriguez, F. 2001, "Setting characteristics and mechanical behaviour of a calcium phosphate bone cement containing tetracycline", *Biomaterials*, vol. 22, no. 9, pp. 897-901.

- Regsegger, P. & Laib, A. 1998, "Microstructural analysis of bone using 3D micro computed tomography in vitro and in vivo", *Journal of Biomechanics*, vol. 31, no. Supplement 1, p. 182.

- Rey C & Freche M 1991, *Apatite chemistry in biomaterial preparation, shaping and biological behaviour*, Bioceramics edn, Butterworth Heinemann, London.

- Rho, J. Y., Hobatho, M. C., & Ashman, R. B. 1995, "Relations of mechanical properties to density and CT numbers in human bone", *Medical Engineering & Physics*, vol. 17, no. 5, pp. 347-355.

- Rho, J.-Y., Kuhn-Spearing, L., & Zioupos, P. 1998, "Mechanical properties and the hierarchical structure of bone", *Medical Engineering & Physics*, vol. 20, no. 2, pp. 92-102.

- Rico, H. 1997, "The Therapy of Osteoporosis and the Importance of Cortical Bone", *Calcified Tissue International*, vol. 61, no. 6, pp. 431-432.

- Rietveld, H. M. 1969, "A profile refinement method for nuclear and magnetic structures", *Journal of Applied Crystallography*, vol. 2, pp. 65-71.

- Ripamonti, U. 1996, "Osteoinduction in porous hydroxyapatite implanted in heterotopic sites of different animal models", *Biomaterials*, vol. 17, no. 1, pp. 31-35.

- Robert J.Majeska 2001, "Cell Biology of Bone," in *Bone Biomechanics Handbook*, 2nd edn, Stephen Corteen Cowin, ed., pp. 2-1-2-24.

- Rohm Pharma. Rohm Pharma Booklet: Regulatory information. Rohm Pharma Polymers 2003. Germany, Rohm Pharma.

- Roques, A., Browne, M., Taylor, A., New, A., & Baker, D. 2004, "Quantitative measurement of the stresses induced during polymerisation of bone cement", *Biomaterials*, vol. 25, no. 18, pp. 4415-4424.

- Rose, L. & Rosenberg, E. 2001, "Bone grafts and growth and differentiation factors for regenerative therapy: a review", *Practical Procedures & Aesthetic Dentistry*, vol. 13, no. 9, pp. 725-734.

- Roy V.Talmage, Stephen A.Grubb, Hirotashi Norimatsu, & Carole J.VanderWiel 1980, "Evidence for an important physiological role for calcitonin", *Proceedings of the National Academy of Sciences*, vol. 77, no. 1, pp. 609-613.

- Ruan, G., Feng, S. S., & Li, Q. T. 2002, "Effects of material hydrophobicity on physical properties of polymeric microspheres formed by double emulsion process", *Journal of Controlled Release*, vol. 84, no. 3, pp. 151-160.

- Ruchholtz, S., Tager, G., & Nast-Kolb, D. 2004, "The periprosthetic total hip infection", *Unfallchirurg*, vol. 107, no. 4, pp. 307-317.

- Russell T.Turner & Jean D.Sibonga 2009, *Effects of Alcohol Use and Estrogen on Bone* .

- Ryshkewitch, E. 1953, "Compression Strength of Porous Sintered Alumina and Zirconia 9. to Ceramography", *Journal of the American Ceramic Society*, vol. 36, no. 2, pp. 65-68.

- S Gitelis & G.T.Brebach 2002, "The treatment of chronic osteomyelitis with a biodegradable antibiotic-impregnated implant", *Journal of Orthopaedic Surgery*, vol. 10, no. 1, pp. 53-60.

- S.J.Kalita, S.Bose, H.L.Hosick, & A.Bandyopadhyay 2002, "Porous Calcium Aluminate Ceramics for Bone-Graft Applications", *Journal of Materials Research*, vol. 17, no. 12, pp. 3042-3049.

- S.Mohsin, F.J.O'Brien, & T.C.Lee 2006, "Osteonal crack barriers in ovine compact bone", *Journal of Anatomy*, vol. 208, pp. 81-89.

- S.Rousseau, J.Lemaitre, M.Bohner, & C.Frei "Long-term aging of Brushite cements in physiological conditions: an in vitro study.", p. 83.

- S.Rousseau, M.Buehler, L.Jordi, & J.Lemaître "Influence Of Magnesium On The Working Characteristics Of Brushite Cements", p. 26.

- S.Takagi, L.C.Chow, S.Hirayama, & A.Sugawara 2003, "Premixed calcium-phosphate cement pastes", *Journal of Biomedical Materials Research Part B: Applied Biomaterials*, vol. 67B, no. 2, pp. 689-696.

- Salgalo, A. J., Coutinho, O. P., & Reis, R. L. 2004, "Bone tissue engineering: state of the art Bioscience", *Macromolecular Bioscience*, vol. 4, no. 8, pp. 743-765.

- Schimandle, J. H. & Boden, S. D. 1997a, "Bone substitutes for lumbar fusion:present and future", *Operative Techniques in Orthopaedics*, vol. 7, no. 1, pp. 60-67.

- Schimandle, J. H. & Boden, S. D. 1997b, "Bone substitutes for lumbar fusion:present and future", *Operative Techniques in Orthopaedics*, vol. 7, no. 1, pp. 60-67.

- Schnieders, J., Gbureck, U., Thull, R., & Kissel, T. 2006, "Controlled release of gentamicin from calcium phosphate--poly(lactic acid-co-glycolic acid) composite bone cement", *Biomaterials*, vol. 27, no. 23, pp. 4239-4249.

- Seal, B. L., Otero, T. C., & Panitch, A. 2001, "Polymeric biomaterials for tissue and organ regeneration", *Materials Science and Engineering: R: Reports*, vol. 34, no. 4-5, pp. 147-230.

- Seeman, E. 2008, "Structural basis of growth-related gain and age-related loss of bone strength", *Rheumatology*, vol. 47, p. iv2-iv8.

- Serge Pérez, Milou Kouwijzer, Karim Mazeau, & Søren Balling Engelsen. Modeling Polysaccharides: Present Status & Challenges. 2009.

- Serraj, S., Micha+»lesco, P., Margerit, J., Bernard, B., & Boudeville, P. 2002, "Study of a hydraulic calcium phosphate cement for dental applications", *Journal of Materials Science: Materials in Medicine*, vol. 13, no. 1, pp. 125-131.

- Shellis, R. P. & Wilson, R. M. 2004, "Apparent solubility distributions of hydroxyapatite and enamel apatite", *Journal of Colloid and Interface Science*, vol. 278, no. 2, pp. 325-332.

- Shinsako, K., Okui, Y., Matsuda, Y., Kunimasa, J., & Otsuka, M. 2008, "Effects of bead size and polymerization in PMMA bone cement on vancomycin release", *Bio-Medical Materials and Engineering*, vol. 18, no. 6, pp. 377-385.

- Sikavitsas, V. I., Temenoff, J. S., & Mikos, A. G. 2001, "Biomaterials and bone mechanotransduction", *Biomaterials*, vol. 22, no. 19, pp. 2581-2593.

- Singh, M. & D.O'Hagan 1998, "The preparation and characterization of polymeric antigen delivery systems for oral administration.", *Advanced Drug Delivery Reviews*, vol. 34, no. 2-3, pp. 285-304.

- Sloan, G. M. 2000, "Posterior Pharyngeal Flap and Sphincter Pharyngoplasty: The State of the Art", *The Cleft Palate-Craniofacial Journal*, vol. 37, no. 2, pp. 112-122.

- Sommerfeldt, Sommerfeldt, D., Rubin, & Rubin, C. 2001, "Biology of bone and how it orchestrates the form and function of the skeleton", *European Spine Journal*, vol. 10, no. 0, p. S86-S95.

- Soriano, I. & Evora, C. 2000, "Formulation of calcium phosphates/poly (d,l-lactide) blends containing gentamicin for bone implantation", *Journal of Controlled Release*, vol. 68, no. 1, pp. 121-134.

- Spivak, J. & Hasharoni, A. 2001, "Use of hydroxyapatite in spine surgery", *European Spine Journal*, vol. 10, no. 0, p. S197-S204.

- Stanton, D. C., Chou, J. C., & Carrasco, L. R. 2004, "Injectable calcium-phosphate bone cement (Norian) for reconstruction of a large mandibular defect: a case report", *Journal of Oral and Maxillofacial Surgery*, vol. 62, no. 2, pp. 235-240.

- Stephen W Hughes 2006, "Measuring liquid density using Archimedes' principle", *Physics Education*, vol. 41, no. 5, pp. 445-447.

- Strube, P., Sentuerk, U., Riha, T., Kaspar, K., Mueller, M., Kasper, G., Matziolis, G., Duda, G. N., & Perka, C. 2008, "Influence of age and mechanical stability on bone defect healing: Age reverses mechanical effects", *Bone*, vol. 42, no. 4, pp. 758-764.

- Sugawara, S., T.Imai, & M.Otagiri 1994, "The controlled release ofprednisolone using alginate gel.", *Pharmaceutical Research* pp. 272-277.

- Supatra Jinawath, Dujreutai Pongkao, Wojciech Suchanek, & Masahiro Yoshimura 2001, "Hydrothermal synthesis of monetite and hydroxyapatite from monocalcium phosphate monohydrate", *International Journal of Inorganic Materials*, vol. 3, no. 7, pp. 997-1001.

- Sven Kurbel, Radivoje Radic, Željko Kotromanovic, Željka Pušeljic, & Boris Kratofil 2003, "A calcium homeostasis model: orchestration of fast acting PTH and calcitonin with slow calcitriol", *Medical Hypotheses*, vol. 61, no. 3, pp. 346-350.

- T.Parker Vail & James R.Urbaniak 1996, "Donor-Site Morbidity with Use of Vascularized Autogenous Fibular Grafts", *Journal of Bone and Joint Surgery*, vol. 78, no. 2, pp. 204-211.

- Tamber H, Johansen P, Merkle H.P, & Gander B 2005, "Formulation aspects of biodegradable polymetric microspheres for antigen delivery.", *Advanced Drug Delivery Reviews*, vol. 57, pp. 357-376.

- Taniwaki, Y., Takemasa, R., Tani, T., Mizobuchi, H., & Yamamoto, H. 2003, "Enhancement of pedicle screw stability using calcium phosphate cement in osteoporotic vertebrae: in vivo biomechanical study", *Journal of Orthopaedic Science*, vol. 8, no. 3, pp. 408-414.

- TenHuisen, K. S. & Brown, P. W. 1998, "Formation of calcium-deficient hydroxyapatite from [alpha]-tricalcium phosphate", *Biomaterials*, vol. 19, no. 23, pp. 2209-2217.

- Theiss, F., Apelt, D., Brand, B., Kutter, A., Zlinszky, K., Bohner, M., Matter, S., Frei, C., Auer, J. A., & von Rechenberg, B. 2005, "Biocompatibility and resorption of a brushite calcium phosphate cement", *Biomaterials*, vol. 26, no. 21, pp. 4383-4394.

- Timothy McTighe, Lorence W.Trick, & James B.Koeneman 1995, "Design Considerations for Cementless Total Hip Arthroplasty," in *Encyclopedic Handbook of Biomaterials and Bioengineering.*, 2 edn, Donald Lee Wise, ed., Marcel Dekker, New York, pp. 3-42.

- Tiourina, O. P. & G.B.Sukhorukov 2002, "Multilayer alginate/protamine microsized capsules: encapsulation of alpha-chymotrypsin and controlled release stdy.", *International Journal ofPharmaceutics*, vol. 242, no. 1-2, pp. 155-161.

- Tofighi, A., Mounic, S., Chakravarthy, P., Rey, C., & Lee, D. 2001, "Setting Reactions Involved in Injectable Cements Based on Amorphous Calcium Phosphate", *Key Engineering Marerials*, vol. Bioceramics 13, pp. 769-772.

- Toshifumi Sugama, Marita Allan, & Janet M.Hill 1992, "Calcium Phosphate Cements Prepared by Acid-Base Reaction", *Journal of the American Ceramic Society*, vol. 75, no. 8, p. 2076.

- Tuan, H. S. & Hutmacher, D. W. 2005, "Application of micro CT and computation modeling in bone tissue engineering", *Computer-Aided Design*, vol. 37, no. 11, pp. 1151-1161.

- Turner, A. S. 2002, "The Sheep as a Model for Osteoporosis in Humans", *The Veterinary Journal*, vol. 163, no. 3, pp. 232-239.

- Vaananen, H. K. 1996, "Biology of bone growth and development", *Bone*, vol. 18, no. 1, Supplement 1, p. S103.

- Vaananen, H. K., Zhao, H., Mulari, M., & Halleen, J. M. 2000, "The cell biology of osteoclast function", *Journal of Cell Science*, vol. 113, no. 3, pp. 377-381.

- Vaccaro, A. R., Chiba, K., Heller, J. G., Patel, T. C., Thalgott, J. S., Truumees, E., Fischgrund, J. S., Craig, M. R., Berta, S. C., & Wang, J. C. 2005, "Bone grafting alternatives in spinal surgery, , , , ,", *The Spine Journal*, vol. 2, no. 3, pp. 206-215.

- Van den Vreken, N. M. F., Pieters, I. Y., Declercq, H. A., Cornelissen, M. J., & Verbeeck, R. 2010, "Characterization of calcium phosphate cements modified by addition of amorphous calcium phosphate", *Acta Biomaterialia*, vol. 6, no. 2, pp. 617-625.

- van der Graaf, S., Schroδn, C. G. P. H., & Boom, R. M. 2005, "Preparation of double emulsions by membrane emulsification--a review", *Journal of Membrane Science*, vol. 251, no. 1-2, pp. 7-15.

- van der Linden, J. C., Birkenhager-Frenkel, D. H., Verhaar, J. A. N., & Weinans, H. 2001, "Trabecular bone's mechanical properties are affected by its non-uniform mineral distribution", *Journal of Biomechanics*, vol. 34, no. 12, pp. 1573-1580.

- van Eijden, T. M. 2000, "Biomechanics of the Mandible", *Critical Reviews in Oral Biology & Medicine*, vol. 11, no. 1, pp. 123-136.

- Vandelli, M. A., Romagnoli, M., Monti, A., Gozzi, M., Guerra, P., Rivasi, F., & Forni, F. 2004a, "Microwave-treated gelatin microspheres as drug delivery system", *Journal of Controlled Release*, vol. 96, no. 1, pp. 67-84.

- Vaughan, E. D. 1996, "The maxillofacial surgeon and cranial base surgery", *British Journal of Oral and Maxillofacial Surgery*, vol. 34, no. 1, pp. 4-17.

- Vereecke, G. & Lemaitre, J. 1990, "Calculation of the solubility diagrams in the system Ca(OH)2-H3PO4-KOH-HNO3-CO2-H2O", *Journal of Crystal Growth*, vol. 104, no. 4, pp. 820-832.

- W.G.Billottee 2002, *Ceramic Materials in "Biomaterials: Principles and Applications* CRC Press, Boca Raton, FL.

- Wachter, N. J., Krischak, G. D., Mentzel, M., Sarkar, M. R., Ebinger, T., Kinzl, L., Claes, L., & Augat, P. 2002, "Correlation of bone mineral density with strength and microstructural parameters of cortical bone in vitro", *Bone*, vol. 31, no. 1, pp. 90-95.

- Wan, L. S. C., P.W.S.Heng, & L.W.Chan 1992, "Drug Encapsulation in Alginate Microspheres by EmulsiJication", *Joumal of Microencapsulation* pp. 309-316.

- Wang, J., Chen, W., Li, Y., Fan, S., Weng, J., & Zhang, X. 1998, "Biological evaluation of biphasic calcium phosphate ceramic vertebral laminae", *Biomaterials*, vol. 19, no. 15, pp. 1387-1392.

- Wang, M. 2003, "Developing bioactive composite materials for tissue replacement", *Biomaterials*, vol. 24, no. 13, pp. 2133-2151.

- Wang, X., Chen, L., Xiang, H., & Ye, J. 2007a, "Influence of anti-washout agents on the rheological properties and injectability of a calcium phosphate cement", *Journal of Biomedical Materials Research Part B: Applied Biomaterials*, vol. 81B, no. 2, pp. 410-418.

- Wang, X., Ye, J., & Wang, H. 2006, "Effects of additives on the rheological properties and injectability of a calcium phosphate bone substitute material", *Journal of Biomedical Materials Research Part B: Applied Biomaterials*, vol. 78B, no. 2, pp. 259-264.

- Wang, Y., Chang, H. I., Wertheim, D. F., Jones, A. S., Jackson, C., & Coombes, A. G. A. 2007b, "Characterisation of the macroporosity of polycaprolactone-based biocomposites and release kinetics for drug delivery", *Biomaterials*, vol. 28, no. 31, pp. 4619-4627.

- Watase, M. & Nishinari, K. 1980, "Rheological properties of agarose-gelatin gels", *Rheologica Acta*, vol. 19, no. 2, pp. 220-225.

- William R.Moore, Stephen E.Graves, & Gregory I.Bain 2001, "Synthetic bone graft substitutes", *ANZ Journal of Surgery*, vol. 71, no. 6, pp. 354-361.

- Williams, D. 1979, "Mechanical properties of biomaterials and bioceramics symposium", *Journal of Biomedical Engineering*, vol. 1, no. 1, pp. 67-69.

- Wong, L. H., Tio, B., & Miao, X. 2002, "Functionally graded tricalcium phosphate/fluoroapatite composites", *Materials Science and Engineering: C*, vol. 20, no. 1-2, pp. 111-115.

- Wu, P. C., Huang, Y. B., Chang, J. S., Tsai, M. J., & Tsai, Y. H. 2003, "Design and evaluation of sustained release microspheres of potassium chloride prepared by Eudragit«", *European Journal of Pharmaceutical Sciences*, vol. 19, no. 2-3, pp. 115-122.

- Wu, X. P., Yang, Y. H., Zhang, H., Yuan, L. Q., Luo, X. H., Cao, X. Z., & Liao, E. Y. 2005, "Gender differences in bone density at different skeletal sites of acquisition with age in Chinese children and adolescents", *Journal of Bone and Mineral Metabolism*, vol. 23, no. 3, pp. 253-260.

- Xia, Z., Grover, L. M., Huang, Y., Adamopoulos, I. E., Gbureck, U., Triffitt, J. T., Shelton, R. M., & Barralet, J. E. 2006, "In vitro biodegradation of three brushite calcium phosphate cements by a macrophage cell-line", *Biomaterials*, vol. 27, no. 26, pp. 4557-4565.

- Xu HH, Quinn JB, Takagi S, Chow LC, & Eichmiller FC 2001, "Strong and macroporous calcium phosphate cement: Effects of porosity and fiber reinforcement on mechanical properties", *Journal of Biomedical Materials Research*, vol. 57, no. 3, pp. 457-466.

- Yang, Q., Troczynski, T., & Liu, D. M. 2002, "Influence of apatite seeds on the synthesis of calcium phosphate cement", *Biomaterials*, vol. 23, no. 13, pp. 2751-2760.

- Yao, J., Radin, S., Leboy, S., & Ducheyne, P. 2005, "The effect of bioactive glass content on synthesis and bioactivity of composite poly (lactic-co-glycolic acid)/bioactive glass substrate for tissue engineering", *Biomaterials*, vol. 26, no. 14, pp. 1935-1943.

- Yavuzer, R. & Jackson, I. T. 2001, "Partial Lip Resection with Orbicularis Oris Transposition for Lower Lip Correction in Unilateral Facial Paralysis", *Plastic and Reconstructive Surgery*, vol. 108, no. 7.

- Yingling, V. R., Davies, S., & Silva, M. J. 2001, "The Effects of Repetitive Physiologic Loading on Bone Turnover and Mechanical Properties in Adult Female and Male Rats", *Calcified Tissue International*, vol. 68, no. 4, pp. 235-239.

- Z.Schwartz, J.Y.Martin, D.D.Dean, J.Simpson, D.L.Cochran, & B.D.Boyan 1996, "Effect of titanium surface roughness on chondrocyte proliferation, matrix production, and differentiation depends on the state of cell maturation", *Journal of Biomedical Materials Research*, vol. 30, no. 2, pp. 145-155.

- Zahirul, M., Khan, I., tedul, H. P., Kurjakovi&cacute, & , N. 2000, "A pH-Dependent Colon-Targeted Oral Drug Delivery System Using Methacrylic Acid Copolymers. II. Manipulation of Drug Release Using Eudragit® L100 and Eudragit S100 Combinations", *Drug Development and Industrial Pharmacy*, vol. 26, no. 5, pp. 549-554.

- Zheng Shu, X., Liu, Y., Palumbo, F. S., Luo, Y., & Prestwich, G. D. 2003, "In situ crosslinkable hyaluronan hydrogels for tissue engineering", *Biomaterials*, vol. 25, no. 7-8, pp. 1339-1348.

- Zioupos P, Currey J.D, & Casinos A 2000, "Exploring the effects of hypermineralisation in bone tissue by using an extreme biological example.", *Connective Tisssue Research*, vol. 41, no. 3, pp. 229-248.